Alireza Shadmani
Mohammad Reza Nikoo
Amir H. Gandomi

Ocean Wave Energy Technology

Fundamentals of Wave Farm Design

Springer

Ocean Wave Energy Technology

Alireza Shadmani · Mohammad Reza Nikoo ·
Amir H. Gandomi

Ocean Wave Energy Technology

Fundamentals of Wave Farm Design

Springer

Alireza Shadmani
Faculty of Engineering and Information Technology
University of Technology Sydney
Sydney, NSW, Australia

Amir H. Gandomi
Faculty of Engineering and Information Technology
University of Technology Sydney
Sydney, NSW, Australia

Mohammad Reza Nikoo
Department of Civil and Architectural Engineering
Sultan Qaboos University
Muscat, Oman

ISBN 978-3-031-95039-1 ISBN 978-3-031-95040-7 (eBook)
https://doi.org/10.1007/978-3-031-95040-7

This Springer imprint is published by the registered company Springer Nature Switzerland AG
The registered company address is: Gewerbestrasse 11, 6330 Cham, Switzerland

To my family and friends, whose unwavering support and boundless curiosity inspire me to push the boundaries of ocean innovation

Preface

The ocean is one of Earth's largest sources of natural energy, and many people see wave energy as a promising path toward clean, renewable power. Our interest in this field began when we first studied ocean engineering and saw how waves can be both powerful and complex. Over time, we realized it is important to combine theory and practice to design and deploy effective wave energy systems.

In this book, we share the basics of wave energy and show how wave energy converters can be designed, tested, and improved. We have worked to keep the ideas clear, with real-world examples that connect theory to actual projects. Our hope is that students, researchers, and engineers will find useful guidance and gain new insights into wave energy. Throughout the book, theoretical concepts are complemented by practical considerations, numerical methods, and illustrative case studies. The aim is not only to present the established knowledge but also to highlight the ongoing challenges and future directions that will shape the next generation of wave energy technology.

By bringing together research and practical lessons learned, we aim to support future progress in this area. We hope this book will serve as a helpful resource and encourage more work on harnessing the power of the ocean. Looking beyond the technical aspects, we also believe it is important to consider the social and environmental impacts of wave energy development. Wider acceptance of ocean-based power depends on responsible design and planning, as well as collaboration between engineers and local communities. By addressing these issues, we can help ensure that wave energy becomes a lasting source of clean power.

Ultimo, Australia — Alireza Shadmani
Muscat, Oman — Mohammad Reza Nikoo
Sydney, Australia — Amir H. Gandomi

Acknowledgements I am deeply grateful to the many individuals whose expertise made this book possible. Special gratitude goes to my mentors, including Prof. Amir H. Gandomi and Dr. Mohammad Reza Nikoo, who sparked my fascination for ocean renewable energy.

Competing Interests The authors have no competing interests to declare that are relevant to the content of this manuscript.

Contents

Chapter 1
Wave Energy Fundamentals and Calculation

Abstract Ocean wave energy represents one of the most promising yet underutilized renewable energy resources available globally. This chapter establishes the essential theoretical and practical frameworks for understanding wave energy fundamentals and quantification methods necessary for effective wave farm design. Drawing from oceanography, fluid dynamics, and renewable energy engineering, it presents wave energy as a concentrated form of solar energy transferred through wind interactions with the ocean surface, resulting in a resource characterized by high energy density, relative predictability, and minimal environmental footprint compared to other renewable technologies. The chapter is structured to provide comprehensive coverage across four interconnected sections. The introduction to wave energy offers historical context and basic principles, positioning this resource within the broader renewable energy landscape while explaining the physical mechanisms of wave formation and energy transport. The wave energy potential assessment section examines global and regional resource distribution, detailing measurement technologies and characterization parameters including significant wave height, energy period, directional properties, and seasonal variations essential for site selection. Wave energy calculation methods form the technical core, presenting both linear wave theory and spectral analysis techniques for quantifying energy flux in regular and irregular sea states, alongside mathematical models for resource estimation across varying environmental conditions. The final section provides illuminating case studies from diverse geographical contexts that demonstrate practical application of assessment methodologies, illustrating the complete process from data acquisition through resource characterization to energy yield prediction while addressing real-world challenges in measurement accuracy, long-term variability, and climate change impacts on resource projections.

Keywords Wave energy resource · Spectral analysis · Energy flux quantification · Resource variability · Site assessment methodology

A. Shadmani et al., *Ocean Wave Energy Technology*,
https://doi.org/10.1007/978-3-031-95040-7_1

1.1 Introduction to Wave Energy

Ocean wave energy has a long history of interest, dating back to early observations in the eighteenth century when inventors first began to imagine capturing the power of ocean waves. During the Industrial Revolution, a few pioneers even attempted to build wave energy devices, but technological limitations hindered progress. It was not until the oil crisis of the 1970s that renewed interest in alternative energy led to significant research and development in wave energy. Nowadays, as the world seeks sustainable alternatives to fossil fuels, ocean wave energy is once again capturing attention. With increasing awareness of climate change and the need to diversify energy sources, wave energy is emerging as a significant player in the renewable energy landscape. Utilizing the natural, rhythmic motion of the ocean's waves, this form of energy has the potential to provide clean, reliable electricity to coastal communities and beyond, contributing to global efforts in reducing carbon emissions and mitigating climate change impacts [1].

Wave energy is a concentrated form of solar energy: the sun produces temperature differences across the globe, causing winds that blow over the ocean surface. These winds create ripples that grow into swells, which can travel thousands of miles with virtually no loss of energy. The power density of these waves is much higher compared to wind or solar power, making wave energy a highly efficient renewable resource. Unlike other forms of renewable energy, wave energy benefits from the natural amplification of energy through the wind-wave interaction, which concentrates energy into powerful, consistent wave forms.

It is important to note that deep-water waves should not be confused with the waves seen breaking on the beach. When a wave reaches shallow water (roughly when the water depth is less than half a wavelength), it slows down, its wavelength decreases, and it grows in height, ultimately leading to breaking. This process, known as wave shoaling, results in the dissipation of energy through turbulence and friction with the seabed. The major losses of energy occur through breaking and friction with the seabed, meaning that only a fraction of the resource reaches the shore. Because of these losses, most wave energy devices are placed in deeper waters, where waves maintain their energy and can be harnessed more efficiently.

A wave carries both kinetic and gravitational potential energy. The total energy of a wave depends roughly on two factors: its height (H) and its period (T). The power carried by the wave is proportional to H^2 and to T and is usually given in Watt per meter of incident wave front. For example, the coastline of Western Europe is blessed with an average wave climate of about 50 kW of power for each meter width of the wave front [2]. The overall resource (around 2 TW) is of the same order of magnitude as the world's electricity consumption. A conservative estimate is that it is possible to extract 10–25% of this, suggesting that wave power could make a significant contribution to the energy mix [3]. These numbers put into perspective the sort of demand that human beings apply to natural resources, and the urgent need to find sustainable solutions. Global wave energy potential is considerable. The Intergovernmental Panel on Climate Change (IPCC) special report on renewable

energy estimated the theoretical potential at about 29,500 TWh/year, surpassing global electricity consumption [4]. Yet, Gunn and Stock-Williams [3] suggested that the technically exploitable resource is between 1700 and 3500 TWh/year. However, the actual exploitable wave energy varies based on local conditions, technological capabilities, and economic factors. Clemente et al. [5] highlights its high energy density, predictability, and relative consistency compared to other renewables. Unlike wind or solar, wave patterns can be forecast several days ahead, and wave energy is especially reliable in certain regions, in which Clemente et al. [6] underscored wave energy's potential contribution to the renewable mix.

As of 2024, the wave energy sector is still in development, with ongoing investment and research addressing efficiency, environmental concerns, and integration into energy systems. To better understand the wave energy formation, in the following a clear understanding of wave generation and its energy calculation are presented.

Ocean waves, both on the surface and below, transfer energy away from their sources, which are excited by forces such as gravitational potential, earthquakes, and interactions with floating bodies. Among the various types of ocean waves, swell waves and local wind waves are particularly suited for energy harnessing. Swell waves originate from distant storms and travel to coastlines as concentrated wind energy, often arriving when local winds have subsided. Wind waves, on the other hand, form through surface friction as winds blow across vast ocean areas, converting the wind's energy into wave motion. The energy within these waves is both kinetic, from particle movement, and potential, from water elevation above sea level. As a result, regions with consistent, strong wave activity offer ideal conditions for energy extraction. The formation of ocean waves involves a complex interaction of disturbing and restoring forces. Wind-generated waves begin as small ripples, growing larger as the wind sustains them until they reach a maximum size, where energy input and losses reach equilibrium. Once fully developed, these waves can travel long distances as swell waves, continuing even after the winds that created them have ceased. All waves are influenced to some degree by both local and previous wind conditions, with no fundamental difference in their hydrodynamics.

In general, in ocean wave terminology, wind sea refers to waves actively growing under the influence of local winds, while swell describes waves that have left their storm area and spread out with minimal energy loss. These swells can travel across deep waters—defined as depths exceeding one-third of the wavelength—without being affected by the seabed. Typically, an offshore view reveals multiple wave trains of varying wavelengths and directions. Unlike a single-frequency sinusoidal wave, real sea waves consist of many ordinary waves of differing frequencies and directions. This understanding of wave dynamics and the energy waves carry forms the basis for harnessing ocean waves as a renewable energy source. Figure 1.1 illustrates the relationship between different types of ocean waves based on their wave period and relative energy. The wave types are categorized across a spectrum from capillary waves, with very short periods (around 0.1 s) and low energy, to trans-tidal waves, with periods up to 24 h. As the wave period increases, so do the type and potential impact of the waves. For instance, gravity-capillary waves and ordinary gravity waves, with periods of up to 30 s, carry moderate energy. Moving to longer

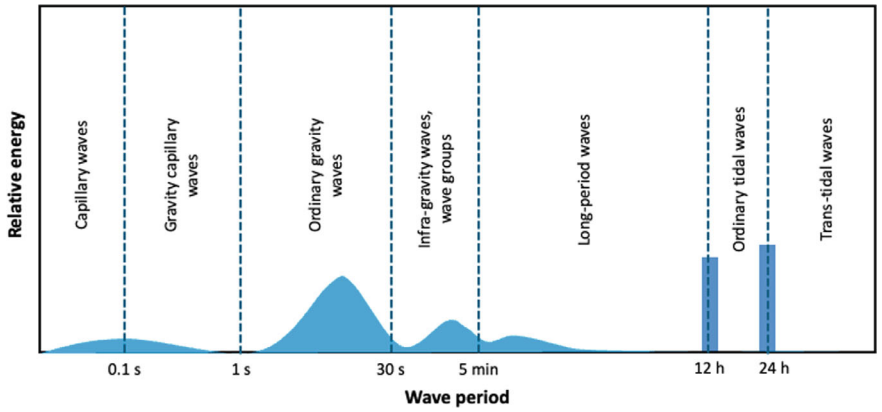

Fig. 1.1 The types of waves that may occur in the ocean [8]

periods, infra-gravity waves, which last several minutes, and long-period waves, such as seiches, storm surges, and tsunamis, show increased energy and significant impact. The longest periods are associated with ordinary tidal waves and trans-tidal waves, which are driven by lunar and solar influences. This spectrum demonstrates how both period and energy level influence the classification and impact of oceanic wave types [7].

The simplest description of wave motion is the regular, sinusoidal, or monochromatic waves illustrated in Fig. 1.2. In this description, all the waves have the same height and wavelength, and the time between wave crests is also constant and is defined as the wave period [9]. In monochromatic waves, the energy is proportional to the square of the wave height and the square of the wave period. In deep water, this energy is divided equally between the potential energy of the moving surface and the kinetic energy of the subsurface water particle movements. It should be noted that the wave motion is a moving energy packet and that the water particles do not move with the wave [10]. They are simply agitated when the waves arrive and oscillate around some fixed position. Only energy is transmitted through the water. An important point to note, though, is that waves begin to lose their energy as they come into shallower water near the shore.

Typically, wave is considered as a sinusoidal variation at the water surface elevation and can be defined as having a height H, which is the vertical distance from the wave crest to the wave trough, a wavelength, λ, which is the distance between two similar points of the wave, and the wave period, T, which is the time taken for the wave to repeat, which is depicted in Fig. 1.2. Additionally, it is useful to define other wave parameters:

$$s = \frac{H}{\lambda} \rightarrow \text{wave steepness} \tag{1.1}$$

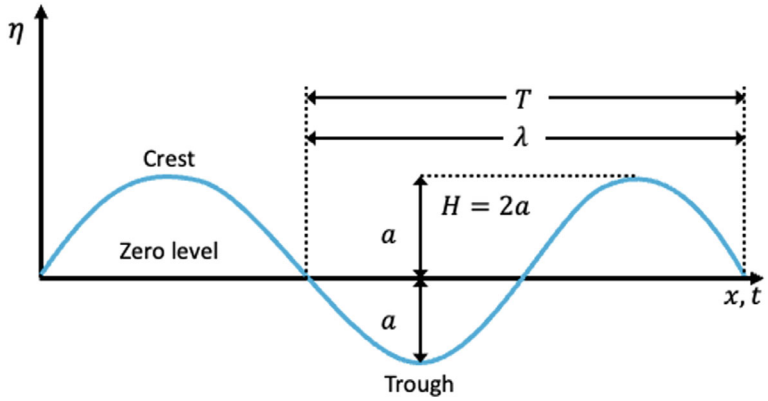

Fig. 1.2 Definition of wave parameters over a sinusoidal wave [8]

$$k = \frac{2\pi}{\lambda} \rightarrow \text{wave number} \tag{1.2}$$

$$\omega = \frac{2\pi}{T} \rightarrow \text{wave frequency} \tag{1.3}$$

Of these additional parameters, the wave steepness is often used to distinguish between linear and nonlinear waves. Typically, if the steepness is less than 0.01, then the linear wave relationships are valid, but as the steepness increases then linear theory becomes less accurate and higher-order wave models such as the 5th order Stokes waves are more appropriate [11]. However, it is very difficult to use the higher-order wave models for analyzing anything other than regular waves and so linear wave theory is often used for waves much steeper than 0.01 [12].

The theoretical foundations of wave dynamics were established by pioneers like Airy (1845) [13] and Stokes (1847) [14], who developed linear and nonlinear wave motion theories. Their fundamental definition of wave dynamics is the foundation of wave energy calculation. Wave energy density, or the energy within a wave system, depends on wave height and wavelength. Wave energy and height are related quadratically, means a small increase in height significantly boosts energy potential [15].

An important characteristic of ocean waves is that they are generally dispersive, which means that the energy in the wave does not travel at the same velocity as the wave profile [16]. For instance, the effect of dispersion can be seen when a stone is dropped into water or the wave paddles in a wave tank stop generating waves. In this case waves appear to be left behind the main wave and are travelling at a slower velocity than the wave crests due to the wave energy. The velocity of a wave crest is typically called the wave celerity, c, and the velocity of the energy propagation is typically called the group velocity, C_g. In deep water, the group velocity is equal to a half of the wave celerity, but in general the group velocity is given by:

$$C_g = \frac{1}{2}\left[1 + \frac{\frac{4\pi d}{\lambda}}{\sinh\left(\frac{4\pi d}{\lambda}\right)}\right]c \tag{1.4}$$

Moreover, not only does the group velocity vary with water depth, but the wave celerity also varies with water depth and is given by:

$$c = \frac{\lambda}{T} = \frac{gT}{2\pi}\tanh\left(\frac{2\pi d}{\lambda}\right) \tag{1.5}$$

This is called the dispersion equation and defines the wavelength based on the wave period and water depth. Accordingly, the water surface elevation ζ is given by:

$$\zeta = \frac{H}{2}\cos\left[2\pi\left(\frac{x}{\lambda} - \frac{t}{T}\right)\right] \tag{1.6}$$

However, this variation in water surface elevation is the result of an elliptical motion of the water particles, which also extends far below the water surface, with the amplitude of motion decreasing exponentially with depth. Thus, the vertical displacement of the water particles $\zeta(z)$ is expressed as follows:

$$\zeta(z) = \frac{H}{2}\cos\left[2\pi\left(\frac{x}{\lambda} - \frac{t}{T}\right)\right]\frac{\sinh\left[\frac{2\pi(z+d)}{\lambda}\right]}{\sinh\left[\frac{2\pi d}{\lambda}\right]} \tag{1.7}$$

and the horizontal displacement $\xi(z)$ is denoted by:

$$\xi(z) = -\frac{H}{2}\sin\left[2\pi\left(\frac{x}{\lambda} - \frac{t}{T}\right)\right]\frac{\cos\left[\frac{2\pi(z+d)}{\lambda}\right]}{\sinh\left[\frac{2\pi d}{\lambda}\right]} \tag{1.8}$$

Thus, in deep water, the water particle motions are circular, but they become more elliptical as the water depth decreases. Moreover, the variation in water particle motion is dependent on the water depth relative to the wavelength, and this is often used to define three regions of water depth: (1) deep water where the seabed does not affect the waves and typically requires the water depth to be greater than half the wavelength, (2) shallow water where there is no variation in horizontal water particle motion with water depth and typically requires the water depth to be less than 1/20th of a wavelength, and (3) intermediate depth that exists between these two extremes [11].

At a depth of half a wavelength, the wave-induced motions are only approximately 4% of these at the surface and thus could be considered insignificant [10]. However, it should always be remembered that these limits are somewhat arbitrary, and since they depend on the wavelength this means that the definition of water depth is not fixed. That is, a site may be defined as being in deep water for a short wave, whilst the same site for a different wave may be in intermediate water. Thus, care should

always be taken to determine which reference wavelength should be used to define the relative depth. For wave energy, it is particularly important to recognize this condition, because many wave energy devices defined as "deep-water" devices, are typically deployed in what many oceanographers would define as intermediate water depths [17, 18].

The present chapter is intended to convey an overview of the knowledge accrued until now. The main subject is to elaborate on the energy associated with ocean waves. The assessment procedures for wave energy potential will be discussed in the following section. Moreover, the mathematical description of wave energy extraction is presented in the third section of this chapter. In the final section with concluding remarks, several case studies are provided to present the calculation and assessment of wave energy in different regions.

1.2 Wave Energy Potential Assessment

Accurately assessing the potential of wave energy is essential for site selection, technology development, and economic feasibility, as emphasized in [19–21]. This assessment relies on a combination of measurement techniques and modeling approaches to provide a comprehensive understanding of wave resources. In-situ measurements, conducted mainly with wave buoys and Acoustic Doppler Current Profilers (ADCPs), yield precise data on wave height, period, and direction. Wave buoys measure these parameters directly from the ocean surface, while ADCPs, typically installed on the seabed, use sound waves to analyze water movement, offering detailed wave characteristics.

Remote sensing technologies complement these direct measurements, expanding the scope of wave energy assessment. Satellite altimetry, using radar altimeters, provides global wave height data, enabling broad coverage of ocean conditions. Synthetic Aperture Radar (SAR) technology further enhances this capability, delivering high-resolution images of ocean surface waves, particularly useful for remote or inaccessible areas. Together, remote sensing and in-situ measurements form the observational foundation for wave energy potential assessment. This complex process is essential to determine where and how wave energy can be harnessed effectively and sustainably, as illustrated in Fig. 1.3.

The global distribution of wave energy potential is uneven, with certain regions exhibiting exceptional resources. A detailed assessments of wave energy highlighted key areas with high potential, including Western and Northern Europe (particularly the UK, Ireland, Norway, and Portugal), the North American Pacific Northwest, the southern tips of Africa and South America, and the southern coastlines of Australia and New Zealand. These regions experience consistent, powerful waves driven by global wind patterns and vast ocean expanses, making them prime candidates for wave energy development [18, 22, 23]. While global assessments offer a broad overview, detailed regional studies are essential for practical wave energy projects. For example, in Europe, Rusu and Onea [24] evaluated wave energy potential across

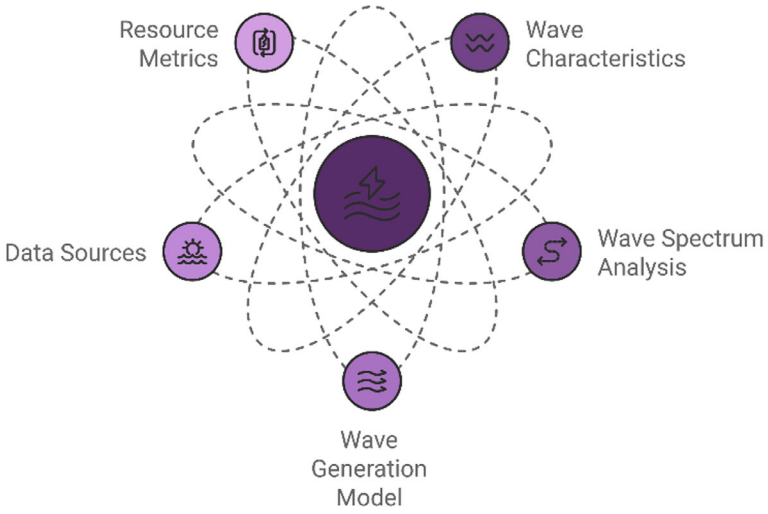

Fig. 1.3 Elements of wave energy potential assessment

European coastal environments, noting the exceptional resources off the western coasts of Ireland and Scotland, where average wave power levels exceed 70 kW/m in some areas. In North America, Lenee-Bluhm et al. [25] identified significant wave resources along the US West Coast, particularly in Washington, Oregon, and Northern California, with García-Medina et al. [26] providing high-resolution nearshore characterizations for the Pacific Northwest. In the Southern Hemisphere, Hemer et al. [27] assessed Australia's wave energy resources, highlighting the southern coastline, while Gorman et al. [28] documented significant potential along New Zealand's western and southern coasts. However, detailed discussion of case studies in various regions will be discussed in Sect. 1.3.

The wave energy potential of a given location is shaped by a complex interplay of geographical, meteorological, and oceanographic factors. Geographical elements include fetch (the distance over which wind blows unobstructed), bathymetry (the depth and shape of the seabed), and coastline orientation. Larger fetch typically generates more energetic waves, while bathymetry influences wave behavior as they approach the shore. The angle at which waves approach the coast, determined by coastline orientation, can also significantly impact wave energy. Meteorological factors, especially global and local wind patterns, are primary drivers of wave formation. Seasonal variations and extreme weather events like storms can amplify wave energy, though they pose challenges for device durability. Additionally, oceanographic factors such as large-scale currents and variations in water density (due to temperature and salinity) influence wave patterns and energy content. Understanding these factors is crucial for accurately assessing wave energy potential and for developing effective wave energy technologies. Temporal and spatial variations in wave height and period are essential for general wave energy formulations, incorporating

correction factors and coefficients of variation [29, 30]. Regional assessments using geo-statistical methods help evaluate spatial variations in wave height, essential for identifying optimal points for energy extraction [31]. By analyzing wave energy potential along coastlines, regions with higher energy yields can be pinpointed, guiding the strategic placement of energy harvesting facilities. Therefore, accurate modeling of wave height and period is vital for effective wave energy assessment, enabling improved predictions and optimizations of energy extraction.

The performance of wave energy devices is influenced by the temporal, directional, and spectral characteristics of ocean waves, as these determine the relationship between average omni-directional wave power and average power generation. Temporal consistency in wave climates is particularly valuable, as stable sea states allow power plants to operate closer to optimal conditions, enhancing system efficiency. However, wave climates vary with meteorological conditions, leading to daily, seasonal, and annual fluctuations that impact power generation, which an example of monthly variation of significant wave height and wave period is demonstrated in Fig. 1.4. Locations with consistent wave climates are generally more favorable, as they provide more predictable energy outputs. Thus, understanding the temporal characteristics of wave climates is essential to optimize wave energy device performance and predict power generation accurately.

The directional characteristics of a wave climate are influenced by both the directional spread of individual sea states and the overall directional variation of all sea states. Only isolated, omni-directional devices may not be significantly affected by these variations. Generally, an increase in directional variation can reduce average power generation, as devices are less likely to align optimally with incoming waves. The directional characteristics of a wave climate depend on its location, which determines the range of weather systems generating the winds and waves that shape the local wave climate. Therefore, considering directional characteristics is essential when assessing a potential wave energy site [32].

Finally, the spectral characteristics of a wave climate are linked to the wave spectrum of individual sea states and the overall spectral variation across all sea states.

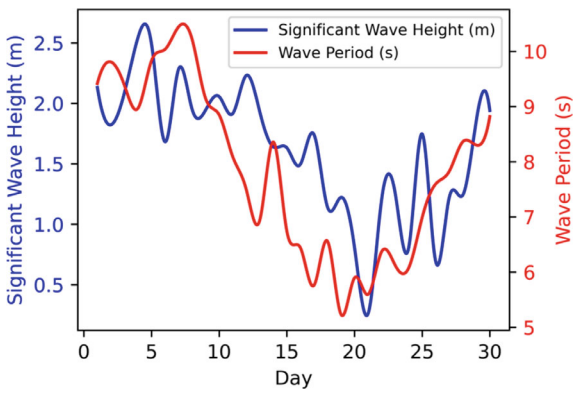

Fig. 1.4 Example of the variation of the significant wave height and wave period over one month

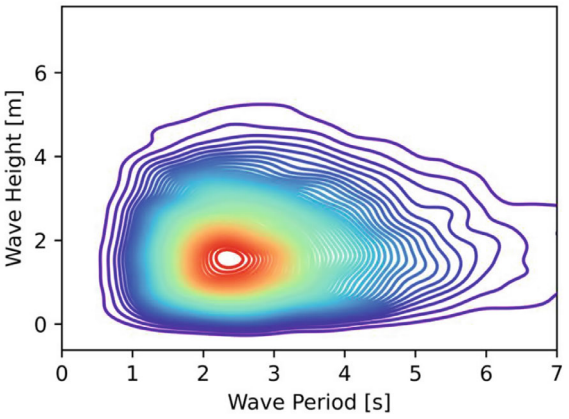

Fig. 1.5 Example of scatter diagram of wave height and period

Spectral characteristics are particularly important because the efficiency of many devices depends on wave frequency. Wave power at certain frequencies may be more effective for energy extraction than at others. Consequently, assessing the spectral characteristics of a potential site is crucial, especially in relation to the spectral response of devices intended for deployment [33].

Once a site of interest has been identified, a scatter diagram is often used to characterize its wave climate. Figure 1.5 illustrates an example scatter diagram, a frequency table indexed by a representative wave period (typically the peak, zero-crossing, or energy period) and a representative wave height, which usually is the significant wave height. A scatter diagram provides more detailed information about the wave climate than the average omni-directional wave power.

Firstly, table resolution can affect the scatter diagram's accuracy, as sea states may vary significantly within a single cell, especially for small significant wave heights. For example, a cell representing wave heights between 0.5 and 1.0 m may contain sea states with a potential 4:1 variation in wave power. Although these variations may have a minor impact on overall wave power estimates, any potential distortions should be considered. Additionally, scatter diagrams lack information on the temporal, directional, or spectral distribution of sea states within a single cell, all of which can impact wave energy device performance. This issue is sometimes mitigated by creating multiple scatter diagrams for different wave directions or seasons, but practical limits exist on how many diagrams can be effectively used. Overall, scatter diagrams of wave height and period offer a comprehensive description of the wave climate at a location, as shown in Fig. 1.5, and are essential for calculating long-term energy production and understanding wave energy variability.

Furthermore, the wave rose, illustrated in Fig. 1.6, is a commonly used representation of the wave climate. It provides a graphical view of average wave power or significant wave height from various directional sectors. Seasonal wave roses can also be created to offer insights into seasonal variations in wave climate, which is particularly helpful in regions where different meteorological conditions affect wave characteristics at different times of the year.

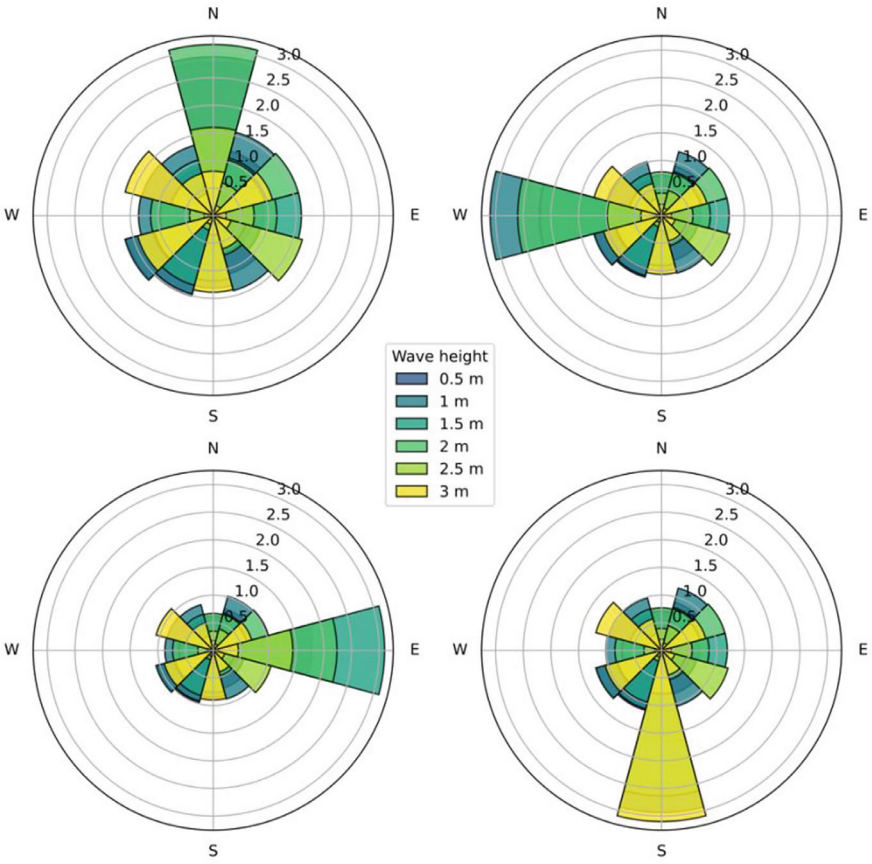

Fig. 1.6 Example of wave roses

Characterizing the wave climate with single parameters—such as average omni-directional wave power, scatter diagrams, or wave roses—provides only a partial understanding of potential power generation. Whenever possible, using the full time-series of directional wave spectra is recommended for estimating a device's average power generation [34, 35]. When a complete dataset is not available or is impractical to use, it is essential to recognize the increased uncertainty in power generation estimates and that the performance of a wave energy device at different sites may not correlate directly with simple parameters like average wave power. Despite their limitations in power prediction, wave climate representations are valuable for understanding device performance. As knowledge about a device improves, specific wave climate characteristics may be identified that allow for a reasonable estimate of the device's performance based on climate data. Until then, it is important to be aware of the limitations and potential distortions that simplified wave climate characterizations might introduce in power estimates. The average omni-directional wave

power is the most common characterization of the wave resource for the assessment of wave energy. This seems, and likely is, a reasonable characterization since to extract significant amounts of wave energy the incident wave power must also be significant; without waves there is no wave power. The key factor to consider is that when comparing potential sites, the use of the average omni-directional wave power obscures information regarding the temporal, directional, and spectral characteristics of the wave climate that may be important to the average power capture. In fact, how these characteristics may affect the average power generation will vary with the device and so it is difficult to be overly prescriptive regarding the extent of distortion that may be due to using average omni-directional wave power as a proxy for average power generation. One method to compensate for the potential distortion is to provide information on other aspects of the wave climate simultaneously with the average omni-directional wave power. Examples of this additional information could include the ratio of maximum wave power to average wave power, the average directionality coefficient, the average spectral width, and/or the average energy period. Unfortunately, whilst this additional information does provide more details of the characteristics of the wave resource that may suggest the relative strengths and weaknesses of particular sites, it still does not provide a clear indication of how a device's power generation may differ between locations.

Whilst it is frustrating that a single parameter, or even set of parameters, cannot be used to assess the suitability of a potential device deployment site, this is the state of the wave energy industry at the moment. The rich diversity of device concepts currently being developed means that there are multiple relationships between the wave resource and power generation. Moreover, it is possible that a particular device concept may be most suitable at one location, whilst another device concept is more suitable at another location. Thus, there may not be the complete convergence onto a single concept as in wind energy, due to the potentially greater diversity of wave resource characteristics compared to wind resource characteristics, which is generally successfully characterized simply by the average wind speed.

Although not associated with a particular device concept, a useful illustration of the dangers of using the average omni-directional wave power as a proxy for power generation is in assessing the effect of water depth on the incident wave power. For instance, in a certain region, the average omni-directional wave power offshore may decrease as it approaches the shore. To assess the extent that this reduction in average omni-directional wave power may translate to a reduction in potential power generation, it is necessary to consider how the change in average omni-directional wave power has occurred. Consideration of the wave propagation process indicates that there are six main processes responsible for the change in average omni-directional wave power, namely: shoaling, refraction, diffraction, depth-induced wave breaking, bottom friction, and wind growth, which will be elaborated in the next section.

To this end, the wave spectrum is a fundamental component for accurately assessing wave energy potential, as it quantifies the distribution of energy across different frequencies and directions. This spectrum, influenced by factors like wind speed, water depth, and geographic features, provides a statistical description of the sea state by representing the water surface as the sum of sinusoidal waves with

varied frequencies, amplitudes, and directions. The wave spectrum allows for a more precise understanding of power density and wave characteristics than viewing waves as simple, regular oscillations. This superposition of waves results in a comprehensive representation known as the wave spectrum, which is crucial for predicting significant wave height, period, and overall wave energy potential.

Statistical approaches are essential in wave energy calculations, especially for long-term resource assessment and device performance estimation [36]. These methods involve analyzing probability distributions of wave heights and periods, often using data collected over several years or even decades. The Rayleigh distribution is frequently used to model wave height distributions within a sea state, while the log-normal distribution is commonly applied to wave periods, as shown in Fig. 1.7 [37–39]. Exceedance probabilities, which indicate the percentage of time that wave conditions exceed specific thresholds, are valuable for estimating potential energy production. For example, the widely used P95 measure represents wave power that is exceeded 95% of the time, offering a conservative estimate of the available resource, as depicted in Fig. 1.8 [40, 41].

Long-term statistical analyses provide insights into seasonal and interannual variability in wave energy resources, essential for project planning and economic feasibility. Techniques such as extreme value analysis are used to estimate the magnitude and frequency of extreme wave events, which are critical for the structural design and survivability assessment of wave energy devices [41]. Additionally, statistical methods help quantify uncertainty in wave energy estimates, often using techniques like bootstrap resampling or Monte Carlo simulations to establish confidence intervals in resource assessments [42, 43]. Long-term hindcast studies used historical wind data to simulate wave conditions over several decades, creating a robust statistical basis for evaluating wave energy resources [2]. These studies typically employed global wave models to generate a time series of wave parameters, which are then analyzed to derive metrics relevant to wave energy, such as mean wave power and its variability. The wave spectrum is crucial in these assessments, as it provides insights into the distribution of energy across different wave components. This is particularly valuable because wave energy devices are often optimized for specific frequency ranges, making the spectral characteristics of a site influential in technology selection and device performance. Together with other metocean parameters such as water depth, marine current speed/direction, and wind speed/direction, this can be used to estimate the power capture and design parameters for any wave energy device deployed at the location. However, typically it is not possible to work with this amount of data (or the data is not available) and so a characterization of the wave climate is used. The wave climate characterization can essentially be one of two types: the characterization of the wave climate at a single point or the characterization of the wave climate over an area. However, it is important to recognize that in either case the characterization results in a compression of the details on the wave climate and so does not contain all the information that may be relevant to the performance of a wave energy device.

The directional properties of the wave spectrum are also key when assessing the potential for directional wave energy devices. Advanced assessment techniques often

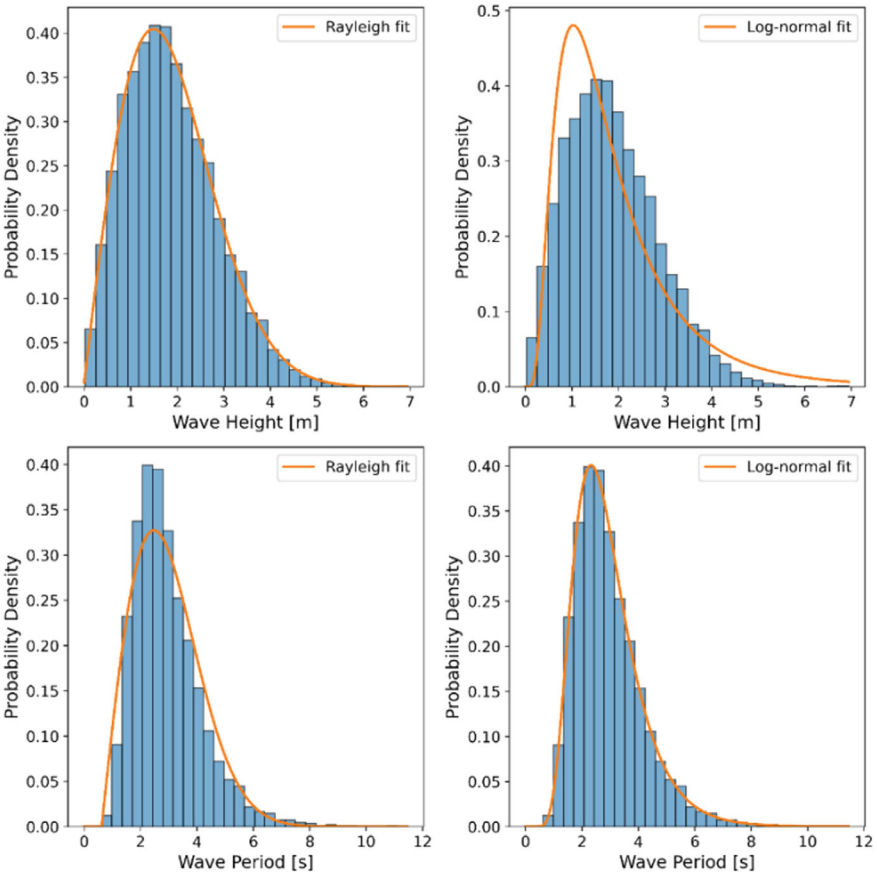

Fig. 1.7 Wave height and period distribution fitted by Rayleigh and log-normal distributions

combine spectral wave models with high-resolution bathymetric data and local wind fields to create detailed maps of wave energy potential. These assessments considered not only mean wave power but also factors such as temporal variability, extreme wave events, and practical extraction limitations, providing a realistic estimate of the technically exploitable wave energy resource.

The wave spectrum is commonly represented by the variance density spectrum, while specialized investigations frequently employ canonical models—most notably the Pierson-Moskowitz spectrum for fully developed seas and the JONSWAP (Joint North Sea Wave Project) spectrum for fetch-limited conditions. These theoretical constructs are central to wave energy resource assessments, providing a mathematically rigorous framework for characterizing the inherently irregular, multidirectional nature of ocean wave fields. By analyzing the ocean surface into its constituent frequency components, it is possible to capture the spatio-temporal heterogeneity of wave energy across a spectrum of frequencies (or wave periods) and directions,

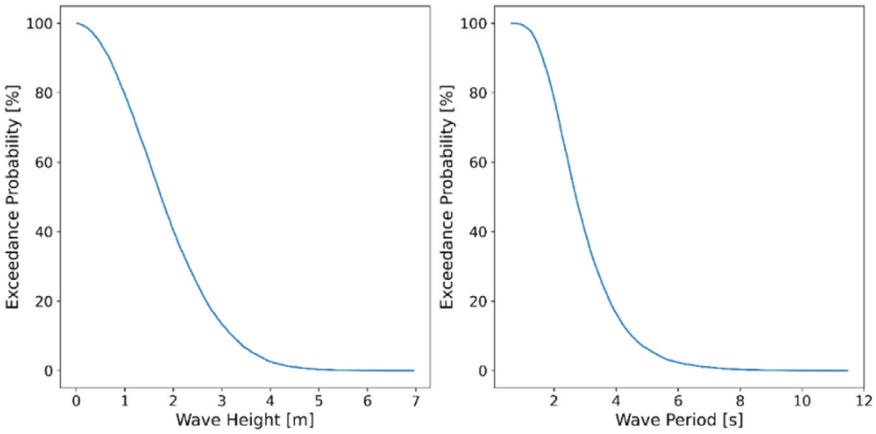

Fig. 1.8 Exceedance probability of wave height and period

thus offering a comprehensive view of the prevailing wave climate in a given locale. Moreover, spectral models can be adapted or combined to accommodate unique regional characteristics—ranging from localized wind forcing to bathymetric influences—further enhancing the reliability of resource estimations and the robustness of predictive simulations.

The JONSWAP spectrum is commonly used to represent the sea state that is not fully developed. The Pierson-Moskowitz and JONSWAP spectra are expressed as follows, respectively:

$$S(\omega) = \frac{\alpha g^2}{\omega^5} \exp\left[-\beta\left(\frac{\omega_p}{\omega}\right)^4\right] \tag{1.9}$$

$$S(\omega) = \frac{\alpha g^2}{\omega^5} \exp\left[-\frac{5}{4}\left(\frac{\omega_p}{\omega}\right)^4\right] \gamma^{\exp\left[-\frac{(\omega-\omega_p)^2}{2\sigma^2\omega_p^2}\right]} \tag{1.10}$$

In Pierson-Moskowitz, α is equivalent to 0.0081, β is 0.74, and $\omega_p = \frac{g}{U_{19.5}}$. Additionally, in JONSWAP, $\alpha = 0.076\left(\frac{U_{10}^2}{F_g}\right)^{0.22}$, $\omega_p = 22\left(\frac{g^2}{U_{10}F}\right)^{\frac{1}{3}}$, $\gamma = 3.3$, and σ is decided as follows:

$$\sigma = \begin{cases} 0.07 \rightarrow \omega \leq \omega_p \\ 0.09 \rightarrow \omega > \omega_p \end{cases} \tag{1.11}$$

Moreover, $S(\omega)$ is the spectral variance density, ω_p is the peak frequency, g is the gravitational acceleration, U_{10} is the wind speed at a height of 10 m, F is the fetch length, and ω is the wave component frequency. In addition to the wind speed and fetch length, the JONSWAP spectrum is also defined by the peak enhancement factor γ. This parameter defines how the peak of the spectrum is as shown in Fig. 1.9.

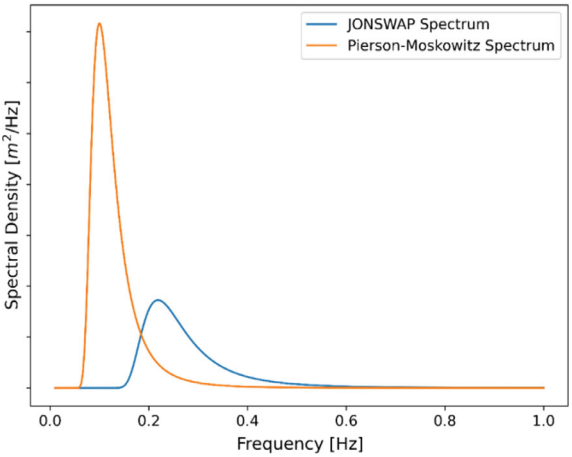

Fig. 1.9 Two common wave spectrums

Comparison of Eqs. (1.9) and (1.10) reveal that the spectral shapes of the JONSWAP and Pierson-Moskowitz spectra are identical when the peak enhancement factor of the JONSWAP spectrum equals 1.0. Thus, it can be inferred that the bandwidth of the spectrum is dependent on its state of development with new and developing seas having a narrower bandwidth, so that the wave components are all at similar frequencies and fully developed seas having a broader bandwidth, with the wave energy spread over a larger range of frequencies.

To facilitate understanding, the discussion above only considers sea states that have been generated by a single source of wind. However, in reality, the sea state at a single location may have waves generated from a number of different sources of winds from different directions with different speeds and fetch lengths. Where there are two distinct sources of waves then the sea state is called bi-modal and has two peaks with different peak directions and frequencies. Figure 1.10 shows an example of a bi-modal sea state. cases where there are more than two sources of wind result are called multi-modal sea states. Although there will be some interaction between the waves from the different sources, typically this interaction is small, and the spectra can generally be linearly superimposed without too much loss of accuracy (at least when they are not close to breaking).

A primary goal of wave energy resource evaluation is to quantify the magnitude of power accessible in the wave field across various spatial and temporal scales. Through spectral analysis, key parameters—such as significant wave height and the energy period—are derived with greater precision. These parameters inform standard formulations of wave power flux, typically expressed in kW per meter of wave crest, and serve as critical indicators of resource availability. Furthermore, long-term observational records, drawn from in-situ measurements, e.g., wave buoys, satellite altimetry, or comprehensive numerical wave hindcasts, provide data on seasonal, interannual, and spatial variations in the wave climate. This wealth of information is

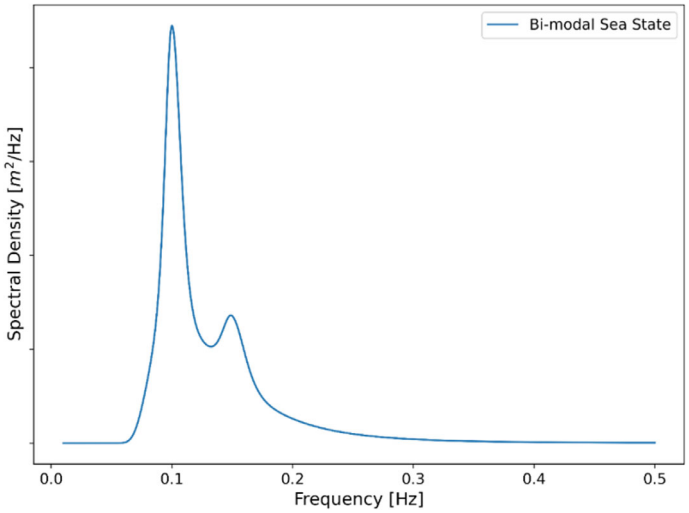

Fig. 1.10 Bi-modal sea state

indispensable for identifying regions with heightened wave energy potential, illuminating how meteorological factors, including evolving wind patterns and large-scale climate oscillations, can modulate wave regimes.

In addition to this, wave generation models are fundamental to assess wave energy potential, particularly over large spatial scales and extended time periods. These models simulate the physical processes behind ocean wave creation and evolution. Wave generation is primarily driven by wind forcing, where energy is transferred from the wind to the water surface through complex air-sea interactions. Foundational studies described the mechanisms of resonance and shear flow instability, which contribute to wave growth [44, 45]. Building on these principles, modern wave generation models—such as those in third-generation spectral wave models like WAVEWATCH III and SWAN (Simulating WAves Nearshore)—incorporate advanced parameterizations for wind input, nonlinear wave-wave interactions, and energy dissipation processes. These models solve the wave action balance equation, capturing the evolution of the wave spectrum over space and time, which will be elaborated in the following section.

As waves move away from their generation area, they undergo transformations due to interactions with bathymetry, currents, and environmental factors. Processes such as shoaling, refraction, diffraction, and wave breaking significantly influence wave characteristics near the coast. Nearshore transformation models, often based on mild-slope or Boussinesq-type equations, simulate these coastal processes with higher resolution. Integrating large-scale wave generation models with nearshore transformation models is essential for comprehensive wave energy assessments, enabling accurate predictions from deep ocean to coastal waters. Overall, the calculation of wave energy is another important aspect of wave energy potential assessment. It is

crucial for understanding how to quantify the energy available in ocean waves and how to estimate the power output of wave energy devices, where principles of wave energy calculations will be elaborated in the next section.

1.3 Wave Energy Calculation Methods

Wave energy calculation methods are the basis of wave energy resource assessment and play a pivotal role in the design, optimization, and deployment of wave energy devices. These methods encompass a wide spectrum of approaches, ranging from fundamental analytical techniques to advanced numerical models and sophisticated spectral analysis, as shown in Fig. 1.11. The primary objective of these methods is to accurately quantify the energy contained in ocean waves and estimate the potential power that can be extracted by wave energy devices. A clear understanding of wave energy calculation methods is foundational not only for assessing energy resources but also for ensuring accurate measurements and interpretations of wave parameters, like significant wave height, that inform device design and site selection. Significant wave height, a key metric in wave energy assessments, has multiple definitions based on observational or analytical techniques, each providing slightly different insights into wave characteristics. Recognizing the method used to determine significant wave height is essential for consistency, as slight variations between methods can affect energy estimates, especially in shallow or steep wave conditions. This highlights the importance of precise and consistent terminology in wave energy calculations to improve reliability across all stages of wave energy development, from resource assessment to device deployment.

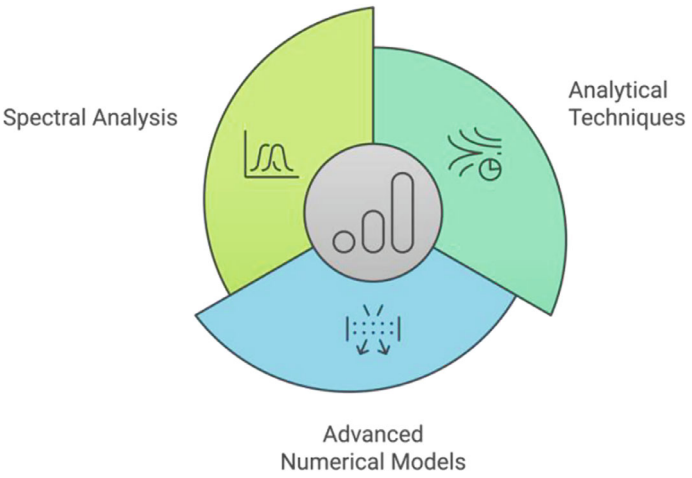

Fig. 1.11 Different approaches for wave energy calculation

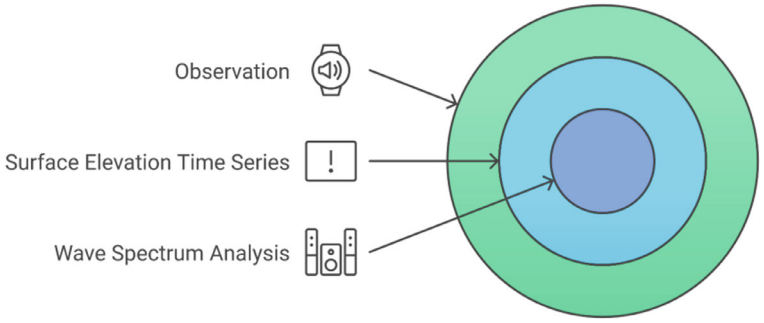

Fig. 1.12 Methods for measuring significant wave height

Recalling the introduction to this section, it was noted that there are three different definitions of the significant wave height: the first based on observation, the second based on analysis of a record of the surface elevation time series, and the third one is based on the wave spectrum. It is important to be aware of which one is being used, demonstrated in Fig. 1.12. The first method is never used nowadays; however, wave data from both the other methods is still commonly used. Thus, it is good practice when referencing the significant wave height to use a subscript to identify the method, with the subscript '1/3' used when the significant wave height is based on the average height of the third highest waves and the subscript 'm_0' when the significant wave height is based on the wave spectrum. Unfortunately, in many cases the significant wave height is identified by the subscript 's' and the method used to generate it is unknown. As noted above, the difference between the methods in deep water for a moderate sea state is relatively small, typically about 1%; however, the difference increases progressively as the waves steepen and/or water depth decreases.

In wave energy, the preferred representative wave height is the significant wave height derived from the spectral moments of the wave spectrum, H_{m_0}:

$$H_{m_0} = 4\sqrt{\int_0^\infty S(\omega)d\omega} \tag{1.12}$$

This is because it is effectively based on the energy in the waves and as such is directly related to the average wave power density. To show this, it is necessary to recognize that with linear super-position the power in each wave can be considered independently and then summed together to give the total average wave power density. Therefore, consider a single wave component then the wave power is given by:

$$J(\omega) = \rho g S(\omega).C_g(\omega) \tag{1.13}$$

where the first half of the right-hand side of the equation is the energy in the wave and the second half of the right-hand side is the velocity at which the energy is propagating, known as group velocity [6]. The speed that the wave energy propagates depends on the wave frequency ω and water depth h and is given by:

$$C_g(\omega) = \frac{1}{2}\frac{\omega}{k(\omega)}\left(1 + \frac{2k(\omega)h}{\sinh 2k(\omega)h}\right) \tag{1.14}$$

where $k(\omega)$ is defined by the dispersion equation:

$$\omega^2 = gk(\omega)\tanh k(\omega)h \tag{1.15}$$

Using the assumption of linear super-positioning, the average wave power density for the sea state is given by the integral of the wave components:

$$J = \int_0^\infty \rho g S(\omega).\frac{1}{2}\frac{\omega}{k(\omega)}\left(1 + \frac{2k(\omega)h}{\sinh 2k(\omega)h}\right)d\omega \tag{1.16}$$

To progress further, it is useful to define the moments of the spectrum m_n as:

$$m_n = \int_0^\infty S(\omega)\omega^n d\omega \tag{1.17}$$

Then, the wave energy period T_e can be defined as the ratio of the first negative moment of the spectrum to the zeroth moment of the spectrum as given by the following equation:

$$T_e = \frac{m_{-1}}{m_0} \tag{1.18}$$

And the significant wave height can be used directly in the calculation of the wave power density. Consequently, the omni-directional wave power J can be defined in deep water as:

$$J = \frac{\rho g^2 H_{m_0}^2 T_e}{64\pi} \tag{1.19}$$

In addition to defining significant wave height and energy period, the moments of the spectrum can also be used to characterize other aspects of a sea state. For example, the relative spreading of energy across wave frequencies, known as the spectral bandwidth ϵ_0, can be defined as the standard deviation of the period variance density normalized by the energy period, as follows:

$$\epsilon_0 = \sqrt{\frac{m_0 m_{-2}}{m_{-1}^2} - 1} \tag{1.20}$$

Moreover, it is possible to make a spectral estimate of the mean zero-crossing period of the waves T_z, which is given by:

$$T_z \cong T_{02} = \sqrt{\frac{m_0}{m_2}} \tag{1.21}$$

This spectral estimate of the mean zero-crossing period of a sea state is valuable, as it enables the scaling of a spectrum based on assumptions about spectral shape and the mean zero-crossing period, a common parameter for defining historical wave resource data. Likewise, the spectrum can be scaled using the peak period T_p, which is also frequently used to characterize wave resource data.

Using these expressions, it is also possible to calculate the ratio between different measures of the wave period for particular spectral shapes. This can be especially useful when it is considered necessary to convert between representations of the wave period. For example, for a JONSWAP spectrum with peak enhancement factor, $\gamma = 3.3$, the ratios of the wave periods are $1.12T_e = 1.29T_z = T_p$. For many devices, the directional characteristics of the sea state will also be important. The directionally resolved wave power density $J(\theta)$ is a key directional characteristic of the sea state as it defines the wave power propagation in a particular direction. The directional wave spectrum can be used to calculate the variation in the directionally resolved wave power density $J(\theta)$ as given by:

$$\begin{gathered} J(\theta) = \rho g \int_{-\pi}^{+\pi} \int_{0}^{\infty} S(\omega, \varphi) C_g(\omega) \delta d\omega . d\varphi \\ \begin{cases} \delta = 1 \rightarrow \cos(\theta - \varphi) \geq 0 \\ \delta = 0 \rightarrow \cos(\theta - \varphi) < 0 \end{cases} \end{gathered} \tag{1.22}$$

Additional directional parameters that characterize a sea state include the direction of maximum directionally resolved wave power density and the directionality coefficient, which is the ratio of the maximum directionally resolved wave power density to the omni-directional wave power density, as defined in Eq. (1.19). Another important characteristic, especially when considering transient effects, is wave groupiness, the tendency for larger waves to occur in groups. Nonlinear processes, particularly in shallow water, contribute to wave groups, though spectral bandwidth also plays a role; narrow-banded spectra generally exhibit higher levels of wave groupiness than broad-banded spectra. A common measure of wave groupiness is the average run length, or the average number of consecutive waves that exceed a specified threshold, such as the significant or mean wave height.

To accurately model and analyze these complex wave characteristics, numerical wave models play a crucial role. These models incorporate physical processes such as

wave generation, dissipation, and nonlinear interactions to predict wave behavior in different environments. Among them, spectral wave models are particularly effective in capturing the influence of directional parameters, wave groupiness, and spectral bandwidth on wave dynamics. By resolving wave energy across multiple frequencies and directions, they provide a more detailed representation of sea states, making them essential tools for coastal engineering and oceanographic studies. One such widely used spectral wave model is SWAN, which is designed to simulate the evolution of wave conditions in coastal and nearshore environments. By incorporating directional wave parameters, spectral characteristics, and nonlinear interactions such as wave groupiness, SWAN provides a comprehensive framework for assessing wave generation, propagation, and transformation. Its ability to resolve complex physical processes makes it an indispensable tool for coastal engineering, wave energy resource assessment, and environmental impact studies [46].

The predictive capability of the SWAN model depends on the accurate specification of its input parameters, which define the physical and environmental settings governing wave generation. One of the most critical inputs is wind fields, which drive wave growth by transferring momentum from the atmosphere to the sea surface. These fields are typically obtained from meteorological models, weather stations, or reanalysis datasets [47]. Accurate wind data, both in terms of spatial coverage and temporal resolution, are vital for realistic simulations of wind-driven wave systems. Another crucial input is bathymetry data, representing the topography of the seabed and variations in water depths. Bathymetric features significantly affect wave transformation processes, including refraction, diffraction, and shoaling. High-resolution bathymetric maps allow the model to accurately simulate these effects and predict their impact on wave energy distribution. Boundary conditions are also essential, as they define the incoming wave energy at the edges of the model domain. These conditions are typically derived from regional or global wave models and include spectral descriptions of wave height, period, and direction.

SWAN simulates a wide range of interconnected physical processes that govern wave evolution, depicted in Fig. 1.13. Wave generation by wind is the primary mechanism, where wind stress on the sea surface induces wave growth. The rate of growth depends on factors such as wind speed, duration, and fetch length, with SWAN employing empirical and theoretical formulations to capture these effects. Refraction and diffraction are key processes that redistribute wave energy as waves interact with varying water depths or obstacles. Refraction bends wave paths toward or away from regions of changing depth, concentrating energy in some areas while dispersing it in others. Diffraction occurs when waves encounter barriers such as breakwaters or islands, spreading energy into shadow zones and creating complex interference patterns. These processes are particularly important in harbors and coastal engineering projects where wave directionality and energy distribution must be carefully managed.

Shoaling occurs when waves travel into shallower waters, causing an increase in wave height due to the conservation of energy. This process is significant in determining nearshore wave power and can lead to localized energy amplification, making it a critical factor for wave energy assessments. Nonlinear wave-wave interactions

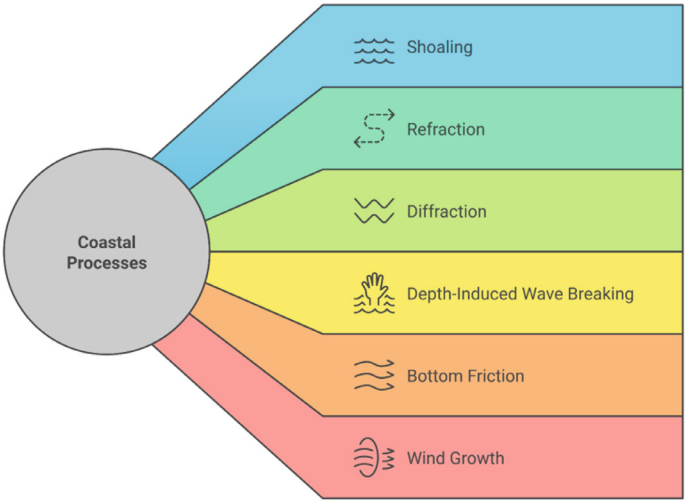

Fig. 1.13 Coastal processes influencing in wave energy calculations

further influence wave spectra by transferring energy between different frequencies, maintaining spectral balance and preventing excessive energy concentration in narrow bands. White capping and wave breaking serve as energy dissipation mechanisms that limit wave growth and prevent overestimation of wave heights. White capping results from wave crest instability, releasing energy as turbulence, while wave breaking occurs predominantly in shallow waters, where waves steepen and collapse. Bottom friction also contributes to energy loss, particularly in regions with rough or mobile seabed, where the interaction between waves and the seabed results in significant dissipation.

SWAN generates a variety of outputs that provide essential insights for coastal and marine applications. One of the most important outputs is significant wave height, representing the average height of the highest one-third of waves in a given period. This parameter is crucial for assessing wave energy potential and is widely used in the design of wave energy devices. The model also provides wave periods, including the energy period and peak period, which describe the dominant wave frequencies and are essential for evaluating energy conversion efficiency. Wave direction and directional spectra offer detailed information about the path waves follow and how energy is distributed across multiple directions. Wave power flux is another key output, quantifying the rate of wave energy transport per unit width of wave crest [48]. Wave power typically expressed in kW per meter, this metric is fundamental for determining the economic feasibility of wave energy projects. SWAN produces spatial distributions of wave energy, visualized through maps and grids that highlight areas with high energy potential. Time series data track the temporal variability of wave parameters, providing insights into seasonal patterns, extreme events, and long-term trends.

A key advantage of SWAN is its ability to generate high-resolution spatial and temporal wave data, making it an invaluable tool for wave energy assessments. By integrating bathymetric, meteorological, and hydrodynamic inputs, SWAN can simulate wave conditions across diverse environments, from open oceans to nearshore regions. This capability allows researchers and engineers to identify optimal locations for wave energy extraction, taking into account factors such as wave height variability, energy period consistency, and directional wave spreading. Additionally, SWAN's outputs facilitate the evaluation of environmental impacts, ensuring that wave energy installations are designed with minimal disruption to coastal ecosystems. The model's predictive power is further enhanced by its adaptability to different grid resolutions and boundary conditions, enabling site-specific analysis for energy resource assessment and infrastructure planning. Iglesias and Carballo [49] demonstrated its effectiveness in identifying high-potential areas for wave energy exploitation along the Spanish coastline. Similarly, Rusu and Guedes Soares [50] applied SWAN to characterize the wave energy resource in the Portuguese nearshore, highlighting the model's capability to provide detailed spatial and temporal wave power distribution. The model's versatility is further exemplified by its coupling with other numerical models. Mel et al. [51] coupled SWAN with a hydrodynamic model to enhance wave predictions in areas with complex bathymetry, a crucial factor in accurate wave energy resource assessment. Moreover, validation studies have played a critical role in establishing SWAN's reliability for wave energy applications. Moeini and Etemad-Shahidi [52] conducted comprehensive validation in Lake Ontario, focusing on parameters relevant to wave energy calculations. Pallares et al. [53] further validated SWAN's performance in predicting extreme wave events in the Mediterranean Sea, an essential aspect for the design and survivability of wave energy devices.

Furthermore, Rogers et al. [54] introduced an enhanced white capping formulation, improving the models' performance in fetch-limited conditions. Salmon et al. [55] implemented a new bottom friction formulation based on the eddy viscosity model, enhancing predictions in shallow water environments. Additionally, the introduction of unstructured grid capabilities by Zijlema et al. [56] marked a significant advancement in SWAN's ability to represent complex coastlines and bathymetry [11]. This development has been particularly beneficial for detailed wave energy resource characterization in coastal areas with intricate geometries. This enhanced flexibility in SWAN's numerical framework not only improves its ability to capture wave dynamics in complex coastal environments but also underscores the importance of precise model calibration. While these advancements refine the model's underlying physics, their effectiveness depends on accurately tuning key parameters to reflect real-world conditions. Consequently, before applying SWAN for wave simulations, a thorough calibration process is necessary to ensure the model's reliability and accuracy in diverse marine environments.

Before utilizing SWAN models for wave simulations, an essential step is the calibration of key parameters to enhance accuracy and reliability. Calibration involves fine-tuning parameters such as bottom friction, white capping, and nonlinear wave interactions to ensure the model realistically represents wave dynamics in a given environment. This process is particularly important when applying SWAN to specific

coastal or offshore regions, where local conditions influence wave behavior. Proper calibration helps improve the agreement between simulated wave characteristics and observed data, making the model more effective for practical applications [57]. Calibration systematically involves adjusting model parameters to closely align simulated outputs with observed data, thereby minimizing discrepancies and improving predictive performance. The calibration process typically begins by selecting representative datasets, which may include in-situ wave measurements, e.g., from wavey buoys, satellite observations, or hindcast data.

A core component of SWAN calibration is the selection and adjustment of several key parameters. Among these, wind input coefficients are particularly influential, as wind forcing is the primary driver of wave generation. The calibration process adjusts the wind growth coefficients and scaling factors to accurately reflect how local and regional wind conditions drive wave development. Equally important is the calibration of white capping dissipation, which governs energy loss due to wave breaking in deeper waters. This parameter ensures a proper balance between wave growth and dissipation, preventing either overestimated wave energy or excessive damping. Bottom friction represents another critical parameter, especially in coastal regions where interactions between the seabed and wave motion significantly affect energy dissipation. During calibration, bottom friction coefficients are fine-tuned to reflect site-specific characteristics such as sediment type and seabed roughness. Nonlinear wave-wave interactions, often modeled through the DIA or other spectral approaches, also require calibration to correctly distribute energy across the frequency spectrum, ensuring realistic wave height predictions. These parameters influence wave generation, propagation, and dissipation processes. The main parameters typically calibrated in SWAN are presented in Table 1.1 [58].

The calibration of SWAN models involves a structured, multi-step process that ensures accurate representation of wave dynamics by fine-tuning key parameters. The following steps provide a detailed procedure for achieving reliable calibration.

- Step 1: Data collection and pre-processing

Observational datasets form the foundation of model calibration. Data from buoys, satellites, or hindcasts are collected and pre-processed to remove noise, fill gaps, and correct anomalies. This ensures that the calibration is not influenced by errors or inconsistencies in the observational data.

- Step 2: Initial model setup

The initial setup of the SWAN model involves inputting baseline parameter values derived from literature, previous studies, or site-specific conditions. These initial values act as a starting point for further calibration adjustments.

- Step 3: Sensitivity analysis

A sensitivity analysis helps identify which parameters most significantly impact model performance. By systematically varying key parameters, researchers can determine their influence on outputs such as wave height, period, and direction, allowing prioritization of parameter adjustments.

Table 1.1 Main parameters in the calibration process of SWAN model

	Parameter	Short description
Wave growth and dissipation parameters	White capping dissipation coefficient (C_{ds})	Controls the dissipation of wave energy due to breaking in deep water
	Bottom friction coefficient (C_{ds})	Determines energy loss due to bottom friction, especially in shallow water
	Depth-induced breaking parameter (γ)	Regulates wave breaking due to depth limitation (commonly calibrated using the Battjes and Janssen model)
	Nonlinear quadruplet interaction coefficient (C_{nl4})	Affects wave energy redistribution through nonlinear interactions
	Triad interaction coefficient (C_{triad})	Governs wave-wave interactions in shallow waters
Wind input parameters	Wind drag coefficient (C_d)	Influences wave growth based on wind forcing
	Exponential growth parameter (A)	Affects wind energy transfer into waves
Numerical and spectral parameters	Directional resolution ($\Delta\theta$)	Determines the number of directional bins for wave energy distribution
	Frequency resolution (Δf)	Defines the discretization of the wave spectrum
Model-specific tuning parameters	Wave breaking threshold (α)	Defines the threshold for depth-induced wave breaking
	Bottom friction formulation	Choice of formulation (e.g., JONSWAP, Collins, Madsen) affects wave damping due to seabed interaction
	Wave reflection coefficient	Governs wave reflections from coastal structures or seabed features

- Step 4: Iterative parameter adjustment

The most impactful parameters, identified during sensitivity analysis, are adjusted iteratively. The model is run for multiple time periods and locations, and each iteration involves comparing model outputs with observational data. Adjustments are made progressively to refine the accuracy of the simulation.

- Step 5: Error minimization

Statistical metrics, such as root mean square root (RMSE), bias, and scatter index, are used to measure discrepancies between modeled and observed results. Through

iterative refinement, these errors are minimized, ensuring the model consistently aligns with real-world data.

- Step 6: Validation

Once the calibration achieves acceptable accuracy, an independent dataset is used to validate the model's robustness. Validation ensures that the model is generalizable and performs reliably under varying conditions beyond the calibration dataset. However, SWAN calibration, while indispensable for accurate wave modeling, encounters several challenges that must be addressed to ensure robust and reliable outputs. The inherent complexity of wave dynamics, combined with practical limitations in data collection and computational power, makes this process both resource-intensive and highly technical.

One of the most significant challenges is the variability of wave conditions across different spatial and temporal scales. Waves are influenced by multiple environmental factors, including local wind fields, bathymetry, and coastal geometry. These variables fluctuate over time and across regions, requiring calibration efforts that can adapt to specific local conditions. Often, a single calibration scenario is insufficient, necessitating multiple simulations and site-specific adjustments to accurately capture dynamic wave behaviors [57]. The availability and quality of observational data pose another major barrier. High-resolution datasets, such as those obtained from wave buoys, satellite altimetry, and field measurements, are often limited, especially in remote or under-monitored regions. This scarcity of reliable data can lead to gaps in the calibration process, potentially affecting the model's predictive accuracy. Researchers must sometimes rely on interpolation techniques or hindcast models to fill these gaps, though this introduces additional uncertainty. Large-domain simulations, particularly those conducted at high spatial and temporal resolutions, require significant computational resources. The iterative nature of the calibration process, involving numerous models runs with incremental parameter adjustments, further exacerbates the computational cost. Balancing accuracy and efficiency are crucial, as overly simplified models may miss critical wave interactions, while highly detailed models can become prohibitively expensive to run [59, 60].

The sensitivity of SWAN models to parameter changes can also complicate calibration. Small changes in wind input coefficients, bottom friction, or white capping dissipation can have disproportionately large effects on model outputs, necessitating meticulous fine-tuning. Conducting sensitivity analyses is essential to identify the most influential parameters and prioritize their adjustment without overwhelming computational resources [47]. To better understand the wave energy calculation by the SWAN model over large areas and long time periods, in the following the mathematical formulations governing the SWAN model will be elaborated. These models solve the wave action balance equation:

$$\frac{\partial N}{\partial t} + \nabla X\,(cN) = \frac{S}{\sigma} \tag{1.23}$$

where N is the action density spectrum, c is the propagation velocity in the geographical and spectral space, S represents source and sink terms including wind input, nonlinear wave-wave interactions, and energy dissipation processes, and σ is intrinsic frequency. By coupling these wave models with geographical information, it is possible to produce detailed spatial maps of wave energy potential, accounting for bathymetric effects and coastal features. The action density is used instead of the energy density $E(\sigma, \theta)$ because in the presence of currents, action density is converted while energy density is not. For instance, SWAN represents the wave field as a two-dimensional wave action density spectrum $N(\sigma, \theta)$. Since wave action is conserved in the presence of currents, this formulation provides a more robust representation of wave dynamics. The wave action balance equation is expressed as:

$$\frac{\partial N}{\partial t} + \nabla x.\left(c_g N\right) + \frac{\partial (c_\sigma N)}{\partial \sigma} + \frac{\partial (c_\theta N)}{\partial \theta} = \frac{S}{\sigma} \tag{1.24}$$

where c_g, c_σ, c_θ are the group velocity governing wave energy transport in geographical space, propagation velocities in the frequency and directional domains, respectively. The terms in this equation describe wave energy propagation, frequency shifting due to varying currents and depth, and directional spreading effects. The right-hand side of the equation (S/σ) represents the net energy input and dissipation processes, which are crucial for accurate wave modeling.

The total wave energy is obtained by integrating over all frequencies and directions:

$$E_{total} = \rho g \iint E(\sigma, \theta) d\sigma d\theta \tag{1.25}$$

where ρ is water density, g is gravitational acceleration, and $E(\sigma, \theta) = N(\sigma, \theta) \times \sigma$, which is the wave energy density spectrum, related to wave action density. This integration provides the total energy available in the wave field, which is fundamental for wave energy resource assessments.

The SWAN model accounts for various physical processes through source/sink terms as follows:

$$S = S_{in} + S_{nl} + S_{ds} + S_{bot} + S_{br} \tag{1.26}$$

where parameters on the right-hand side of the above equation are wind input, nonlinear wave-wave interactions, dissipation due to white capping, bottom friction, and depth induced breaking, respectively. The wind input term quantifies the energy transferred from the wind to the wave field. It is often parameterized using the linear growth mechanism proposed by Janssen [61]:

$$S_{in} = A.\rho_{air}.\left(\frac{u^2}{c}\right).E(\sigma, \theta) \tag{1.27}$$

where A is an empirical coefficient, ρ_{air} is the air density, u is the wind speed at 10 m above sea level, and c is the phase velocity of the wave. Nonlinear interactions among waves redistribute energy between spectral components without adding or removing total energy. This process is significant in deep-water conditions and is modeled using the Boltzmann integral:

$$S_{nl} = \iint T\left(N, N'\right) d\sigma d\theta \tag{1.28}$$

where T represents the energy transfer function. This mechanism enables wave energy to spread across frequencies and directions, shaping the spectral distribution. White capping represents energy loss due to wave breaking in deep water, parameterized using the Hasselmann formulation:

$$S_{ds} = -\Gamma.\sigma.(kH_s)^p.E(\sigma, \theta) \tag{1.29}$$

where Γ is an empirical coefficient, k is the wave number, H_s is the significant wave height, p is an exponent, typically set to 2. This term is crucial for balancing excessive wave growth due to wind forcing. Bottom friction dissipates wave energy as waves interact with the seabed, modeled using empirical formulations such as the JONSWAP model:

$$S_{bot} = -C_{bf} k^2 E(\sigma, \theta) \tag{1.30}$$

where C_{bf} is a friction coefficient depending on seabed roughness. As waves propagate into shallow water, they break when the wave height exceeds a threshold based on water depth. The Battjes and Janssen [62] formulation represents this process. This term ensures dissipation in the surf zone.

$$S_{br} = -\frac{Q_b}{H_{\max}} E(\sigma, \theta) \tag{1.31}$$

Several other well-established spectral wave models are widely used for global and regional wave energy assessment. A pioneering third-generation wave model developed in the late 1980s by the WAMDI group. WAM was one of the first models to integrate the full spectral energy balance with modern source term physics such as wind input, nonlinear interaction, and dissipation, and proved capable of realistic wave predictions on oceanic scales. It laid the groundwork for subsequent models. WAM is still used and forms the basis of the wave models in major weather centers.

An advanced model developed by NOAA/NCEP, effectively a successor of WAM. WAVEWATCH III is a third-generation spectral wave model that solves the random-phase spectral action density equation for waves across the globe. It introduced numerous improvements in numeric and physics over its predecessors, allowing for flexible grid schemes, improve source term packages, and modular expansion.

WAVEWATCH III is designed for global and regional scales, and it is used operationally for wave forecasting. For instance, NOAA runs a global WAVEWATCH III model to provide wave forecasts and hindcasts, and it serves as the backbone for many wave atlases. The model can be run on regular latitude-longitude grids or curvilinear grids, and recent versions even support unstructured meshes. This model can output detailed spectral information, but for wave energy applications typically the significant wave height and energy period are used to compute the wave power flux since wave power per unit crest length is proportional to square of significant wave height and energy period. This model's reliability has been demonstrated in numerous validation results.

Additionally, a spectral wave model developed by DHI as part of the MIKE suite of marine modeling tools. MIKE 21 SW is also a third-generation model and includes all the standard source term physics for wind-wave growth, nonlinear interactions, and dissipation similar to WAM/SWAN. One distinguishing feature of MIKE 21 SW is its use of unstructured mesh grids. Instead of a fixed rectangular grid, it allows a flexible mesh that can be refined in areas of interest and coarsened in open ocean, which can greatly improve computational efficiency. This flexibility is advantageous for wave energy assessment. One can run MIKE 21 simulation that has high resolution around wave nested models. MIKE 21 is a proprietary model. It has been validated against measurements in various regions, and studies have shown it produces results comparable to other spectral models when properly calibrated. For instance, in the Indian Ocean, MIKE 21 hindcasts were validated against buoy and satellite altimeter data, shadowing generally good agreement [63].

Besides wave energy calculation, there are several phenomena that are influencing the wave propagation and wave energy flux, namely shoaling, refraction, diffraction, depth-induced wave breaking, bottom friction, and wind growth, as depicted in Fig. 1.13.

Shoaling can be understood by considering a wave propagating into shallower water. When a wave propagates into shallower water, the wave group velocity changes, but the change in group velocity is not accompanied by a change in energy flux. Thus, conservation of energy means that the wave height must get larger to keep the total energy flux constant. It can be visualized as a bunching up of the incident waves so that they increase in height as illustrated in Fig. 1.14.

To understand refraction, consider a wave propagating at an angle to the depth contours. In this case, the dispersion equation tells us that the part of the wave crest in shallow water will travel slower resulting in a turning of the direction of wave propagation. This effect explains why on the beach all the waves appear to come from a direction approximately orthogonal to the coastline, as depicted in Fig. 1.15.

Refraction causes waves to change direction, making their propagation more perpendicular to seabed depth contours. This process reduces directional spreading, concentrating the wave approach as the water depth decreases. While refraction causes a reduction in wave height by spreading the wave energy over a larger area, it is important to remember that the process is energy-conserving and does not alter the energy traveling orthogonally to the depth contours.

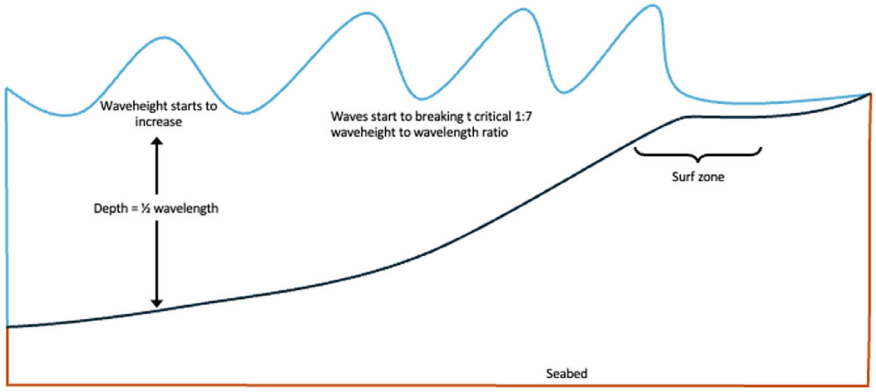

Fig. 1.14 Change in wave shape due to water depth [8]

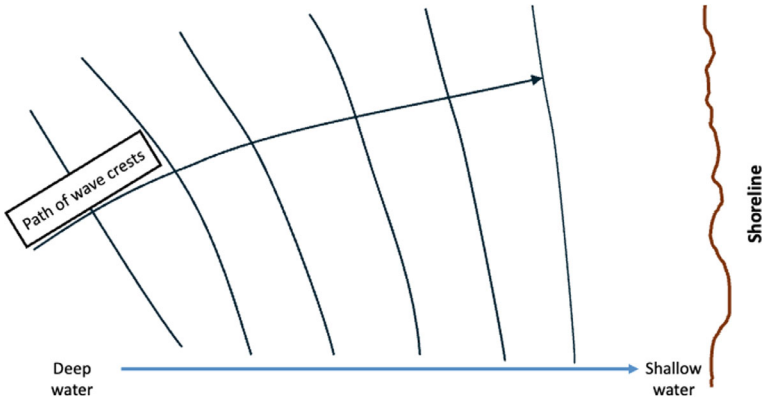

Fig. 1.15 Wave refraction near the shore due to a change in water depth [8]

The impact of refraction on average omni-directional wave power—and thus power generation—depends on the directional sensitivity of the wave energy device. An isolated device that is insensitive to wave direction will experience a similar reduction in power generation as the average omni-directional wave power decreases. However, for a larger area-sensitive device, incident wave power is defined by the wave power incident on the area. If this area is aligned with depth contours, refraction has no effect on incident wave power due to energy conservation. In most cases, however, the area will not be perfectly aligned with depth contours, and refraction will alter the power incident on it, with the effect increasing as the angle between the area and depth contours grows. Thus, the suitability of using average omni-directional wave power as a proxy for power generation depends on the specific device characteristics and deployment configuration.

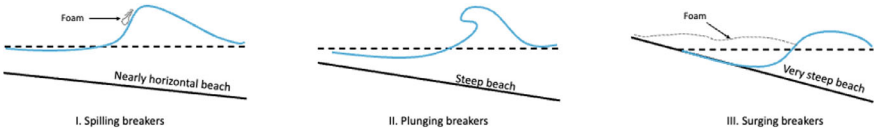

Fig. 1.16 Classification of breaking waves [8]

Diffraction occurs when waves meet a surface-piercing obstacle such as an island, headland, or breakwater. Without diffraction, the waves would continue to travel in the same direction leaving a region of calm water in the lees of the obstacle. However, diffraction means that the waves will bend so that there are waves behind the obstacle. The amount of diffraction depends on the wavelength, with the longer waves diffracting to a greater extent than the shorter waves. If there is more than one source of diffraction, e.g., either side of an island, then a diffraction pattern may form where there are areas of increased and decreased wave height due to constructive and destructive interference. Although diffraction means that waves will occur on the leeward side of an obstacle, generally these waves will be smaller than the incident waves (except in the special case of constructive interference) so the wave resource behind an obstacle is likely to be smaller than the seaward wave resource.

Wave breaking occurs when the horizontal wave particle velocity becomes greater than the wave celerity. When this occurs, the wave will spill energy in the form of breaking waves. Depth-induced wave breaking is related to the steepening of the waves in shallow water due to shoaling. When the wave height is greater than about 0.8 of the water depth (or about 0.14 of the wavelength), then the waves break. There are three different types of breaking waves: spilling, plunging, and surging, as shown in Fig. 1.16, depending on the wave and seabed steepness.

In water depths greater than about 10 m, most waves will not break and so it is tempting to consider that this process is not significant in assessing the suitability of using average omni-directional wave power to compare offshore and nearshore sites. However, the average omni-directional wave power includes energy from all events irrespective of its exploitability. It includes the wave energy in storms, which at the offshore site, in deep water, may have 40–50 times the wave power of the average wave power. Thus, although storms may only occur infrequently, they may make a relatively large contribution to the average wave power and account for perhaps 15–20% of the total wave energy. On the contrary, at the nearshore site, the wave energy in a storm is a much smaller multiple of the average wave power because depth-induced wave breaking has limited the wave energy in a storm that reaches the nearshore but not affected the wave power in the most commonly occurring seas. The proportion of the total wave energy contained in storms is important since it is largely un-exploitable, either because the device power generation is limited by the plant rating, or because it must shut down in order to survive the storm. Thus, because the average omni-directional wave power does not distinguish whether the wave energy is exploitable, it distorts the relative potential power generation at the offshore and nearshore sites.

The reduction of average omni-directional wave power has often been primarily attributed to bottom friction. However, as illustrated above, a significant proportion of the reduction is caused by other factors and in particular refraction [64]. Indeed, for a typical seabed bottom friction only accounts for about 5% of the reduction in average omni-directional wave power. The reduction in spectral wave energy due to bottom friction is complex and varies with depth so that the wave spectrum changes because of bottom friction, although the small amount of energy reduction means that the change in spectrum will also be small. However, as different device concepts have different spectral responses, it is possible that the change in spectral shape will be more significant for one device concept than another. Thus, it is possible that the change in average omni-directional wave power due to bottom friction has a different impact on average power generation for different devices because of their different response characteristics. As there is a larger fetch to the open ocean for the nearshore, it may be expected that wind growth will increase the wave power at this site. Unfortunately, in many cases, the offshore waves are already in equilibrium with the wind because of the large fetch and so they cannot grow significantly between offshore and nearshore. However, when the wind blows from the land there will be minimal fetch for the nearshore site, but the fetch may be significant for the offshore site.

This interplay between fetch length, wind forcing, and wave growth highlights the complexity of wave energy resource assessment, particularly in coastal and nearshore environments. Understanding these dynamics is crucial for accurately estimating wave power potential and optimizing the siting of wave energy converters. In the next section, recent case studies on wave energy assessment will be elaborated and discussed, showcasing how numerical models like SWAN have been applied to analyze wave resource variability, optimize energy extraction, and improve predictions in diverse marine environments. These studies provide valuable insights into the practical challenges and advancements in wave energy research.

While SWAN, WAVEWATCH III, MIKE 21 and other spectral models all operate on similar principles, there are differences in their performance and suitability that are important for wave energy assessments. In terms of core physics, all third-generation models incorporate state-of-the-art source term formulations, and numerous intercomparisons have found that they produce very similar wave predictions given the same inputs [65]. For example, studies comparing SWAN and MIKE 21 for coastal simulations found their results statistically comparable after calibration, with differences usually within the error margins of measurements. Reliability thus depends more on input data and model setup than the choice of model itself. That said, certain models have niche strengths. SWAN includes detailed shallow-water physics by default, which can make it more reliable in surf zones or areas with strong currents, whereas WAVEWATCH III might need additional tuning or cannot resolve very shallow breaking as finely. WAVEWATCH III has been rigorously validated on global scales and benefits from continuous development by a broad community, lending confidence to its results for open-ocean wave climates. MIKE21's reliability has been demonstrated in many projects. One advantage is that DHI provides validated default parameter settings for different regions based on their extensive

experience, which can be useful for new users. In practice, when model predictions are compared to buoy data, errors in significant wave height typically range on the order of 10–15% for well-executed simulations, and energy flux errors are similar or slightly larger (since they involve wave period as well). These error levels are acceptable for resource assessment purposes. Extreme events pose a slightly bigger challenge—models might under-predict the highest waves due to spectral resolution limits or physics saturation, but improvements are continuously being made (e.g., updated wave breaking formulations to better capture extreme seas). Overall, no single model has proven categorically more accurate in all cases; with proper tuning, each can achieve high reliability.

The computational cost of wave modeling can be significant, especially for long-term hindcasts or high-resolution domains. Differences in model algorithms affect how fast they run. WAVEWATCH III and WAM use explicit time-stepping schemes on structured grids, which can become slow if very fine grid spacing is needed (time step restrictions apply to maintain numerical stability). They do however support parallelization (MPI) and multiple grid levels—WW3 can run a mosaic of nested grids simultaneously, which is efficient for global-regional coupling. SWAN, using implicit schemes, allows larger time steps in shallow water, which improves efficiency for high-resolution coastal runs. SWAN also has parallel versions (OpenMP, MPI) but on a single grid its scalability is sometimes limited by memory. MIKE 21 SW's unstructured mesh approach can be highly efficient: it puts computation only where needed. For instance, to simulate an area with many islands, a structured grid model must refine everywhere, whereas MIKE21 can refine around islands and use larger elements elsewhere, saving CPU time. In terms of raw speed, WAVEWATCH III has been optimized over decades and can handle global grids with millions of points; SWAN can bog down if asked to cover a huge domain at high resolution (it's less efficient on oceanic scales). On the other hand, SWAN shines in local domains where you need 100 m-scale resolution and complex physics. A noteworthy development in recent years is leveraging modern high-performance computing (HPC) for wave models. For example, researchers have implemented GPU acceleration for WAM (the model underpinning many global forecasts), achieving impressive speed-ups—a 7-day global wave simulation at 0.125° (~14 km) resolution can now run in only ~ 7.6 min on 8 GPUs, which is dozens of times faster than on traditional CPUs.

Another practical consideration is how easily a model can be set up and integrated into real-world projects. SWAN and WAVEWATCH III are open source, which makes them attractive for academic research and for organizations with in-house modeling expertise. They require preparation of input files (wind, bathymetry, current fields if any) and some familiarity with running numerical models. There is a large user community and extensive documentation for both. MIKE 21, being commercial, comes with a polished user interface and technical support, which can be advantageous for industry users or agencies that prefer a turnkey solution. It simplifies setting up simulations (e.g. through a GUI for mesh generation and boundary conditions), though at the cost of license fees. In terms of coupling with other systems: WAVEWATCH III and WAM are often coupled with atmospheric models (e.g. in weather forecast centers) and even ocean circulation models, making them well-suited for

integrated operational forecasting. SWAN is frequently coupled with coastal circulation models or used in planning studies where it might take outputs from a regional climate model. Data requirements are similar across models—all need wind forcing; bathymetry and currents for higher-fidelity nearshore results. If high-quality wind data are available (satellite-derived winds or reanalysis), these models can be applied almost anywhere in the world. In operational use (e.g., daily wave forecasts or nowcasts), WAVEWATCH III and WAM are more commonly used globally, whereas SWAN often provides localized guidance.

1.4 Case Studies on Wave Energy Assessment

Wave energy assessment case studies have been instrumental in advancing our understanding of ocean renewable energy potential across diverse geographic regions. These studies not only showcase the practical implementation of wave energy conversion technologies but also offer valuable insights into the methodologies used for resource evaluation. Through systematic analyses of various coastal environments, researchers have refined approaches to quantifying and characterizing wave energy resources, leading to more accurate assessments and improved optimization of energy extraction systems. These advancements contribute to the development of more efficient and reliable wave energy solutions, ultimately enhancing their feasibility for large-scale deployment.

Pioneering studies have developed methodologies to assess wave power density across different ocean regions, providing critical data for identifying promising sites for wave energy extraction [66]. An assessment of the Atlantic Marine Energy Test Site (AMETS) off the west coast of Ireland, for example, utilized 12 years of modeled data to analyze annual and seasonal wave characteristics, including significant wave height, energy period, and power. This detailed characterization aids in understanding resource variability, which is essential for effective site selection. Understanding the wave climate—defined by the statistical distribution of wave heights and periods over time—is essential [67]. Another study leveraged historical wave data to analyze the variability and predictability of wave energy resources, shedding light on the temporal availability of wave energy and its correlations with seasonal and interannual climatic patterns [68].

Folley [69] discussed the generation and validation of wave energy resource data using numerical models and site measurements. It also discussed the processes that affect wave propagation and lead to wave transformation. However, it does not provide a direct answer to the fundamentals of wave energy. This work provided an understanding of wave hydrodynamics and energy resources. Moreover, the definition of representative wave height and its estimation by experienced observers was presented in this research. Robertson [70, 71] provided an overview of wave energy resource assessments, including in-situ and remote wave measurement techniques, numerical wave propagation models, parameterizations, and methodologies to quantify the wave resource and minimize uncertainty. Subsequently, Guillou et al. [72]

examined different methods for assessing wave energy resources, including investigations based on observations and numerical simulations. They also highlight the benefits, limitations, and potential of these methods. The International Electrotechnical Commission's technical specification for wave energy resource assessment and characterization is explored by Ramos and Ringwood [73]. They elaborated the methodology using the Irish west coast as a case study. They suggested revisiting certain aspects of the validation and model setup procedures.

According to the abovementioned studies, the most energetic wave climates occur in the mid- to high-latitude oceans, where strong winds and long fetch (uninterrupted distance over water) allow waves to build up significant energy. Notably, the Southern Hemisphere mid-latitudes (approximately 40°–60°S) experience some of the highest wave power levels on earth. Due to the vast uninterrupted expanse of the Southern Ocean encircling Antarctica, waves can propagate and grow virtually unimpeded, resulting in mean wave power densities often exceeding 80 kW/m of wave crest [74], demonstrated in Fig. 1.17. This makes the Southern Ocean and its adjacent sea a dominant source of wave energy. In fact, the maximum average wave power globally has been reported in these Southern Ocean, with individual locations averaging on the order of 100 kW/m or more over long-term periods. Seasonal variations are also pronounced, during austral winter, Southern Ocean wave power peaks even further due to intense storms.

Several regional hotspots stand out for their high wave energy potential. In the Southern Hemisphere, the most energetic coastal regions include the southwestern coasts of South America, e.g., Chile, the waters off South Africa, and the southern coasts of Australia and New Zealand. These areas face the open ocean and directly receive the brunt of Southern Ocean swells, yielding very high wave power densities. In the Northern Hemisphere, the North Atlantic Ocean is the premier wave energy hotspot. The North Atlantic's average wave power can reach on the order of ~ 80 kW/m in its most energetic parts. This energy is felt along adjacent coastlines: the western

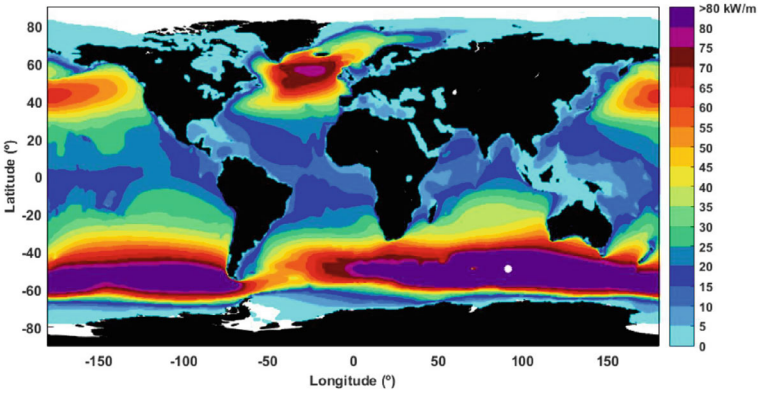

Fig. 1.17 Mean wave power distribution based on ERA5 reanalysis data spanning the 30-year period from 1980 to 2018 [74]

coasts of Europe, e.g., UK, Ireland, Norway, and the eastern coasts of North America experience the highest wave energies in the north, as they are exposed to the Atlantic's prevailing wind and swell patterns. Other notable high-energy regions include the North Pacific, particularly the northwest Pacific affecting East Asia and the northeast Pacific affecting the Pacific Northwest of North America, and the South Pacific, e.g., coasts of Chile and New Zealand, which similarly benefit from long stretches of ocean over which waves can grow. By contrast, enclosed or sheltered basins have much lower wave energy potential. For example, the Mediterrnean Sea, Black Sea, and Baltic Sea have limited fetch and milder wind climates, resulting in low wave power densities (often well below 10 kW/m). tropical regions near the equator also tend to have gentler waves on average, except in storm events, because trade winds are steady but not as strong as mid-latitude westerlies, and tropical storms, while intense, are intermittent. Therefore, equatorial and coastal tropical areas (aside from cyclone-prone zones) are generally lower in wave energy compared to temperate and high-latitude zones.

The European coastline, particularly the western coast of Scotland, is one of the most extensively studied regions for wave energy potential. Recent studies conducted between 2018 and 2023 have documented mean wave power levels ranging from 30–50 kW/m, with exceptional sites around the Hebrides achieving peaks of 85 kW/m during winter months. The European Marine Energy Centre (EMEC) in Orkney has recorded H_s averaging 2.3 m annually, with T_p ranging between 9.5 and 11.5 s. Winter measurements have shown extreme wave heights exceeding 15 m during storm events, with power densities surpassing 140 kW/m. Analysis of wave directionality indicates predominant wave approaches from the west-northwest (280°–310°), carrying approximately 60% of the annual energy flux. These extensive studies provide a foundation for the design and optimization of WECs that are well-suited to the challenging conditions of the North Atlantic.

An assessment by Ferraro et al. [75] examined the wave energy potential off Calabria, Southern Italy, an area with a mild wave climate. This study utilized ECMWF data, validated against buoy data, to assess average yearly and seasonal wave energy at selected hot spots, providing insights into the energy potential at various locations and time scales. By decomposing sea states into a spectrum of individual wave frequencies and amplitudes, spectral analysis offers a detailed understanding of energy distribution within a wave field, as depicted in Fig. 1.18.

The Portuguese continental shelf also demonstrates significant wave energy potential, particularly in its northern region. Detailed measurements reveal average annual wave power levels of 25–35 kW/m, with seasonal variations showing winter averages of 42.5 kW/m and summer minimums of 16.8 kW/m. Long-term data analysis indicates significant wave heights typically range from 1.5–2.8 m, with peak periods between 8–12 s occurring 65% of the time. The most energetic sea states ($H_s > 4$ m, $T_p > 13s$) contribute approximately 35% of the total annual energy, despite occurring only 12% of the time. Water depths between 50–100 m have been found to offer optimal energy density, with a measured 22% reduction in power levels as waves propagate from 100 to 20 m depth contours. The variability in energy

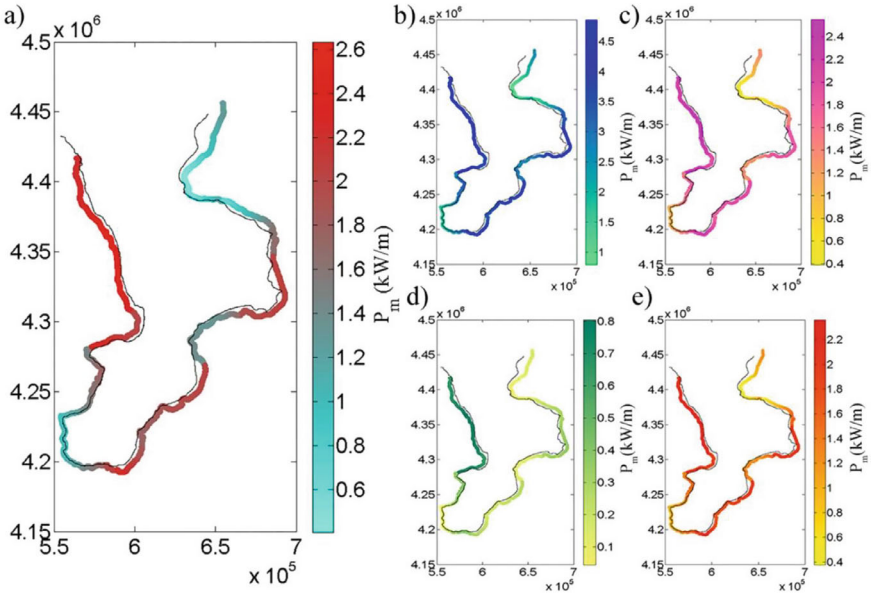

Fig. 1.18 Spatial distribution of mean wave power (Pm) at 100 m depth along the Calabrian coastline, showing interpolated values across multiple time scales: **a** annual average, **b** winter season, **c** spring season, **d** summer season, and **e** autumn season [75]

density emphasizes the importance of precise site selection and device configuration to maximize energy extraction. Studies of the Mediterranean coastlines have also highlighted specific hotspots for wave energy potential, though generally lower compared to oceanic coastlines. In Sardinia, Italy, detailed assessments have shown wave power levels between 8–20 kW/m, with significant contributions during winter. While the Mediterranean exhibits lower wave heights compared to the Atlantic or Pacific coastlines, the region benefits from reduced variability, offering opportunities for consistent, albeit lower, energy generation. In Greece, recent research has shown that the Aegean Sea, particularly near Crete, has an average wave power of 10–15 kW/m, making it a potential candidate for small-scale wave energy converters suited to localized energy needs. The relatively calm conditions of the Mediterranean make it suitable for early-stage technologies and pilot projects aimed at testing and refining wave energy devices.

In more complex wave climates like the Indian Ocean, wave models have been used to understand how monsoons and swells contribute to the resource. A study by Remya et al. [63] performed wave hindcasts in the North Indian Ocean using the MIKE 21 model, validating results against buoy and satellite data. The model generally reproduced the wave climate well, but interestingly, it showed some regional discrepancies: for the Arabian Sea, the model tended to underpredict wave heights during monsoon season. The researchers traced this to the model's wind forcing

and possibly unresolved physics unique to the monsoon, e.g., sudden storm development. They also pointed out the importance of swell arriving from the Southern Indian Ocean—waves. In a related effort, Nayak et al. [76] coupled SWAN with WAM to study how distant swells interact with local wind seas in the Bay of Bengal. This nested model approach captured complex wave spectra, often multi-peaked due to mixed swell and wind waves and helped improve accuracy in estimating wave power along the eastern coast of India. Another study integrated WAVEWATCH III with SWAN for high-resolution forecasting near Puducherry, India—a demonstration of using a coarse global model to drive a fine-scale local model for precise wave energy estimates near the shore. These Indian Ocean case studies show that models can be successfully applied even in challenging wave climates, but they also highlight that model performance can vary. For instance, WAM was found to overestimate smaller waves and underestimate very large waves in the Indian ocean with biases around 0.5–1 m in H_s during extreme events. Recognizing such biases is important for resource assessment so that energy estimates are not overly optimistic or pessimistic, and it guides further model refinement (Fig. 1.19).

The southern coast of Australia and the Tasman Sea is another high-energy region that has been studied via models. Researchers have used SWAN and WAVEWATCH III to map wave energy around Australia's coasts, finding excellent agreement with buoy networks deployed there [77]. One case study along Australia's southwest coast, a region with ~ 40–50 kW/m mean wave power, used a nested SWAN model to simulate nearshore wave conditions over 10 years. The resulting wave power estimates helped identify optimal sites for wave energy converters, and model validation showed errors of less than 5% in mean wave power compared to measurements, e.g., at a buoy off Perth. Additionally, in Pacific Island settings with fringing reefs and complex bathymetry, models like SWAN have been coupled with high-resolution bathymetric data to estimate how much wave energy reaches island coastlines. These cases required inclusion of wave breaking on reefs and island shadowing effects. Once those were incorporated, model estimates of wave energy matched well with

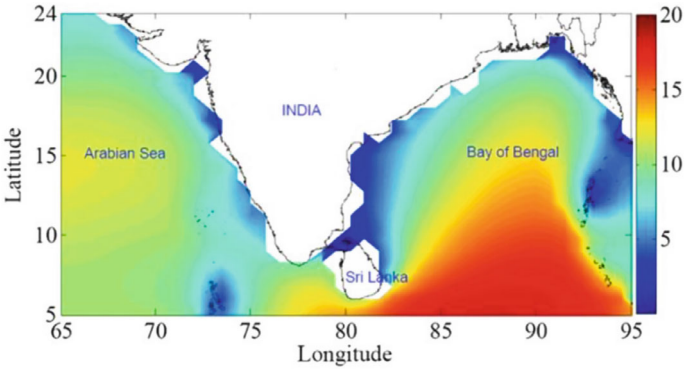

Fig. 1.19 Distribution of annual mean wave power in kW/m in Arabian Sea and Bay of Bengal [76]

the limited data available, demonstrating the model's adaptability to various environments. In New Zealand, the western coast has been highlighted for its wave energy potential, with studies between 2019 and 2023 identifying mean wave power levels of 25–45 kW/m. Sites such as Taranaki have exhibited significant seasonal fluctuations, with winter peaks reaching up to 60 kW/m. These studies also underscore the importance of offshore bathymetry, as energy losses due to wave shoaling were reduced by maintaining energy converters at depths greater than 60 m. Additionally, the Cook Strait—which lies between the North and South Islands—has been identified as an ideal location for wave energy development due to its consistent tidal currents and wave action, providing opportunities for hybrid tidal and wave energy systems. The integration of tidal and wave energy presents unique opportunities for hybrid renewable energy solutions that maximize resource utilization [78] (Fig. 1.20).

The Chilean coast presents some of the highest wave energy potentials globally, with detailed measurements indicating power levels of 40–60 kW/m in the southern regions. Site-specific studies reveal significant wave heights averaging 3.2 m annually, with peak periods between 12–15 s occurring 55% of the time. Deep-water measurements (>100 m depth) show energy densities 30% higher than those at 50 m depth contours. Studies along the Oregon coast document annual average power levels of 25–35 kW/m, with winter peaks reaching 45–55 kW/m. Wave height distributions indicate significant wave heights

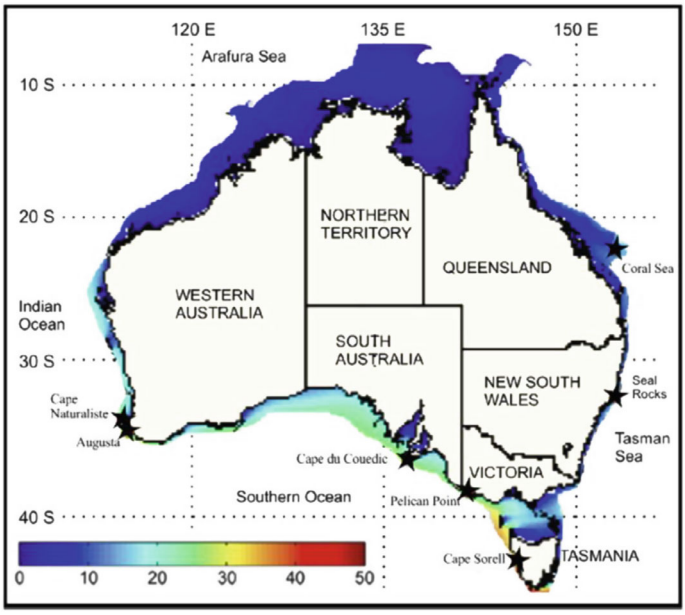

Fig. 1.20 Maps of average wave energy flux (kW/m) for Australia [78]

exceeding 2 m for 70% of the year, with dominant peak periods between 8–12 s accounting for 80% of the annual energy flux. These findings emphasize the potential for substantial energy production in regions characterized by consistent and powerful wave climates, as well as the importance of depth considerations when planning device installations. The Atlantic coast of Canada has also seen increasing interest, with studies off the coast of Nova Scotia and Newfoundland identifying substantial energy potential. Between 2019 and 2022, measurements indicated average annual wave power levels ranging from 20–40 kW/m. The Bay of Fundy, known for its extreme tidal range, has also been studied for its combined wave and tidal potential, offering a unique opportunity for hybrid renewable energy installations.

In South Africa, the west coast near Cape Town has demonstrated considerable wave energy potential, with studies revealing average wave power levels of 30–50 kW/m. Measurements conducted by van Niekerk et al. (2020) indicate significant wave heights ranging from 2–4 m, with frequent storm events pushing wave heights up to 10 m. The consistent westerly winds and vast ocean fetch contribute to this high energy potential. Seasonal analysis indicates that most of the energy flux occurs during winter months, when storm-driven wave action provides opportunities for high power generation. These studies also highlight the challenges posed by extreme wave conditions, necessitating the use of robust and resilient technology capable of withstanding harsh marine environments while maintaining efficient energy capture.

Modern assessment methodologies have achieved remarkable accuracy through multi-instrument approaches. Satellite altimetry data shows correlation coefficients of 0.92 with buoy measurements for significant wave heights, while ADCP measurements demonstrate 95% accuracy in wave period determination. Implementations of the SWAN model show root mean square errors of less than 0.4 m for significant wave heights and 1.2 s for peak periods when compared to buoy data. Machine learning approaches have achieved prediction accuracies of 88–93% for 24-h forecasts of wave power levels. These advancements in assessment technologies are instrumental in reducing uncertainty in wave energy predictions, thereby enhancing the feasibility and planning of wave energy projects. Economic analyses from these studies reveal critical cost factors. Grid connection costs average €1.5–2.5 million per kilometer for offshore cables, while maintenance access requirements indicate optimal wave height limitations of 1.5 m for 80% accessibility. Environmental monitoring data shows seasonal marine mammal activity patterns that require operational adjustments for 15–20% of annual operating hours.

These case studies illustrate the diverse potential for wave energy globally and the importance of site-specific analyses to optimize energy extraction. They underscore the value of integrating multiple data sources—including satellite, buoy, and numerical models—to improve the accuracy of wave energy assessments. The continued development of sophisticated assessment tools and hybrid renewable energy solutions is crucial for unlocking the full potential of wave energy, ultimately contributing to the global pursuit of sustainable and renewable energy sources. Furthermore, the adoption of adaptive management strategies that consider environmental, economic, and technological factors will be essential in ensuring the long-term viability and

scalability of wave energy projects. As the wave energy sector continues to grow, collaboration between governments, research institutions, and private companies will be key to overcoming challenges and accelerating the deployment of wave energy technologies across the world.

The field of wave energy assessment is evolving rapidly, and several advancements are on the horizon that promise to enhance the accuracy and utility of wave generation models. Incorporating real-world observations into wave models, i.e., data assimilation, can greatly improve their accuracy. Presently, global forecasting centers already assimilate wave data—for instance, EMCWF's wave model assimilates satellite altimeter measurements of wave height, and in the latest system this is done in hourly sequential windows rather than 6-hourly, meaning the model's wave field is continuously nudged with observations to keep it on track. This approach, also used in ERA5 reanalysis, has yielded more accurate short-range wave forecasts. In the context of wave energy, future models may use data assimilation not just for forecasting but for hindcasting and resource mapping, blending long-term model runs with buoy and satellite records to reduce bias. The European Space Agency's climate change initiative has produced a 27-year global wave dataset by merging multi-mission altimeter data. Such datasets can serve as both validation and assimilation sources. It can be envisioned as hybrid modeling where a spectral model's output is periodically corrected by observations, leading to a more accurate assessment of wave energy statistics, especially in regions with sparse historical wind data. Additionally, data assimilation of wind fields, e.g., using scatterometer wind observations, can indirectly improve wave model performance, since wind errors are a major error source for waves. Going forward, increased deployment of wave measuring instruments will provide a richer data stream.

As computing power grows, it is becoming feasible to run wave models at unprecedented resolutions and in fully coupled modes. Higher spatial resolution, on the order of 1–5 km globally, and tens of meters nearshore will allow models to capture islands, coastlines, and bathymetric features that currently require parameterizations. For example, ECMWF plans to upgrade its operational wave model grid to ~ 9 km to match the atmospheric model grid, improving coastal wave detail and air-sea coupling. In research settings, extremely high-resolution hindcasts are already underway. A U.S. project recently completed a 32-year hindcast for U.S. coastal waters with ~ 200 m resolution near the coast, using SWAN with over 4 million grid points. The use of unstructured grids and nested grids is making multi-scale modeling more seamless.

Another future direction is better coupling between wave models and other environmental models. Waves do not exist in isolation—they interact with winds, currents, and even influence atmospheric processes through wave-dependent momentum transfer. Fully coupled ocean-atmosphere-wave models can capture feedback, e.g., how waves affect wind stress, or how currents can modulate wave energy). Ensemble modeling (running multiple simulations with slight variations) can quantify uncertainty in wave energy estimates. With more computing power, one could run an ensemble of wave hindcasts using different wind datasets or slightly perturbed physics, to create a probabilistic wave energy resource assessment rather than a single

deterministic estimate. On the more theoretical side, continued improvement of the wave model physics will also benefit wave energy assessment. Research is ongoing to better model extreme waves (rogue wave probabilities, wave breaking limits) which affect the estimation of survivability conditions for wave devices. For energy extraction, models might include the effect of wave farms (arrays of WECs) on the wave field—essentially coupling wave models with energy absorber models to see how much energy is removed and how waves in the lee are reduced. Some wave models have added modules to simulate wave-structure interactions on a bulk level (e.g., SWAN has had experiments in including wave energy device effects as enhanced dissipation).

The rise of artificial intelligence offers new opportunities to complement physics-based wave models. Machine learning algorithms are already being explored for wave forecasting and resource assessment. For example, researchers have developed machine learning models (like neural networks, random forests, etc.) to predict wave characteristics from historical data, or to emulate the behavior of a full wave model much faster. Recent reviews highlight that hybrid approaches, where machine learning algorithms are integrated with numerical wave models, can improve wave energy predictions [79]. One use case is using machine learning to downscale model output: a coarse model might provide general wave conditions, and a trained machine learning model could instantly predict localized wave power at a specific site, having learned from past high-resolution simulations or measurements. Another area is using artificial intelligence to optimize model parameters—for instance, tuning the source term coefficients in WW3 or SWAN using genetic algorithms or neural networks for best match with observed data (some work has been done using machine learning to adjust white capping or wave breaking parameters on the fly to reduce errors). Moreover, artificial intelligence can assist in long-term statistical analysis: instead of running a wave model for 30 years, one could potentially train a machine learning model on a subset and then predict wave energy statistics for the rest, saving computation.

References

1. Izadparast, A.H., Niedzwecki, J.M.: Estimating the potential of ocean wave power resources. Ocean Eng. **38**(1), 177–185 (2011). https://doi.org/10.1016/j.oceaneng.2010.10.010
2. Reguero, B.G., Losada, I.J., Méndez, F.J.: A global wave power resource and its seasonal, interannual and long-term variability. Appl. Energy **148**, 366–380 (2015). https://doi.org/10.1016/J.APENERGY.2015.03.114
3. Gunn, K., Stock-Williams, C.: Quantifying the global wave power resource. Renew. Energy **44**, 296–304 (2012). https://doi.org/10.1016/j.renene.2012.01.101
4. 2024—IPCC. https://www.ipcc.ch/2024/. Accessed 23 Feb 2025
5. Clemente, D., Teixeira-Duarte, F., Rosa-Santos, P., Taveira-Pinto, F.: Advancements on optimization algorithms applied to wave energy assessment: an overview on wave climate and energy resource. Energies **16**(12), 4660 (2023). https://doi.org/10.3390/en16124660
6. Clément, A., et al.: Wave energy in Europe: current status and perspectives. Renew. Sustain. Energy Rev. **6**(5), 405–431 (2002). https://doi.org/10.1016/S1364-0321(02)00009-6

7. Komen, G.J., Cavaleri, L., Donelan, M., Hasselmann, K., Hasselmann, S., Janssen, P.A.E.M.: Dynamics and modelling of ocean waves. https://ui.adsabs.harvard.edu/abs/1996dmow.book.....K (1996). Accessed 23 Feb 2025
8. Pecher, A., Kofoed, J.P. (eds.): Handbook of ocean wave energy. In: Ocean Engineering & Oceanography, vol. 7. Springer International Publishing, Cham (2017). https://doi.org/10.1007/978-3-319-39889-1
9. Olbers, D., Willebrand, J., Eden, C.: Ocean Dynamics. Springer, Berlin, Heidelberg (2012). https://doi.org/10.1007/978-3-642-23450-7
10. Cruz, J. (ed.): Ocean wave energy. In: Green Energy and Technology (Virtual Series). Springer, Berlin, Heidelberg (2008). https://doi.org/10.1007/978-3-540-74895-3
11. Pelinovsky, E., Kharif, C. (eds.): Extreme Ocean Waves. Springer International Publishing, Cham (2016). https://doi.org/10.1007/978-3-319-21575-4
12. Falnes, J., Perlin, M.: Ocean waves and oscillating systems: linear interactions including wave-energy extraction. Appl. Mech. Rev. **56**(1), B3 (2003). https://doi.org/10.1115/1.1523355
13. Administrator: Tides and waves. https://www.whipplelib.hps.cam.ac.uk/special/exhibitions-and-displays/george-darwin/tides-and-waves. Accessed 23 Feb 2025
14. Stokes, G.G. (ed.): On the theory of oscillatory waves. In: Mathematical and Physical Papers in Cambridge Library Collection—Mathematics, vol. 1, pp. 197–229. Cambridge University Press, Cambridge (2009). https://doi.org/10.1017/CBO9780511702242.013
15. Astariz, S., Iglesias, G.: Wave energy vs. other energy sources: a reassessment of the economics. Int. J. Green Energy **13**(7), 747–755 (2016). https://doi.org/10.1080/15435075.2014.963587
16. Kilcher, L., Fogarty, M., Lawson, M.: Marine energy in the United States: An Overview of Opportunities. National Renewable Energy Lab. (NREL), Golden, CO, USA, NREL/TP-5700-78773 (2021). https://doi.org/10.2172/1766861
17. Martinez, A., Iglesias, G.: Wave exploitability index and wave resource classification. Renew. Sustain. Energy Rev. **134**, 110393 (2020). https://doi.org/10.1016/j.rser.2020.110393
18. Guillou, N., Lavidas, G., Chapalain, G.: Wave energy resource assessment for exploitation—a review. J. Mar. Sci. Eng. **8**(9), 705 (2020). https://doi.org/10.3390/jmse8090705
19. Sathyanarayana, A.H., Seelam, J.K.: Wave energy potential along the Indian coast: a comprehensive review. Ocean Eng. **316**, 120033 (2025). https://doi.org/10.1016/j.oceaneng.2024.120033
20. Mwasilu, F., Jung, J.-W.: Potential for power generation from ocean wave renewable energy source: a comprehensive review on state-of-the-art technology and future prospects. IET Renew. Power Gener. **13**(3), 363–375 (2019). https://doi.org/10.1049/iet-rpg.2018.5456
21. Simbolon, R., Sihotang, W., Sihotang, J.: Tapping ocean potential: strategies for integrating tidal and wave energy into national power grids. GEMOY Green Energy Manag. Optim. Yields **1**(1), 49–65 (2024)
22. Ahn, S., Haas, K.A., Neary, V.S.: Wave energy resource characterization and assessment for coastal waters of the United States. Appl. Energy **267**, 114922 (2020). https://doi.org/10.1016/j.apenergy.2020.114922
23. Galano, R.M.C., De Leon, M.P.: Preliminary assessment of potential ocean wave energy resources in the coastal areas of the Philippines. J. Coast. Res. **113**(SI), 665–669 (2025). https://doi.org/10.2112/JCR-SI113-131.1
24. Rusu, L., Onea, F.: Assessment of the performances of various wave energy converters along the European continental coasts. Energy **82**, 889–904 (2015). https://doi.org/10.1016/j.energy.2015.01.099
25. Lenee-Bluhm, P., Paasch, R., Özkan-Haller, H.T.: Characterizing the wave energy resource of the US Pacific Northwest. Renew. Energy **36**(8), 2106–2119 (2011). https://doi.org/10.1016/j.renene.2011.01.016
26. García-Medina, G., Özkan-Haller, H.T., Ruggiero, P.: Wave resource assessment in Oregon and southwest Washington, USA. Renew. Energy **64**, 203–214 (2014). https://doi.org/10.1016/j.renene.2013.11.014
27. Hemer, M.A., et al.: A revised assessment of Australia's national wave energy resource. Renew. Energy **114**, 85–107 (2017). https://doi.org/10.1016/j.renene.2016.08.039

28. Gorman, R.M.: The treatment of discontinuities in computing the nonlinear energy transfer for finite-depth gravity wave spectra. J. Atmospheric Ocean. Technol. **20**(1), 206–216 (2003). https://doi.org/10.1175/1520-0426(2003)020%3c0206:TTODIC%3e2.0.CO;2
29. Özger, M., Altunkaynak, A., Şen, Z.: Stochastic wave energy calculation formulation. Renew. Energy **29**(10), 1747–1756 (2004). https://doi.org/10.1016/j.renene.2004.01.009
30. Özger, M., Altunkaynak, A., Şen, Z.: Statistical investigation of expected wave energy and its reliability. Energy Convers. Manag. **45**(13), 2173–2185 (2004). https://doi.org/10.1016/j.enconman.2003.10.015
31. Altunkaynak, A., Özger, M.: Spatial significant wave height variation assessment and its estimation. J. Waterw. Port Coast. Ocean Eng. **131**(6), 277–282 (2005). https://doi.org/10.1061/(ASCE)0733-950X(2005)131:6(277)
32. Karunarathna, H., Maduwantha, P., Kamranzad, B., Rathnasooriya, H., de Silva, K.: Evaluation of spatio-temporal variability of ocean wave power resource around Sri Lanka. Energy **200**, 117503 (2020). https://doi.org/10.1016/j.energy.2020.117503
33. Christakos, K., Lavidas, G., Gao, Z., Björkqvist, J.-V.: Long-term assessment of wave conditions and wave energy resource in the Arctic Ocean. Renew. Energy **220**, 119678 (2024). https://doi.org/10.1016/j.renene.2023.119678
34. Park, M.-J., Kim, Y.: Probabilistic estimation of directional wave spectrum using onboard measurement data. J. Mar. Sci. Technol. **29**(1), 200–220 (2024). https://doi.org/10.1007/s00773-023-00984-z
35. Zheng, Z., Dong, G., Dong, H., Ma, X., Tang, M.: Research on the methods for separating wind sea and swell from directional wave spectra in finite-depth waters. Ocean Dyn. **74**(2), 113–131 (2024). https://doi.org/10.1007/s10236-023-01592-6
36. Penalba, M., Ulazia, A., Saénz, J., Ringwood, J.V.: Impact of long-term resource variations on wave energy farms: the Icelandic case. Energy **192**, 116609 (2020). https://doi.org/10.1016/j.energy.2019.116609
37. Huang, W., Dong, S.: Joint distribution of significant wave height and zero-up-crossing wave period using mixture copula method. Ocean Eng. **219**, 108305 (2021). https://doi.org/10.1016/j.oceaneng.2020.108305
38. Huang, W., Dong, S.: Statistical properties of group height and group length in combined sea states. Coast. Eng. **166**, 103897 (2021). https://doi.org/10.1016/j.coastaleng.2021.103897
39. Lee, U.-J., Cho, H.-Y., Lee, B.W., Ko, D.-H.: Joint probability distribution of significant wave height and peak wave period using Gaussian copula method. J. Coast. Res. **116**(SI), 96–100 (2024). https://doi.org/10.2112/JCR-SI116-020.1
40. Qin, J.: Evolving probabilistic modeling for long-term significant wave heights with a focus on extremes. Renew. Energy **187**, 362–370 (2022). https://doi.org/10.1016/j.renene.2022.01.069
41. Pires Vieira Serta, C., Haver, S., Li, L.: Statistical modeling and applications of joint distributions for significant wave height, spectral peak period, and peak direction of propagation: a case study in the Norwegian Sea. J. Mar. Sci. Eng. **11**(12), 2372 (2023). https://doi.org/10.3390/jmse11122372
42. Mo, J., Wang, X., Huang, S., Wang, R.: Advance in significant wave height prediction: a comprehensive survey. Complex Syst. Model. Simul. **4**(4), 402–439 (2024). https://doi.org/10.23919/CSMS.2024.0019
43. Muraleedharan, G., Lucas, C., Soares, C.G.: Spectral wave energy period and peak period statistics concomitant with maximum significant wave heights. Coast. Eng. **183**, 104260 (2023). https://doi.org/10.1016/j.coastaleng.2022.104260
44. Miles, J.W.: On the generation of surface waves by shear flows. J. Fluid Mech. **3**(2), 185–204 (1957). https://doi.org/10.1017/S0022112057000567
45. Phillips, O.M.: On the generation of waves by turbulent wind. J. Fluid Mech. **2**(5), 417–445 (1957). https://doi.org/10.1017/S0022112057000233
46. Amarouche, K., Akpınar, A., Rybalko, A., Myslenkov, S.: Assessment of SWAN and WAVEWATCH-III models regarding the directional wave spectra estimates based on Eastern Black Sea measurements. Ocean Eng. **272**, 113944 (2023). https://doi.org/10.1016/j.oceaneng.2023.113944

47. Abu Zed, A.A., Kansoh, R.M., Iskander, M.M., Elkholy, M.: Wind and wave climate south-eastern of the Mediterranean Sea based on a high-resolution SWAN model. Dyn. Atmospheres Oceans **99**, 101311 (2022). https://doi.org/10.1016/j.dynatmoce.2022.101311
48. Wang, L., Li, Y., Zhang, L., Zhang, F., Zheng, C., Luo, C.: Analysis and research on energy transfer from wind to waves based on the SWAN model. In: 2024 International Conference on New Power System and Power Electronics (NPSPE), pp. 235–238 (2024). https://doi.org/10.1109/NPSPE62515.2024.00046
49. Iglesias, G., Carballo, R.: Wave energy and nearshore *hot spots*: the case of the SE Bay of Biscay. Renew. Energy **35**(11), 2490–2500 (2010). https://doi.org/10.1016/j.renene.2010.03.016
50. Rusu, L., Guedes Soares, C.: Wave energy assessments in the Azores islands. Renew. Energy **45**, 183–196 (2012). https://doi.org/10.1016/j.renene.2012.02.027
51. Mel, R.A., Lo Feudo, T., Miceli, M., Sinopoli, S., Maiolo, M.: A coupled wave-hydrodynamical model to assess the effect of Mediterranean storms under climate change: the Calabaia case study. Dyn. Atmospheres Oceans **102**, 101368 (2023). https://doi.org/10.1016/j.dynatmoce.2023.101368
52. Moeini, M.H., Etemad-Shahidi, A.: Application of two numerical models for wave hindcasting in Lake Erie. Appl. Ocean Res. **29**(3), 137–145 (2007). https://doi.org/10.1016/j.apor.2007.10.001
53. Pallares, E., Sánchez-Arcilla, A., Espino, M.: Wave energy balance in wave models (SWAN) for semi-enclosed domains–application to the Catalan coast. Cont. Shelf Res. **87**, 41–53 (2014). https://doi.org/10.1016/j.csr.2014.03.008
54. Rogers, W.E., Hwang, P.A., Wang, D.W.: Investigation of wave growth and decay in the SWAN model: three regional-scale applications. J. Phys. Oceanogr. **33**(2), 366–389 (2003). https://doi.org/10.1175/1520-0485(2003)033%3c0366:IOWGAD%3e2.0.CO;2
55. Salmon, J.E., Holthuijsen, L.H., Zijlema, M., van Vledder, G.P., Pietrzak, J.D.: Scaling depth-induced wave-breaking in two-dimensional spectral wave models. Ocean Model **87**, 30–47 (2015). https://doi.org/10.1016/j.ocemod.2014.12.011
56. Zijlema, M.: Computation of wind-wave spectra in coastal waters with SWAN on unstructured grids. Coast. Eng. **57**(3), 267–277 (2010). https://doi.org/10.1016/j.coastaleng.2009.10.011
57. Shadmani, A., Reza Nikoo, M., Etri, T., Gandomi, A.H.: A multi-objective approach for location and layout optimization of wave energy converters. Appl. Energy **347**, 121397 (2023). https://doi.org/10.1016/j.apenergy.2023.121397
58. Allard, R., Rogers, E., Carroll, S.: User's Manual for the Simulating Waves Nearshore Model (SWAN), p. 171 (2002)
59. Lavidas, G., Venugopal, V.: Application of numerical wave models at European coastlines: a review. Renew. Sustain. Energy Rev. **92**, 489–500 (2018). https://doi.org/10.1016/j.rser.2018.04.112
60. Jiang, Y., et al.: Modeling waves over the Changjiang River Estuary using a high-resolution unstructured SWAN model. Ocean Model **173**, 102007 (2022). https://doi.org/10.1016/j.ocemod.2022.102007
61. Janssen, P.A.E.M.: Quasi-linear theory of wind-wave generation applied to wave forecasting. J. Phys. Oceanogr. **21**(11), 1631–1642 (1991). https://doi.org/10.1175/1520-0485(1991)021%3c1631:QLTOWW%3e2.0.CO;2
62. Battjes, J.A., Janssen, J.P.F.M.: Energy Loss and Set-Up Due to Breaking of Random Waves, pp. 569–587 (2015). https://doi.org/10.1061/9780872621909.034
63. Remya, P.G., Kumar, R., Basu, S., Sarkar, A.: Wave hindcast experiments in the Indian Ocean using MIKE 21 SW model. J. Earth Syst. Sci. **121**(2), 385–392 (2012). https://doi.org/10.1007/s12040-012-0169-7
64. Sartini, L., Antonini, A.: On the spectral wave climate of the French Atlantic Ocean. Ocean Eng. **304**, 117900 (2024). https://doi.org/10.1016/j.oceaneng.2024.117900
65. Fonseca, R.B., Gonçalves, M., Soares, C.G.: Comparing the performance of spectral wave models for coastal areas. J. Coast. Res. **33**(2), 331–346 (2017). https://doi.org/10.2112/JCOASTRES-D-15-00200.1

66. Cornett, A.M.: A global wave energy resource assessment. In: The Eighteenth International Offshore and Polar Engineering Conference, OnePetro (2008)
67. Atan, R., Goggins, J., Nash, S.: A detailed assessment of the wave energy resource at the Atlantic marine energy test site. Energies **9**(11), 967 (2016). https://doi.org/10.3390/en9110967
68. Reguero, B.G., Losada, I.J., Méndez, F.J.: A recent increase in global wave power as a consequence of oceanic warming. Nat. Commun. **10**(1), 205 (2019). https://doi.org/10.1038/s41467-018-08066-0
69. Folley, M., Whittaker, T.J.T.: Analysis of the nearshore wave energy resource. Renew. Energy **34**(7), 1709–1715 (2009). https://doi.org/10.1016/j.renene.2009.01.003
70. Robertson, B.R.D., Hiles, C.E., Buckham, B.J.: Characterizing the near shore wave energy resource on the west coast of Vancouver Island, Canada. Renew. Energy **71**, 665–678 (2014). https://doi.org/10.1016/j.renene.2014.06.006
71. Robertson, B., Dunkle, G., Gadasi, J., Garcia-Medina, G., Yang, Z.: Holistic marine energy resource assessments: a wave and offshore wind perspective of metocean conditions. Renew. Energy **170**, 286–301 (2021). https://doi.org/10.1016/j.renene.2021.01.136
72. Guillou, N., Lavidas, G., Kamranzad, B.: Wave energy in Brittany (France)—resource assessment and WEC performances. Sustainability **15**(2), 1725 (2023). https://doi.org/10.3390/su15021725
73. Ramos, V., Ringwood, J.V.: Exploring the utility and effectiveness of the IEC (International Electrotechnical Commission) wave energy resource assessment and characterisation standard: a case study. Energy **107**, 668–682 (2016). https://doi.org/10.1016/j.energy.2016.04.053
74. Rusu, L., Rusu, E.: Evaluation of the worldwide wave energy distribution based on ERA5 data and altimeter measurements. Energies **14**(2), 394 (2021). https://doi.org/10.3390/en14020394
75. Algieri-Ferraro, D., Aristodemo, F., Veltri, P.: Wave energy resources along Calabrian coasts (ITALY). Coast. Eng. Proc. **35**, 5 (2017). https://doi.org/10.9753/icce.v35.waves.5
76. Nayak, S., Bhaskaran, P.K., Venkatesan, R., Dasgupta, S.: Modulation of local wind-waves at Kalpakkam from remote forcing effects of Southern Ocean swells. Ocean Eng. **64**, 23–35 (2013). https://doi.org/10.1016/j.oceaneng.2013.02.010
77. Liu, J., et al.: A high-resolution wave energy assessment of south-east Australia based on a 40-year hindcast. Renew. Energy **215**, 118943 (2023). https://doi.org/10.1016/j.renene.2023.118943
78. Morim, J., Cartwright, N., Etemad-Shahidi, A., Strauss, D., Hemer, M.: A review of wave energy estimates for nearshore shelf waters off Australia. Int. J. Mar. Energy **7**, 57–70 (2014). https://doi.org/10.1016/j.ijome.2014.09.002
79. Shadmani, A., Nikoo, M.R., Gandomi, A.H., Wang, R.-Q., Golparvar, B.: A review of machine learning and deep learning applications in wave energy forecasting and WEC optimization. Energy Strategy Rev. **49**, 101180 (2023). https://doi.org/10.1016/j.esr.2023.101180

Chapter 2
Boundary Element Methods

Abstract Boundary element methods (BEM) represent a powerful computational approach for modeling wave-structure interactions essential to wave energy converter design and analysis. This chapter presents a rigorous examination of BEM techniques, their mathematical foundations, and their specific applications in wave energy systems. By focusing computation exclusively on boundary surfaces rather than entire fluid domains, BEM offers significant computational efficiency advantages for solving linear and weakly nonlinear hydrodynamic problems, making it particularly valuable in the iterative design optimization processes required for effective wave energy harvesting systems. The chapter is structured to provide comprehensive coverage across five interconnected sections. The introduction to boundary element methods establishes the fundamental mathematical principles underlying BEM, explaining the Green's function formulation, boundary integral equations, and the method's strengths in handling infinite and semi-infinite domains without discretization of the entire fluid region. The second section explores BEM specifically in wave-structure interactions, detailing the linear potential flow theory, radiation-diffraction problems, and the calculation of hydrodynamic coefficients critical for modeling how wave energy converters respond to incident waves. Numerical implementation of BEM forms the technical core of the chapter, covering mesh generation techniques, singularity treatment approaches, solution methods for resulting linear systems, and acceleration techniques that enhance computational efficiency. The application section demonstrates how BEM serves as the foundation for frequency-domain and time-domain models of various wave energy converter types, examining its role in device performance prediction, optimization processes, and array layout design. The final section addresses current challenges in BEM applications, including limitations in modeling extreme waves and strongly nonlinear effects, while exploring emerging hybrid methods, high-order formulations, and coupling techniques with other numerical approaches that promise to extend BEM capabilities for next-generation wave energy converter designs.

Keywords Boundary integral equations · Radiation-diffraction problem · Hydrodynamic coefficients · Frequency-domain analysis · Green's function methods

A. Shadmani et al., *Ocean Wave Energy Technology*,
https://doi.org/10.1007/978-3-031-95040-7_2

2.1 Introduction to Boundary Element Methods

After five decades of development, the boundary element method (BEM) has found a firm footing in the arena of numerical methods for partial differential equations (PDEs) [1]. Comparing to the more popular numerical methods, such as the finite difference method (FDM) and finite element method (FEM), which can be classified as the domain methods, the BEM distinguish itself as a boundary method, meaning that the numerical discretization is conducted at reduced spatial dimensions. For example, for problems in three spatial dimensions, the discretization is performed on the bounding surface only; and in two spatial dimensions, the discretization is on the boundary contour only. This reduced dimension leads to smaller linear systems, less computer memory requirements, and more efficient computation. This effect is most pronounced when the domain is unbounded. Unbounded domain needs to be truncated and approximated in domain methods [2]. The BEM, on the other hand, automatically models the behavior at infinity without the need of deploying a mesh to approximate it. In the modern-day industrial settings, mesh preparation is the most labor intensive and the costliest portion in numerical modeling, particularly for the FEM [3]. Without the need of dealing with the interior mesh, the BEM is more cost effective in mesh preparation. For problems involving moving boundaries, the adjustment of the mesh is much easier with the BEM; hence, it is again the preferred tool. With these advantages, the BEM is indeed an essential part in the repertoire of the modern-day computational tools [4].

In order to gain an objective assessment of the success of the BEM, as compared to other numerical methods, a search is conducted using the Web of Science. Based on the keyword search, the total number of journal publications found in the Science Citation Index Expanded was compiled for several numerical methods. The result clearly indicates that the FEM is the most popular with more than 66,000 entries. The FDM is a distant second with more than 19,000 entries, less than one third of the FEM. The BEM ranks third with more than 10,000 entries, more than half of the FDM. All other methods, such as the finite volume method (FVM) and the collocation method, trail far behind. Based on this bibliographic search, we can conclude that the popularity and versatility of BEM falls behind the two major methods, FEM and FDM. However, BEM's leading role as a specialized and alternative method to these two, as compared to all other numerical methods for partial differential equations, is unchallenged.

Figure 2.1 illustrates the annual number of journal publications related to the Boundary Element Method (BEM) from 2004 to 2024, based on data collected from Springer. The trend shows a steady increase in publications over the two-decade span, starting at 358 publications in 2004 and reaching a peak of 931 in 2023. Despite periodic fluctuations, including a slight decline around 2009 and 2016, the overall trajectory indicates growing academic interest in BEM. Notably, there is a significant drop in 2024, with publications falling to 600, which may reflect either an incomplete dataset for the current year or a shift in research focus. The area plot

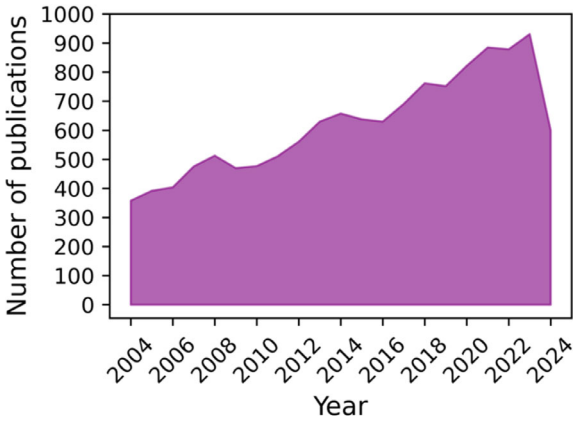

Fig. 2.1 Number of journal articles published by the year about BEM, based on the Springer search engine

effectively highlights the cumulative growth and variations in publication activity over time.

As the BEM is almost mature, it is of interest to visit its history. Although there exist certain efforts toward the writing of the history of the FEM and the FDM, relatively little has been done for the BEM [5]. The present article is aimed at taking a first step toward the construction of a history for the BEM.

Before reviewing its modern development, we shall first explore the rich heritage of the BEM, particularly its mathematical foundation from the eighteenth century to the early twenty-first century. The historical development of the potential theory, Green's function, and integral equations are reviewed [2, 3].

Numerical methods cannot truly prosper until the invention and then the wide availability of the electronic computers in the early 1960s. It is of little surprise that both the FEM and the BEM started around that time. For the BEM, multiple efforts started around 1962. The turning point that launched a series of connected efforts, which soon developed into a movement, can be traced to 1967. In the 1970s, the BEM was still a novice numerical technique but saw an exponential growth. By the end of it, textbooks were written, and conferences were organized on BEM. This article reviews the early development up to the late 1970s, leaving the latter development to future writers [6].

Before starting, we should clarify the use of the term 'boundary element method' in this book. In the narrowest view, one can argue that BEM refers to the numerical technique based on the method of weighted residuals, mirroring the finite element formulation, except that the weighting function used is the fundamental solution of governing equation to eliminate the need of domain discretization [7]. One can view BEM as the numerical implementation of boundary integral equations based on Green's formula, in which the piecewise element concept of the FEM is utilized for the discretization [8]. Even more broadly, BEM has been used as a generic term for a variety of numerical methods that use a boundary or boundary-like discretization. These can include the general numerical implementation of boundary integral equations known as the boundary integral equation method (BIEM) [9], whether

elements are used in the discretization or not; or the method known as the indirect method that distributes singular solutions on the solution boundary; or the method of fundamental solutions in which the fundamental solutions are distributed outside the domain in discrete or continuous fashion with or without integral equation formulation; or even the Trefftz method which distribute non-singular solutions [10]. These generic adoptions of the term are evident in the many articles and many contributions in the BEM solvers. In fact, the theoretical developments of these methods are often intertwined. Hence, for the purpose of the current historical review, we take the broader view and consider into this category all numerical methods for partial differential equations in which a reduction in mesh dimension from a domain-type to a boundary-type is accomplished. More properly, these methods can be referred to as "boundary methods" or "mesh reduction methods." But we shall yield to the popular adoption of the term "boundary element method" for its wide recognition. It will be used interchangeably with the above terms.

To guarantee the boundary-only discretization feature in the BEM, the proper fundamental solutions or Green's functions, which satisfy the considered differential governing equations of the boundary value problems in advance, need to be known [10]. For unbounded or infinite domain problems and thin-body problems, the BEM has the inherent advantage over the domain-discretization methods [11]. Moreover, by introducing the iso-geometric analysis (IGA), the BEM can be easily coupled with the standard CAD techniques due to the boundary-only representation requirement, which has been widely applied to a variety of elliptic problems, such as Laplace equation [12, 13], Helmholtz equation [14, 15], electromagnetics [16, 17], elastodynamics [18, 19], and crack problems [20]. Although the use of the fundamental solutions provides several excellent computational properties, one must pay the price of dealing with the numerical calculation of the singular integrals involving the fundamental solutions in the BEM implementation, which is usually mathematically complex and time-consuming.

More recently, several recent investigations used BEM to solve the problem of wave-structure interactions, specifically wave energy converters (WECs) [21–24]. BEM solves the linearized hydrodynamic wave-structure interaction problem. It uses a boundary integral formulation of the Laplace equation, which is potential flow, modeling the fluid domain boundaries with a mesh of panels. By enforcing boundary conditions, e.g., no flow through the body surface, linearized pressure on the free surface, and appropriate radiation conditions, BEM solvers compute quantities like added mass, radiation damping, and wave excitation forces on the WEC. These quantities describe how the device radiates waves when it oscillates and how incoming waves exert forces on it, i.e., diffraction effects. Using BEM results, one can predict the device's motion response, often given as response amplitude operator (RAOs), and ultimately estimate power absorption when coupled with a power take-off (PTO) model. In the following, the application of BEM in wave-structure interaction, its numerical implementation, and modeling the WECs will be discussed.

2.2 BEM in Wave-Structure Interaction

The interaction between waves and structures is a great concern in ocean engineering, naval architecture, coastal engineering, and other disciplines. The effects of the waves on the structures generally include the contribution of the water inertia, the viscosity, and the free surface variation. For large-scale structures, the influence of the water viscosity is negligible, and the wave force can be solved by the potential flow theory [25]. Under the assumption of the potential flow, the wave diffraction and radiation problems can be solved with the Laplace equation and the related initial and boundary conditions. For the steady state problem under the action of regular waves, a time factor can be separated out, and the problem can be solved in the frequency domain.

The BEM based on the Green's function is widely used to solve the interaction between the wave and the complex ocean engineering structures. A notable aspect of using the free-surface Green's function is that it inherently satisfies the conditions at infinity and the free surface, so the formulation requires only the body surface integral. For the frequency domain problem of the wave interaction with a structure in the horizontally unbounded domain, the integrations on the free surface, the seabed and a vertical cylinder surface at infinity can be removed with the application of the Green's function satisfying the scattering wave boundary conditions at those surfaces. Thus, with the BEM based on the Green's function, only the body surface is required to be discretized to distribute the unknowns on the body surface. In this way, the memory requirement, the computation loads, and the tedious preparation work on meshing are greatly reduced. Therefore, the BEM enjoys many advantages over other domain numerical methods. Initially, Hess and Smith [26] introduced the constant panel method to calculate the water flow around a 3D body. Then the method was widely used in the wave interaction with marine structures, such as Faltinsen [27] and Garrison et al. [28]. In the constant panel method, a 3D body surface is discretized by a set of quadrilateral or triangular plane elements, and the unknown sources are distributed at the center of each panel and the strength of the source is constant in a panel. Finally, a set of simultaneous equations can be obtained with the application of the boundary conditions, and the strength of the sources can thus be determined.

For a body with a curved surface, the discretized surface by a set of plane panels might not be smooth, even not continuous. In order to obtain accurate computation results, a large number of panels must be used to reduce the roughness of the body surface at the expense of the computational efficiency. In addition, the spatial derivative of the velocity potential on the body surface cannot be calculated in one panel, and this will also increase the difficulty in programming and computation.

Since the late 1980s of the twenty-first century, the higher-order BEM (HOBEM) was considered to study the wave interaction with ocean structures [29, 30] and ships [31, 32]. In HOBEM, the body surface is discretized into a set of curved quadrilateral or triangular elements. Thus, the body geometry and physical quantities, such as the velocity potential, on the body surface are expressed as functions of its nodal values by using the same shape functions. In this way, a curved body surface can be reconstructed with a small number of high order elements with high accuracy, and

the same accurate potential result can be obtained with a small number of high order elements as that with many constant panels. To balance the computational accuracy and the difficulty in the meshing preparation, the second order element is generally adopted in programming [33, 34].

For the second order quadrilateral element, it is possible to use the Lagrange interpolation method with eight nodes or the Hermite interpolation method with nine nodes [35]. In the Lagrange interpolation method, the eight nodes are generally arranged at edges and corners of a quadrilateral element, and in the Hermite interpolation method, the other node is arranged at the center of the element generally. In this way, for a body discretized with NE elements, the linear equations generated by nine nodes elements have apparently NE dimensions more than those generated by eight nodes elements with the same number of elements. If the body geometry and the velocity potential do not change abruptly in one element, the Lagrange interpolation method will have the same accuracy as that of the Hermite interpolation method but with a higher efficiency. Therefore, the Lagrange interpolation method has more extensive applications in hydrodynamic analysis.

Because the unknowns of a HOBEM are distributed at nodes, with a continuous variation within the element, it also has the following advantages in the numerical analysis: (1) it is convenient to calculate the hydrodynamic pressure at any position on the body surface by an interpolation of the nodal values in an element and it is easy to combine a HOBEM with a FEM for the structural analysis with different meshes, (2) the velocity potential at the waterline can be obtained directly and the wave run-up at the waterline can be computed accurately, as is required for computing the air-gap height of an offshore platform, (3) the spatial derivative of the velocity potential on the body surface can be computed easily and accurately, as is required in the calculation of the second order velocity potential and the second order force and moment on a structure. The velocity potential and its spatial derivatives at any point in a high order element can be determined by the nodal velocity potentials with shape functions. Thus, the velocity potential is continuous on the whole-body surface. The spatial derivative of the velocity potential is continuous inside the element, but not necessarily across elements. To make the spatial derivative of the velocity potential also consistent on the body surface, the spline functions might be used to fit the surface geometry and the velocity potential on the piecewise smooth body. One method is to use the B-spline functions to describe the coordinates of the body geometry and the velocity potential on the body surface, and to determine the expansion coefficients of the velocity potentials by the BEM. It is called the B-spline based BEM, which has been applied for the analysis for wave structure interaction problems [36, 37]. The spline function is a piecewise defined polynomial function, with a high degree of smoothness at the connection points of polynomial pieces, which are called the knots, or the control points. With the application of higher order spline functions, the higher order spatial derivatives of the velocity potential can also be obtained.

When the spline functions are used in fitting a function, the local change of the function will generate variations of the simulation results in the whole domain. Because of the above characteristics the spline function-based BEM might be used to obtain satisfactory results with fewer pieces, but not very accurate results with the

increase of the piece numbers. In addition, for bodies with an unsmooth surface or with regions where the velocity potential changes abruptly, the body surface should be divided into several smooth patches firstly, and then the spline function is used to simulate the geometric and physical values in each patch. For a complex ocean engineering structure, how to divide the structure surface into patches is not an easy job. Therefore, the application of the spline BEM is not as convenient and flexible as the application of the HOBEM in practice.

With the development of ocean engineering, the scale of the structures becomes larger and larger, and the number of structure components is increasing greatly. To study those problems, the BEM has a fatal weakness as its coefficient matrix is full. $O(N^2)$ operations are required to form the coefficient matrix, $O(N^2)$ computer storage to store it, and $O(N^2)$ operations to solve it, even with an iterative method, where N is the number of unknowns. For a body, if its length scale increases 10 times, its area scale will increase 100 times and the number of computation operations, and the computer storage will increase 10,000 times. This growth rate will result in a large computation burden and storage requirement for computers to solve the problem of wave interaction with a large-scale structure or many bodies. For a large-scale calculation, some fast algorithms with high speed and low storage were proposed, such as: the fast multipole method (FMM) [38], the recorrected fast Fourier transform method (pFFT) [39, 40], and the wavelet transform method [41, 42]. They can be divided into two categories in view of reducing computer storage and speeding up calculation. One is only to store the product of the full matrix and the trial vector with an acceleration calculation method for speeding up the calculation, instead of storing the full matrix, the other is to compress the full matrix with a kind of spectral transform method, and to store a new matrix of finite bandwidth. These methods were applied to the computation of wave interaction with structures and provide a solution to the problem of very large structures or many structures. However, for different problems and calculation models, different integral equations are set up based on different Green functions. Thus, different methods and techniques must be applied in implementing a low storage accelerated method for them.

The BEM method continues to be a vital tool in the analysis of wave-structure interactions, with recent research focusing on enhancing its capabilities and expanding its applications. Over the past decade, significant advancements have been made in improving the method's accuracy, efficiency, and ability to handle complex scenarios in marine and offshore engineering. One area of development has been in the refinement of HOBEM formulations. Teng et al. [43] presented an advanced HOBEM for analyzing wave-current interactions with structures, improving both accuracy and efficiency for complex flow conditions. This work builds on earlier higher-order methods, pushing the boundaries of what can be achieved in terms of computational precision. Similarly, Feng et al. [44, 45] introduced a novel desingularized Morino formulation that enhances the stability and accuracy of BEM for wave radiation and diffraction problems, as depicted in Fig. 2.2, addressing some of the numerical challenges that have long plagued the method.

Bao et al. [47] developed an accelerated BEM using the adaptive cross approximation technique, significantly reducing computational time for large-scale radiation

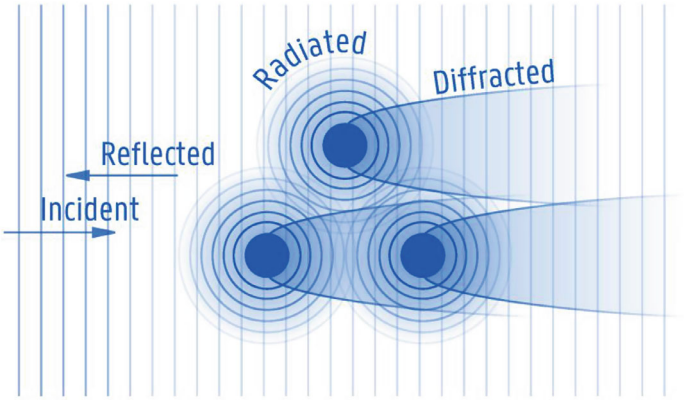

Fig. 2.2 Components of wave interactions [46]

and diffraction problems. Their method showed promise for optimization studies involving multiple design iterations. Additionally, Zheng et al. [48] proposed a FMM-BEM for 3D wave-structure interaction analysis, demonstrating its efficiency in handling problems with many degrees of freedom. Additionally, Zhou et al. [49] developed a second-order time-domain HOBEM to analyze the performance of oscillating water column (OWC) WEC integrated into coastal structures. These recent developments demonstrate the ongoing evolution of BEM in wave-structure interaction problems. From improving fundamental numerical techniques to tackling complex multi-physics scenarios, the method continues to adapt to the changing needs of marine and offshore engineering. As computational power increases and numerical methods refine, BEM is likely to remain a crucial tool in understanding and designing for the complex interactions between waves and structures in the marine environment. To this end, the following sections will explore the numerical implementation of BEM and its application in modeling various WECs.

2.2.1 Fundamentals of BEM

To understand more about the fundamentals of BEM, the foundation of potential flow theory is necessary. Linear potential flow theory has been the cornerstone of wave-structure interaction analysis for decades due to its simplicity and computational efficiency. The theory assumes small-amplitude waves and motions, allowing for linearization of the free surface boundary conditions. In the linear theory, the velocity potential $\phi(x, y, z, t)$ satisfies the Laplace equation in the fluid domain:

$$\nabla^2 \phi = 0 \tag{2.1}$$

Under small assumption of small-amplitude waves, the problem is formulated in the frequency-domain, where the velocity potential is decomposed into its time-harmonic form:

$$\Phi(x, y, z, t) = \Re\left\{\phi(x, y, z)e^{-i\omega t}\right\} \tag{2.2}$$

To fully describe the wave-structure interaction problem, it is important to consider the decomposition of the velocity potential, the hydrodynamic forces acting on the structure, and the role of nonlinear effects in real-world applications. In the presence of a structure, the total velocity potential $\phi(x, y, z)$ can be decomposed into three main components:

$$\phi = \phi_I + \phi_D + \phi_R \tag{2.3}$$

Each component represents a different aspect of the wave interaction:

1. Incident wave potential (ϕ_I)

The incident wave potential represents the undisturbed wave field approaching the structure. For a monochromatic plane wave propagating in the x-direction in deep water, the incident potential is:

$$\phi_I = \frac{ig}{\omega}e^{kz}e^{i(kx-\omega t)} \tag{2.4}$$

This solution satisfies Laplace's equation and the linearized free-surface condition.

2. Diffracted wave potential (ϕ_D)

When waves encountered the structure, they are scattered in different directions. The resulting diffracted wave potential ϕ_D represents the modification of the wave field due to the presence of the body. It satisfies the same boundary conditions as the incident wave, except that it ensures no motion of the structure in the diffraction problem (fixed structure):

$$\frac{\partial \phi_D}{\partial n} = -\frac{\partial \phi_I}{\partial n} \rightarrow on\, S_B(\text{body surface}) \tag{2.5}$$

The diffracted waves radiate outward and must satisfy the radiation condition at infinity, ensuring only ongoing waves exist at large distances.

3. Radiated wave potential (ϕ_R)

If the structure is allowed to oscillate (as in the radiation problem), it generates additional waves, known as radiated waves. The radiated wave potential ϕ_R describes waves emitted due to the body's oscillatory motion in one or more of its six rigid body degrees of freedom (surge, sway, heave, roll, pitch, yaw). If the structure moves with velocity $\mathbf{V}_{\text{body}}$, the radiation potential satisfies:

$$\frac{\partial \phi_R}{\partial n} = \boldsymbol{V}_{body}.\boldsymbol{n} \rightarrow on\, S_B \text{ (body surface)} \tag{2.6}$$

Like the diffracted wave potential, ϕ_R must also satisfy the radiation condition at infinity.

Each of these components plays a fundamental role in determining the hydrodynamic forces acting on the structure. The forces exerted on a structure arise from different hydrodynamic effects. These forces can be classified into four main components:

$$F_{total} = F_{FK} + F_{Diff} + F_{Rad} + F_{HS} \tag{2.7}$$

- Froude-Krylov force (F_{Rad})

The Froude-Krylov force is the force exerted by the unperturbed incident wave field on the structure. It arises from the pressure distribution due to the incident wave potential and is computed using Bernoulli's equation:

$$p = -\rho \frac{\partial \phi}{\partial t} - \frac{1}{2}\rho |\nabla \phi|^2 - \rho g z \tag{2.8}$$

For small waves, the dominant term is the first one, leading to the Froude-Krylov force:

$$F_{FK} = -\int_{S_B} \rho \frac{\partial \phi_I}{\partial t} \boldsymbol{n} dS \tag{2.9}$$

The force depends solely on the incident wave field and does not account for the structure's influence on the waves.

- Diffraction force (F_{Rad})

The diffraction force results from the scattered (diffracted) wave field and arises due to wave reflection and modifications around the structure. It is computed from the diffracted potential ϕ_D:

$$F_{Diff} = -\int_{S_B} \rho \frac{\partial \phi_D}{\partial t} \boldsymbol{n} dS \tag{2.10}$$

This force is particularly important for large structures, where the body significantly disturbs the wave field.

- Radiation force (F_{Rad})

The radiation force accounts for the waves generated by the structure's motion. It can be further divided into added mass and wave damping effects:

$$F_{Rad} = -\int_{S_B} \rho \frac{\partial \phi_R}{\partial t} \boldsymbol{n} dS \tag{2.11}$$

The added mass effect arises because the fluid surrounding the structure accelerates with it, effectively increasing its inertia. The wave damping effect represents the energy radiated away as waves due to the body's motion. These two effects are commonly expressed using hydrodynamic coefficients:

$$F_{Rad} = -A_{ij}\ddot{\xi}_j - B_{ij}\ddot{\xi}_j \tag{2.12}$$

where A_{ij} and B_{ij} are the added mass and wave radiation damping coefficients, and ξ_j represents the body motion in mode j.

- Hydrostatic restoring force (F_{HS})

For floating bodies, an additional force arises due to buoyancy. The hydrostatic restoring force is due to changes in displacement caused by body motion and is given by:

$$F_{HS} = -C_{ij}\xi_j \tag{2.13}$$

where C_{ij} is the hydrostatic stiffness matrix, which depends on the body's shape and buoyancy characteristics.

It is worth noting that (i) the excitation force is defined as $F_e = F_{FK} + F_d$ and (ii) $F_{hs} + F_g = 0$ when a floating WEC body is at rest in still water. When the body deviates from its equilibrium, the hydrostatic pressure provides a restoring force in the modes of heave, roll, and pitch, depending on the mismatch between buoyancy and gravity. For incident linear waves, an analytical solution generally exists. However, analytical solutions for ϕ_D and ϕ_R only exist for some simple WEC shapes, e.g. sphere, cylinder, etc. [50, 51]. For arbitrary WEC geometries, it is difficult to find analytical solutions for ϕ_d and ϕ_r, and BEMs are generally used to obtain numerical approximations of ϕ_d and ϕ_r.

The notable BEM solvers are WAMIT, NEMOH, AQWA, AQUA+, and WADAM in the frequency domain, and ACHIL3D in the time domain. A comparison study between forces. The next section will elaborate more on the details of the BEM numerical implementation and various aspects of this method. In the following, a comparison of NEMOH, WAMIT, and ANSYS-AQWA—three widely used codes—in terms of accuracy, computational efficiency, and usability will be provided. These tools all solve the linear radiation/diffraction problem but differ in numerical formulation and user interface, which the overview of each solver presented in Fig. 2.3. The details of each solver will be elaborated in the next section.

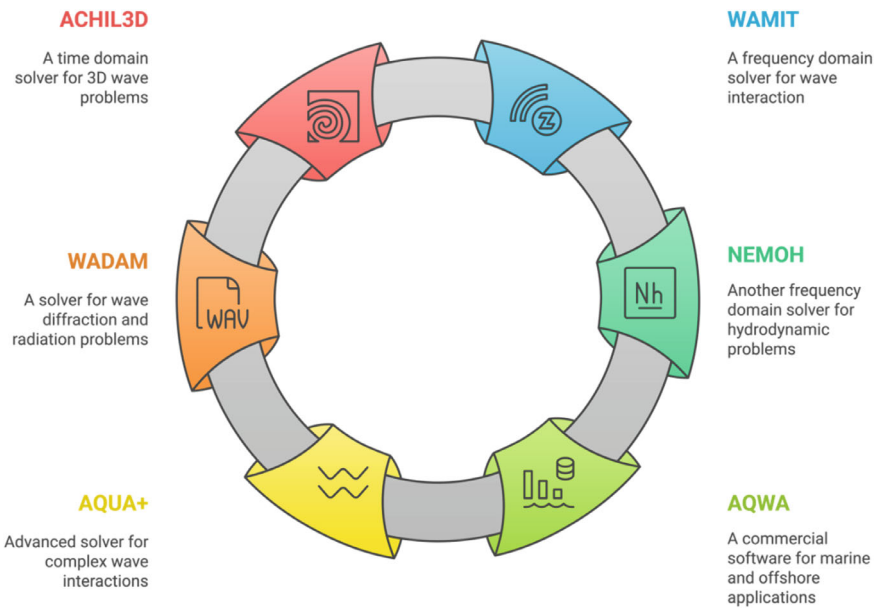

Fig. 2.3 Overview of BEM solvers

2.3 Numerical Implementation of BEM

BEM derives its numerical framework from integral formulations of PDEs, typically the Laplace equation or the Helmholtz equation, depending on the specific physical problem. For wave-structure interaction, BEM is generally grounded in linear potential flow theory, assuming irrotational and incompressible fluid motion, presented in Eq. (2.1). This equation describes a flow regime free of vorticity, where fluid motion can be fully characterized by the scalar potential ϕ. Applying Green's second identity to the governing PDE transforms it into a boundary integral equation (Eq. (2.14)):

$$c(x)\phi(x) = \int_{\Gamma} \left[G(x,y)\frac{\partial \phi(y)}{\partial n} - \phi(y)\frac{\partial G(x,y)}{\partial n} \right] d\Gamma(y) \tag{2.14}$$

where

- $c(x)$ is a geometrical coefficient determined by the position of x, with $c(x) = 0.5$ for smooth boundaries.
- $G(x, y)$ is the Green's function, representing the fundamental solution to the Laplace equation.
- $\partial G/\partial n$ and $\partial \phi/\partial n$ denote the normal derivatives of the Green's function and velocity potential, respectively on the boundary Γ.

This integral equation forms the basis of the BEM for solving wave-structure interaction problems, where unknowns are typically distributed over the boundary, significantly reducing the dimensionality of the problem compared to domain-based methods. For example, a 3D problem involving the entire fluid domain is reduced to a 2D problem along the boundary.

Green's function forms the kernel of the integral equation and encapsulates the influence of the boundary geometry and conditions. For problems involving infinite or semi-infinite domains, the free-space Green's function is commonly used, expressed in Eq. (2.15):

$$f(x) = \begin{cases} G(x,y) = \frac{1}{4\pi|x-y|}, & 3D \\ G(x,y) = -1/2\pi \log|x-y|, & 2D \end{cases} \tag{2.15}$$

Proper handling of the kernel, especially near singularities, is critical to maintaining numerical accuracy and solution stability. To transform the boundary integral equation into a numerically solvable form, the boundary Γ is discretized into a finite number of boundary elements or panels. The unknowns, such as the potential ϕ and its normal derivative $\partial\phi/\partial n$, are approximate using shape functions defined over the elements. Key aspects of the implementation of BEMs are as follows:

- Boundary discretization: The boundary Γ is divided into small elements, such as line segments in 2D or surface panels in 3D. These boundary elements represent local approximations of the unknown quantifies-potential ϕ and its normal derivative $\partial\phi/\partial n$. The density and distribution of these elements are crucial for capturing sharp boundary variations, especially around corners and edges [52].
- Shape function approximation: Within each boundary element, shape functions approximate the variation of unknowns. Linear or quadratic shape functions are commonly used depending on the required accuracy. Linear functions are computational cheaper but may introduce approximation errors for highly curved or irregular boundaries, whereas higher-order functions provide better accuracy at the cost of additional computation [24].
- Collocation method: The collocation method selects specific points within each element, often at the centroid or nodes, where the integral equation is evaluated. This converts the integral equation into a set of algebraic equations. Alternative methods, such as Galerkin's method, which uses weighted residuals, can also be applied for higher precision [17].
- Numerical integration: The boundary integrals are evaluated using numerical quadrature techniques. For regular integrals, Gaussian quadrature is often sufficient. However, integrals involving singularities require specialized techniques, such as singularity subtraction or adaptive integration, to avoid numerical instability. For self-influence terms where the Green's function becomes singular, analytical integration may be necessary [53].
- System of linear equations: The discretized form of the boundary integral equation results in a linear system of equations $Ax = b$, where A contains influence

coefficients determined by the Green's function and boundary conditions, x represents the unknowns (potential and its normal derivative), and b is derived from the known boundary data [2].

- Solution of the linear system: The linear system is solved using either direct or iterative methods. For smaller problems, direct solvers like Gaussian elimination or LU decomposition are typically employed. However, for large-scale applications, iterative solvers, e.g., conjugate gradient or GMRES, coupled with preconditioning techniques provide computational efficiency [54].

These computational strategies from the foundation of modern BEM solvers used in wave-structure interaction studies. Various BEM-based software packages implement these techniques, enabling accurate hydrodynamic analysis for complex geometries. Purposefully, the number of usages of each of the following packages from 2010 to 2024 is presented in Fig. 2.4.

WAMIT, developed at MIT, is one of the oldest and most validated BEM codes in marine hydrodynamics [55]. It uses a potential formulation and offers both low-order (panel) and high-order (B-spline) discretization options. WAMIT's high-order solver can represent the potential with continuous B-splines, which improves accuracy for smooth bodies at the cos of more complex setup [56]. Most users, however, use the low-order mode with flat quadrilateral panels, which is analogous to what NEMOH uses. WAMIT has been extensively benchmarked—its results are often treated as a reference standard in wave energy research. For example, in a code comparison study, WAMIT solutions for a floating platform were used as the reference to evaluate open-source codes [57].

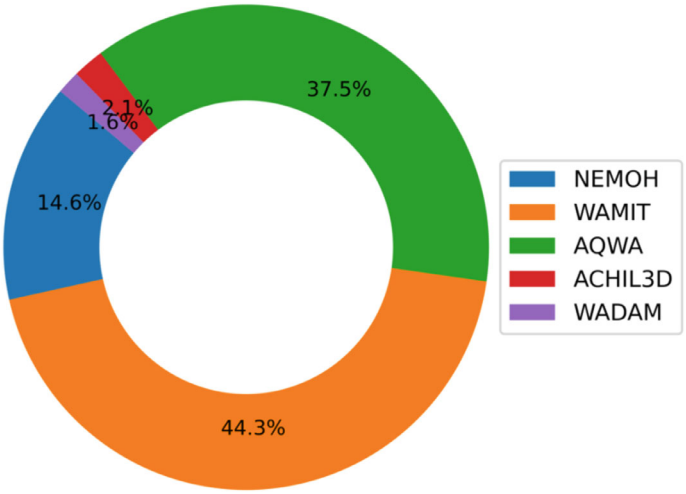

Fig. 2.4 Number of usages of various BEM packages

In terms of accuracy, WAMIT reliably computes added mass, damping, and excitation forces provided the mesh is of good quality and issues like irregular frequencies are handled. WAMIT also supports advanced features such as second-order wave force calculations and multiple bodies with coupling, which add to its versatility. Computationally, WAMIT is quite efficient in solving the linear problem [58, 59]. It can employ symmetry to reduce computation, allowing up to two symmetry planes, so a quarter or half of a symmetric structure can be modeled [57]. This multi-symmetry option can drastically cut down the number of panels and computation time for symmetric WECs, e.g., axisymmetric point absorbers or symmetric floats, an advantage over some codes that allow only one symmetry plane. WAMIT's solver is well-optimized and can run on modest hardware for single devices, though large cases will scale in runtime.

NEMOH, originally released in 2014 by developers at École Centrale de Nantes, is an open-source BEM code dedicated to first-order wave loads [60]. It uses a low-order panel method and like WAMIT requires a mesh of the body surface. One key difference is that NEMOH is limited to quadrilateral panels. If a geometry mesh has triangles, they must be converted to quads before running NEMOH. With regard to accuracy, NEMOH's computation is theoretically equivalent to a low-order BEM like WAMIT's panel method, and many studies have found that NEMOH's results agree closely with WAMIT for a variety of problems. For instance, Uçar et al. [61] compared NEMOH and WAMIT on added mass, damping, and excitation for several vessels and reported overall good agreement, with differences appearing mainly at low periods (high frequency) where NEMOH's results were somewhat less accurate. Heave and pitch RAOs from NEMOH aligned well with WAMIT, but NEMOH showed slight underestimation in heave added mass and damping at very short-wave periods. These discrepancies might stem from NEMOH's numerical scheme, e.g., difficulties at irregular frequencies or less sophisticated integration of singularities. Spurious solutions that occur at certain frequencies for closed bodies—are a known issue for BEM codes. WAMIT offers an automatic removal technique, whereas NEMOH historically required the user to damp out or avoid those frequencies. Newer versions or user-developed fixes, like adding internal free-surface tanks or using open-boundary conditions, have improved NEMOH's handling of this issue. On the computational efficiency front, NEMOH tends to be slightly slower than WAMIT for comparable mesh sizes, partly due to less optimization and the lack of multi-symmetry support. In practice, NEMOH can require a finer mesh to reach the same accuracy as WAMIT's high-order option, which means more elements and longer run times. One study noted that a newer solver (HAMS) could achieve results closer to WAMIT's with significantly less computational cost than NEMOH, which in that comparison was ~ 10–20 times slower than HAMS for similar accuracy [62]. Nonetheless, NEMOH's big advantage is usability and accessibility. It has been integrated as a backend in tools like WEC-Sim and python libraries, e.g., NEMOH capabilities in the python-based backend code Capytaine [63, 64]. However, using NEMOH effectively may require more manual effort in mesh preparation and result processing. In summary, NEMOH is a capable tool that, with careful use, can match

the accuracy of commercial codes of linear problems, though it may be less efficient and less turnkey than paid alternatives.

ANSYS-AQWA is a commercial suite within the ANSYS software ecosystem, used in offshore engineering for ship and offshore structure hydrodynamics, including WECs [65]. AQWA uses a linear panel method similar to WAMIT and NEMOH and can model bodies in the frequency domain and even simulate time-domain responses with Morison elements and moorings included. In terms of accuracy, AQWA's frequency-domain results have been found at the same level with other BEM codes. For example, one study comparing AQWA and NEMOH for ship motion analysis found that, when using sufficiently refined meshes, all codes produced very similar added mass, damping, and RAOs [61]. AQWA's results have also been used as a benchmark in wave energy studies. It is considered reliable for first-order hydrodynamics. AQWA might use internal algorithms to handle irregular frequencies and like WAMIT, support multiple bodies and advanced features.

On computational speed, AQWA can handle large numbers of panels, but mesh density will impact runtime as with any BEM [66]. One case reported a mesh convergence study with AQWA over 55,000 panels were used on half a hull, which took a substantial amount of CPU time, whereas coarser meshes in the few thousand range solved in minutes [67]. This shows that AQWA's performance scales with problem size, and for most WECs the panel count is moderate. AQWA's usability is a strong point, especially for industry users. It comes with a graphical interface and is integrated with ANSYS workbench, allowing users to import meshes including both quadrilateral and triangular panels, which it will internally convert. This software also allows the inclusion of mooring lines and PTOs in a time-domain simulation module, meaning a user can do and end-to-end simulation within one environment. In summary, AQWA provides accuracy comparable to WAMIT and is efficient for typical WEC analyses. Its drawbacks are the cost and the fact that its algorithms are closed source (Table 2.1).

The successful implementation of BEM relies on addressing several advanced challenges that influence accuracy, computational efficiency, and scalability. These considerations are essential for handling large-scale wave-structure interaction problems or complex configurations such as arrays of WECs.

- *Singularity handling and desingularization techniques*

One of the major challenges in BEM is dealing with the singular behavior of the Green's function, particularly when evaluating integrals near or at collocation points. The kernel of the integral equation becomes singular when the source point coincides with the field point, potentially leading to numerically. The singular component of the integral is extracted analytically and treated separately, leaving the remaining integral to be evaluated numerically. This method is widely used due to its balance of accuracy and computational effort. In desingularized BEM, collocation points are chosen slightly off the boundary surface, avoiding the singularity entirely. Although this method reduces the impact of singularities, careful selection of offset distances is required to maintain solution accuracy. In some cases, certain integrals involving

Table 2.1 Comparative analysis of BEM software packages for wave-structure interaction in WECs

Software licensing	Key capabilities	Strengths	Limitations	WEC-specific features	Computational efficiency	User interface	Documentation and support
NEMOH open source	Linear potential flow analysis Radiation-diffraction problems First-order hydrodynamic coefficients Regular and irregular waves Panel method implementation	Free and open-source Excellent Transparent calculation process Adaptable through source code access Good for educational purposes	Limited higher-order capabilities No built-in second-order effects Performance issues with very large meshes Limited non-linear effects modeling No forward-speed effects	Widely used in WEC research Compatible with WEC-Sim Well-suited for array analysis Good for conceptual design phases Frequency-domain coefficients for WEC control	Moderate efficiency Parallelization possible but limited Memory-intensive for complex geometries Computational time increases significantly with mesh refinement	Command-line based Third-party tools needed for pre/post-processing	Well-documentation
WAMIT commercial	Higher-order BEM formulation Comprehensive linear and second-order analysis Multiple body interactions Forward speed capabilities Advanced control surface modeling	Highly optimized algorithms Robust solver for complex geometries	High licensing cost Closed-source implementation	Extensive WEC-specific capabilities Power take-off modeling Mooring analysis integration Multi-body WEC modeling Generalized modes for flexible bodies	Efficient memory management Parallel processing capabilities Handles large problems effectively Optimized Green functions	Text-based interface Third-party pre/post-processing needed	Extensive documentation Validation examples

(continued)

Table 2.1 (continued)

Software licensing	Key capabilities	Strengths	Limitations	WEC-specific features	Computational efficiency	User interface	Documentation and support
ACHIL3D limited availability	Linear potential flow solver Domain decomposition approach Specialized for complex geometries Good for multi-body problems	Efficient domain decomposition Good for closely spaced structures Handles complex geometries well Reduced memory requirements	Limited commercial availability Less established user base Fewer validation cases available Limited integration with other tools	Multi-body WEC analysis Array interaction modeling Efficient for farm layouts	Efficient domain decomposition Good handling of complex interactions Specialized memory-saving algorithms Moderate parallel processing	Research-oriented interface Limited GUI capabilities	Limited documentation Research papers as primary reference Limited user community Minimal structured support
WADAM commercial	Linear and weakly nonlinear analysis Frequency and time domain Comprehensive load analysis Strong post-processing	Seamless integration with DNV tools Comprehensive offshore design workflow Industry standard in offshore engineering Regular validation and updates Robust hydrodynamic analysis	High licensing costs Primarily focused on offshore structures Less WEC-specific functionality Closed-source implementation Limited customization options	Good for floating WECs Strong in structural response Limited specific WEC optimization Better for survivability analysis	Good performance Optimized for marine structures Efficient frequency domain solver Structured mesh handling Industry-hardened algorithms	Workflow-oriented interface Good visualization tools Industry-standard workflows	Comprehensive documentation

(continued)

Table 2.1 (continued)

Software licensing	Key capabilities	Strengths	Limitations	WEC-specific features	Computational efficiency	User interface	Documentation and support
AQWA ANSYS commercial	Linear and second-order analysis Time and frequency domain Specialized diffraction/radiation Integrated with ANSYS suite Coupled analysis capabilities	Integration with other ANSYS products Strong visualization capabilities Well-established in industry Regular updates and improvements Coupling with structural analysis	High licensing cost Resource-intensive Generic offshore focus Closed-source implementation Complex workflow for beginners	Limited WEC-specific features Good for structural response Moorings and PTO modeling Survival condition analysis Requires customization for WECs	Moderate BEM efficiency Good for standard problems Memory-intensive GPU acceleration options	Modern GUI interface Integrated pre/post-processing Part of ANSYS Workbench Visualization tools integrated Workflow management	Extensive documentation
AQWA + ANSYS commercial	Enhanced AQWA capabilities Advanced nonlinear features Specialized marine modules Extreme condition modeling Advanced coupling options	Extended nonlinear capabilities Advanced hydrodynamic modeling Enhanced post-processing Better extreme condition handling Improved multi-body interactions	Complex setup requirements Significant computational demands	Advanced wave-structure interaction Good for complex WEC designs Enhanced array modeling Improved survivability analysis Advanced PTO modeling options	Advanced solver technology Better handling of complex problems Higher computational demands Enhanced parallelization Improved convergence algorithms	Advanced GUI Comprehensive toolkit Extensive visualization options Integration with simulation workflow	Premium documentation

singularities can be solved analytically, particularly for canonical geometries, e.g., spheres or cylinders, providing exact contributions without numerical error.

- *Efficient matrix assembly and storage techniques*

The BEM formulation typically leads to dense, fully populated coefficient matrices due to the global influence of boundary conditions. As the number of boundary elements increases, the memory and computational demands grow quadratically or worse, posing challenges for large-scale problems. One strategy to improve efficiency is the FMM, which approximates the long-range interactions between distant boundary elements using hierarchical clustering, reducing the complexity of matrix assembly and solution from $O(N^2)$ to approximately $O(N \log N)$ or better. This technique is particularly effective for problems with many elements. Hierarchical matrices, also known as $\mathcal{H}$-matrices, this approach exploits low-rank approximations of matrix blocks corresponding to far-field interactions. It reduces storage requirements while maintaining acceptable accuracy. For specific problems, such as highly sparse domains or localized interactions, sparsification techniques can be employed to reduce computational costs.

- *Parallel and distributed computing*

For wave energy simulations involving large WEC arrays, the computational burden necessitates parallel and distributed computing solutions. Decomposing the problem into smaller subdomains or leveraging modern high-performance computing architectures can significantly accelerate the simulation process. One approach to parallelism is the domain decomposition. The physical domain is divided into subdomains, each solved independently with communication between subdomains occurring at boundaries. This is particularly effective for massively parallel environments. There are other approaches for this issue, such as task-based parallelism and hybrid methods, for large simulations, combining inter-code communication using MPI with OpenMP can optimize resource utilization across clusters.

- *Handling nonlinear and time-dependent problems*

Most BEM implementations are based on linear wave theory but extending the method to handle nonlinear and time-dependent problems is critical for accurately simulating extreme waves and offshore applications. Incorporating higher-order boundary conditions and nonlinear terms in the integral equation can capture second-order effects, such as wave run-up and steep waves. While frequency-domain formulations are computationally efficient for steady-state problems, time-domain BEM is essential for transient simulations involving wave impact, mooring dynamics, and WEC start-up or shutdown conditions. Iterative approaches, such as Newton-Raphson methods, are used to solve the nonlinear system of equations arising from strong wave-structure interactions.

- *Wave energy array effects and multi-body interactions*

For wave energy farms consisting of multiple WECs, BEM models must account for device interactions, wave interference, and array layout optimization. Accurate

modeling of wave shadowing, where upstream WECs alter wave conditions for downstream devices, is essential for optimizing array performance. BEM models must capture how closely spaced devices can either amplify or dampen incoming waves, affecting energy extraction efficiency. Large arrays require parallel computing frameworks to handle the global influence matrix efficiently while ensuring accurate inter-device interaction modeling.

To better understand the application of BEM in various WEC models and its advancements in recent years, the next section will elaborate on these aspects.

2.4 Application of BEM in Wave Energy Converter Models

When designing a WEC, and at several stages of development, numerical modeling is pivotal. In this section, only the hydrodynamic numerical modeling is considered. It is critical at an early stage, as it allows several iterations of the same concept to be tested in the fastest way possible, but it is equally critical in later stages, when envisaging new generations of machines and/or trying to optimize control routines.

To this end, the difference between working in the frequency or in the time domain must be elaborated. Basically, frequency domain solutions of the equations of motion rely on the assumption that the incident waves are the result of the superposition of single harmonic waves. Linear wave theory is used, i.e., body motions are assumed small when compared with the wavelength, and thus, the problem can be split into two: the diffraction problem, where the body is fixed and subject to an incoming wave field, and the radiation problem, where the body is forced to move in otherwise undisturbed fluid. The velocity potential is obtained by the sum of the diffraction potential and all the radiation potentials, which can be associated with the wave exciting forces and moments and with the hydrodynamic coefficients, i.e., added mass and damping, respectively. With such results the motions of the body can be derived, and these are usually expressed in a non-dimensional form through the RAO. Additional constraints can be introduced by external mass, damping of stiffness matrices (e.g., to assess the influence of different mooring arrangements or of different power take-off settings).

When nonlinear effects are significant, time domain solutions need to be implemented. There are several ways to derive such models, but in the majority of cases, the nonlinear analysis is based on direct pressure integration over the body surface at each time step of the simulation [68]. Simplifications, like reducing the body surface to a mean wetted surface, can be implemented, leading to a considerable reduction in the computational time that is required to run the simulations at the expense of the maximum possible accuracy. The main difference to the frequency domain approach is therefore the possibility of adding nonlinear effects in the equations of motion, which are typically linked with convolution integrals that consider effects that persevere after the motion of the body stops (hence such integrals are sometimes referred to as ‘memory functions’). To this date, the frequency domain approach has

been used in a much larger number of applications than the time domain equivalent [69–71].

There are various types of WECs, each with unique operating principles and hydrodynamic characteristics, as demonstrated in Fig. 2.5. The application of BEM varies depending on the specific WEC type, and in the following discussion, its implementation for different WECs will be explored.

The use of pure BEM codes to study WECs was at first linked with the study of OWC plants. Brito-Melo et al. [73, 74] modified the AQUADYN code originally developed at École Centrale de Nantes, producing a specific version dedicated to OWCs (AQUADYN-OWC). The major modification was associated with the supplementary radiation problem imposed by the oscillatory movement of the water in the inner chamber, which was solved by modifying the boundary condition through the pressure distribution. The study, conducted in the scope of the development of the Pico plant, showed an increasing level of depth: the initial configuration assumed an isolated structure surrounded by an infinite fluid domain, whilst the final geometry included the neighboring coastline and bathymetry. Comparisons were made with a 1:35 scale model, validating the numerical results.

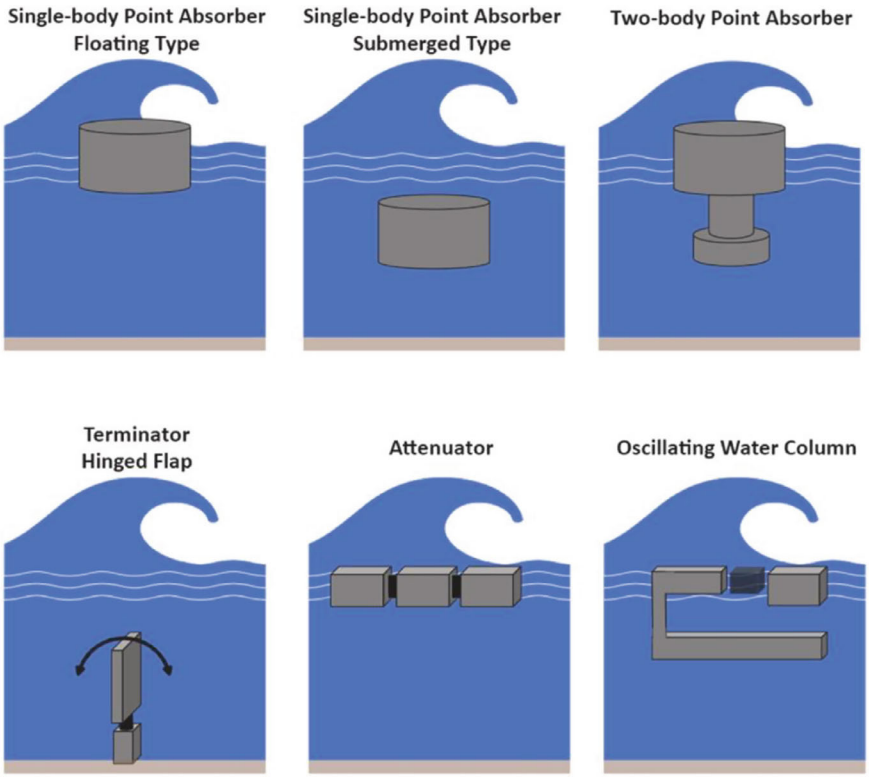

Fig. 2.5 Various types WECs categorized by their operating principles [72]

One of the most notable applications of BEM in WECs is in the prediction of wave-induced forces and moments on devices such as OWCs, point absorbers, attenuators, and overtopping devices. OWCs, for example, have been extensively studied using BEM due to the complexity of air-water interactions within their chambers. In a study by Ruehl et al. [75], a BEM-based model was developed to simulate the hydrodynamics of a floating OWC under varying wave conditions. The study demonstrated the ability of BEM to accurately predict internal water surface displacements and optimize the geometry of the air chamber for maximum energy extraction. Similarly, the experimental validation of BEM-based models by Pecher et al. [76] revealed that discrepancies between numerical and physical models could be minimized by incorporating advanced boundary conditions to account for nonlinear effects. As a result, BEM continues to serve as a crucial design tool for engineers working on OWC systems, facilitating improvements in power capture efficiency and turbine performance.

Modeling OWCs with BEM is more complex because the interior free surface oscillation must be represented. A common linear modeling approach is to treat the moving water column as an "equivalent piston" moving inside the device. BEM codes like WAMIT have features to handle this: one can model the OWC as a floating body with an additional mode corresponding to the internal water surface motion (sometimes implemented via a fictitious mass or a second body representing the piston of water). In frequency domain, this allows calculation of the pneumatic chamber resonance and the hydrodynamic interactions between the chamber and external waves. BEM has been widely used and validated for OWCs, especially fixed OWCs integrated into breakwaters or onshore structures. For example, Delauré and Lewis [77] and Raghavan et al. [78] performed 3D BEM modeling of a fixed OWC and found good agreement with experimental results. Similarly, Dash et al. [79] used a BEM approach to analyze OWC hydrodynamics and compared predictions to measured data, validating the linear model for a range of wave conditions. These studies, among others, established that linear potential flow can capture the primary dynamics of OWCs (such as the chamber's natural period and the trend of capture efficiency) when the wave amplitudes are small. In industry, the commercial BEM code WAMIT has been a go-to tool for OWC design studies and has been cross-verified against physical modeling. Open-source BEM codes initially struggled with OWCs due to modeling limitations. Notably, the standard approach in NEMOH (an open-source BEM solver) was to model the internal water surface as a thin disk—an approximation that proved ineffective in many cases. his oversimplification led to poor results, since a thin disk at the free surface does not accurately represent the inertia and coupling of the full water column. Researchers addressed this by using a multi-body BEM formulation. Penalba et al. [56] demonstrated that one can model the OWC chamber and the internal free-surface as two coupled bodies (the structure plus an "imaginary piston" body representing the water column) in NEMOH. By extending the piston body down to the length of the internal water column, they achieved much better agreement with experimental data. In essence, the multi-body approach allows the internal water motion to be properly accounted for in the equations of motion. Studies have even coupled BEM with CFD to improve OWC modeling—for example,

Simonetti et al. [80] showed that while CFD can capture nonlinear air-compressibility and viscous effects in OWCs, BEM predictions are reasonably accurate for primary response and come at a fraction of the computational cost. As Delauré and Lewis [77] performed BEM simulations for a single chamber OWC similar to Mutriku's OWC design, more recently, Faÿ [81] reported on Mutriku's actual performance and noted that linear models could predict annual energy production reasonably when calibrated, but underpredicted losses in real irregular wave condtions, owing to turbine inefficiencies and nonlinear wave effects. These findings underscore that BEM is powerful for relative comparisons and design optimization, but absolute predictions may need calibration or correction factors.

A device like the Ocean Energy (OE) buoy, which is a floating OWC, has been the subject of coupled BEM and PTO studies. In model tests, the OE buoy's motion and pneumatic pressure were recorded and compared to a simulation that combined a BEM hydrodynamic model (for the floating structure and internal water column) with an air compressibility model for the Wells turbine. The frequency-domain BEM provided the added mass, damping, and excitation forces for both the buoy's rigid body modes and the internal water piston mode. Those parameters were used in a coupled frequency-domain solution for the system. The comparison showed that predicted heave and pitch RAOs, as well as pressure oscillation amplitude, matched the experiment within ~ 5% in the linear regime, validating the use of BEM for such complex devices. Any discrepancies were mostly attributed to simplifications in the turbine model and linearization of airflow damping. Overall, BEM remains an indispensable tool for OWC analysis, used for initial design (to size the chamber and turbine for the expected wave climate) before higher-fidelity or specialized models are applied.

Point absorbers, often considered the simplest type of WEC, are also extensively modeled using BEM. A study by Li and Yu [82] synthesized various numerical methods for point absorber modeling and highlighted BEM as a key approach due to its ability to provide accurate predictions of hydrodynamic coefficients, including added mass and radiation damping. In research conducted on the Seabased AB WEC (a point absorber developed in Sweden); BEM was used to simulate the heaving motion of the buoy under irregular wave conditions. The results showed that accurate modeling of PTO mechanisms using BEM significantly enhanced the system's energy absorption efficiency [83]. Many studies have modeled these devices as axisymmetric or simple geometries, such as spheres, cylinders, and cones, using panel methods. For instance, a spherical or cylindrical buoy's added mass and damping in heave can be computed with a frequency-domain BEM solver, and the results used to predict heave RAOs and absorbed power. Because point absorbers are often omni-directional (axisymmetric), a BEM analysis in two dimensions (for axisymmetric bodies) or using symmetry planes is possible, further reducing computational effort. Numerous validation studies have shown BEM's efficacy for point absorbers. For example, BEM predictions for the heave motion of a simple buoy have been compared to wave tank tests, generally showing good agreement in the linear regime. In cases where discrepancies arose, it was often due to neglected viscous effects or nonlinearities rather than fundamental flaws in the BEM. Researchers have found that including

an empirical viscous drag term can improve match with experiments—a common approach is to augment the BEM-computed force with a Morison-type drag force proportional to velocity squared. This accounts for energy dissipation due to flow separation (vortex shedding) around the device, which pure potential flow BEM cannot capture. Despite such limitations, linear BEM remains the starting point for point absorber design and analysis. For instance, Raghavan et al. [62] used BEM (via the HAMS code) to compute hydrodynamic coefficients and RAOs for a cylindrical heaving point absorber, finding good agreement with a benchmark solver (WAMIT).

Many small-scale tank tests of heaving buoys have been compared to BEM predictions. In one example, a small-scale heaving buoy was tested in regular waves and the measured heave RAO was compared with linear BEM results [84]. The linear model captured the resonance peak and general RAO shape well, but slightly overpredicted motion at resonance due to the absence of viscous damping in the simulation. By adding a quadratic damping term (tuned to free-decay tests), the modified BEM model matched the experimental RAO almost exactly. This work confirmed that the primary hydrodynamic forces are captured by potential flow theory, and the remaining discrepancy can be attributed to viscous effects not in the BEM. Another study by Giorgi et al. [85, 86] looked at nonlinear motion of a heaving buoy. They extended the model to include a nonlinear Froude-Krylov force accounting for instantaneous submergence and found improved correlation with experimental extreme motion and drift compared to the purely linear model. This suggests that while linear BEM is a good first approximation, certain regimes, such as large waves, large motion amplitude, benefit from augmenting the model with nonlinear hydrodynamic components.

Another significant case study is the modeling of the Pelamis WEC, an attenuator device consisting of a series of cylindrical segments that bend with wave action. Renzi and Dias [87] used BEM to model the wave-induced bending moments along the length of the Pelamis device and analyzed how segment coupling affected overall power output. Their findings showed that optimizing the length and configuration of the segments using BEM simulations could maximize energy absorption while minimizing mechanical stresses. Additional studies, such as those by Child and Venugopal [88], confirmed that BEM-based modeling of Pelamis devices in array configurations provided valuable insights into wave interactions between individual units, allowing for the optimization of farm layouts to avoid destructive interference and maximize constructive wave interactions. A notable case study is the Pelamis P1, which is a three-hinged attenuator. Researchers used WAMIT to model the Pelamis and calculate the motion of each segment and hinge forces under various wave conditions [89]. By applying a linear PTO damping at the hinges in the model, they could predict the power output and even reconstruct the device's published power matrix. The BEM-based results for Pelamis showed good agreement with the device's design power matrix in moderate wave conditions, confirming that linear hydrodynamic models can capture the energy absorption mechanism of attenuators. This study also extended to multiple Pelamis devices in an array, using WAMIT to examine how spacing and relative orientation affect performance. Such analyses are important for wave farms:

BEM can quickly evaluate array interactions (e.g., shadowing or constructive interference effects) by computing the diffraction of waves by one device onto others. The Pelamis P1 underwent sea trials in Scotland in the mid-2000s, and its developers published a power matrix. A validation study [90] attempted to reproduce this power matrix using WAMIT and a time-domain model. They modeled each Pelamis segment in WAMIT and included hinge PTO damping linearly. WAMIT produced the frequency-dependent hinge motion amplitudes and phase lags. These were then converted to time-domain using radiation impulse response functions and run in irregular wave spectra corresponding to the sea states of the power matrix. The simulated average power in each sea state closely matched the Pelamis reported values for moderate wave conditions, e.g., sea states with $H_s \sim 2{-}3$ m and $T_p \sim 8{-}10$ s. In high sea states, means very large waves, the simulation overpredicted power because the real device actively cut off or limited PTO damping to avoid damage—a control strategy not captured in the simple linear model. This work validated that for operational seas, linear BEM combined with a basic time-domain model can predict full-scale WEC performance. Additionally, Pelamis's measured motions were compared to RAOs from WAMIT. The trends were well-matched, although WAMIT slightly misestimated the relative phase between adjacent modules in some wave periods, possibly due to neglecting viscous hinge damping. Overall, the Pelamis case demonstrated that BEM could scale up to multi-body, full-scale devices and provide credible predictions, as long as engineers account for control and friction differences when interpreting results.

Furthermore, attenuators, being elongated, are more directionally sensitive than point absorbers. In practice, a device like Pelamis is aligned with prevailing wave direction. Its moorings allow it to weathervane into the waves. If waves come at oblique angles, the response and power capture can change significantly. BEM can quantify this by running the simulation for different wave incidence angles. Typically, the highest response is in head-on seas, while performance drops in oblique or broadside waves. This highlights that in assessing an attenuator's annual energy production, one must integrate over the directional spectrum of the site's wave climate. BEM codes enable such analysis by providing RAOs as a function of wave direction. Other multi-body WECs, such as hinged flaps or multi-float systems, are conceptually similar in BEM modeling [91, 92]. Each element is a body with its own radiation/diffraction properties, and coupling terms are included. Provided the motion between bodies is not too large (so that linear assumptions hold reasonably), BEM can be very effective. For example, one study applied BEM, i.e., HAMS and WAMIT, to an oscillating wave surge converter (a large flap hinged at the bottom) in addition to a point absorber, demonstrating that the code could handle both types of devices with good accuracy [93]. In summary, for attenuators and other multi-body WECs, BEM offers a way to model complex device geometries and interactions in a computationally efficient manner, although it may require careful setup, e.g., meshing each body, specifying joint conditions, and often needs to be supplemented with separate structural/mechanical analysis for the hinge behavior.

BEM has also been instrumental in the design of overtopping devices, such as the Wave Dragon, which captures wave energy by allowing water to flow over a

ramp into a storage reservoir. Kofoed et al. [94] conducted prototype testing of the Wave Dragon and used BEM models to simulate wave run-up and overtopping rates under different wave climates. Their results showed that BEM simulations closely matched experimental data, validating their use for predicting energy capture in real sea conditions. Furthermore, the study demonstrated that optimizing the slope and width of the overtopping ramp using BEM could significantly improve energy output. Subsequent research expanded on this work by coupling BEM with optimization algorithms to iteratively refine device geometry for site-specific wave conditions [95].

Beyond individual devices, BEM has played a critical role in analyzing WEC arrays and farm configurations. In wave energy farms, the interaction of radiated and diffracted wave fields between devices can result in constructive or destructive interference, significantly impacting overall energy capture. Babarit [96] conducted extensive BEM-based simulations to study the performance of WEC arrays and demonstrated that the spatial arrangement of devices could lead to significant gains or losses in efficiency. For example, by positioning devices to harness constructive interference, overall power output was increased by up to 30% in some configurations. Similarly, Han et al. [97] examined the effect of device spacing and alignment using BEM models and concluded that proper optimization of array layouts is crucial for minimizing negative interactions and maximizing wave farm efficiency. The DOE-sponsored WEC Array project compared WAMIT and NEMOH predictions of array interaction factors to basin tests; BEM could predict the trend of constructive/destructive interference well, though some amplitude discrepancies arose due to wave scattering between devices that introduced slight nonlinear effects not in the model.

Additionally, BEM is often coupled with time-domain solvers and other numerical methods to account for nonlinear wave effects and structural dynamics. Chu et al. [98] demonstrated the coupling of BEM with CFD to capture viscous losses and nonlinear wave phenomena that are typically neglected in linear BEM models. Their results indicated that the coupled approach provided more accurate predictions of power output, particularly in extreme sea states. Similarly, BEM-FEM coupling has been employed to evaluate structural integrity and fatigue life in WECs, especially for devices subjected to large dynamic loads. For example, a study by Tang et al. [32] used BEM-FEM simulations to predict stress distributions within the mooring lines and structural components of a floating structure, ensuring that designs met long-term durability requirements.

In summary, across these studies, linear BEM has consistently proven capable of capturing the primary hydrodynamic behavior of WECs. Discrepancies tend to emerge in regimes where assumptions are violated, such as strong nonlinearities, extreme motions, or unmodeled physics like PTO control and mooring line dynamics. By validating BEM models against experiments and field data, researchers refine the models—often by adding supplemental damping or tuning parameters—to increase accuracy. These case studies build confidence that BEM, despite its limitations, is a sound foundation for WEC performance evaluation.

Beyond the accuracy of BEM models, another crucial aspect of WEC analysis is understanding how wave conditions influence performance. The efficiency of a WEC depends not only on its design but also on environmental factors, such as wave height, period, and direction, as well as location-specific characteristics like water depth and overall wave climate. BEM is commonly used to assess these dependencies by computing device response over a range of conditions [67]. In a linear model, wave height has no impact on the RAO or efficiency—doubling the wave amplitude results in a proportional doubling of the motion amplitude, while the absorbed power increases quadratically, as power is proportional to the square of the wave amplitude in linear theory. Thus, linear BEM would predict the same performance (capture width ratio, etc.) for a 1 m wave as for a 2 m wave of the same period, aside from scaling. However, nonlinear effects become more significant at higher wave heights. For instance, a point absorber that performs efficiently in 1 m waves might see its efficiency plateau or drop in 4 m waves due to PTO limits or viscous losses. A study on the Gulf of Guinea found the point absorber's efficiency peaked at a certain moderate wave height (~ 2 m); at larger waves (4 m) the absolute power was higher (because more energy is available and the device resonated at those conditions), but the efficiency (fraction of available wave energy captured) was lower [99]. This suggests that beyond a certain wave height, the device could not absorb proportionally more energy—possibly a sign of reaching its stroke limits or increased losses. BEM alone would not capture those saturation effects, but by integrating BEM with device-specific limits, like maximum stroke or PTO force, one can evaluate how performance changes with wave height. Generally, designers ensure the WEC can survive and continue operating (maybe in a de-tuned mode) in high waves, even if efficiency drops. From a BEM analysis perspective, multiple wave heights are usually examined in irregular wave simulations using a spectrum and BEM-derived transfer functions, one can compute expected power output. This is done for many H_s and T_p pairs to create a power matrix. That power matrix combined with a site's wave height distribution yields the annual energy.

Wave period is perhaps the most critical factor for WEC performance. WECs are typically designed to resonate or at least respond strongly in a certain period range. BEM is used to identify the natural periods of the device (where added mass and stiffness interplay leads to large motions). For example, a heaving buoy might have a resonance in heave around $T = 8\,s$. At that period, the RAO for heave motion (or the non-dimensional capture width) will be maximal. At periods far from resonance (too low or too high), the response and power absorption drop off. BEM calculations across frequencies can produce a frequency response curve: for instance, the power capture vs. wave period might show a peak around 11 s for a given PTO setting. If the wave period is much shorter, for instance 5 s, the buoy cannot respond fast enough—BEM would show a small motion amplitude and thus low absorbed power. If the wave period is much longer, approximately 20 s, the excitation force itself might diminish, since the buoy effectively rides the long swell with little oscillation, again leading to low power. Thus, matching a WEC's response to the prevailing wave periods at a site is crucial. BEM is instrumental in this: designers adjust parameters (size, geometry, PTO stiffness) in the BEM model to tune the device's natural period.

Bandwidth is another consideration—some devices have a narrow optimal period range, others a broader one. A broad frequency response is generally desirable to maintain performance across variable sea states. Techniques like introducing multiple oscillation modes or actively controlling the PTO can widen the effective bandwidth (these can also be evaluated in frequency domain by looking at adjusted damping matrices). In summary, BEM analysis of wave period effects allows engineers to produce a power spectral density or a capture width vs. period plot, which directly feeds into energy yield calculations for a given wave climate.

Wave direction relative to the WEC matters for non-axisymmetric devices. Point absorbers that are symmetric (e.g. a vertical cylinder) are essentially insensitive to wave direction—waves from any horizontal direction produce the same heave response. In contrast, attenuators and terminators (elongated or direction-specific WECs) show strong directional dependence. An attenuator like Pelamis must align with incoming waves; if waves arrive at a 30° angle off the nose, the excitation forces on each segment become asymmetric and the hinge motions may reduce, lowering power output. BEM codes can compute directional excitation and RAOs by varying the incident wave angle in the simulation. For Pelamis, one would run cases from 0° (head-on) to 90° (broadside) to map out the sensitivity. Typically, head-on (0°) yields maximum performance, and by 90° the device might capture very little (since the wave is along its side, causing mostly negligible hinge motion). Some devices, like oscillating wave surge converters (OWSCs—flap type devices mounted on the seabed), are also direction-dependent: they need waves roughly perpendicular to their face. If waves come at an angle, the effective width presented to the wave is less and the response can drop. Directionality is a key part of wave resource assessment—many sites have a predominant wave direction, but also a spread (e.g., North Atlantic waves might come mostly from west, but with some spread). WECs like attenuators might be moored to passively realign to the dominant wave direction or must be designed to handle a range of approach angles. BEM simulations across directions help quantify how misaligned seas affect annual energy production. If a site has a wide directional spread, an axisymmetric WEC (like a point absorber) might have an advantage of equal performance from all directions, whereas a strongly directional WEC might underperform unless it actively yaws into the waves.

The local water depth can influence WEC hydrodynamics. Many BEM codes, including WAMIT, NEMOH, AQWA, can simulate finite water depth by using a modified Green's function or image method for the bottom. Finite depth primarily affects long waves—when the wavelength is large relative to depth, the wave kinematics are altered and so are the hydrodynamic coefficients. For example, a point absorber in 50 m depth will have a different added mass at a 20 s period wave than it would in very deep water, because the wave-induced pressure field is influenced by the bottom. For oscillating surging devices nearshore (like bottom-hinged flaps), depth is obviously critical (they wouldn't exist in deep water). BEM can include the seabed as a fixed boundary (usually assuming a flat horizontal bottom). If a WEC is placed on a shoal or slope, strictly one would need a more complex model; but often an average depth is assumed. Mooring systems also interact with depth (e.g., catenary moorings require sufficient depth), though moorings are handled outside of BEM

as discussed later. As for geographical location: depth is one factor, distance from shore (which can correlate with wave spectrum changes due to fetch or sheltering) is another.

Different regions of the world have very different wave climates, which profoundly affects WEC performance and design. For instance, the North Atlantic off Western Europe has among the world's highest wave energy potentials, with average power densities on the order of 40–60 kW/m and extremes well above 100 kW/m. Specific sites facing the North Atlantic can see average wave power ~ 87 kW/m. On the other hand, semi-enclosed seas like the Baltic Sea or the Mediterranean have much lower averages (5–15 kW/m typical), but also gentler extreme conditions. WEC developers often initially test in milder sites and later move to more energetic sites. For example, the Mediterranean Sea, while less energetic, offers a less punishing environment for prototypes (fewer extreme storms). A device optimized for Mediterranean conditions (with mostly small-to-medium, short-period waves) might not perform optimally if directly placed in North Atlantic swells without retuning. The frequency distribution of waves is key—North Atlantic has a lot of long-period swell (10–15 s dominant periods), whereas the Mediterranean might have shorter wind-sea (5–8 s) dominating. If a WEC's natural period is around 7 s to match the Med, it will be off-resonance and suboptimal in the Atlantic. Conversely, a heavy device tuned for 12 s Atlantic swell might hardly ever reach resonance in the Mediterranean's shorter waves. BEM-based analysis allows designers to quantify these effects by generating power matrices for multiple sites. A study by Onea and Rusu [100] assessed several WEC designs at sites from the Iberian Atlantic coast to the Black Sea. They found that the capacity factor (fraction of max energy output achieved on average) of a given WEC varied widely by location—e.g., around 22% in a moderate Irish Atlantic site, but only a few percent in the low-energy Baltic, and up to ~ 37% in winter months at the very energetic locations. This aligns with the idea that WEC performance correlates with how well the wave climate overlaps with the device's optimal operating range. If the wave climate shifts (due to seasonal patterns or long-term climate change), the WEC's performance will shift accordingly. Therefore, location-specific optimization is often pursued: using BEM, one can adjust design parameters for each target site's wave spectrum to maximize annual energy. This might mean altering the mass distribution (to change natural periods) or PTO damping characteristics. Some WEC designs even aim to be broadly adaptable; for example, the Inertial Sea Wave Energy Converter (ISWEC) was engineered specifically for the Mediterranean's lower-energy, shorter-period waves. In summary, wave climate and geography impact WEC performance strongly, and BEM modeling is a critical tool in evaluating those impacts. It provides the quantitative link between wave conditions (height, period, direction) and device response/power, enabling the creation of site-specific performance estimates and guiding the design for different regions.

Overall, despite its many advantages, BEM does have certain limitations. One significant drawback is its reliance on linear potential flow theory, which assumes small-amplitude waves and inviscid fluids. While this assumption is valid for many operational conditions, it can lead to inaccuracies in extreme waves, where nonlinear effects, such as wave breaking and viscous dissipation, become dominant. Addressing

this limitation requires hybrid approaches or extensions of BEM that incorporate nonlinear boundary conditions. Recent advancements include adaptive panel methods and parallel computing techniques, which aim to reduce the computational cost of large-scale simulations while extending BEM's applicability to more complex wave scenarios.

2.5 Challenges and Future Directions in BEM

2.5.1 Challenges

The BEM remains a crucial computational technique in marine and offshore engineering, known for its ability to handle problems in unbounded domains with minimal discretization. However, to extend its utility for increasingly complex wave-structure interactions, researchers are working to address current challenges related to nonlinear dynamics, computational efficiency, multi-body interactions, and multi-physics modeling. These ongoing advancements will further establish BEM as an indispensable tool for the development of next-generation WECs and offshore infrastructure. Several challenges have been presented in the following based on the recent advancements.

2.5.1.1 Nonlinear Wave Effects and Higher-Order Formulations

One of the most significant limitations of current BEM implementations is their reliance on linear or weakly nonlinear wave theory, which restricts their accuracy in capturing steep waves, wave breaking, and violent wave-structure interactions. Practical marine environments-especially those involving WECs operation under energetic sea states-frequently exhibit strongly nonlinear behavior that cannot be adequately captured by linear models. Addressing this limitation involves the development of higher-order BEM formulations capable of resolving second- and third-order effects, such as wave diffraction, wave run-up, and nonlinear radiation. Time-domain approaches, which iteratively solve the governing equations to handle transient nonlinear interactions, are gaining traction. Additionally, hybrid models that couple BEM with fully nonlinear solvers, such as those based on the Navier-Stokes equations, show promise in resolving localized nonlinear phenomena, including wave breaking, overtopping, and vortex shedding. These advancements will provide more robust simulations, capturing complex interactions between waves and offshore structures.

Classical BEM assumes linear wave theory—small wave slopes and small body motions—and a fixed geometry (usually about the mean position). This excludes nonlinear phenomena like steep waves, wave breaking, or very large motion excursions. WECs can experience nonlinear Froude-Krylov forces (when a large wave

effectively sees a changing body geometry), slamming forces if parts of the structure emerge and re-enter the water, and nonlinear hydrostatic restoring when motion is large. Standard BEM cannot capture these because it solves a linearized boundary value problem. To handle moderately nonlinear motions, some models use a body-nonlinear approach (updating the body position and integrating hydrostatic forces accurately but still using linear radiation/diffraction)—however, this often requires time-domain simulation rather than frequency domain. Researchers have developed extensions like the weak-scatterer approximation, where the free-surface condition is applied on the actual instantaneous position of the body (to first order) but still linearized about a calm sea. Fully nonlinear BEM (sometimes called a Numerical Wave Tank using potential flow) is an active research area—these models use time stepping and can handle large waves and motions without linearization. These models employ techniques like Mixed Eulerian-Lagrangian (MEL) to update the free surface at each step. However, the challenge is that they become computationally intensive. Fully nonlinear 3D simulations ran about 100 times slower than real time, which is impractical for long simulations or design iterations. Thus, fully nonlinear BEM is typically used to study specific extreme events or to verify the range of validity of linear models, rather than replace linear BEM for routine design.

In summary, linear BEM works well for most operational sea states and provides the foundation for understanding WEC dynamics, but for extreme waves and survival conditions, additional nonlinear modeling or experiments are required. The inability of linear BEM to predict phenomena like parametric resonance (in some cases WECs can exhibit parametric resonance in pitch or roll under certain periodic excitation) or coupled nonlinear aero-hydro dynamics (in OWCs at large amplitudes) is a limitation that the industry addresses by a combination of higher-fidelity simulations and safety factors in design.

2.5.1.2 Computational Burden and Scalability Improvements

BEM inherently produces fully populated, dense coefficient matrices due to the global influence of boundary conditions through Green's functions. For large-scale problems, such as wave farms or floating offshore structures, these matrices can lead to computational intractability in both memory usage and processing time. Addressing this computational bottleneck has led to the development of advanced numerical techniques. The FMM reduces the computational complexity of matrix assembly and inversion from $O(N^2)$ to $O(N \log N)$ or better by approximating long-range interactions. Hierarchical matrices ($\mathcal{H}$-matrices) further reduce memory requirements by exploiting low-rank approximations in far-field interactions. Parallel computing and GPU-accelerated solvers have also emerged as critical solutions, enabling simulations involving thousands of interacting devices. These advancements are essential for applications like wave farm optimization, where device interactions can significantly influence energy capture.

Even though BEM is computationally faster than CFD, it can still become demanding for complex scenarios. If one wants to simulate a large array of WECs

(dozens of devices interacting hydrodynamically), the number of unknowns in the BEM system increases with all the bodies and can lead to very long computation times or high memory usage. Also, BEM traditionally handles zero forward speed problems (stationary or freely floating bodies in waves). If a WEC has significant current or forward velocity (not usually the case, except perhaps for current-assisted systems or if considering a hybrid wave-current device), standard BEM formulations would need modifications (e.g., adding a steady flow potential—this gets complicated and is not common in wave energy modeling). Another challenge is mesh generation, where creating a good-quality mesh for complex geometries can be time-consuming. Poor meshes (too few panels in high-curvature areas, or too many panels causing numerical ill-conditioning) can lead to inaccurate results. NEMOH's limitation to quadrilateral panels, for instance, means some automatic meshing tools cannot be used directly, requiring extra steps to preprocess the geometry. Irregular frequencies were mentioned earlier—they are false solutions of the integral equations that occur at certain frequencies for closed bodies (like a hollow OWC chamber or any body that traps a volume of fluid). If not dealt with, they appear as spikes in the added mass/damping results. WAMIT, Capytaine, and HAMS have methods to remove these (e.g., internal tank method, or solving a supplementary system), but simpler codes might require the user to manually identify and ignore those frequency points or apply numerical damping. This is a technical challenge in using BEM that requires understanding the theory.

Finally, the radiation condition (Sommerfeld condition at infinity) is enforced via analytical Green's functions in many codes (for open water), but if one tries to use BEM in a confined or semi-confined domain (like near a wall or in a channel), standard formulations don't directly apply—specialized Green's functions or large domains with damping zones are needed. Some advanced BEM models include damping beaches or absorbing boundary conditions in the computational domain for time-domain simulations, which adds complexity but is important for preventing artificial reflections in numerical wave tanks.

2.5.1.3 Coupling BEM with Structural Models and FSI

Predicting structural deformation, fatigue, and failure due to wave loading requires the integration of BEM with structural solvers to simulate the dynamic response of flexible offshore structures and WECs. FSI models that combine BEM with finite element methods (FEM) have been developed to capture the interaction between hydrodynamic forces and structural deformation. Iterative coupling techniques ensure numerical stability and convergence, particularly for highly flexible components or large deformations.

2.5.1.4 Multi-body Interactions and Wave Farm Optimization

Large arrays of WECs or floating platforms introduce complex wave-structure and inter-device interactions, including wave shadowing, constructive or destructive interference, and wake effects. These interactions can either enhance or diminish the performance and energy output of individual devices. Extending BEM formulations to accurately capture these effects is a critical research focus.

Advanced optimization algorithms are being developed to determine the optimal configurations and layouts of devices within wave farms. By coupling these algorithms with large-scale parallel BEM implementations, researchers can explore various configurations and evaluate their impacts on overall performance and energy capture efficiency. This capability is crucial for designing wave farms that maximize energy extraction while minimizing destructive interference and operational losses.

2.5.1.5 Addressing Viscous and Turbulence Effects

Traditional BEM assumes inviscid potential flow, which neglects the effects of viscous dissipation and turbulence-factors that are often significant in real-world scenarios, particularly around structures and during wave breaking. Hybrid models that couple BEM with CFD solvers capable of resolving the Navier-Stokes equations offer a promising solution. These models allow for the accurate simulation of localized viscous phenomena while retaining the computational efficiency of BEM in the far-field. Additionally, viscous correction models integrated directly into the BEM framework provide an efficient alternative by approximating energy dissipation without the need for fully volumetric simulations. These hybrid approaches strike a balance between computational cost and accuracy, making them ideal for problems involving wave-structure interactions in turbulent or dissipative environments.

BEM is built on the assumption of an ideal inviscid fluid (potential flow), meaning it does not directly account for viscous effects such as drag, flow separation, and vortex shedding. In many WECs, viscous phenomena are non-negligible—for example, a heaving buoy can shed vortices at sharp edges, or a pitching flap can cause flow separation along its surface. These effects manifest as additional damping or altered excitation forces that linear potential flow misses. In practice, modelers incorporate viscous effects in a simplified way. The common approach is to add a Morison drag term or other empirically derived damping terms to the equations of motion. Morison's equation (originally for slender structures) has a quadratic drag term $F_D = \frac{1}{2}\rho C_D A|v|v$, which is velocity-squared damping. By tuning the drag coefficient C_D (often using data from decay tests or oscillation tests), one can reasonably approximate the energy dissipation due to viscosity. This is routinely done in WEC simulation frameworks; for instance, WEC-Sim (a time-domain simulator) allows users to specify a nonlinear drag on each body in addition to the linear radiation damping from BEM. Such tuned "viscous damping" terms are crucial to match experimental observations of decay rates or response in resonance. Another limitation is that BEM predicts no lift forces in symmetric bodies (because potential flow

would reattach smoothly). However, a device with a sharp geometry might experience some lift or asymmetrical force due to flow separation in certain motions. These subtle effects are typically small for WEC shapes (which are often rounded to avoid extreme separation) but could be important for devices like an oscillating wave surge flap (where flow separation at the edges can significantly alter the torque). At present, pure BEM cannot capture vortex-induced loads or turbulence, so these must either be accounted for empirically or by coupling BEM with CFD in critical areas. For example, a hybrid model might use BEM for global wave forces but add a CFD-based correction for a turbulent loading on a particular appendage. Recognizing this limitation, designers apply safety margins: a BEM prediction of absorbed power might be optimistic if viscous losses are ignored, so they might calibrate against scaled tests to ensure the predicted power is realistic.

2.5.1.6 Free Surface Tracking and Nonlinear Boundary Updates

Accurate tracking of the free surface is essential for simulations involving large waves or significant nonlinear surface deformation, such as wave breaking or wave overtopping. Traditional BEM implementations face challenges in updating the free surface boundary conditions at each time step, often leading to inaccuracies in predicting wave evolution. To overcome these issues, boundary-fitted moving meshes have been developed to dynamically adapt to the evolving free surface geometry. Level-set methods, which represent the free surface implicitly, are coupled with BEM to capture complex wave interactions, including wave merging and breaking. Particle-based methods, such as smoothed particle hydrodynamics (SPH), are also being integrated into BEM frameworks to manage extreme surface deformations and nonlinearity.

2.5.1.7 Multi-physics Coupling and Real-Time Control

As offshore energy projects scale up, simulations must account for multi-body interactions and multi-physics effects, including hydrodynamic, aerodynamic, and structural dynamics. Multi-body systems, such as arrays of WECs or floating offshore platforms with multiple substructures, require accurate modeling of mooring dynamics, tether forces, and hydrodynamic coupling between bodies.

BEM models are being expanded to simulate these collective behaviors under varying environmental conditions, enabling optimized system-level performance. Integrating BEM with real-time control models allows devices to dynamically adjust their responses to changing wave conditions, thereby maximizing energy output and minimizing structural fatigue. Multi-physics platforms combining BEM with atmospheric and oceanic models provide a comprehensive approach to simulating offshore environments. The BEM continues to be a foundational tool in marine and offshore engineering, offering efficiency and adaptability for wave-structure interaction problems. However, its future relevance depends on overcoming limitations posed by nonlinear dynamics, large-scale applications, and multi-physics challenges.

Advances in higher-order formulations, hybrid models, and scalable computing are ensuring that BEM remains a critical enabler of innovations in wave energy, offshore wind, and coastal protection systems. As the demand for sustainable offshore energy grows, BEM's versatility will be central to meeting emerging engineering challenges.

2.5.1.8 Mooring and PTO Interactions

WECs are usually moored (except some fixed devices) and have PTO mechanisms—both of which interact with device motions. However, BEM by itself handles only the hydrodynamics of the free-floating body, typically assuming no external forces other than gravity and hydrostatics. Mooring forces and PTO forces must be introduced externally. In frequency-domain analysis, a common approach is to linearize these forces as equivalent springs and dampers. For instance, a catenary mooring can be linearized around an operating point to provide an approximate linear stiffness in surge/heave, which can be added to the equations of motion. A PTO (e.g., a hydraulic damper or linear generator) is often modeled as a linear damping term (and sometimes a stiffness if there's spring restoring or end-stop effects). These appear as additional terms in the dynamic equation: $M\ddot{x} + C_{hydro}(\omega)\dot{x} + K_{hydro}x + K_{mooring}x + B_{PTO}\dot{x} = F_{exc}(\omega)$. One must be careful because mooring dynamics can be highly nonlinear (especially for slack moorings that can go taut or for moorings with drag on lines). Tools like WEC-Sim address this by coupling to a mooring dynamics module (e.g., MoorDyn) that can simulate the mooring line behavior in time domain. Frequency-domain BEM analysis cannot capture mooring line dynamics like snap loads or line inertia; it can only include a linearized stiffness and perhaps a constant damping. This limitation means that certain platform motions (e.g., slow drift due to mooring elasticity, or asymmetry due to one mooring line engaging) are outside the scope of standard BEM analysis. The interaction of moorings with wave-frequency motion can also be significant: for example, a taut mooring line can increase the heave natural frequency of a device or induce couplings between heave and pitch. If not included, the BEM model's predicted resonance might be off. Therefore, in high-fidelity models, one would integrate the BEM hydrodynamics with a separate structural/mooring solver. BEM codes themselves usually allow simply adding a constant or linear spring to approximate moorings. Similarly, PTO damping might not be purely linear (some PTOs have nonlinear control or saturation), but in frequency-domain modeling it's assumed linear to use linear theory. This means BEM-based predictions of power assume an ideal linear PTO. If the real control strategy deviates (e.g., latching control, or tuning those changes with wave amplitude), a direct frequency-domain result might misestimate performance. In summary, mooring and PTO effects are not inherently included in BEM—they are added in post-processing or in coupled simulations. This is a limitation in that a "plain" BEM simulation of a device might show it drifting off or not constrained properly (since moorings aren't there), and one must incorporate those correctly to simulate the actual device. It's an area where time-domain modeling (with BEM input) is often preferred for fully capturing system behavior.

2.5.2 Future Directions

The future of WEC modeling likely involves more integrated software environments. BEM will be one component of a holistic design tool that might include structural analysis (to check stresses), control simulation (to implement advanced PTO strategies), and economic assessment (to connect performance with cost). Efforts like the Wave Energy Converter SIMulator (WEC-Sim) already integrate BEM results with time-domain dynamics, control, and moorings. We foresee BEM solvers being more tightly coupled with these tools—possibly even running in real-time co-simulation for controllers (for instance, a controller design tool might call a BEM solver on-the-fly to get wave force coefficients as it optimizes control). Additionally, as arrays and farms become a focus (for scaling up power output), BEM will be extended to handle multiple devices and interactions more efficiently. This could include considering shared moorings or platforms (e.g., a multi-WEC platform where hydrodynamics and structural modes interact). Some industry efforts are looking at combined wind-wave platforms; here, BEM (for the floaters) might need to work alongside blade-element momentum theory (for a wind turbine on the platform)—multi-physics coupling will be important. Finally, as an advancement in practice, the community is moving towards more open validation data and standardized benchmarks for WEC modeling. This will indirectly advance BEM by highlighting where models deviate and need improvement. Projects like the Wave Energy Code Comparison Project (WECCCOMP) involved numerous codes (including BEM-based) being compared on set scenarios. These collaborative efforts identify outliers and drive improvements (e.g., fixing bugs or adding features in codes like NEMOH). Future benchmarks may include more nonlinear cases, pushing BEM tools to adopt some nonlinear capabilities or smarter coupling. The continued feedback loop between experimental testing (like at new open-sea test sites) and BEM prediction will refine the tools.

References

1. Hall, W.S.: Boundary element method. In: Hall, W.S. (ed.) The Boundary Element Method, pp. 61–83. Springer Netherlands, Dordrecht (1994). https://doi.org/10.1007/978-94-011-0784-6_3
2. Kythe, P.K.: An Introduction to Boundary Element Methods. CRC Press, Boca Raton (2020). https://doi.org/10.1201/9781003068693
3. Cheng, A.H.-D., Cheng, D.T.: Heritage and early history of the boundary element method. Eng. Anal. Bound. Elem. **29**(3), 268–302 (2005). https://doi.org/10.1016/j.enganabound.2004.12.001
4. Gwinner, J., Stephan, E.P.: Advanced Boundary Element Methods: Treatment of Boundary Value, Transmission and Contact Problems. Springer Series in Computational Mathematics, vol. 52. Springer International Publishing, Cham (2018). https://doi.org/10.1007/978-3-319-92001-6
5. Liu, Y.J., et al.: Recent advances and emerging applications of the boundary element method. Appl. Mech. Rev. **64**(3), 030802 (2012). https://doi.org/10.1115/1.4005491

6. Beskos, D.E.: Boundary element methods in dynamic analysis. Appl. Mech. Rev. **40**(1), 1–23 (1987). https://doi.org/10.1115/1.3149529
7. Kane, J.H., Maier, G., Tosaka, N., Atluri, S.N. (eds.): Advances in Boundary Element Techniques. Springer Series in Computational Mechanics. Springer, Berlin, Heidelberg (1993). https://doi.org/10.1007/978-3-642-51027-4
8. Hsiao, G.C.: Boundary element methods—an overview. Appl. Numer. Math. **56**(10), 1356–1369 (2006). https://doi.org/10.1016/j.apnum.2006.03.030
9. Constanda, C., Doty, D., Hamill, W.: Boundary Integral Equation Methods and Numerical Solutions. Developments in Mathematics. Springer International Publishing, Cham (2016). https://doi.org/10.1007/978-3-319-26309-0
10. Langer, U., Steinbach, O.: Recent advances in boundary element methods. Comput. Methods Appl. Math. **23**(2), 297–299 (2023). https://doi.org/10.1515/cmam-2023-0037
11. Katsikadelis, J.T.L.: Boundary element technology. In: Katsikadelis, J.T. (ed.) The Boundary Element Method for Engineers and Scientists, 2nd edn., pp. 113–149. Academic Press, Oxford (2016). https://doi.org/10.1016/B978-0-12-804493-3.00005-9
12. Takahashi, T., Matsumoto, T.: An application of fast multipole method to isogeometric boundary element method for Laplace equation in two dimensions. Eng. Anal. Bound. Elem. **36**(12), 1766–1775 (2012). https://doi.org/10.1016/j.enganabound.2012.06.004
13. Lesnic, D.: The boundary element method for solving the Laplace equation in two-dimensions with oblique derivative boundary conditions. Commun. Numer. Methods Eng. **23**(12), 1071–1080 (2007). https://doi.org/10.1002/cnm.947
14. Takahashi, T., Hamada, T.: GPU-accelerated boundary element method for Helmholtz' equation in three dimensions. Int. J. Numer. Methods Eng. **80**(10), 1295–1321 (2009). https://doi.org/10.1002/nme.2661
15. Blyth, M.G., Pozrikidis, C.: A comparative study of the boundary and finite element methods for the Helmholtz equation in two dimensions. Eng. Anal. Bound. Elem. **31**(1), 35–49 (2007). https://doi.org/10.1016/j.enganabound.2006.07.005
16. Chen, L., et al.: Reduced order isogeometric boundary element methods for CAD-integrated shape optimization in electromagnetic scattering. Comput. Methods Appl. Mech. Eng. **419**, 116654 (2024). https://doi.org/10.1016/j.cma.2023.116654
17. Buffa, A., Hiptmair, R.: Galerkin boundary element methods for electromagnetic scattering. In: Ainsworth, M., Davies, P., Duncan, D., Rynne, B., Martin, P. (eds.) Topics in Computational Wave Propagation: Direct and Inverse Problems, pp. 83–124. Springer, Berlin, Heidelberg (2003). https://doi.org/10.1007/978-3-642-55483-4_3
18. Shaaban, A.M.: A review article: isogeometric boundary element analysis in engineering applications. Int. J. Hydromechatronics **5**(4), 366–396 (2022). https://doi.org/10.1504/IJHM.2022.127039
19. Su, R., Zhang, X., Tangaramvong, S., Song, C.: Adaptive scaled boundary finite element method for two/three-dimensional structural topology optimization based on dynamic responses. Comput. Methods Appl. Mech. Eng. **425**, 116966 (2024). https://doi.org/10.1016/j.cma.2024.116966
20. Hwu, C.: Boundary element analysis. In: Hwu, C. (ed.) Anisotropic Elasticity with Matlab, pp. 339–448. Springer International Publishing, Cham (2021). https://doi.org/10.1007/978-3-030-66676-7_15
21. Kazemi, S., Incecik, A.: Application of direct boundary element method to three dimensional hydrodynamic analysis of interaction between waves and floating offshore structures. In: ASME 2004 23rd International Conference on Offshore Mechanics and Arctic Engineering, American Society of Mechanical Engineers Digital Collection, pp. 755–761 (2008). https://doi.org/10.1115/OMAE2004-51429
22. Newman, J.N., Lee, C.-H.: Boundary-element methods in offshore structure analysis. J. Offshore Mech. Arct. Eng. **124**(2), 81–89 (2002). https://doi.org/10.1115/1.1464561
23. Guo, B., Wang, T., Jin, S., Duan, S., Yang, K., Zhao, Y.: A review of point absorber wave energy converters. J. Mar. Sci. Eng. **10**(10), 1534 (2022)

24. Shi, K. (石凯元), Zhu, R. (朱仁传): Efficient spectral coupled boundary element method for fully nonlinear wave–structure interaction simulation. Phys. Fluids **35**(5), 057121 (2023). https://doi.org/10.1063/5.0151990
25. Papillon, L., Costello, R., Ringwood, J.V.: Boundary element and integral methods in potential flow theory: a review with a focus on wave energy applications. J. Ocean Eng. Mar. Energy **6**(3), 303–337 (2020). https://doi.org/10.1007/s40722-020-00175-7
26. Hess, J.L.: Development and application of panel methods. In: Cruse, T.A. (ed.) Advanced Boundary Element Methods, pp. 165–177. Springer, Berlin, Heidelberg (1988). https://doi.org/10.1007/978-3-642-83003-7_18
27. Faltinsen, O.M.: Second order nonlinear interactions between waves and low frequency body motion. In: Horikawa, K., Maruo, H. (eds.) Nonlinear Water Waves, pp. 29–43. Springer, Berlin, Heidelberg (1988). https://doi.org/10.1007/978-3-642-83331-1_3
28. Garrison, C.J.: Interaction of oblique waves with an infinite cylinder. Appl. Ocean Res. **6**(1), 4–15 (1984). https://doi.org/10.1016/0141-1187(84)90023-3
29. Vaz, G., Falcão de Campos, J.A.C., Eça, L.: A numerical study on low and higher-order potential based BEM for 2D inviscid flows. Comput. Mech. **32**(4), 327–335 (2003). https://doi.org/10.1007/s00466-003-0490-8
30. Teng, B., Gou, Y.: BEM for wave interaction with structures and low storage accelerated methods for large scale computation. J. Hydrodyn. Ser. B **29**(5), 748–762 (2017). https://doi.org/10.1016/S1001-6058(16)60786-2
31. He, G., Kashiwagi, M.: Time-domain analysis of steady ship-wave problem using higher-order BEM. Int. J. Offshore Polar Eng. **24**(01), 1–10 (2014)
32. Tang, Y., Sun, S.-L., Abbasnia, A., Guedes Soares, C., Ren, H.-L.: A fully nonlinear BEM-beam coupled solver for fluid–structure interactions of flexible ships in waves. J. Fluids Struct. **121**, 103922 (2023). https://doi.org/10.1016/j.jfluidstructs.2023.103922
33. Min, E.-H., Kim, M.: Fully nonlinear wave interaction with 2D floating body including nonlinear sloshing tank. Ocean Eng. **307**, 118063 (2024). https://doi.org/10.1016/j.oceaneng.2024.118063
34. Zhou, X., Cheng, Y., Pan, S.: Time-domain higher-order boundary element method for simulating high forward-speed ship motions in waves. China Ocean Eng. **38**(5), 904–914 (2024). https://doi.org/10.1007/s13344-024-0071-5
35. Chen, R., Li, M., Ding, D.: A higher-order BEM discretization scheme for the EEG forward problem. In: 2024 Photonics & Electromagnetics Research Symposium (PIERS), pp. 1–3 (2024). https://doi.org/10.1109/PIERS62282.2024.10618161
36. Wei, Q., Xiang, J.: B-spline wavelet boundary element method for three-dimensional problems. Acta Mech. **232**(8), 3233–3257 (2021). https://doi.org/10.1007/s00707-021-03009-1
37. Landrini, M., Grytøyr, G., Faltinsen, O.M.: A B-spline based BEM for unsteady free-surface flows. J. Ship Res. **43**(01), 13–24 (1999). https://doi.org/10.5957/jsr.1999.43.1.13
38. Fast multipole boundary element method|Engineering mathematics and programming. Cambridge University Press. https://www.cambridge.org/be/academic/subjects/engineering/engineering-mathematics-and-programming/fast-multipole-boundary-element-method-theory-and-applications-engineering. Accessed 02 Mar 2025
39. Ibáñez, M.T., Power, H.: An efficient direct BEM numerical scheme for phase change problems using Fourier series. Comput. Methods Appl. Mech. Eng. **191**(21), 2371–2402 (2002). https://doi.org/10.1016/S0045-7825(01)00416-9
40. Yan, H., Liu, Y., Yue, D.K.P.: An efficient computational method for nonlinear three-dimensional wave-wave and wave-body interactions. J. Hydrodyn. **18**(1), 84–88 (2006). https://doi.org/10.1007/BF03400428
41. He, Y., Zhang, X., Zhang, T., Wang, C., Geng, J., Chen, X.: A wavelet immersed boundary method for two-variable coupled fluid-structure interactions. Appl. Math. Comput. **405**, 126243 (2021). https://doi.org/10.1016/j.amc.2021.126243
42. Harris, J.C., Dombre, E., Benoit, M., Grilli, S.T., Kuznetsov, K.I.: Nonlinear time-domain wave-structure interaction: a parallel fast integral equation approach. Int. J. Numer. Methods Fluids **94**(2), 188–222 (2022). https://doi.org/10.1002/fld.5051

43. Teng, B., Song, Z.: Extension of the frequency-domain pFFT method for wave structure interaction in finite depth. China Ocean Eng. **31**(3), 322–329 (2017). https://doi.org/10.1007/s13344-017-0038-x
44. Feng, A., You, Y., Cai, H.: An improved Rankine source panel method for three dimensional water wave problems. Int. J. Nav. Archit. Ocean Eng. **11**(1), 70–81 (2019). https://doi.org/10.1016/j.ijnaoe.2018.02.001
45. Feng, A., Sheng, L.: Numerical simulations of water wave problems with current effect. J. Mar. Sci. Technol. **24**(3), 738–755 (2019). https://doi.org/10.1007/s00773-018-0585-8
46. Verbrugghe, T., et al.: Coupling methodology for smoothed particle hydrodynamics modelling of non-linear wave-structure interactions. Coast. Eng. **138**, 184–198 (2018). https://doi.org/10.1016/j.coastaleng.2018.04.021
47. Bao, Y., Song, J., Liu, Z.: BEM based adaptive cross approximation algorithm for solving low frequency problems. In: 2018 IEEE International Symposium on Antennas and Propagation & USNC/URSI National Radio Science Meeting, pp. 2505–2506 (2018). https://doi.org/10.1109/APUSNCURSINRSM.2018.8608465
48. Zheng, X., Ji, M., Li, X., Zhou, S., He, X.: FMM-BEM algorithm based on improved free surface Green's function. Chaos Solitons Fractals **153**, 111497 (2021). https://doi.org/10.1016/j.chaos.2021.111497
49. Zhou, Y., Ning, D., Liang, D., Cai, S.: Nonlinear hydrodynamic analysis of an offshore oscillating water column wave energy converter. Renew. Sustain. Energy Rev. **145**, 111086 (2021). https://doi.org/10.1016/j.rser.2021.111086
50. Cho, I.H., Kim, M.H.: Hydrodynamic performance evaluation of a wave energy converter with two concentric vertical cylinders by analytic solutions and model tests. Ocean Eng. **130**, 498–509 (2017). https://doi.org/10.1016/j.oceaneng.2016.11.069
51. Bharath, A., Nader, J.-R., Penesis, I., Macfarlane, G.: Nonlinear hydrodynamic effects on a generic spherical wave energy converter. Renew. Energy **118**, 56–70 (2018). https://doi.org/10.1016/j.renene.2017.10.078
52. Dehghan, M., Hosseinzadeh, H.: Improvement of the accuracy in boundary element method based on high-order discretization. Comput. Math. Appl. **62**(12), 4461–4471 (2011). https://doi.org/10.1016/j.camwa.2011.10.023
53. Wu, H., Zhang, C., Zhu, Y., Li, W., Wan, D., Noblesse, F.: A global approximation to the Green function for diffraction radiation of water waves. Eur. J. Mech. BFluids **65**, 54–64 (2017). https://doi.org/10.1016/j.euromechflu.2017.02.008
54. Falnes, J., Kurniawan, A.: Ocean Waves and Oscillating Systems: Linear Interactions Including Wave-Energy Extraction, vol. 8. Cambridge University Press (2020)
55. Payne, G.: A modular graphical user interface for WAMIT. In: 7th European Wave and Tidal Energy Conference, Porto, Portugal, EWTEC, 2007. https://www.research.ed.ac.uk/en/publications/a-modular-graphical-user-interface-for-wamit. Accessed 08 Mar 2025
56. Penalba, M., Kelly, T., Ringwood, J.: Using NEMOH for modelling wave energy converters: a comparative study with WAMIT (2017)
57. Sheng, W., et al.: Hydrodynamic studies of floating structures: comparison of wave-structure interaction modelling. Ocean Eng. **249**, 110878 (2022). https://doi.org/10.1016/j.oceaneng.2022.110878
58. Eng, Y.-H., Chin, C.-S., Lau, M.W.-S.: Added mass computation for control of an open-frame remotely-operated vehicle: application using WAMIT and MATLAB. J. Mar. Sci. Technol. **22**(4) (2014). https://doi.org/10.6119/JMST-013-0313-2
59. Sjökvist, L., et al.: Calculating buoy response for a wave energy converter—a comparison of two computational methods and experimental results. Theor. Appl. Mech. Lett. **7**(3), 164–168 (2017). https://doi.org/10.1016/j.taml.2017.05.004
60. Kurnia, R., Ducrozet, G.: NEMOH: open-source boundary element solver for computation of first- and second-order hydrodynamic loads in the frequency domain. Comput. Phys. Commun. **292**, 108885 (2023). https://doi.org/10.1016/j.cpc.2023.108885
61. Uçar, M., Uzunoğlu, E., Oğuz, E.: Comparison and evaluation of open-source panel method codes against commercial codes. Gemi Ve Deniz Teknol. **221**(86), 108 (2022). https://doi.org/10.54926/gdt.1106386

62. Raghavan, V., Lavidas, G., Metrikine, A.V., Mantadakis, N., Loukogeorgaki, E.: A comparative study on BEM solvers for wave energy converters. In: Trends in Renewable Energies Offshore. CRC Press (2022)
63. Ancellin, M., Nguyen, N.: Case studies of BEM solver accuracy with the open-source code Capytaine. In: ASME 2024 43rd International Conference on Ocean, Offshore and Arctic Engineering, American Society of Mechanical Engineers Digital Collection (2024). https://doi.org/10.1115/OMAE2024-127995
64. Ancellin, M., Dias, F.: Capytaine: a Python-based linear potential flow solver. J. Open Source Softw. **4**(36), 1341 (2019)
65. Thanh Ta, D., Phan, Q.N., Truong, T.T.: Hydrodynamic analysis of point absorber wave energy converters using ANSYS Aqwa. J. Phys. Conf. Ser. **2949**(1), 012047 (2025). https://doi.org/10.1088/1742-6596/2949/1/012047
66. Ghesmi, M., von Graefe, A., Shigunov, V., Friedhoff, B., el Moctar, O.: Comparison and validation of numerical methods to assess hydrodynamic loads on mechanical coupling of multiple bodies. Ship Technol. Res. **66**(1), 9–21 (2019). https://doi.org/10.1080/09377255.2018.1482100
67. Mahmoud, M., Abdelkareem, M.A., Olabi, A.G.: Modeling and simulation of wave energy. In: Olabi, A.G. (ed.) Renewable Energy—Volume 2: Wave, Geothermal, and Bioenergy, pp. 85–101. Academic Press, 2024. https://doi.org/10.1016/B978-0-323-95211-8.00002-6
68. Yavuz, H., McCabe, A., Aggidis, G., Widden, M.B.: Calculation of the performance of resonant wave energy converters in real seas. Proc. Inst. Mech. Eng. Part M J. Eng. Marit. Environ. **220**(3), 117–128 (2006). https://doi.org/10.1243/14750902JEME44
69. Filippas, E.S., Belibassakis, K.A.: A nonlinear time-domain BEM for the performance of 3D flapping-wing thrusters in directional waves. Ocean Eng. **245**, 110157 (2022). https://doi.org/10.1016/j.oceaneng.2021.110157
70. Lei, J., Shao, C., Zhang, C.: Frequency-domain fundamental solutions and boundary element method for consistent couple stress elastodynamic problems. Int. J. Numer. Methods Eng. **124**(22), 4992–5019 (2023). https://doi.org/10.1002/nme.7335
71. Kelly, T., Zabala, I., Peña-Sanchez, Y., Ringwood, J., Henriques, J., Blanco, J.M.: A post-processing technique for removing 'irregular frequencies' and other issues in the results from BEM solvers. Int. J. Mar. Energy **5**(1), 123–131 (2022)
72. Shadmani, A., Nikoo, M.R., Gandomi, A.H., Chen, M., Nazari, R.: Advancements in optimizing wave energy converter geometry utilizing metaheuristic algorithms. Renew. Sustain. Energy Rev. **197**, 114398 (2024). https://doi.org/10.1016/j.rser.2024.114398
73. Brito-Melo, A., Sarmento, A.J.N.A., Clément, A.H., Delhommeau, G.: A 3D boundary element code for the analysis of OWC wave-power plants. In: The Ninth International Offshore and Polar Engineering Conference, OnePetro (1999)
74. Brito-Melo, A., Sarmento, A.J.N.A., Clement, A.H., Delhommeau, G.: Hydrodynamic analysis of geometrical design parameters of oscillating water column devices. In: 3rd European Wave Energy Conference, Patras, France, 1998. https://hal.science/hal-01155731. Accessed 08 Mar 2025
75. Ruehl, K., Porter, A., Posner, A., Roberts, J.: Development of SNL-SWAN, a validated wave energy converter array modeling tool (2013)
76. Pecher, R.: Breaking the symmetry with the multi-point well connection method. In: SPE Reservoir Simulation Symposium, OnePetro (2015). SPE-173302-MS. Accessed 08 Mar 2025
77. Delauré, Y.M.C., Lewis, A.: 3D hydrodynamic modelling of fixed oscillating water column wave power plant by a boundary element methods. Ocean Eng. **30**(3), 309–330 (2003). https://doi.org/10.1016/S0029-8018(02)00032-X
78. Raghavan, V., Simonetti, I., Metrikine, A.V., Lavidas, G., Cappietti, L.: A new numerical modelling framework for fixed oscillating water column wave energy conversion device combining BEM and CFD methods: validation with experiments. Ocean Eng. **301**, 117543 (2024). https://doi.org/10.1016/j.oceaneng.2024.117543
79. Dash, S.K., Koley, S., Zheng, S. (郑思明): Performance of an oscillating water column wave energy converter device under random ocean waves and ocean currents. Phys. Fluids **36**(10), 107165 (2024). https://doi.org/10.1063/5.0232117

80. Simonetti, I., Cappietti, L., El Safti, H., Oumeraci, H.: Numerical modelling of fixed oscillating water column wave energy conversion devices: toward geometry hydraulic optimization. In: ASME 2015 34th International Conference on Ocean, Offshore and Arctic Engineering, American Society of Mechanical Engineers Digital Collection (2015). https://doi.org/10.1115/OMAE2015-42056
81. Faÿ, F.-X., et al.: Comparative assessment of control strategies for the biradial turbine in the Mutriku OWC plant. Renew. Energy **146**, 2766–2784 (2020). https://doi.org/10.1016/j.renene.2019.08.074
82. Yu, Y.-H., Li, Y.: Reynolds-averaged Navier-Stokes simulation of the heave performance of a two-body floating-point absorber wave energy system. Comput. Fluids **73**, 104–114 (2013). https://doi.org/10.1016/j.compfluid.2012.10.007
83. Giannini, G., Day, S., Rosa-Santos, P., Taveira-Pinto, F.: A novel 2-D point absorber numerical modelling method. Inventions **6**(4), 75 (2021). https://doi.org/10.3390/inventions6040075
84. Li, D., et al.: Two-buoy and single-buoy floating wave energy converters: a numerical comparison. Energy **296**, 131219 (2024). https://doi.org/10.1016/j.energy.2024.131219
85. Giorgi, G., Penalba, M., Ringwood, J.: Nonlinear hydrodynamic models for heaving buoy wave energy converters. In: Asian Wave and Tidal Energy Conference, pp. 1–10. Singapore (2016). https://mural.maynoothuniversity.ie/id/eprint/9418/. Accessed 08 Mar 2025
86. Giorgi, G.: Performance assessment of a parametric-resonance wave energy converter: change of instability intensity going from regular to irregular waves. In: The 34th International Ocean and Polar Engineering Conference, OnePetro (2024)
87. Renzi, E., Dias, F.: Hydrodynamics of the oscillating wave surge converter in the open ocean. Eur. J. Mech. BFluids **41**, 1–10 (2013). https://doi.org/10.1016/j.euromechflu.2013.01.007
88. Child, B.F.M., Venugopal, V.: Optimal configurations of wave energy device arrays. Ocean Eng. **37**(16), 1402–1417 (2010). https://doi.org/10.1016/j.oceaneng.2010.06.010
89. Gobato, R., Gobato, A., Fedrigo, D.F.G.: Study Pelamis system to capture energy of ocean wave (2015). https://doi.org/10.48550/arXiv.1508.01106. *arXiv*: arXiv:1508.01106
90. Ghaedi, A., Sedaghati, R., Mahmoudian, M., Bazyari, S.: Reliability modeling of wave energy converters based on pelamis technology. Electr. Power Syst. Res. **227**, 109977 (2024). https://doi.org/10.1016/j.epsr.2023.109977
91. Choiniere, M., Davis, J., Nguyen, N., Tom, N., Fowler, M., Thiagarajan, K.: Hydrodynamics and load shedding behavior of a variable-geometry oscillating surge wave energy converter (OSWEC). Renew. Energy **194**, 875–884 (2022). https://doi.org/10.1016/j.renene.2022.05.169
92. Nguyen, N., Davis, J., Tom, N., Thiagarajan, K.: Theoretical modeling of a bottom-raised oscillating surge wave energy converter structural loadings and power performances. Appl. Ocean Res. **149**, 104031 (2024). https://doi.org/10.1016/j.apor.2024.104031
93. Raghavan, V., Lavidas, G., Metrikine, A.V.: Comparing open-source BEM solvers for analysing wave energy converters. J. Phys. Conf. Ser. **2647**(7), 072002 (2024). https://doi.org/10.1088/1742-6596/2647/7/072002
94. Kofoed, J.P., Frigaard, P., Friis-Madsen, E., Chr, H.: Sørensen, "Prototype testing of the wave energy converter wave dragon." Renew. Energy **31**(2), 181–189 (2006). https://doi.org/10.1016/j.renene.2005.09.005
95. Castro-Santos, L., Bento, A.R., Guedes Soares, C.: The economic feasibility of floating offshore wave energy farms in the North of Spain. Energies **13**(4), 806 (2020). https://doi.org/10.3390/en13040806
96. Babarit, A.: On the park effect in arrays of oscillating wave energy converters. Renew. Energy **58**, 68–78 (2013). https://doi.org/10.1016/j.renene.2013.03.008
97. Han, M., Cao, F., Shi, H., Zhu, K., Dong, X., Li, D.: Layout optimisation of the two-body heaving wave energy converter array. Renew. Energy **205**, 410–431 (2023). https://doi.org/10.1016/j.renene.2023.01.100
98. Chu, B. (储备) et al.: Viscous effects on the hydrodynamic performance of a two-body wave energy converter with a damping plate. Phys. Fluids **36**(9), 092116 (2024). https://doi.org/10.1063/5.0230250

99. Oyegbemi, K.O., Charles, O.U., Ibiaba, D.: Performance analysis of a point absorber wave energy converter in Nigerian West Coast; Gulf of Guinea. Int. J. Mar. Eng. Innov. Res. **8**(2) (2023). https://doi.org/10.12962/j25481479.v8i2.16718
100. Rusu, E., Onea, F.: The expected dynamics of the European offshore wind sector in the climate change context. J. Mar. Sci. Eng. **11**(10), 2023 (1967). https://doi.org/10.3390/jmse11101967

Chapter 3
Wave Energy Converter Principles and Geometry Design

Abstract Wave energy converters (WECs) represent sophisticated engineering systems designed to transform the irregular, oscillatory motion of ocean waves into usable electrical power. This chapter examines the critical relationship between WEC device principles and their geometric design, highlighting how form directly influences functionality across diverse operational environments. By understanding the fundamental physical interactions between device geometry and wave hydrodynamics, engineers can develop more efficient, resilient, and economically viable wave energy solutions. The chapter is structured to provide comprehensive coverage across five interconnected sections. The fundamentals of WECs section establishes the core operating principles and classification systems, detailing energy extraction mechanisms, degrees of freedom, and power take-off approaches that determine overall system architecture. The geometry design principles section explores how specific geometric parameters—including scale, proportion, shape characteristics, and orientation—influence hydrodynamic response factors such as added mass, radiation damping, and resonance bandwidth, with dedicated analysis of geometric considerations for different WEC types. Optimization techniques in WEC geometry design presents advanced methodologies spanning from analytical approaches to sophisticated computational methods including high-fidelity CFD simulations, parametric optimization algorithms, and emerging machine learning applications that enable multi-objective design optimization across competing performance criteria. The case studies section provides detailed examples of geometry optimization in prominent WEC designs, demonstrating how theoretical principles translate into practical design decisions within specific operational contexts. The final section examines future trends in WEC design, including multi-functional structures serving purposes beyond energy generation, bio-inspired geometries leveraging evolutionary adaptations found in marine organisms, and adaptive morphing systems capable of reconfiguring to optimize performance across varying wave conditions.

Keywords Wave energy converter · Geometric optimization · Hydrodynamic response · Resonance bandwidth · Bio-inspired design

A. Shadmani et al., *Ocean Wave Energy Technology*,
https://doi.org/10.1007/978-3-031-95040-7_3

3.1 Fundamentals of WECs

Wave energy converters (WECs) are advanced engineering systems designed to capture and convert the immense kinetic and potential energy of ocean waves into mechanical power or electricity. This energy, driven by atmospheric winds and large-scale weather systems, provides a perpetual and largely untapped source of power along coastlines worldwide.

When waves encounter a WEC, a complex interaction occurs between the incident wave field and the device. In linear hydrodynamics, the total wave field is considered as a superposition of three components, as explained in Sect. 2.2. In effect, the WEC absorbs energy from the incident wave by emitting waves that reduce the wave energy propagating past it. Energy conservation demands that the "missing" wave energy is transferred into the device. Thus, optimal energy capture often involves the WEC radiating a wave that destructively interferes with the incident wave on the downstream side, effectively trapping energy in the device.

Crucially, a WEC must oscillate in tune with the waves to absorb energy. The principle of resonance is often exploited. When the device's natural oscillation frequency matches the incoming wave frequency even small waves can drive large-amplitude motions. At resonance, the wave-induced excitation force is in phase with the device's velocity, so the device efficiently absorbs energy, which is known as resonant or tuned absorption. Off-resonance, much of the wave energy is reflected or remains in the wave, yielding lower capture. In practice, WECs interact with irregular sea, so maintaining resonance over a range of frequencies is challenging. Nonetheless, the core wave-body interaction physics remains. The device extracts energy by exerting force on the water through wave radiation and diffraction effects and having the water do work on the device in return.

Most WECs are essentially oscillators that absorb energy from waves by moving back and forth. Common modes of motion include heave, surge, pitch/roll, or internal water sloshing in terminator devices. As waves pass, the device (or part of it) oscillates relative to a reference frame, which could be the seabed, a stationary structure, or another body. This relative motion is a key. For instance, a floating buoy moving up and down can pull against a fixed reference or a heavier second body, doing work in the process. The wave's alternating forces lead to an oscillatory force-displacement cycle, and by introducing a PTO damping, the kinetic energy of oscillation can be extracted as work. Essentially, the WEC behaves like a damped mass-spring system. Wave excitation drives the mass (device) against a spring (hydrostatic restoring force) and a damper (the PTO). When tuned properly, especially near resonance, the motion is sizable, and the PTO damper can optimally extract energy by being in phase with velocity. To maximize energy extraction, WECs rely on an integrated network of mechanical, hydraulic, and electrical components especially designed for different wave conditions and deployment environments. The success of a WEC installation depends on the proper integration of its subsystems and their ability to adapt to environmental variations. WEC designs are diverse—over a thousand concepts have been

reported historically [1]—but they are commonly classified by operating principle and configuration.

During each wave cycle, the wave induces a force on the device and moves it. For example, lifting a buoy on the wave crest and dropping it in the trough, thereby doing work. The mechanical energy of this motion is then converted by the PTO into electricity or other forms. Resonance greatly amplifies this process: at resonance, the device oscillates with maximum amplitude for a given wave input, and the phase alignment means the PTO sees a force and velocity aligned for maximum power transfer. However, WECs must also avoid phase mismatches that would cause the device to alternately give energy back to the waves (as "reactive power"). In multi-degree-of-freedom devices, several oscillation modes can be exploited (e.g. an overtopping device might convert heave motion into potential energy of elevated water, etc.). No matter the design, the fundamental mechanism is wave-induced oscillatory motion to mechanical work extraction [2]. The wave's energy is transferred to an oscillating body or fluid, and through that motion is fed into a PTO. By properly designing the geometry and inertial properties, WECs maximize coupling with waves (often by length scale tuning to wave wavelength) and use resonance to increase energy transfer. This conversion mechanism is inherently cyclic and oscillatory, requiring robust design to handle continuously changing loads and bidirectional motion.

Therefore, in the next section, a classification of various WECs based on their operational principles and geometric configurations will be presented.

3.2 Geometry Design Principles for WECs

The geometry of WEC fundamentally dictates its efficiency, stability, and adaptability to varying marine conditions. As WECs interact with dynamic wave environments, their geometrical configuration must balance energy capture efficiency, mechanical robustness, and cost-effective maintenance. The design of a WEC's geometry influences how it interacts with incident waves, determines its resonance characteristics, and affects key operational metrics such as power output, durability, and survivability [3]. Accordingly, a fundamental aspect of WEC design involves understanding wave-structure interactions and optimizing resonance effects.

Resonance occurs when the natural frequency of the WEC aligns with the dominant wave frequencies at the deployment site, significantly enhancing energy capture efficiency. Achieving resonance requires precise adjustments to the device's geometry, mass distribution, and overall structural properties. Additionally, successful WEC design must account for:

- Site-specific wave resource assessments: Evaluating local wave conditions ensures that the device is appropriately tuned for optimal performance.
- Device survivability: Designing for extreme wave events and environmental conditions is critical to long-term operation.

Fig. 3.1 Main categories of WECs with an example device

- Environmental impact mitigation: Consideration of marine ecosystems, coastal impacts, and regulatory requirements is necessary to minimize adverse effects.

Incorporating these factors into the design and deployment process ensures that WECs operate efficiently and sustainably, contributing to the broader renewable energy landscape. To optimize these benefits, it is crucial to understand the different classes of WECs, each defined by unique operational principles and geometric configurations tailored to specific wave energy capture mechanisms (Fig. 3.1). These devices can be broadly categorized into six distinct classes, as the characteristics of each category is depicted in Fig. 3.2:

(1) Oscillating water columns (OWC)
(2) Point absorbers
(3) Attenuators
(4) Terminators
(5) Overtopping devices
(6) Submerged pressure differential.

OWCs are devices that trap a column of air above a column of water inside a partially submerged chamber. As waves enter and exit the chamber, the water column rises and falls, acting like a piston on the air above it. This wave-induced air pressure drives a bi-directional turbine (often a Wells turbine that rotates in the same direction regardless of airflow) to generate electricity. The chamber is open below the waterline to allow wave interaction, and as waves pass, the air is alternately compressed and decompressed, producing an oscillating air flow through the turbine. OWCs can be onshore or offshore. Their working principle is analogous to a wind turbine but driven by oscillating air flow induced waves rather than steady wind. While the Wells turbine in an OWC has a moderate efficiency (~50–60%) compared to a unidirectional turbine, it is effective for the OWC's oscillating airflow. OWCs are one

of the more mature WEC technologies, with several prototypes and even commercial installations, e.g., the Mutriku breakwater OWC plan in Spain [4]. Studies show that chamber geometry strongly influences performance. For instance, a comparative study found a curved front wall and bottom profile produced higher pneumatic pressure and turbine power than a simple flat-bottom chamber. A circular curved bottom helps concentrate the oscillating water mass, yielding greater efficiency than triangular or stepped bottoms [5]. Similarly, the orifice (turbine) size relative to chamber volume must be tuned: too large and the pneumatic damping is low (water column oscillates freely but does less work on air), too small and the chamber is stiff (reflects waves). Onshore OWCs often optimize geometry for the dominant swell period at the deployment site, achieving resonance that greatly amplifies the internal water motion.

Offshore (floating) OWCs come in various geometries. Spar-buoy OWCs (a long vertical cylinder with an internal chamber, e.g. OceanEnergy's OE35 buoy [6]), backward-bent duct buoys (BBDB) which have an L-shaped chamber open at the bottom and facing the waves, and multi-chamber barge designs [7]. Floating OWCs introduce additional degrees of freedom—the entire device can heave, pitch, or surge, which interacts with the internal water oscillation. The geometry must therefore balance hydrodynamic stability with pneumatic performance [8]. A tall spar OWC has high inertia and remains relatively stable, allowing the water column to oscillate nearly as if fixed. In contrast, a shorter barge OWC will move more, potentially in phase with the water column and thus altering the effective amplitude. Geometric studies have examined adding skirts or damping plates to floating OWCs to adjust their motion response. Common geometric parameters for floating OWCs are the chamber draft (depth of opening), the waterplane area or outer hull size (affecting its heave natural period), and again the turbine orifice. For example, the OE35 buoy (35 m diameter hull) uses a large radial chamber to ensure sufficient air volume and a draft ~ 10 m to capture pressure variations, and its hull geometry yields a heave period around the wave period for resonance. Many floating OWCs are slack-moored and can survive by submerging the mouth below extreme wave troughs, avoiding strong slamming. For instance, the Mighty Whale (an early floating OWC test barge in Japan) had a wide, stable geometry and survived typhoons by virtue of its bulk and closed air valves to cushion impact. For floating OWCs, the geometry is a compromise between maximizing air column oscillation and maintaining platform stability. A floating OWC's efficiency can rival that of other types if the chamber is large—the OE35 (an 826-ton device) targets 500 kW power, using its sheer size to capture energy. Survivability for OWCs, particularly floating ones, relies on geometry too. A low center of gravity and broad beam can ensure the OWC does not overturn in storms.

Onshore OWCs have shown reliable long-term operation; their rigid geometry (often concrete) easily withstands wave impacts, and by design, waves mainly enter the chamber rather than directly slamming a structure. The energy capture of a well-designed OWC is significant. Mutriku's chambers each generate ~ 18 kW average (with ~ 30 kW turbine capacity) from ~ 2–3 m Atlantic swells, thanks to geometric resonance. Onshore OWCs share structural loads with the coastline or breakwater in which they are built, often an advantage—the breakwater provides wave protection for the chamber to some extent, and in return the OWC can contribute to coastal protection

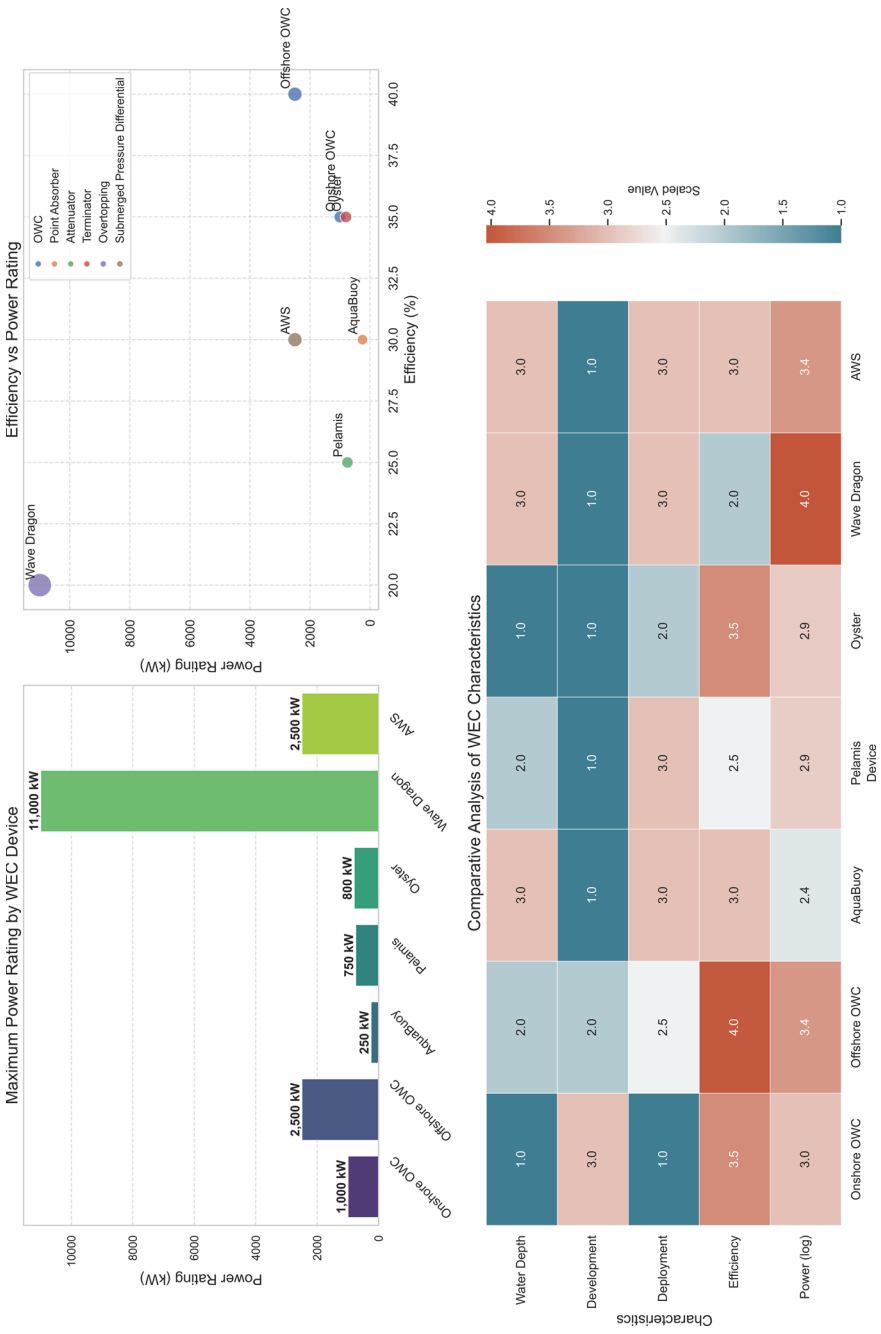

Fig. 3.2 Comparative analysis of various WEC characteristics

and power production simultaneously. One downside is that fixed OWCs are not easily tuned after construction; hence getting the geometry right is critical [9].

Recent research into OWC geometry has focused on innovative chamber designs: U-OWC and multi-chamber systems, and tunable geometry [10]. A U-shaped OWC (with a U-tube duct under water connecting to the chamber) allows more parameters (like duct length, diameter) to tweak resonance. For floating OWCs, experiments like those on the spar-buoy OWC have refined how draft and diameter affect the dual-mode (platform + water column) dynamics [11]. Additionally, there is interest in hybrid geometries—e.g., an OWC combined with a point absorber or an oscillating flap in one platform (to capture multiple modes) [12, 13]. As OWCs involve both hydrodynamics and aerodynamics, sophisticated coupled models now optimize the chamber geometry along with turbine characteristics. The consensus in recent literature is that geometry optimization of OWCs can significantly improve performance (capture width and phase tuning) without major cost increase, making it a high-impact design area.

Point absorbers are typically buoy-like devices that absorb wave energy in all directions (omnidirectional) through the vertical heave or pitching motion of a buoy relative to a reference frame (such as a seabed anchor or an internal mass) [14]. Point absorbers are usually compact (small relative to wavelength) floating structures at or near the surface, moving with the waves. The wave-induced motion (heave, surge, or pitch) is resisted by a PTO mechanism, e.g., a hydraulic piston or linear generator, converting the oscillatory motion into electricity. A well-known example is the heaving buoy, where a buoy's up-and-down motion is converted via a linear generator or hydraulic system. These devices can also have internal oscillating masses, e.g., a pendulum or gyroscope, instead of an external reference. For instance, devices like the SEAREV [15] and ISWEC [16] use an internal pendulum or gyroscope to harvest energy from the hull's motion. These types of WECs operate effectively by tuning their natural oscillation to the incoming wave frequency (resonance) to maximize energy absorption. These devices are one of the most widely studied WEC types due to their simplicity and promising performance [14, 17]. The AquaBuoy, for example, was a floating buoy ~ 5 m in diameter that absorbed energy through heave (up-down motion) of the buoy and an internal water column [18]. Point absorbers typically have simple axisymmetric geometries (cylinder, sphere, cone, etc.), so that they respond similarly to waves from any direction. The buoy's geometry—size, shape, draft—directly influences its natural resonance frequency and RAO. A well-chosen geometry will resonate in the dominant wave period, amplifying motion and power capture. Research in recent years has compared a wide range of shapes. Cylinders (with flat or conical bottoms), spheres, cones, and hybrid profiles.

For instance, one study found that a cylinder with a conical bottom outperforms a flat-bottom cylinder in heave, yielding higher RAO, absorbed power, and capture width ratio [19]. Likewise, comparing five hull shapes for a heaving buoy showed that the optimal radius and draft depend on the shape; no single shape is universally best, underscoring that geometry must be tuned to the site wave spectrum. This type of device, by virtue of its small size, have a limited instantaneous capture area, but they can achieve high relative absorption through resonance and motion control [20, 21].

From a survivability perspective, point absorbers benefit from being omnidirectional and often slack-moored—in extreme seas, they can simply heave with waves or submerge rather than resist them. Simpler geometry (e.g. a sphere) distributes stress uniformly and has no sharp corners for stress concentrations. Some designs (like the hemisphere-bottom buoy) tend to submerge under very large waves, effectively shedding excess wave energy. Still, extreme heaving can lead to large mooring loads or stroke limits; thus, many point absorbers include end-stop dampers or submergence control. The AquaBuoy design, for instance, had a tuned hose-PTO that naturally limited force at end extremes. In terms of scalability, point absorbers are highly modular—many small buoys can be deployed in an array to scale up power output. Their geometry is relatively easy to mass-produce (e.g. steel spheres or cylinders), though each unit is lower power (~ tens or hundreds of kW). This modularity and the benign geometry (essentially a buoy) make them attractive for survivability: if a storm destroys some units, others remain, and replacement is straightforward.

Recent theoretical and computational developments have provided clearer guidelines on point absorber geometry. High-fidelity simulations (including nonlinear effects) have shown, for example, that dome or cone-shaped bottoms can reduce viscous losses and improve off-resonance capture. Designers also increasingly consider two-body point absorbers (a float and a reacting mass)—while not single-body geometry per se, the relative size of the two bodies is a geometric optimization problem. Studies report that two-body systems can significantly broaden the frequency bandwidth of absorption at the cost of added complexity [22]. On the experimental side, various scaled buoy shapes have been tested in wave basins to validate numerical predictions. One notable finding is that geometric tweaks to the bottom profile (concave, convex, etc.) can alter the pressure distribution and radiation pattern, thus tuning the damping characteristics [23]. As a result, current design practice for point absorbers involves iterating on geometry (often with smooth, curved profiles defined by Bézier or spline curves) to achieve an optimal balance of added mass and radiation damping that maximizes average power over a site's wave spectrum [22].

Attenuators are long multi-segment floating structures oriented parallel to the wave direction along the wave crests. These devices "ride" the waves and extract energy from the relative motion of their segments as waves travel down their length. Hinges or joints between segments experience flexing as the wave crest and trough pass along the device [24]. Hydraulic rams or other PTO at the hinges resist this bending motion and generate power. The classic example is the Pelamis attenuator, a multi-segment snake-like device (approximately 120–180 m long) where waves induce bending at joints to drive hydraulic generators [25]. By aligning with wave direction, attenuators capture energy from the wave's horizontal undulation. Their geometry (length and segment spacing) is often chosen, approximately half the wavelength to maximize the relative motion between segments. Attenuators tend to operate in offshore sites with long-period swells. They have the advantage of modular segmentation which can ease transportation and potentially allow flexible response to waves, but they require robust joints to survive bending forces [26–28].

As waves propagate along the length, the segments flex at the hinges, and this relative motion drives hydraulic PTO units in the joints. Key geometric parameters include the segment length and draft, and the hinge spacing. Optimization studies indicate that these dimensions strongly affect performance [29]. Longer segments increase capture in longer-period waves, but if too long, the device may bridge over shorter waves, reducing absorption. Likewise, segment draft i.e., submergence, influences which wave heights are effectively engaged. A recent survey notes that for Pelamis-type attenuators, the length and draught of each segment, and the distance between segments should be optimized to maximize hydrodynamic performance. Too close spacing can cause segments to interfere, whereas too far reduces coupling. The attenuator's geometry enables it to ride waves in a snaking motion, attenuating wave energy over its length. This yields a high capture width relative to its narrow cross-section. Pelamis achieved utility-scale outputs (~750 kW per device) with a long slender geometry that is modular and scalable (more segments can be added for longer devices). Notably, longer attenuators tend to capture more energy in long-period swells, while shorter ones respond better to shorter waves—a trade-off in geometry selection. For survivability, the segmented geometry is advantageous: the hinges allow flexibility so that the device can conform to steep waves rather than breaking. However, large waves can induce extreme hinge angles, so end-stop mechanisms are installed to prevent over-bending at joints [30]. Pelamis's joints were engineered to lock or limit motion beyond safe angles, sacrificing some energy capture in extreme seas to save the structure. The slim cylindrical sections also weathervane (passively align) into the wave direction, presenting a narrow profile to head-on storm waves—another geometric survivability feature [18, 31].

Empirical tests on scaled attenuators (e.g. the multi-cylinder M4 device) showed that bottom shape and device scale affect capture width ratio, indicating designers can tweak hull cross-sections (circular vs. rectangular) and overall size to improve efficiency. Recent work also considers using variable geometry in attenuators—for instance, adjustable draft or deployable flaps—to retune the device in different sea states, analogous to how Pelamis could actively adjust its PTO damping per joint. Modern simulation tools (WEC-Sim, etc.) allow detailed modeling of multi-body attenuators, capturing the complex hydrodynamic interactions between segments. In the past five years, studies have explored novel attenuator geometries such as hinged rafts and multi-float designs (e.g. the M4 with four hinged buoys) [30]. These investigations optimize segment count vs. performance, showing diminishing returns beyond a certain number of bodies due to internal wave cancellations. There is also growing experimental evidence on scaling: one comparison found that a larger-scale attenuator had better efficiency per unit length than a smaller-scale version, due to relatively lower friction and end losses [30]. Overall, the Pelamis-class attenuator remains a reference design; recent improvements aim to refine joint design (reducing stress concentration) and hull shapes (for improved hydrodynamics and easier deployment). The geometry-driven balance between energy capture and structural articulation continues to be a focal point of attenuator WEC design.

Oscillating wave surge converters (OWSC) often simply called surge of flap devices, these WECs typically consist of a hinged flap or paddle that oscillates

back and forth with the horizontal movement of water particles (surge motions) in waves [32]. They are termed "terminators" because they interact with and absorb wave energy by presenting a broad surface (flap) perpendicular to the wave direction, effectively terminating the wave. The flap is usually hinged at the bottom (seabed) or sometimes at the surface, and as waves pass, the flap swivels like a door swinging in the waves. PTO systems often hydraulic cylinders at the hinge resist this motion and convert it to electricity [33, 34]. Examples include the Oyster device, a large bottom-hinged flap in nearshore waters [35], and the WaveRoller, a bottom-hinged plate [33]. Another famous design is Salter's duck, a teardrop-shaped oscillating cam that bobbed in pitch like a duck nodding—it achieved very high energy capture in trials (the duck's shape was highly optimized for wave absorption) [36]. Terminator devices typically are deployed in nearshore or intermediate depths where surge motion is strong, and wave directionally is consistent. They can achieve high efficiencies in energy capture by sweeping a large area of the wave front but aligning them to predominant wave direction and engineering the hinge for extreme loads are key challenges.

OWSCs like Aquamarine Power's Oyster consist of a large buoyant flap hinged at the seabed (or a substructure) and protruding above the water surface [37]. Incoming waves drive the flap to oscillate in surge, harnessing the horizontal water particle motion. the geometry—a broad, rectangular panel—presents a large capture area to incoming wave fronts, enabling strong wave coupling and high energy absorption. The Oyster flap (about 18 m by 12 m in Oyster 800) effectively acts as a terminator, intercepting wave energy over its width. Hydrodynamic studies show OWSCs can achieve high capture efficiency; for example, optimizing flap shape can boost the capture factor ~ 30% (from ~ 0.37 to 0.48) relative to a flat rectangular flap. Recent bio-inspired designs mimicking scallop shapes yielded a seaward-curved flap that improved energy capture by increasing hydrodynamic pressure differentials across the flap. The flap's size, thickness, and submergence depth are crucial geometry parameters—a taller/wider flap can capture more waves thrust but faces higher bending moments. To balance this, researchers optimize OWSC aspect ratios and may add features like cambered surfaces or flow vanes to enhance torque without excessive loads. The OWSC's geometric advantage is strong wave coupling in the surf zone, which yields high power output to an onshore PTO, e.g., Oyster's hydraulic pistons, even in moderate waves. Oyster demonstrated capture width ratios exceeding its 12 m width in certain seas, making OWSCs among the most efficient WECs in shallow water. At the same time, geometry is tuned for survivability—the simplicity of a single moving flap with few subsea moving parts improves reliability. In extreme waves, the hinged flap can freely deflect to avoid damage. This inherent compliance is a key survivability feature. Unlike rigid structures, a flap can shed loads by going with the flow. Recent CFD studies of OWSCs confirm that reducing flap width or submerging it deeper lowers wave impact forces at a modest efficiency trade-off. Some modern OWSC designs even allow retracting or lowering the panel during storms. Thus, geometry optimization seeks an efficient profile to maximize surge excitation while ensuring the structure can withstand or avoid peak loads.

The last five years have seen extensive numerical modeling and experimental wave tank testing of OWSC geometries. For instance, Wang and Liu [38] optimized a scallop-edge flap via a radial-basis surrogate and found an ideal curvature that maximized power across varying wave periods. Other studies analyzed bottom-hinged vs. mid-depth hinged flaps, flap arrays, and the influence of bottom slope on OWSC performance since nearshore bathymetry affects surge motions. Experimentally, scale models of device like Oyster have validated that capture efficiency peaks at an optimal flap width-to-depth ratio, beyond which added width brings diminishing returns due to wave shielding and structural strain. Overall, OWSC geometry research emphasizes achieving broadband absorption while maintaining a robust, compliant structure.

Overtopping devices mimic a low-head hydropower dam concept. They use wave action to collect water in a reservoir above the mean sea level, then release it through turbines [37]. In practice, overtopping devices have structures (ramps or funnels) that waves rush up or over, filling a raised reservoir. The Wave Dragon is a well-known overtopping device: it has large wing-like arms to focus waves on a central ramp; waves overtop into a basin and then flow out through low-head hydro turbines to generate power. Because they rely on a head difference, overtopping generally is very large structures—Wave Dragon, for instance, was envisioned at 260 m width, 4–7 MW capacity for an optimized design [39]. Overtopping devices can be floating (offshore Wave Dragon) or fixed as part of breakwaters/coastal structures (e.g. the SeaWave Slot-Cone Generator integrated into a breakwater [40], which had multiple tiered reservoirs). While conceptually simple, they require handling large volumes of water; thus, efficiency gains often come from large scale and concentration of wave energy. One issue is that typical ocean waves have limited height, so overtopping volumes (and thus head for the turbines) are modest, leading to lower overall efficiency in practice (often $< 30\%$ wave-to-wire). Still, their advantage is using proven low-head hydro turbines and potentially serving double-duty as coastal protection structures.

According to recent reviews, key design parameters for overtopping include the reflector angle, ramp shape, freeboard height, and device draft. For instance, a gentler ramp slope can improve capture of a wide range of wave heights but may result in a larger (costlier) structure [41]. Wave Dragon's reflectors are adjustable in angle to suit wave climates—a narrower angle channels more wave energy into the trap for small waves, while a wider angle can be used in energetic seas to avoid overloading. The Wave Dragon is essentially a terminator spanning a broad frontage, so it can capture a large percentage of incident wave energy. Its conversion process is two-stage (waves to potential energy, then to electricity via turbines), with reported overall efficiencies around 20–30% [42]. The geometry plays a big role: too low a freeboard and waves will frequently overtop (high capture but risk spilling and structural strain); too high and few waves overtop (missed energy). Optimizing this geometry is an active area—experiments have shown that adding wave focusing walls or curvature to the reflectors increases overtopping flow rates and hence power output.

On the survivability front, Wave Dragon's massive size and slack mooring give it passive protection. Floating overtopping devices ride the waves, alleviating some

impact—indeed, one CFD analysis showed the device can heave and pitch under large waves without structural failure [43]. However, because it presents a large target, extreme waves impart huge forces: a simulation study found that increasing significant wave height from 1.5 to 4.5 m caused a 6.5-fold increase in wave impact force on Wave Dragon [42]. Thus, structural resilience demands robust hull construction (often in concrete or heavily reinforced steel) and possibly survival modes like opening additional overflow gates or submerging the structure slightly to let waves pass over. Scalability of overtopping is both a benefit and a challenge—they can be built very large (multi-MW capacity), but costs scale quickly with size. New concepts like the WaveCat (a V-shaped dual-hull overtopping) and the Sea Slot-Cone Generator (SSG) (a stepped reservoir overtopping) aim to use geometry more efficiently [44]. For example, SSG uses multiple smaller reservoirs at different heights; geometry optimization of the ramp and slots ensures each wave overtops at least one level, increasing overall capture across wave conditions. In recent years, computational modeling (using CFD and wave basin tests) has greatly enhanced understanding of overtopping flow and geometry interaction. Researchers now simulate overtopping rates over varied ramp shapes—one study compared overtopping with straight, concave, and convex ramps, finding that a curved ramp can reduce reflection and increase reservoir fill rate in certain wave regimes. The use of dual and multi-level reservoirs (as in Wave Dragon vs. SSG) has been explored to capture a broader range of wave heights efficiently. Additionally, the integration of overtopping devices into coastal structures (e.g. overtopping breakwaters) is a geometric co-design problem: the structure must function as both a seawall and an energy device. Such hybrid designs benefit from shared costs, and the fixed geometry can be optimized (e.g. modifying the crest shape of a breakwater-OWEC to enhance wave capture). The comparative analysis of Wave Dragon and WaveCat in literature shows that planform geometry (the layout of collectors) strongly influences directional capture performance [45]. WaveCat's angled hulls proved advantageous in directional wave climates, whereas Wave Dragon's symmetric spread works well for head-on waves [46]. Overall, overtopping WEC development is refining large-scale geometry for maximal collection efficiency while employing materials and structural forms (like pontoon-supported reservoirs) that can survive the harsh ocean environment.

Submerged pressure differential devices (e.g. the Archimedes Wave Swing) are placed fully underwater (often near the seabed) [47]. Waves passing overhead cause pressure changes that drive an internal floater or diaphragm up and down, generating power from that motion. The geometry here is typically axisymmetric and sealed—in AWS, a domed top "piston" moving within a cylindrical chamber. Important geometric parameters include the diameter of the floater (horizontal cross-section), its stroke (gap), and the submergence depth of the device. Submergence is crucial: being deeper reduces the wave-induced pressure differential (improving survivability but reducing power), while being shallower increases excitation but exposes the device to stronger forces. Thus, geometry optimization seeks an optimal submergence. Studies show that fully submerged one-body devices are highly sensitive to submergence depth—even a small change can significantly alter hydrodynamic performance [48].

By being submerged, AWS-type devices inherently avoid the violent surface motions; survivability is enhanced since storm waves pass overhead with less pressure fluctuation at depth. Indeed, the AWS concept touts the ability to endure extreme seas with minimal risk, a stark contrast to surface-borne devices. However, the trade-off is that the available energy (pressure differential) is smaller than at the surface. To compensate, the geometry often must have a large area (diameter) to intercept sufficient wave pressure force. The original AWS prototype (circa 2004) had a ~ 6 m diameter floater and produced on the order of (tens of) kW in moderate waves. Recent trials of an updated AWS demonstrated peaks of 80 kW from a 7 m diameter, 50-ton device, exceeding expected performance by ~ 20% [49]. Crucially, tuning is key to power capture. AWS uses an air spring (an internal air volume) whose pressure can be adjusted to tune the oscillation frequency. This tuning effectively changes the device's stiffness, analogous to altering geometry. By dynamically tweaking internal pressure, the system adapts to wave periods for resonance, greatly boosting efficiency across sea states. Geometry influences this tuning range (a larger volume or different shape changes the baseline stiffness). For structural resilience, the shape of the floater and chamber must handle repeated pressure cycling—a rounded dome is ideal to distribute stress.

Modern design of pressure-differential WECs has introduced variable-geometry features to broaden their operational envelope. For example, researchers at NREL proposed a submerged plate WEC with deployable flaps that can open or close, effectively changing the device's width and added mass in different wave frequencies [50]. Simulations showed that such variable geometry can "reduce wave and PTO loading" in storms and "tune the radiation coefficients" to improve power capture in various sea states. In essence, the device could morph to a low-loading shape (smaller projected area) when waves are large, and a high-capture shape when waves are moderate. This concept improved the theoretical capacity factor by ensuring the device isn't overwhelmed in large seas. On the computational front, fully coupled time-domain models now capture the nonlinear dynamics of submerged WECs (including compressible air springs and end-stop limits). There is also exploration of multi-float or array configurations. For instance, clustering multiple AWS units into one platform for multi-MW output. Geometrically, this raises questions of spacing and shielding between units (like arrays of point absorbers). Nevertheless, the single-unit geometry has matured [51]. The AWS's latest design uses a tension-tether mooring and self-installing buoy, showing that thoughtful geometry (compact cylindrical form) can simplify deployment and maintenance. In summary, submerged pressure differential WECs leverage geometry for reliability, using large cross-sectional area and tunable internal volumes to capture energy, all while remaining inherently robust against the ocean's fury [52].

Despite the variety, all WECs share the goal of oscillating a mass or fluid against a resisting force to produce energy. The horizontal shape can also be non-circular: one recent optimization found that if waves come predominantly from one direction, an elliptical planform (elongated across the wave front) outperforms a circular one by capturing more pressure variation. Only in an omni-directional wave climate does the optimal planform revert to a circular shape. The diverse WEC geometries each

offer advantages and trade-offs. Table 3.1 provides a side-by-side comparison of key features. In general, terminator-style devices (OWSCs, fixed OWCs, overtopping) intercept more wave front and can achieve higher efficiencies (capture width) but require robust structures to manage forces. Attenuators and point absorbers are more easily scaled in number, with modular units providing flexibility and incremental installation, though each unit may capture less individually. Submerged designs sacrifice some capture potential for superior survivability and steadier output. Geometry optimization has emerged as a critical tool across all types, leveraging computational models to refine shapes for maximum annual energy production while ensuring structural limits are respected [53]. No single geometry excels in all metrics; the optimal choice depends on wave climate, desired power, and deployment constraints. Recent advances show that adaptive or morphing geometries (adjustable flaps, movable ballast, tunable chambers) can offer the best of both worlds—high efficiency in normal seas and safe survival in extreme seas. Going forward, a synergy of smart geometry and control will likely define the next generation of WECs.

Asymmetric geometries are employed in wave-focusing systems to direct and concentrate wave energy toward specific components of the WEC. By altering the hull shape or integrating guiding surfaces, these systems maximize the energy captured per unit area. This design strategy is particularly useful in multi-device wave farms. Newer WEC designs are integrating multi-functional geometries that combine energy capture with other marine applications, such as acting as coastal protection barriers or artificial reefs. These designs not only improve energy production but also provide environmental benefits and infrastructure support [54–56].

One of the most critical design considerations in WEC geometry is achieving optimal hydrodynamic performance, which entails maximizing energy absorption while ensuring that the device maintains stability under various sea states. The geometric configuration directly affects the device's ability to achieve resonance with incoming waves, a key factor in maximizing power output. According to Beringer et al. [57, 58], optimizing the shape and number of hydrodynamically active bodies in a WEC system is crucial for ensuring that the system resonates with the dominant wave frequencies at a given deployment site. Their study explored the role of tapered float geometries, which enhance heave and surge motion, thereby improving energy absorption across a range of wave conditions. The tapered shape was particularly effective at mitigating destructive wave interference and ensuring consistent energy output. Moreover, the principle of geometric scalability is important when considering WEC arrays, where multiple devices are deployed to work collectively. The spacing and orientation of devices within the array must be optimized to minimize destructive interference while promoting constructive wave interactions. Numerical simulations performed by Beringer et al. [57] showed that geometric configurations involving staggered arrays outperformed linear arrays in terms of overall energy capture, with efficiency gains of up to 20%. These findings emphasize that the geometric arrangement of WECs in arrays can have a profound impact on the total power output of wave farms.

WECs with multi-degree-of-freedom (MDOF) capabilities have gained attention due to their ability to capture energy from multiple modes of wave-induced motion,

Table 3.1 Comparative summary of WEC geometries

WEC type and example	Geometry and key features	Energy absorption and efficiency	Structural resilience and scalability
OSWC, e.g., Oyster	Large bottom-hinged flap (terminator) in nearshore Flap width ~ comparable to wave span; mostly vertical plate oscillating in surge Recent designs include curved or cambered flaps for improved hydrodynamics	Strong coupling to horizontal wave motion (surge) Efficient at low-frequency swells; high capture width when tuned Geometry tunes natural period to wave period. A flat rectangular flap ~ 30–40% capture factor, improved shapes up to ~ 48% capture factor Hydrodynamic interactions: reflects and absorbs—acts like a partial wave barrier	Hinge and flap designed to deflect under extreme waves, avoiding rigid impact Few moving parts subsea, improving reliability Needs strong foundation/piles Survivability via compliance Scalable by increasing flap width or installing multiple flaps in an array
Attenuator, e.g., Pelamis	Long multi-body floating structure aligned with waves Typical: 3–5 segments, each 20–40 m long Semi-submerged with optimized diameter and length per segment Joints allow pitching between sections	Absorbs energy from wave flexure along its length Optimal segment length ~ on the order of a wave half-length to straddle crest-trough efficiently Capture width can be large, but each mode is narrower-band Efficiency improved by tuning segment dimensions and PTO damping per hinge Hydrodynamics mainly in pitch and heave at joints with minimal reflect Length, spacing, draft geometry affect bandwidth of absorption	Flexible geometry aids survivability—joints relive stress by bending rather than rigidly resisting waves. End-stop devices prevent excessive hinge angles Floating and slack-moored, it weathervanes heads-on to waves, reducing sideways loads Scalable by adding length/segment or deploying multiple devices in parallel

(continued)

Table 3.1 (continued)

WEC type and example	Geometry and key features	Energy absorption and efficiency	Structural resilience and scalability
Point absorber, e.g., AquaBuoy	Compact buoy oscillating in one or more DOFs Can be single-body or two-body Draft usually ~ buoy radius scale	Small device relative to wavelength—absorbs from all directions Relies on resonance for high frequency Maximum theoretical capture width ~ one wavelength, but practical CWR ~ 20–50% in peak conditions	Simplicity and compliance yield good survivability Buoy rides waves; extreme waves tend to lift it rather than break it End-stop limits or submergence control protect PTO from over-stroke
Overtopping, e.g., Wave Dragon	Very large footprint terminator with collectors spanning wide angle and a ramp leading to a reservoir Typically floating barge or platform	Converts wave energy to potential energy—performance measured by overtopping rate and turbine efficiency Geometry dictates capture: collector angle focuses waves Efficiency can be moderate due to multiple conversion stage, but large waves yield high absolute power	Massive structure lends inherent robustness but faces huge wave forces Floating overtopppers are slack-moored and can vertically accommodate wave motion, mitigating impact shocks Structure must sustain slow-varying loads from reservoir weight and rapid impact loads on the ramp Scalable to very high capacities by enlarging width and reservoir

(continued)

Table 3.1 (continued)

WEC type and example	Geometry and key features	Energy absorption and efficiency	Structural resilience and scalability
Submerged pressure differential, e.g., Archimedes Wave Swing	Submerged axisymmetric buoy tethered to seabed or inside a silo Moves in heave due to pressure change above Geometry factors are area, internal air volume, and submergence depth	Absorbs energy from pressure fluctuations rather than surface motion Most effective at resonance: geometry and air-spring tuned to wave frequency By design, frequency bandwidth is narrow but can be widened via control Low radiation loss and minimal surface wave disturbance can have high hydrodynamic efficiency	Outstanding survivability, located sub-surface, avoiding breaking wave impact Can survive extreme sea by virtue of reduced pressure amplitudes at depth 15 m
OWC, e.g., Mutiku and OE Buoy	Onshore: Concrete/ steel chamber built into a shore/ breakwater; opening to sea at front near waterline Chamber size (width, depth) and aperture shape fixed. Offshore: Floating hull with internal air chamber (often spar or barge) Geometry parameters: chamber volume, opening diameter, draft of opening, overall hull form (for floaters)	Captures wave compression of air—essentially a pneumatic spring-mass system Efficiency hinges on matching the oscillating water column's natural period to wave period Fixed OWCs often achieve stable efficiencies ~ 50–70% (wave to pneumatic) at resonance, then ~ 30–40% turbine efficiency to electricity Floating OWCs have slightly lower peak efficiency due to additional body motion degrees, but can be designed for broad resonance	Onshore OWCs: Very robust—essentially a hollow breakwater; proven to survive decades and easy maintenance Offshore OWCs: Floating platform must endure wave forces, where ballast and hull ensure stability, so it does not capsize

such as heave, pitch, and surge. The geometric configuration of MDOF systems is a key determinant of their ability to efficiently harvest wave energy from different wave directions and amplitudes. A study investigated MDOF WECs with varying geometries, focusing on how changes in the shape and size of the primary body influenced power capture in irregular wave conditions [59]. Their results indicated that WECs

with optimized cylindrical and conical geometries were more effective at capturing wave energy due to their reduced hydrodynamic damping and improved response to multi-directional waves. Additionally, the geometric placement of internal components, such as PTO systems and mooring lines, plays a significant role in optimizing performance. Research by Kurniawan et al. [60] highlighted those internal geometries tailored to minimize mechanical losses during energy conversion resulted in higher overall efficiency. Their study showed that incorporating flexible geometries in PTO systems allowed the device to adapt dynamically to varying sea conditions, preventing energy loss and structural overloading.

In OWCs, the geometry of the chamber and air duct significantly affects the device's efficiency and operational range. Optimizing the shape, size, and internal configuration of the chamber is essential for maximizing the oscillation of water and airflow through the turbine. Recent advancements in geometric design have focused on multi-chamber configurations, which improve the absorption of a broader range of wave frequencies. De Lima et al. [61] investigated multi-chamber OWCs with varying internal partition geometries and demonstrated that partition spacing and chamber depth had a direct impact on wave-induced pressure distribution and energy output. The optimized design resulted in a 35% increase in energy absorption compared to traditional single-chamber OWCs. Furthermore, the geometric optimization of air ducts has been shown to enhance turbine efficiency by reducing airflow resistance and turbulence. Elatife and Marjani [62] explored the effect of curved and tapered duct geometries in compact twin radial impulse turbines and found that optimized duct designs improved airflow velocity and energy capture by 15%. Their findings emphasize the importance of tailoring internal geometries to complement external wave interactions, creating a fully integrated design for optimal performance.

The geometry of WECs significantly affects the interaction of the device with ocean waves, determining the efficiency of energy absorption through wave diffraction, radiation, and reflection. Each of these hydrodynamic phenomena is directly influenced by the shape, orientation, and scale of the device, making geometry a fundamental design condition for optimizing wave energy capture. Understanding how these interactions contribute to power absorption and how size influences device performance relative to different wave conditions is key to the successful deployment of wave energy farms [63]. The shape of a WEC directly determines how incident waves interact with its structure and the extent to which wave energy is diffracted, radiated, or reflected. Wave diffraction occurs when incident waves encounter an obstacle, such as a point absorber or an attenuator, causing the wave to bend around the device. Diffraction is most prominent when the size of the device is comparable to or smaller than the incident wavelength. For example, in the case of point absorbers, their compact, typically axisymmetric shape enables omnidirectional diffraction, allowing energy to be absorbed efficiently from waves coming from various directions [64]. As waves bend around the device, part of the wave energy is dissipated, while the remainder interacts with the structure to produce mechanical energy.

Radiation, on the other hand, refers to the generation of secondary waves by the motion of the WEC itself. The effectiveness of this process depends on the shape and dynamic response of the device. For example, when a WEC oscillates in

response to an incoming wave, it radiates waves outward, which interact with the incoming wave field and influence the net power absorbed. The efficiency of radiation is maximized when the device's oscillation frequency matches the wave frequency [65]. Geometric optimization is critical here, as the shape of the device affects the amplitude and phase of the radiated waves. For instance, floating cylindrical devices radiate waves differently compared to flat or tapered structures, with cylindrical devices typically generating broader radiation patterns [66]. Wave reflection occurs when waves encounter a rigid or semi-rigid surface, causing part of the wave energy to be reflected toward the sea. Devices with large flat surfaces or sharp edges, such as overtopping devices or vertical OWCs, tend to reflect a significant portion of the incident wave energy if not properly optimized. Excessive reflection can lead to reduced absorption efficiency, as less wave energy is available for conversion. Therefore, curved or sloped geometries are often employed to minimize reflections and enhance energy capture by promoting wave entry and interaction with the internal components of the device [67, 68]. For example, overtopping devices are designed with sloped ramps to guide waves into an energy capture chamber, reducing reflection while increasing the potential energy of the overtopping water [69]. Furthermore, the interplay between diffraction, radiation, and reflection must be carefully considered in array configurations, where multiple WECs interact hydrodynamically. Improper geometric arrangements can lead to destructive interference, where waves radiated or reflected by one device negatively affect the performance of neighboring devices. Advanced numerical simulations and experimental studies are thus used to optimize device spacing and alignment, ensuring constructive interference and maximal energy capture [70].

The size of a WEC relative to the wavelength of incident waves is another critical factor that influences its ability to efficiently extract energy. The concept of the capture width ratio quantifies the relationship between the effective width of the WEC and the wavelength highlighting how different device sizes perform under varying wave conditions [71]. Point absorbers can achieve high efficiencies across a wide range of wavelengths due to their ability to oscillate with incoming waves in multiple directions. However, their efficiency tends to decrease in long-wavelength conditions, where larger devices or arrays become necessary. On the other hand, larger devices, such as attenuators and overtopping devices, are typically designed to span multiple wavelengths. Attenuators, which are long, segmented devices aligned parallel to the wave direction, are highly effective in long-wavelength environments, where their extended length allows them to capture wave energy over a large surface area. For example, devices like Pelamis WEC demonstrate how increasing the device length relative to the incident wavelength can enhance power output by capturing energy along the full extent of the wave crest [72]. However, this increase in size often comes with structural and maintenance challenges, particularly in rough sea conditions where larger devices experience higher mechanical stresses. The relationship between device size and wavelength also impacts the device's resonance characteristics. Resonance occurs when the natural frequency of a WEC aligns with the frequency of the incoming wave, resulting in maximum energy transfer. Point absorbers, due to their small size, can be tuned to resonate with a wide range of wave

frequencies, making them ideal for regions with diverse wave climates. In contrast, larger devices, such as OWCs, are more effective in environments with stable and predictable wave periods, as their size allows them to resonate with longer, more powerful waves [66].

These design principles and emerging innovations underscore the critical role geometry plays in advancing WEC technology. The geometry of a WEC plays a pivotal role in determining its efficiency, structural integrity, and overall performance. Proper geometry design not only maximizes wave energy absorption but also ensures durability in harsh marine environments and cost-effective operation over the device's lifespan. Therefore, in the next section, several optimization techniques utilized for WEC geometry design will be examined.

3.3 Optimization Techniques in WEC Geometry Design

The optimization of WEC geometry is a multidisciplinary challenge that aims to maximize energy efficiency, ensure structural resilience, and minimize costs. Due to the dynamic nature of wave environments and the complex interactions between wave motion and structural response, achieving optimal designs requires sophisticated techniques that integrate physics-based simulations, computational models, and real-world testing. Optimization also involves addressing trade-offs among various design objectives, such as maximizing power output while maintaining durability and minimizing environmental impact. By addressing the interactions between WEC structures and dynamic ocean environments, advanced optimization methods seek to balance performance with durability [73]. A variety of optimization techniques have been developed to find the best geometric design for a WEC, often defined by one or multiple objectives, such as power, cost, survivability, etc.

Over the past two decades, numerous studies have applied optimization algorithms to WEC hull shapes and dimensions, aiming to maximize energy production while minimizing cost [53]. Essentially, one defines an objective function that quantifies the "goodness" of a particular design—for example, annual energy output, or a multi-objective combination like maximizing power capture and minimizing structural weight. The optimization algorithm then adjusts the geometry parameters within defined bounds to find an optimal or improved design. The design variables might include device dimensions, such as radius, draft, length, shape profiles, geometric proportions, or even parametrized shape descriptors.

Geometry optimization investigations have been carried out recently for different WEC types and objective functions. These objectives are presented initially presented by Shadmani et al. [3]. However, common objective functions for WEC geometry optimization include:

- Maximizing absorbed power or energy, e.g., maximize the annual energy production (AEP) for a given site wave climate, or maximize the capture width at a target wave period. This is a natural objective since the primary goal is energy

output. Sometimes the objective is to maximize power in a representative sea state or maximize across a spectrum of sea states, possibly weighted by occurrence probability.

- Minimizing cost or cost-of-energy, in which the objective may be to minimize the levelized cost of energy (LCOE), which incorporates not just power output but also device cost, which is tied to geometry and possibly maintenance costs. Since structural costs often scale with size, there is an implicit trade-off, i.e., bigger devices capture more power but cost more, so an optimal LCOE finds a sweet spot.
- Minimizing structural loads or improving survivability metrics, where treated as constraints, but can be objectives in multi-objective optimization. For instance, an objective could be to minimize the maximum bending moment in the device or minimize the mooring load, to favor designs that are easier to survive extreme events.
- Maximizing efficiency or capture ratio: instead of absolute power, one might maximize non-dimensional performance like CWR at a range of periods. This can yield shapes that are fundamentally hydrodynamically optimal, independent of scale.
- Other objectives might include maximizing bandwidth or maximizing some robustness measure, etc. In multi-objective settings, algorithms seek a Pareto optimal set of designs showing trade-offs between objectives.

The formulation of the optimization problem is crucial. A poorly chosen objective or constraints can lead to unrealistic designs, e.g., extremely large devices that ignore cost, or shapes that are impractical. Best practices are to incorporate both performance and practically in the objectives/constraints [30, 53]. For example, one study might constrain the geometry such that the device volume is fixed and then maximize power. Another might set a required power and minimize volume.

Basically, these methods use derivatives of objective functions to iteratively adjust design variables until an optimal solution is reached. There are various types of optimization algorithms developed and utilized for the geometry optimization of WECs. Several methods are presented and reviewed by Shadmani et al. [3] and Garcia-Teruel and Forehand [53].

There are two broad classes of optimization methods. Gradient-based techniques are highly effective for problems with continuous design spaces and well-defined objective functions. However, challenges arise when local optima are present, which may require careful initialization and refinement. Examples include steepest descent, conjugate gradient, sequential quadratic programming (SQP), and other nonlinear programming techniques. They are efficient when the problem is smooth and gradients can be obtained, either via analytical differentiation of a model, finite differences, or an adjoint method. In WEC shape optimization, adjoint methods have been utilized to compute gradients for shape changes, which is very powerful for high-dimensional shape parameterizations [74]. The advantage of gradient methods is faster convergence to a local optimum; however, this method can get stuck in local optima and require the design space to be smooth and differentiable, which might not hold if a

shape change causes a different wave breaking pattern. This technique also requires an initial guess—a poor initial geometry might converge to a suboptimal solution.

Heuristic or global search methods, include genetic algorithms (GA), evolutionary strategies, particle swarm optimization (PSO), differential evolution (DE), simulated annealing, etc. These types of methods do not require gradient information; instead, it explores the design space by evaluating many designs and using stochastic rules to evolve towards better designs. For instance, GAs, inspired by the principles of natural selection and evolution explore large design spaces by generating populations of potential solutions and evolving them through selection, crossover, and mutation. This approach is particularly well-suited for nonlinear and multi-modal design problems, where traditional methods may struggle to converge. By allowing diverse exploration, GAs can discover innovative configurations, such as optimal hull shapes and mooring configurations, that might otherwise remain undetected. Real-world WEC design often involves conflicting objectives, such as maximizing power output while minimizing structural mass and cost. DE and PSO have also been applied effectively. A study comparing algorithms found that some derivative-free methods achieved similar optimum results to gradient methods but with more evaluations [30], highlighting a trade-offs between computational effort and the assurance of finding a global optimum. Multi-objective optimization frameworks generate a Pareto front, offering a set of optimal trade-offs between competing criteria. Designers can then select solutions that best align with project-specific goals, such as balancing energy yield and environmental impact [75]. Sometimes hybrid approaches, e.g., a global search to get near the optimum region, then a gradient method to fine-tune, or multiple random initial points for a gradient method to sample multiple basins of attraction.

Numerous studies demonstrate the gains possible through optimization. For instance, Li et al. [76] demonstrated the effectiveness of GAs in optimizing the geometry of multi-cylinder floating point absorbers. The study focused on multi-objective optimization, balancing energy efficiency and mechanical stability by adjusting parameters such as cylinder spacing, buoyancy distribution, and draft depth. The optimized configuration resulted in a 30% increase in power output compared to traditional designs, emphasizing the value of evolutionary optimization in enhancing WEC performance. Similarly, Elatife and Marjani [77] used GAs in the design of compact twin radial impulse turbines, optimizing parameters such as blade angle, chamber width, and turbine placement. Their optimization process revealed that a slight modification in the turbine chamber geometry could increase energy capture efficiency by up to 15%. The robustness of GAs in navigating complex design spaces makes them ideal for optimizing geometrically complex WECs that operate under dynamic sea states.

Nature-inspired algorithms, such as particle swarm optimization (PSO) and differential evolution (DE), have also gained traction in recent years. Yang et al. [75] highlighted the application of PSO in optimizing resonant unit cell geometries within WEC arrays. By fine-tuning the spacing and shape of individual units, the study achieved constructive wave interference, leading to significant improvements in overall array efficiency. These findings underscore the potential of evolutionary algorithms in optimizing large-scale WEC farms, where individual device interactions

can have a cumulative impact on power output. The hydrodynamic performance of OWCs is largely dependent on the geometric configuration of their chambers and the arrangement of turbines. Ning et al. [78] introduced a novel multi-chamber, multi-turbine (MCMT) technology to enhance the efficiency of OWCs. By varying chamber widths and turbine positions, their study optimized the flow of air and water through the device, resulting in a 35% increase in power output compared to conventional single-chamber OWCs. Their results emphasize that multi-chamber designs can better accommodate varying wave frequencies and improve overall energy capture.

Multi-objective optimization frameworks are essential for balancing conflicting design goals, such as maximizing energy capture while ensuring structural integrity. Arrosyid et al. [79] applied a multi-objective optimization framework to the design of multi-cylinder floating point absorbers. Using Pareto optimization, the study identified configurations that minimized structural fatigue and mooring tensions while maximizing power output. Their optimized design achieved a 20% improvement in power capture while reducing maintenance costs due to lower stress on structural components. Housner and Wynn [80] also explored multi-objective optimization in the context of the iProTech pitching inertial pump (PIP) WEC. By simultaneously optimizing variables such as buoy size, pitching frequency, and internal pump mechanics, the study achieved an optimal configuration that increased energy absorption by 18% and improved device longevity. These studies demonstrate the effectiveness of multi-objective optimization in addressing practical challenges associated with large-scale WEC deployment. Bionic and nature-inspired designs are increasingly being explored as a means of improving WEC performance. Li et al. [81] developed a bionic raft design inspired by natural floating organisms, optimizing its segmented curvature and flexibility to enhance wave energy capture. Experimental results showed that the bionic design outperformed traditional flat designs by 22%, primarily due to its ability to adapt to changing wave profiles and reduce energy loss through excessive motion. Talaat et al. [82] further explored flexible geometries mimicking marine organisms, using optimization algorithms to design WECs capable of self-adaptive responses to wave fluctuations. Their findings suggest that nature-inspired designs can enhance hydrodynamic performance and stability, making them suitable for long-term deployment in harsh marine environments.

CFD simulations are indispensable for analyzing complex wave-structure interactions, pressure distributions, and flow patterns around WECs [30]. By simulating a variety of operating conditions, designers can iteratively optimize geometries, such as hull shapes and submerged surfaces, to enhance energy transfer and reduce energy losses due to turbulence or drag. High-fidelity CFD models can capture the nonlinear and stochastic nature of wave environments, providing detailed insights into performance [79]. Machine learning-based optimization accelerates the design process by reducing the computational burden of evaluating large design spaces. Surrogate models approximate the performance of WECs based on a limited set of high-fidelity simulations, allowing for rapid exploration of design variations. Neural networks and support vector machines can also be used to predict optimal configurations, improving the efficiency of optimization workflows [83, 84]. Physical prototypes remain essential for validating computational models and ensuring real-world

performance aligns with theoretical predictions. Scaled models of WECs are tested in wave tanks to observe their behavior under controlled conditions, including varying wave heights and periods. The data collected helps refine computational models and identify potential issues related to structural stress, fatigue, and resonance [85].

Computational optimization techniques form the backbone of modern WEC design strategies, with CFD and BEM being the primary numerical tools for simulating wave-structure interactions. Computational models are often integrated with optimization algorithms to streamline the design process and reduce computational costs. Pinto Júnior et al. [86] demonstrated the use of exhaustive search techniques combined with axisymmetric CFD simulations to optimize the hydro-pneumatic chamber geometry of OWCs. Their results showed that even small adjustments in the chamber's curvature could significantly improve energy capture efficiency by aligning the device's resonance frequency with that of incoming waves. Similarly, Lee et al. [87] studied submerged block geometries using phase regulators to control wave focusing, thereby optimizing power output and minimizing energy losses through destructive interference. Another computational approach involves surrogate modeling, which approximates the system's behavior using a simplified model and reduces the need for time-consuming simulations. Ezhilsabareesh et al. [88] applied surrogate modeling with response surface techniques to optimize the design of OWCs and floating point absorbers. Their study demonstrated that integrating genetic algorithms with surrogate models allowed for efficient exploration of design parameters, reducing computational time by 60% while achieving an overall 25% improvement in energy absorption. These findings highlight the importance of combining computational fluid models with optimization algorithms to identify optimal geometric configurations quickly.

Modern optimization techniques, including CFD simulations and multi-objective optimization algorithms, have been developed to tackle these complexities, leading to improved performance and cost-efficiency in WEC designs [53]. The effectiveness of WEC geometry design hinges on a set of critical variables, each of which influences the interaction between the device and incoming waves. Key variables include the aspect ratio, i.e., length-to-width ratio, surface area, hydrodynamic shape, and submerged depth, all of which impact the energy absorption rate, device stability, and structural loads. The aspect ratio of a WEC, defined as the ratio of its length to width, is a key determinant of how effectively it interacts with waves. Devices with high aspect ratio, such as attenuators and elongated oscillating structures, have been shown to perform well in long-wavelength environments by capturing energy over an extended surface area [89]. In contrast, point absorbers, which generally have lower aspect ratios and compact, axisymmetric designs, are better suited for regions with short-period waves and variable wave directions, as they can capture energy omnidirectionally. However, increasing the aspect ratio can introduce mechanical challenges, particularly by amplifying wave-induced forces on the device's structure. A study by Shadman et al. [90] has demonstrated that tuning the aspect ratio based on local wave spectra can significantly enhance power capture without overstressing the device. For instance, an optimized length-to-width ratio for attenuators operating in the North Atlantic led to a 20% improvement in wave energy absorption

while maintaining structural integrity. Balancing these ratios is critical for achieving high efficiency while ensuring the device's mechanical resilience under extreme sea conditions.

Recent research has applied machine learning techniques alongside numerical simulations to optimize these parameters simultaneously, balancing the trade-offs between power absorption and mechanical constraints [91]. For example, while larger surface areas typically lead to greater energy capture, they also increase hydrodynamic drag and material costs, making optimization necessary to achieve an ideal balance. Thus, surface area plays a pivotal role in determining how much wave energy a device can intercept and convert into usable energy. Larger surface areas generally lead to higher energy absorption rates, as more wave energy is intercepted. However, increasing the size of the capture surface also raises construction and maintenance costs and can lead to higher hydrodynamic drag, which reduces efficiency [92]. To mitigate this trade-off, optimization techniques often involve adjusting the ratio of submerged surface area to the overall volume of the device. By optimizing this ratio, designers can enhance buoyancy and wave interaction while minimizing unnecessary material use and structural complexity. Garcia-Teruel et al. [92] demonstrated that the relationship between power output and submerged volume is not linear; rather, optimal designs typically involve moderate increases in surface area that maximize energy capture without excessively increasing costs. For example, overtopping devices, which rely on large ramps to guide water into collection reservoirs, must be designed with surface areas large enough to capture sufficient wave energy while minimizing drag from turbulent flows. Through multi-objective optimization methods, researchers have achieved significant improvements in the energy-to-cost ratio, by fine-tuning the external dimensions of these devices [93].

The shape of a WEC affects how it interacts with waves, including how it generates secondary waves (radiation), reflects incident waves, and experiences drag forces. Streamlined bodies are typically optimized to reduce hydrodynamic resistance, which enhances energy efficiency by minimizing energy losses due to drag. Non-streamlined bodies, on the other hand, create regions of high-pressure differential, leading to increased energy capture but at the expense of greater hydrodynamic loads [94]. The choice between streamlined and non-streamlined designs depends on the intended operational environment. For example, point absorbers with rounded or tapered shapes perform well in turbulent sea conditions because their streamlined design minimizes drag while allowing for efficient energy absorption. In contrast, flat or non-streamlined devices are advantageous in regions with steady wave conditions, as they can maximize power absorption without needing to account for rapid wave-induced stresses. Study by Rahimi et al. [95] has shown that optimized streamlined shapes can increase energy capture by up to 30% to traditional non-optimized designs.

The vertical position, or submerged depth, of a WEC influences its interaction with both surface and subsurface waves. Surface waves typically carry more energy, making shallow-submerged devices effective in capturing this energy. However, shallow placement also exposes the device to extreme wave events and increases the likelihood of mechanical failure. On the other hand, deeper submersion provides

stability and consistent energy absorption from longer-period subsurface waves, though this may reduce the overall power captured from high-energy surface waves [96]. For point absorbers, optimizing the submerged depth involves balancing proximity to the wave crest with protection from large wave-induced forces. A study by Bouali and Larbi [97] has found that for floating WECs in the Mediterranean, a submersion depth of approximately 5 m was ideal, offering both optimal energy capture and reduced exposure to extreme waves. According to these studies and objective functions presented in the recent investigations, a usage percentage of each objective function is illustrated for each WEC type in Fig. 3.3.

The efficiency of WECs is not solely determined by submersion depth but also strongly influenced by their geometric configurations. Each device's geometry directly affects its ability to interact effectively with wave energy, impacting overall performance, durability, and operational efficiency. Given the heterogeneous nature of WEC systems, each variant exhibits unique operational mechanisms, distinct engineering challenges, and specific opportunities for optimization. Examining specific case studies on geometry design provides insights into how strategic adjustments in the structural aspects of these devices can significantly enhance their performance. Therefore, the following section explores various case studies, highlighting how geometry optimization has been leveraged to achieve improved wave energy capture and reliability across different WEC categories.

Following the thorough review of various WEC types, optimization techniques, and objective functions, a comprehensive analysis has been carried out to express the importance of optimization techniques in WEC geometry optimization. Accordingly, definition of each objective function is presented in Table 3.2.

Figure 3.4 illustrated the average usage percentage of key objective functions employed in single-objective optimization studies across different WEC types. The analysis reveals that certain objective functions exhibit a higher frequency of application depending on the WEC configuration. For instance, the *AEP* objective function demonstrates consistently high usage in 1B-PA devices, particularly in floating configurations, where energy maximization is often the primary design focus. Conversely, objective functions such as *Pressure* and $P_{turbine}$ are predominantly associated with OWC systems, reflecting the significance of internal pressure dynamics and turbine performance in these devices. The figure highlights the distinct optimization priorities that arise due to the varying energy conversion mechanisms and structural configurations of each WEC type. Additionally, Fig. 3.5 presents comparative analysis displaying the distribution of average usage percentages of optimization techniques applied in single-objective and multi-objective optimization approaches, satisfied by WEC type. In the single-objective domain, heuristic and metaheuristic algorithms such as GA, PSO, and DE are prevalent across most WEC types, reflecting their robustness and adaptability in solving nonlinear and complex optimization problems. In contrast, multi-objective optimization studies exhibit a dominant reliance on algorithms like NSGA-II and multi-objective GA, which are specifically designed to handle trade-offs between competing objectives. The distinct algorithm preferences between single- and multi-objective approaches underscore the methodological differentiation required to address varying design objectives in WEC geometry optimization.

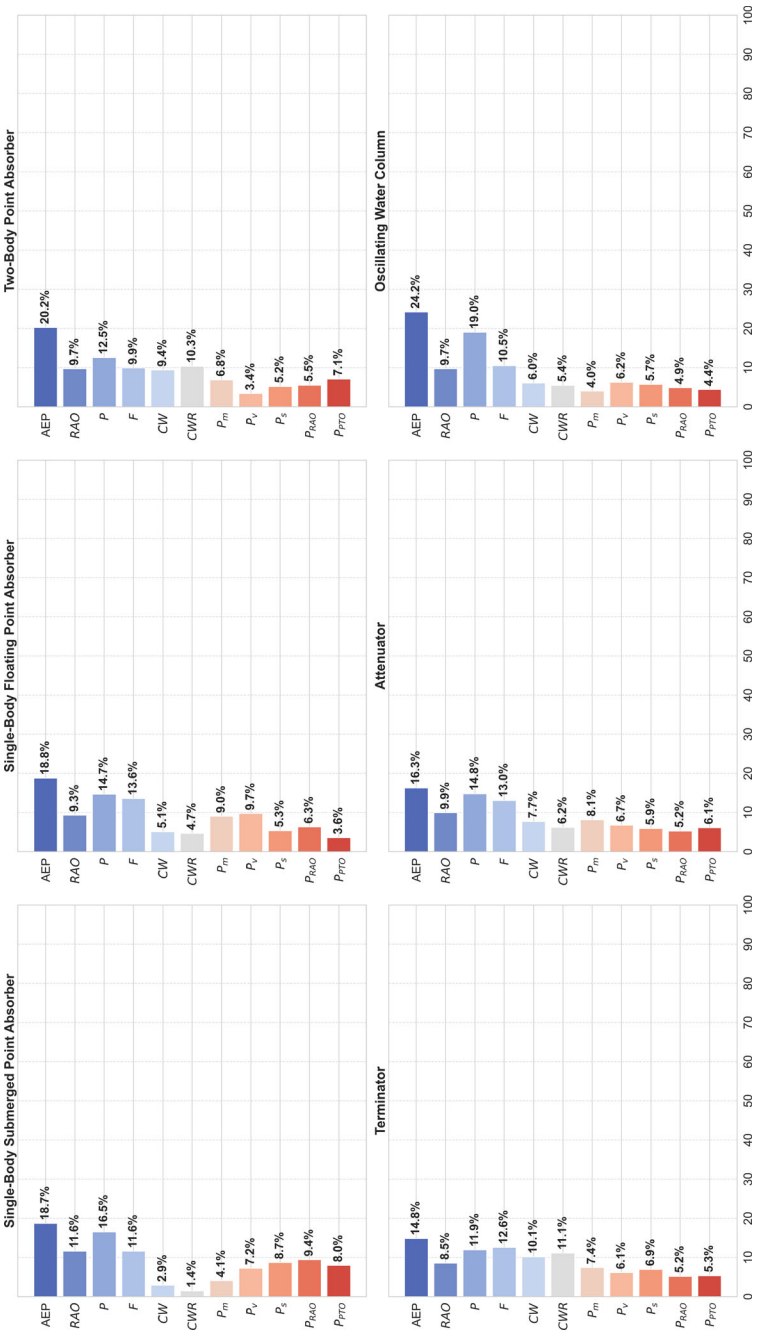

Fig. 3.3 Usage percentage of utilized objective functions in each WEC type

Table 3.2 Definition of various objective functions in WEC geometry optimization

Objective function	Definition
AEP	Annual energy production—total energy produced by the WEC over a year
RAO	Response amplitude operator—ratio of WEC motion amplitude to wave amplitude
P	Average power—mean power output of the WEC
F	Force—hydrodynamic forces on the WEC structure
C_W	Capture width—measure of the power extraction capability
C_{WR}	Capture width ratio—capture width normalized by device characteristic dimension
P_m	Maximum power—peak power output
P_v	Power variance—measure of power output stability
P_s	Survival probability—structural survivability in extreme conditions
P_{RAO}	Power-RAO relationship—power output as a function of motion response
P_{PTO}	Power take-off power—power extracted by the PTO system
$P_{turbine}$	Turbine power—power output of the turbine (especially for OWC)
Pressure	Pressure differential—particularly relevant for OWC and submerged devices

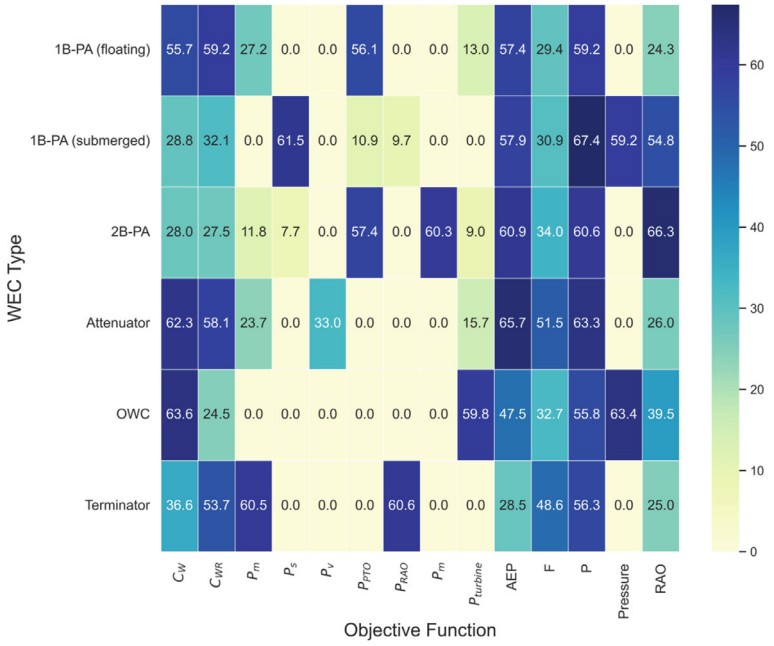

Fig. 3.4 Average usage percentage of objective functions by WEC type

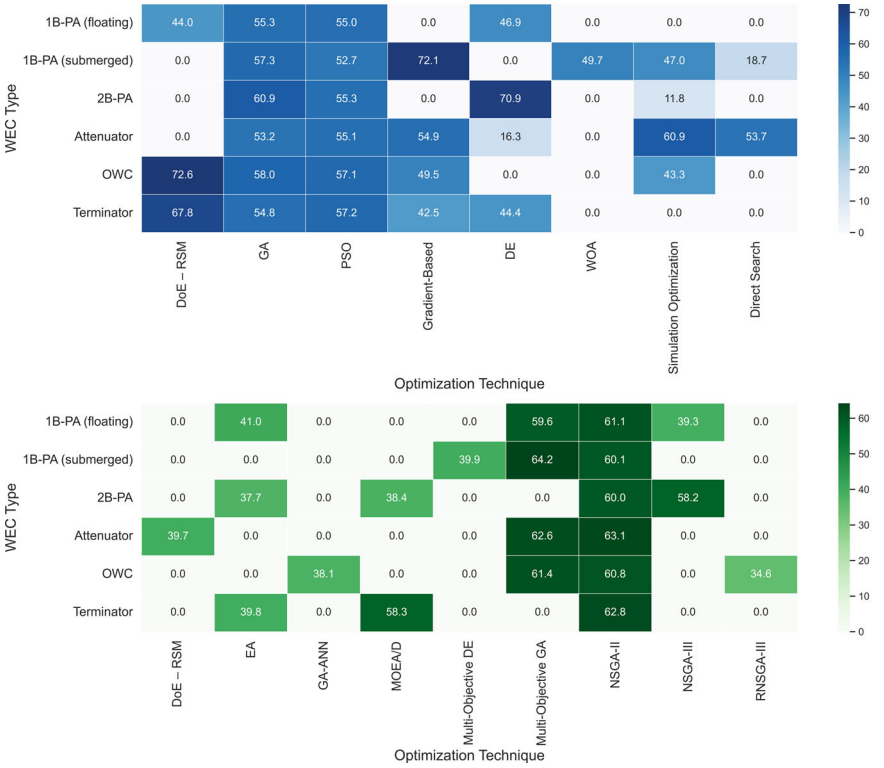

Fig. 3.5 Single-objective and multi-objective optimization techniques by WEC type

Moreover, the correlation between individual objective functions and the optimization techniques utilized in single-objective optimization studies depicted in Fig. 3.6. This figure underscores a pattern where certain algorithms are preferentially selected based on the specific optimization objective. For example, GA and PSO show significant prevalence in maximizing AEP and C_{WR}, objectives that are typically associated with maximizing energy absorption and conversion efficiency. Alternatively, techniques such as gradient-based methods and simulation optimization are more frequently associated with structural objectives like F and P, which demand high precision evaluating physical constraints. This correlation analysis facilitates the identification of best practice pairings between objective functions and optimization techniques within the WEC design optimization landscape. Therefore, a comparison of top performing optimization algorithms based on their average usage percentage across single-objective and multi-objective approaches has been carried out, shown in Fig. 3.7. In single-objective optimization, GA and PSO consistently dominate, attributed to their ease of implementation and global search capabilities in high-dimensional design spaces. In the multi-objective domain, NSGA-II emerges as the most utilized algorithm, owing to its effectiveness in generating Pareto-optimal

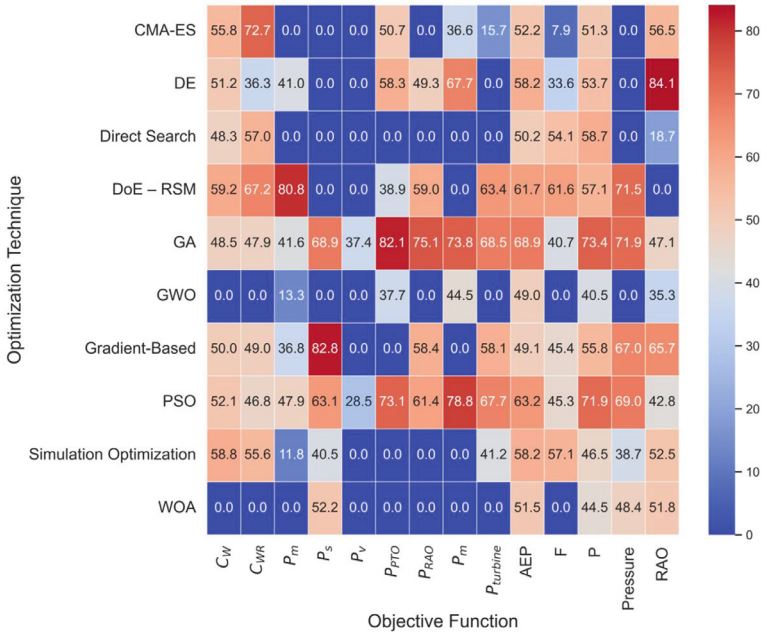

Fig. 3.6 Average usage percentage of objective functions by optimization technique

solutions while maintaining diversity among solutions. This comparative analysis emphasizes the methodological divergence between the two optimization paradigms and highlights the algorithms that have gained widespread acceptance in the WEC optimization community.

Figure 3.8a provides a breakdown of the most commonly optimized objective functions for each WEC type, derived from single-objective optimization studies. The figure indicates that *AEP* remains the predominant optimization target for point absorber devices, reflecting the emphasis on maximizing energy yield in these systems. For OWCs, *Pressure* and $P_{turbine}$ objectives are more frequently addressed, consistent with their reliance on air compression and turbine efficiency for energy conversion. The variation in optimization priorities across different WEC configurations underscores the influence of device architecture and operational principles on the selection of objective functions in performance optimization studies. Furthermore, Fig. 3.8b highlights the most prevalent multi-objective function combinations employed in optimization studies, along with their distribution across different WEC types. Commonly addressed objective pairs include $AEP + C_{WR}$ and $AEP + P$, representing the trade-offs between maximizing energy production and optimizing capture efficiency or power stability. The figure demonstrates the association of specific objective combinations with WEC types, such as the frequent optimization of $AEP + Pressure$ in OWC systems. This analysis underscores the complex nature

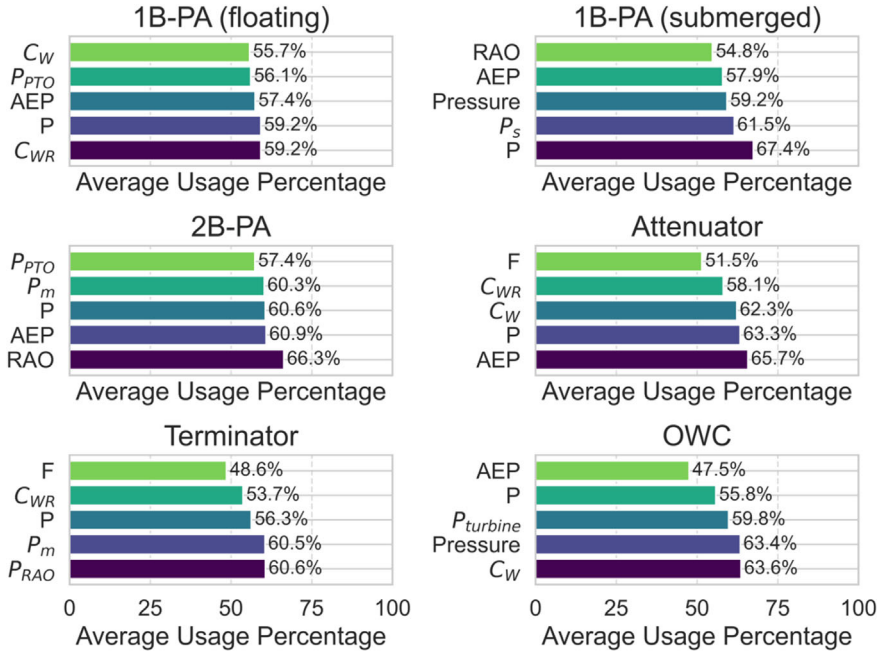

Fig. 3.7 Top objective functions for different WECs

of WEC design optimization, where balancing competing objectives is critical for achieving optimal device performance under varying operational conditions.

Further, Fig. 3.9 presents the comparative effectiveness of various optimization techniques in addressing key objective functions, namely AEP, P, and C_{WR}. This figure identifies the most effective algorithms for each objective based on average usage percentage, with GA and PSO consistently ranking among the top techniques for maximizing AEP and C_{WR}. These results reflect the efficacy of these algorithms in exploring large, nonlinear search spaces commonly encountered in energy maximization problems.

3.4 Case Studies in Geometry Design for Enhanced Performance

Real-world case studies offer valuable insights into the practical implementation of WEC geometry optimizations. By analyzing specific applications, researchers and engineers can better understand the trade-offs between design parameters, operational efficiency, and environmental constraints. The following case studies illustrate the impact of optimized geometry on performance and highlight key points in this manner.

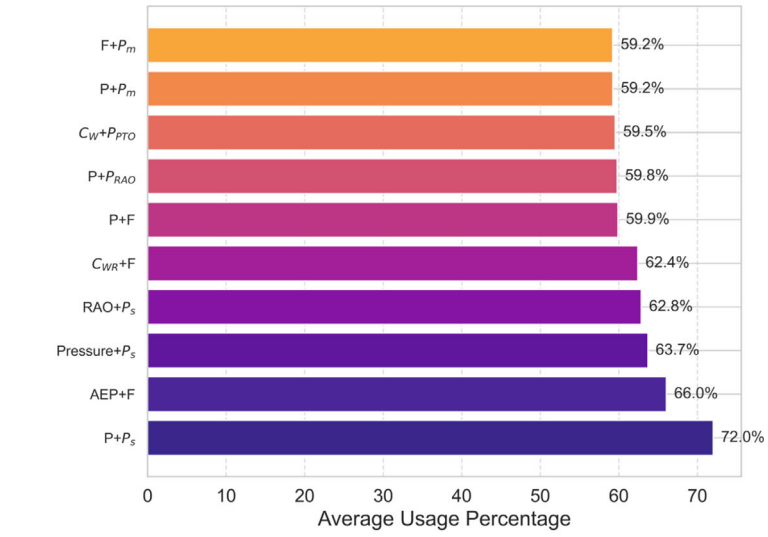

(a)

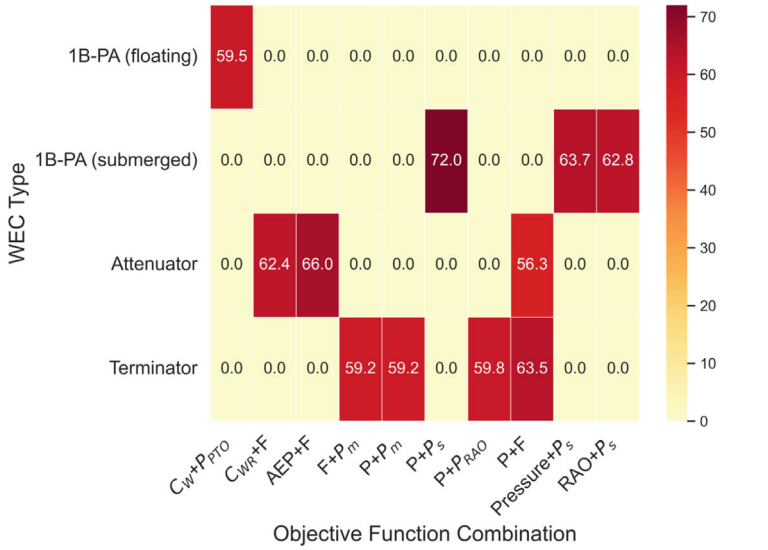

(b)

Fig. 3.8 **a** Top multi-objective combinations **b** multi-objective function combinations by WEC type

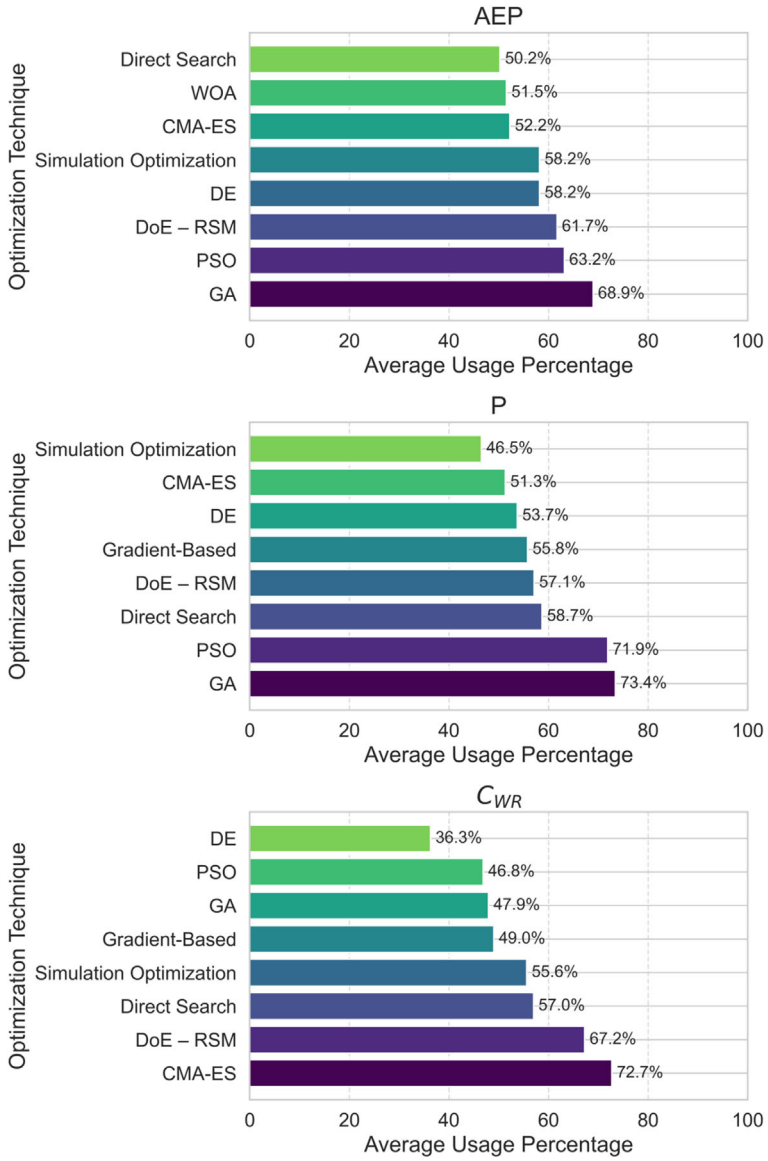

Fig. 3.9 Most effective techniques for three important objective functions

3.4.1 Case Study 1: Point Absorber Geometry Optimization

A point absorber WEC deployed in a moderate-energy coastal site was initially designed based on theoretical estimates of wave interaction. Early operational data revealed suboptimal heave responses, resulting in inefficient energy capture during

peak wave conditions. CFD simulations indicated that the issue was due to an insufficient draft depth, which limited the buoy's resonance with the site's dominant wave frequency. To address this, a series of design iterations were conducted by Guo et al. [98] on a two degrees of freedom point absorber, with incremental changes to the buoy's draft and diameter. The simulations evaluated how these modifications influenced energy capture and stability. Wave tank experiments confirmed the effectiveness of the optimized design, demonstrating a 22% increase in energy yield. The final design not only improved power output but also enhanced survivability by ensuring that the buoy-maintained stability during high-energy wave events.

Manawadu et al. [99] conducted a comprehensive study using Smoothed Particle Hydrodynamics (SPH) modeling to investigate the performance of a heaving point absorber with a novel buoy geometry. They explored 395 cases of varying buoy dimensions and wave conditions, identifying optimal configurations that increased energy absorption by 25% compared to conventional designs. Their findings demonstrated that the optimized buoy achieved better resonance characteristics, allowing for efficient energy capture across a range of wave frequencies. The study further highlighted the importance of tuning the submerged volume and draft depth to account for varying sea states, improving the device's adaptability and stability. Further advancements were made by Arrosyid et al. [79] through a case study involving multi-cylinder floating point absorbers. Using multi-objective GA, artificial neural network, and multi-criteria decision-making, they optimized the key geometrical parameters including outer radius, bottom radius, and draft, where the applied technique balanced CWR and low cost. Their optimized design resulted in a 30% improvement in overall power output by enhancing the device's ability to capture and utilize wave energy more effectively. The study demonstrated that multi-buoy systems with optimized geometries offer greater potential for scalable wave farms, where individual units can be arranged to minimize destructive interference while promoting cooperative energy capture.

Recent innovations in WEC design have focused on multi-axis systems capable of capturing wave energy from multiple directions and modes of oscillation. One prominent example is the TALOS-WEC system, described by Nasr Esfahani et al. [56], which incorporates multi-axis and multi-degree-of-freedom mechanisms. The TALOS-WEC consists of interconnected arms that can pivot and adjust their orientation based on incoming wave direction, allowing the device to optimize its energy capture dynamically. This adaptable design was shown to achieve 40% higher energy efficiency compared to fixed-axis systems, particularly in variable sea conditions. The study highlighted that geometric flexibility, and real-time adjustments were key to maintaining resonance with changing wave profiles and maximizing power output. Additionally, Shadmani et al. [100] investigated the geometry optimization of this unique type of WEC structure. They employed many-objective optimization algorithms and studied various geometrical configuration for multi-axis WEC, where they found cylindrical and octagonal geometries as optimal configurations. The effectiveness of multi-axis designs was further demonstrated in a case study involving the integration of X-structured nonlinear configurations [101]. This design utilized a novel inverter mechanism to amplify wave-induced forces and enhance

energy capture under extreme wave conditions. The X-shaped geometry allowed for efficient energy transfer from high-amplitude waves, reducing power fluctuations and stabilizing output. The study concluded that non-traditional geometric configurations, particularly those incorporating nonlinear elements, have great potential for addressing the challenges of intermittent wave energy.

Moreover, Guo et al. [14] investigated the effect of various buoy shapes, including spherical, conical, and hemispherical designs, on the CWR. The study found that a conical buoy provided up to 20% higher CWR compared to conventional cylindrical shapes due to its reduced drag and optimized interaction with the wave field. Multi-objective optimization approaches have further refined point absorber geometries by simultaneously adjusting variables such as aspect ratio, draft, and submerged depth. Shadmani et al. [54] demonstrated that an optimized aspect ratio combined with a variable submersion depth resulted in higher energy absorption during some extreme wave events. By tuning the submerged depth to match 10% of the dominant wave height, energy absorption improved by 15%, with additional benefits in device stability. This optimization allowed point absorbers to efficiently handle a range of wave periods without requiring structural modifications, making them suitable for deployment in varying wave climates.

The Wave Star device took a unique geometric approach. Instead of one big absorber, it used an array of many small floats (half-sphere buoys) mounted on a structure like pins on an axle [102]. The Wave Star prototype had 20 floats (10 on each side of a platform) that would go up and down with waves, driving hydraulic pumps. The geometry essentially sampled the waves along a length, with floats spaced so that as a wave passes down the line, each float hits its peak at a different time, smoothing power output. Importantly, the entire array could be jacked up above the waterline during storms.

3.4.2 Case Study 2: OWC Design Optimization

Initial designs of OWCs exhibited significant energy losses due to turbulent airflow and inefficient pressure transfer within the chamber. The geometry of the chamber, including its width, depth, and tilt angle, significantly influences the device's energy absorption efficiency and operational range. CFD simulations helped identify optimal configurations that improved the compression efficiency of the trapped air [103]. The optimization process also considered structural robustness to ensure that the device could withstand dynamic loads from wave impacts. The final design increases power output, enhances turbine efficiency, and maintains stability during extreme wave events.

Song et al. [104] conducted a case study to assess the impact of chamber tilt angles on the hydrodynamic performance of an offshore OWC. By varying the tilt angle and analyzing wave interactions using numerical simulations, they found that optimal tilt configurations improved airflow velocity and power output by 20%, particularly in environments with sloped seabed. The study emphasized that geometric

adjustments to match site-specific wave conditions can greatly enhance device efficiency and operational versatility. In another study, Qian et al. [105] examined the performance of multi-chamber OWCs with varying internal partitions and chamber dimensions. Their simulations revealed that multi-chamber configurations absorbed a broader range of wave frequencies compared to single-chamber designs, achieving a 35% increase in overall energy capture. The study demonstrated that by optimizing the spacing and size of internal partitions, designers could enhance resonance and improve wave-induced pressure distribution within the chamber, ultimately boosting energy output. This approach to geometric tuning has important implications for expanding the operational range of OWCs in real-world deployments, making them more suitable for regions with irregular wave patterns.

Geometric optimization is not limited to the external structure of WECs but extends to internal components such as turbines and air ducts in hybrid systems. Elatife and Marjani [77] conducted a case study on the design of compact twin radial impulse turbines used in OWCs. By optimizing the curvature of turbine blades and the cross-sectional area of air ducts, they enhanced airflow dynamics and increased power output by 15%. Their optimized design was particularly effective at capturing energy from low-amplitude waves, expanding the operational range of the system. This case study emphasized the importance of integrating internal and external geometric optimization to achieve comprehensive improvements in device performance. Zhang et al. [106] explored bio-inspired flexible turbine geometries that could adapt dynamically to changing wave forces. By mimicking natural systems, such as the flexible appendages of marine organisms, the study demonstrated that turbine blades with adaptable curvature could maintain high efficiency even under fluctuating wave conditions. The results suggested that bio-inspired designs could improve the durability and operational lifespan of WECs while reducing maintenance requirements in harsh marine environments.

OWCs rely on the movement of waves within a partially submerged chamber to compress air and drive a turbine. The geometry of the chamber, including the cross-sectional shape and the size of the air outlet, has a significant impact on energy capture. Rosati [107] conducted a comparative study of rectangular, trapezoidal, and tapered chamber designs, demonstrating that a tapered design with a reduced inlet achieved 30% higher power output compared to traditional rectangular chambers. The improved performance was attributed to increased air compression efficiency, which enhanced the airflow through the turbine. Another study by Elhanafi and Kim [108] explored the optimization of chamber inclination and length, showing that OWCs with inclined chambers performed better in variable sea states due to their wider resonance bandwidth. This design improvement allowed the device to maintain efficiency across a broader range of wave periods, particularly in regions with seasonal wave variability. CFD simulations confirmed that inclined chambers reduced wave reflection and increased the effective capture of wave energy by optimizing the pressure differential within the chamber. Additionally, metaheuristic algorithms have been used to optimize the placement of OWCs within wave farms. By considering wave directionality and chamber geometry simultaneously, researchers

have enhanced energy capture by reducing destructive wave interference between devices [109].

3.4.3 Case Study 3: Attenuator Optimization

The performance of attenuators depends heavily on their longitudinal geometry, segment stiffness, and length-to-width ratio. An attenuator WEC operating in a high-energy offshore site was optimized to improve energy absorption on its hinges. The original design, while effective under moderate wave conditions, experienced mechanical wear and performance degradation during prolonged exposure to large waves [110].

In one study, GA was applied to evaluate various segment lengths, hinge stiffness configurations, and submersion depths [33]. The optimization process focused on achieving a balance between energy absorption and mechanical durability, where it showed the performance improvements by a 30% increase in power output. The optimized design extended the operational lifespan of the device and reduced maintenance costs.

By increasing the length of the Pelamis relative to the wavelength, Vakili et al. [111] showed that power absorption improved by 18% in regions with long-wavelength conditions. However, this increase in length also resulted in higher mechanical stresses at the segment joints, necessitating further optimization of materials and structural reinforcements to maintain durability. Additionally, varying the segment stiffness along the length of the device allowed for better adaptation to changing wave heights, reducing the likelihood of mechanical fatigue. CFD models have also been used to optimize submersion depth, showing that positioning attenuators at a depth corresponding to half the wave height can reduce wave-induced stresses while maintaining high energy capture efficiency [112]. This optimization strategy enhances the overall performance and longevity of the device, making it more cost-effective in long-term deployments.

3.4.4 Case Study 4: Optimizing Overtopping Devices

Overtopping devices are designed to capture wave energy by allowing waves to flow over a sloped or stepped ramp into a reservoir, where the water is stored temporarily before being released through turbines to generate power. The optimization of the ramp geometry, reservoir dimensions, and hydraulic pathways is critical for ensuring that the maximum amount of wave energy is captured and converted into usable electricity. Optimization studies have investigated various design parameters, including ramp angle, height, and curvature, as well as the dimensions of the storage reservoir and the configuration of turbine channels, to balance water capture efficiency with hydraulic head and energy losses.

One of the key optimization strategies involves adjusting the ramp angle to maximize the overtopping rate while minimizing wave reflection and energy dissipation. Sayar [113] demonstrated that a ramp angle of approximately 45° with a curved surface provides a significant improvement in wave capture compared to traditional flat designs. This optimization was achieved using numerical simulations that modeled the interaction of different wave heights and periods with various ramp geometries. The curved surface design reduced wave breaking and allowed for smoother water flow into the reservoir, which increased the overtopping volume by 20% without requiring structural changes to the device. Similarly, An et al. [114] highlighted that gradual transitions between the ramp and reservoir further reduce energy losses and turbulence within the captured water.

Another optimization technique focused on slope ratio and guide-vane number for the reservoirs of multi-level CROWN overtopping device [41]. This study found the smaller opening mouth width of the lower reservoir benefits the overtopping performance of the upper reservoir. The optimized shape parameters could be employed for practical design of a prototype multi-level overtopping device. It is also emphasized that shallow reservoirs with a broader surface area are effective in capturing large volumes of overtopped water; however, they can suffer from higher evaporation losses and increased flow resistance. To mitigate these effects, hybrid optimization techniques can be employed. One such approach is the use of metaheuristic algorithms, which explore multiple design configurations simultaneously to identify the optimal combination of reservoir dimensions and ramp geometries [3].

3.5 Future Trends in WEC Design

Looking ahead, the field of wave energy conversion is poised to benefit from emerging technologies and novel design concepts that could significantly influence WEC geometries. Future WEC designs will likely be smarter, more adaptable, and more integrated than those of the past. In this section, we outline some key trends and possibilities for the future of WEC geometry and concept design, including new materials, biomimetic approaches, AI-driven optimization, and the integration of wave energy with other systems.

Innovation in wave energy is continuing to produce new types of devices. One trend is towards multi-mode or multi-axis converters, which can capture energy from waves in several degrees of freedom simultaneously. An example is the EU-backed TAPAS or M4 devices that combine heave, pitch, and surge modes in one system, or the TALOS concept which proposes a multi-axis point absorber. These devices often have geometries that are not traditional—e.g., a cluster of floats connected in different orientations—aiming to absorb more wave energy from complex sea states. Another concept is the variable-geometry WEC that we touched on: future devices may actively change their shape or dimensions in response to wave conditions (e.g., inflatable absorbers that can deflate in storms, or extendable arms that deploy in calm seas and retract in rough seas). The NREL-led “Variable Geometry WEC (VGWEC)”

project is exploring such ideas, hypothesizing that shapeshifting could maintain high efficiency across a wider range of conditions while shedding loads when needed.

Nature has evolved myriad ways to harvest energy from fluids (for locomotion, feeding, etc.), and engineers are increasingly looking to biomimicry for inspiration in WEC design. In future WEC geometries, we may see features inspired by marine animals or plants—for example, dolphin or whale tails that efficiently oscillate might inspire flap shapes; the way kelp sways in waves could inspire flexible tethered devices. A preliminary study noted that "biomimetics and creatures could contribute to novel design inspiration for wave energy converters, as seen in many other engineering fields." This suggests using evolutionary algorithms not just in a computational sense but guided by solutions nature already found. For instance, the Nenuphar WEC concept (named after a water lily) tries to mimic how lily pads oscillate with waves. Biomimetic approaches might lead to geometries that are distributed and compliant (like a mat or carpet that oscillates with waves—indeed a "wave carpet" concept has been researched for wave absorption using a thin flap on the seafloor). These kinds of designs may have lower visual profile (environmentally friendly) and inherently survive by yielding to waves rather than fighting them.

Building on what was discussed in Sect. 3.3, the future will undoubtedly see more artificial intelligence and machine learning being used to conceive and refine WEC geometries. Instead of manually testing a few shapes, AI can explore vast design spaces, including unconventional shapes that a human designer might not think of. Machine learning models can be trained on simulation or experimental data to predict performance of new shapes with high speed, allowing iterative optimization guided by algorithms. Already, researchers have used neural networks and advanced regression (like XGBoost) to optimize an asymmetric device's geometry with promising results. In the future, one could imagine a generative design algorithm that, given certain constraints (size, site wave spectrum, etc.), creates an optimal geometry from scratch—potentially something quite novel. Additionally, AI will play a role in operational control of devices (which indirectly affects effective geometry or how geometry is used). Intelligent control can, for example, adjust a device's ballast (hence geometry) on the fly, or reposition devices ahead of storms. This blurs the line between geometry and operation: an AI might effectively "reshape" a device's function by reconfiguring modular geometry (like locking certain joints or flooding certain ballast tanks to alter natural period).

Integrating WECs with other renewable energy systems, such as offshore wind turbines and floating solar panels, is gaining attraction to maximize resource utilization and improve overall energy generation. Hybrid systems can share infrastructure, such as mooring and cabling, reducing installation and maintenance costs. They also provide a more consistent energy output by diversifying the sources of renewable energy, making them ideal for large-scale deployments. Offshore wind turbines are now common; there is interest in adding wave energy converters to wind platforms to utilize the space and infrastructure. For instance, the base of a floating wind turbine could have an integrated ring of OWCs or a set of small flaps around it. Or a mooring line could have an energy absorber attached. The geometries here need to be compatible with the wind structure—likely compact and not interfering with turbine

operations. This could drive WECs to be smaller, modular, and attachable. Already, some pilot projects (like the EU-funded W2Power) looked at attaching wave devices to floating wind platforms.

As discussed, integrating WECs into breakwaters is promising. Future coastal infrastructure might routinely embed OWCs or overtopping devices, shaping the geometry of breakwaters to also function as energy devices. This dual-use trend means WEC geometry will be partly dictated by civil coastal engineering needs (e.g., specific cross-section of a seawall), but also that energy devices can be larger and more rigid (because they're literally part of a concrete structure). Instead of single devices, we'll see wave farms with dozens of units. The geometry of the array layout (spacing, staggering) is a new design element—essentially designing at a higher level. Future farm design will use models to optimize not just each device's geometry, but their collective geometry in the ocean (their positions and interactions). This could include intentionally shaping the farm to focus waves (like a lens) or shadowing to protect certain devices from extremes.

These future trends illustrate the transformative potential of wave energy technology to become a foundation of the global renewable energy landscape. By combining forefront research with sustainable practices, WECs are poised to deliver reliable, scalable, and environmentally friendly power from the world's oceans.

References

1. Guo, B., Ringwood, J.V.: A review of wave energy technology from a research and commercial perspective. IET Renew. Power Gener. **15**(14), 3065–3090 (2021). https://doi.org/10.1049/rpg2.12302
2. Azam, A., et al.: Wave energy evolution: knowledge structure, advancements, challenges and future opportunities. Renew. Sustain. Energy Rev. **205**, 114880 (2024). https://doi.org/10.1016/j.rser.2024.114880
3. Shadmani, A., Nikoo, M.R., Gandomi, A.H., Chen, M., Nazari, R.: Advancements in optimizing wave energy converter geometry utilizing metaheuristic algorithms. Renew. Sustain. Energy Rev. **197**, 114398 (2024). https://doi.org/10.1016/j.rser.2024.114398
4. Garrido, A.J., Garrido, I., Lekube, J., de la Sen, M., Carrascal, E.: OWC on-shore wave power plants modeling and simulation. In: 2016 IEEE International Conference on Emerging Technologies and Innovative Business Practices for the Transformation of Societies (EmergiTech), pp. 43–49 (2016). https://doi.org/10.1109/EmergiTech.2016.7737308
5. Garrido, A.J., Villasante, A., Garrido, I.: Mutriku's offshore wave power plant capture chamber model validation. In: 2024 IEEE 67th International Midwest Symposium on Circuits and Systems (MWSCAS), pp. 491–494 (2024). https://doi.org/10.1109/MWSCAS60917.2024.10658860
6. Wimalaratna, Y.P., et al.: Comprehensive review on the feasibility of developing wave energy as a renewable energy resource in Australia. Clean. Energy Syst. **3**, 100021 (2022). https://doi.org/10.1016/j.cles.2022.100021
7. Portillo, J.C.C., Henriques, J.C.C., Gato, L.M.C., Falcão, A.F.O.: Model tests on a floating coaxial-duct OWC wave energy converter with focus on the spring-like air compressibility effect. Energy **263**, 125549 (2023). https://doi.org/10.1016/j.energy.2022.125549
8. Carrelhas, A.A.D., Gato, L.M.C., Henriques, J.C.C., Marques, G.D.: Estimation of generator electrical power output and turbine torque in modelling and field testing of OWC wave energy

converters. Energy Convers. Manag. X **19**, 100384 (2023). https://doi.org/10.1016/j.ecmx.2023.100384
9. Pawitan, K.A.: Development of oscillating water column and wave overtopping—wave energy converters in Europe over the years. In: Samad, A., Sannasiraj, S.A., Sundar, V., Halder, P. (eds.) Ocean Wave Energy Systems: Hydrodynamics, Power Takeoff and Control Systems, pp. 109–131. Springer International Publishing, Cham (2022). https://doi.org/10.1007/978-3-030-78716-5_4
10. Boccotti, P.: Comparison between a U-OWC and a conventional OWC. Ocean Eng. **34**(5), 799–805 (2007). https://doi.org/10.1016/j.oceaneng.2006.04.005
11. Carlo, L., Iuppa, C., Faraci, C.: A numerical-experimental study on the hydrodynamic performance of a U-OWC wave energy converter. Renew. Energy **203**, 89–101 (2023). https://doi.org/10.1016/j.renene.2022.12.057
12. Jalani, M.A., Saad, M.R., Samion, M.K.H., Imai, Y., Nagata, S., Abdul Rahman, M.R.: Numerical study on a hybrid WEC of the backward Bent Duct Buoy and point absorber. Ocean Eng. **267**, 113306 (2023). https://doi.org/10.1016/j.oceaneng.2022.113306
13. Cheng, Y., Song, F., Dai, S., Yuan, Z., Incecik, A.: Broadband wave energy extraction by a dual-PTO hybrid system of a comb-type breakwater and an oscillating flap. Energy Convers. Manag. **297**, 117670 (2023). https://doi.org/10.1016/j.enconman.2023.117670
14. Guo, B., Wang, T., Jin, S., Duan, S., Yang, K., Zhao, Y.: A review of point absorber wave energy converters. J. Mar. Sci. Eng. **10**(10), 1534 (2022)
15. Cordonnier, J., Gorintin, F., De Cagny, A., Clément, A.H., Babarit, A.: SEAREV: case study of the development of a wave energy converter. Renew. Energy **80**, 40–52 (2015). https://doi.org/10.1016/j.renene.2015.01.061
16. Khedkar, K., Nangia, N., Thirumalaisamy, R., Bhalla, A.P.S.: The inertial sea wave energy converter (ISWEC) technology: device-physics, multiphase modeling and simulations. Ocean Eng. **229**, 108879 (2021). https://doi.org/10.1016/j.oceaneng.2021.108879
17. Shami, E.A., Zhang, R., Wang, X.: Point absorber wave energy harvesters: a review of recent developments. Energies **12**(1) (2019). https://doi.org/10.3390/en12010047
18. Jahangir, M.H., Alimohamadi, R., Montazeri, M.: Performance comparison of pelamis, wavestar, langley, oscillating water column and Aqua Buoy wave energy converters supplying islands energy demands. Energy Rep. **9**, 5111–5124 (2023). https://doi.org/10.1016/j.egyr.2023.04.051
19. Dang, T.D., Phan, C.B., Ahn, K.K.: Design and investigation of a novel point absorber on performance optimization mechanism for wave energy converter in heave mode. Int. J. Precis. Eng. Manuf. Green Technol. **6**(3), 477–488 (2019). https://doi.org/10.1007/s40684-019-00065-w
20. Ramli, M.A., Mustapa, M.A., Rozali, R.H., Azrulhisham, E.A.: Hydrodynamic performance of heaving motion on cylinder and conical two-body point absorber in low wave energy. IOP Conf. Ser. Earth Environ. Sci. **1046**(1), 012010 (2022). https://doi.org/10.1088/1755-1315/1046/1/012010
21. Kim, S.-J., Koo, W., Kim, M.-H.: The effects of geometrical buoy shape with nonlinear Froude-Krylov force on a heaving buoy point absorber. Int. J. Nav. Archit. Ocean Eng. **13**, 86–101 (2021). https://doi.org/10.1016/j.ijnaoe.2021.01.008
22. Xu, Q., et al.: Experimental and numerical investigations of a two-body floating-point absorber wave energy converter in regular waves. J. Fluids Struct. **91**, 102613 (2019). https://doi.org/10.1016/j.jfluidstructs.2019.03.006
23. Rahimi, A., et al.: Numerical and experimental study of the hydrodynamic coefficients and power absorption of a two-body point absorber wave energy converter. Renew. Energy **201**, 181–193 (2022). https://doi.org/10.1016/j.renene.2022.10.103
24. Wang, J., Wang, S., Jiang, Q., Xu, Y., Shi, W.: Effect of different raft shapes on hydrodynamic characteristics of the attenuator-type wave energy converter. China Ocean Eng. **37**(4), 645–659 (2023). https://doi.org/10.1007/s13344-023-0055-x
25. Matamala, P., et al.: Numerical and experimental assessment of the hydrodynamic behaviour of an attenuator wave energy converter device. In: Trends in Renewable Energies Offshore. CRC Press (2022)

26. Liao, Z., et al.: Modelling and control tank testing validation for attenuator type wave energy converter—part I: experiment setup and control-oriented modelling. IEEE Trans. Sustain. Energy **14**(3), 1747–1757 (2023). https://doi.org/10.1109/TSTE.2023.3246172
27. Liao, Z., et al.: Modelling and control tank testing validation for attenuator type wave energy converter—part II: linear noncausal optimal control and deterministic sea wave prediction tank testing. IEEE Trans. Sustain. Energy **14**(3), 1758–1768 (2023). https://doi.org/10.1109/TSTE.2023.3246173
28. Sun, T., et al.: Modelling and control tank testing validation for attenuator type wave energy converter—part III: model predictive control and robustness validation. IEEE Trans. Sustain. Energy **14**(3), 1737–1746 (2023). https://doi.org/10.1109/TSTE.2023.3246171
29. Capper, J., Mi, J., Li, Q., Zuo, L.: Numerical analysis and parameter optimization of a portable two-body attenuator wave energy converter. In: International Design Engineering Technical Conferences and Computers and Information in Engineering Conference, American Society of Mechanical Engineers, p. V010T10A005 (2021)
30. Guo, B., Ringwood, J.V.: Geometric optimisation of wave energy conversion devices: a survey. Appl. Energy **297**, 117100 (2021)
31. Gobato, R., Gobato, A., Fedrigo, D.F.G.: Study Pelamis system to capture energy of ocean wave (2015). https://doi.org/10.48550/arXiv.1508.01106. *arXiv*: arXiv:1508.01106
32. Cheng, Y., Xi, C., Dai, S., Ji, C., Cocard, M.: Wave energy extraction for an array of dual-oscillating wave surge converter with different layouts. Appl. Energy **292**, 116899 (2021). https://doi.org/10.1016/j.apenergy.2021.116899
33. Liu, Y., Mizutani, N., Cho, Y.-H., Nakamura, T.: Nonlinear hydrodynamic analysis and optimization of oscillating wave surge converters under irregular waves. Ocean Eng. **250**, 110888 (2022). https://doi.org/10.1016/j.oceaneng.2022.110888
34. Liu, Y., Mizutani, N., Cho, Y.-H., Nakamura, T.: Performance enhancement of a bottom-hinged oscillating wave surge converter via resonant adjustment. Renew. Energy **201**, 624–635 (2022). https://doi.org/10.1016/j.renene.2022.10.130
35. Jahangir, M.H., Houmani, A., Kargarzadeh, A.: A theoretical assessment of energy efficiency of wave tower as an oscillating wave surge converter. Ocean Eng. **295**, 116748 (2024). https://doi.org/10.1016/j.oceaneng.2024.116748
36. He, G., Zhao, C., Liu, C., He, R., Luan, Z.: Power absorption and dynamic response analysis of a hybrid system with a semi-submersible wind turbine and a Salter's duck wave energy converter array. Energy **305**, 132210 (2024). https://doi.org/10.1016/j.energy.2024.132210
37. Ghasemipour, N., Izanlou, P., Jahangir, M.H.: Feasibility study on utilizing oscillating wave surge converters (OWSCs) in nearshore regions, case study: along the southeastern coast of Iran in Oman sea. J. Clean. Prod. **367**, 133090 (2022). https://doi.org/10.1016/j.jclepro.2022.133090
38. Wang, Y., Liu, Z.: A bionic design of oscillating wave surge energy converter based on scallops. Energy **304**, 132236 (2024). https://doi.org/10.1016/j.energy.2024.132236
39. Moradi, M., Ilinca, A.: Analyzing wave dragon under different wave heights using flow-3D: a computational fluid dynamics approach. Water **17**(5), 613 (2025). https://doi.org/10.3390/w17050613
40. Vicinanza, D., Margheritini, L., Contestabile, P., Kofoed, J.P., Frigaard, P.: Seawave slot-cone generator: an innovative caisson breakwaters for energy production. In: Coastal Engineering 2008. World Scientific Publishing Company, pp. 3694–3705 (2009). https://doi.org/10.1142/9789814277426_0306
41. Liu, Z., Zhang, G.: Overtopping performance of a multi-level CROWN wave energy convertor: a numerical study. Energy **294**, 130795 (2024). https://doi.org/10.1016/j.energy.2024.130795
42. Erselcan, İ.Ö., Özkan, D., Sulukan, E., Uyar, T.S.: Wave energy conversion technologies. In: Uyar, T.S., Javani, N. (eds.) Renewable Energy Based Solutions, pp. 345–361. Springer International Publishing, Cham (2022). https://doi.org/10.1007/978-3-031-05125-8_14
43. da Silveira Paiva, M., et al.: Geometrical evaluation of an overtopping wave energy converter device subject to realistic irregular waves and representative regular waves of the sea state that occurred in Rio Grande—RS. Processes **13**(2), 335 (2025). https://doi.org/10.3390/pr13020335

44. Xu, X., et al.: An integrated approach for the decision of wave energy converter deployment based on forty-five-years high-resolution wave climate modeling. Energy **305**, 132238 (2024). https://doi.org/10.1016/j.energy.2024.132238
45. Fernandez, H., et al.: The new wave energy converter WaveCat: concept and laboratory tests. Mar. Struct. **29**(1), 58–70 (2012). https://doi.org/10.1016/j.marstruc.2012.10.002
46. Allen, J., Iglesias, G., Greaves, D., Miles, J.: Physical modelling of the effect on the wave field of the WaveCat wave energy converter. J. Mar. Sci. Eng. **9**(3) (2021). https://doi.org/10.3390/jmse9030309
47. Mahdy, A., Hasanien, H.M., Aleem, S.H.E.A., Al-Dhaifallah, M., Zobaa, A.F., Ali, Z.M.: State-of-the-art of the most commonly adopted wave energy conversion systems. Ain Shams Eng. J. **15**(1), 102322 (2024). https://doi.org/10.1016/j.asej.2023.102322
48. de Sousa Prado, M.G., Gardner, F., Damen, M., Polinder, H.: Modelling and test results of the Archimedes wave swing (2006). https://doi.org/10.1243/09576509JPE284
49. Al-Dhaifallah, M., Mahdy Ahmed, A., Hasanien, H.M., Ali, Z.M., Ali Ebrahim, E., Abdel Aleem, S.H.E.: Dynamic performance enhancement of nonlinear AWS wave energy systems based on optimal super-twisting control strategy. Ain Shams Eng. J. **15**(5), 102732 (2024). https://doi.org/10.1016/j.asej.2024.102732
50. Jenne, S., et al.: HERO WEC V1: Design and Experimental Data Collection Efforts. National Renewable Energy Laboratory (NREL), Golden, CO, USA, NREL/TP-5700-91741 (2024). https://doi.org/10.2172/2482265
51. Czech, B., Bauer, P., Polinder, H., Korondi, P.: Modeling and simulating an Archimedes Wave Swing park in steady state conditions. In: 2009 13th European Conference on Power Electronics and Applications, pp. 1–10. https://ieeexplore.ieee.org/abstract/document/5278939?casa_token=LSpVt6BzawsAAAAA:AIRObAfVunD2s5v8qBbZOsJyoNvFCKTf8XrtOphdBSqTHDroOXbSo76r4e0mPMBeY-XN69o (2009). Accessed 12 Mar 2025
52. Nath, R., Kankar, P.K., Gupta, V.K.: Study of Archimedes Wave Swing Harvester for Indian Ocean. In: Parinov, I.A., Chang, S.-H., Kim, Y.-H. (eds.) Advanced Materials, pp. 545–556. Springer International Publishing, Cham (2019). https://doi.org/10.1007/978-3-030-19894-7_42.
53. Garcia-Teruel, A., Forehand, D.I.M.: A review of geometry optimisation of wave energy converters. Renew. Sustain. Energy Rev. **139**, 110593 (2021)
54. Shadmani, A., Nikoo, M.R., Gandomi, A.H., Chen, M.: An optimization approach for geometry design of multi-axis wave energy converter. Energy **301**, 131714 (2024). https://doi.org/10.1016/j.energy.2024.131714
55. Zhang, C., Li, D., Ding, Z., Liu, Y., Cao, F., Ning, D.: Wave energy converter with multiple degrees of freedom for sustainable repurposing of decommissioned offshore platforms: an experimental study. Appl. Energy **376**, 124204 (2024). https://doi.org/10.1016/j.apenergy.2024.124204
56. Nasr Esfahani, F., Sheng, W., Ma, X., Hall, C.M., Aggidis, G.: Innovations in wave energy: a case study of TALOS-WEC's multi-axis technology. J. Mar. Sci. Eng. **13**(2), 279 (2025). https://doi.org/10.3390/jmse13020279
57. Beringer, C.K., Bosma, B., Robertson, B.: A numerical and experimental study of wave energy converter number of bodies and degrees of freedom. In: Social Science Research Network, Rochester, NY: 5022459 (2024). https://doi.org/10.2139/ssrn.5022459
58. Beringer, C.K., Bosma, B., Robertson, B.: Wave energy converter bodies and degrees of freedom impacts on power, motion, and control: a numerical and experimental study. In: Social Science Research Network, Rochester, NY: 4917632. https://papers.ssrn.com/abstract=4917632 (2024). Accessed 13 Mar 2025
59. Beringer, C.K., Bosma, B., Robertson, B.: Degrees of freedom effects on a laboratory scale WEC point absorber. Proc. Eur. Wave Tidal Energy Conf. **15**(1), 29–35 (2023). https://doi.org/10.36688/ewtec-2023-380
60. Waskito, K.T., Geraldi, A., Ichi, A.C., Yanuar, Rahardjo, G.P., Al Ghifari, I.: Design of hydraulic power take-off systems unit parameters for multi-point absorbers wave energy converter. Energy Rep. **11**, 115–127 (2024). https://doi.org/10.1016/j.egyr.2023.11.042

61. de Lima, Y.T.B., et al.: Study of the geometry of an oscillating water column device with five chambers coupled under regular waves through the constructal design method. Fluids **9**(4), 86 (2024). https://doi.org/10.3390/fluids9040086
62. Elatife, K., El Marjani, A.: Design optimization and analysis of a compact twin radial impulse turbine for wave energy conversion. Results Eng. **24**, 103561 (2024). https://doi.org/10.1016/j.rineng.2024.103561
63. Choiniere, M., Davis, J., Nguyen, N., Tom, N., Fowler, M., Thiagarajan, K.: Hydrodynamics and load shedding behavior of a variable-geometry oscillating surge wave energy converter (OSWEC). Renew. Energy **194**, 875–884 (2022). https://doi.org/10.1016/j.renene.2022.05.169
64. Performance optimization techniques on point absorber and oscillating water column wave energy converter: a comprehensive review. IEEE Journals & Magazine | IEEE Xplore. https://ieeexplore.ieee.org/abstract/document/10844294. Accessed 13 Mar 2025
65. Jin, H., Zhang, H., Zheng, S., Xu, D.: Characteristics of a two-dimensional periodic wave energy converter array. Renew. Energy **222**, 119834 (2024). https://doi.org/10.1016/j.renene.2023.119834
66. Adibzade, M., Akbari, H.: Spectral approach to evaluate multi-body floating wave energy converters in complex sea states. Ocean Eng. **286**, 115567 (2023). https://doi.org/10.1016/j.oceaneng.2023.115567
67. Garcia-Teruel, A., Forehand, D.I.M.: Manufacturability considerations in design optimisation of wave energy converters. Renew. Energy **187**, 857–873 (2022). https://doi.org/10.1016/j.renene.2021.12.145
68. Cotten, A., Forehand, D.I.M.: Optimisation of a novel, sloped module, multibody wave energy converter, using an efficient modelling technique. Renew. Energy **162**, 727–742 (2020). https://doi.org/10.1016/j.renene.2020.07.091
69. Formentin, S.M., Zanuttigh, B., van der Meer, J.W.: A neural network tool for predicting wave reflection, overtopping and transmission. Coast. Eng. J. **59**(1), 1750006-1–1750006-31 (2017). https://doi.org/10.1142/S0578563417500061
70. Singh, D., Paul, A.R., Samad, A.: Performance estimation of a two-body wave energy converter for the East Coast of India. Environ. Prog. Sustain. Energy **43**(6), e14468 (2024). https://doi.org/10.1002/ep.14468
71. Rashidi, S., Nikseresht, A.H.: Numerical investigation of the response of the hybrid wave energy converter including oscillating water column and horizontal floating cylinder to irregular waves. Energy **301**, 131717 (2024). https://doi.org/10.1016/j.energy.2024.131717
72. Shipon, M.R., Ali, M.S., Kabir, M.A., Abdullah-Al-Mamun, Md., Farrok, O.: Pelamis wave energy converter. In: Farrok, O., Islam, M.R. (eds.) Oceanic Wave Energy Conversion: Advancement of Electrical Generators, pp. 45–66. Springer Nature, Singapore (2024). https://doi.org/10.1007/978-981-99-9814-2_3
73. Shadmani, A., Nikoo, M.R., Gandomi, A.H., Wang, R.-Q., Golparvar, B.: A review of machine learning and deep learning applications in wave energy forecasting and WEC optimization. Energy Strategy Rev. **49**, 101180 (2023). https://doi.org/10.1016/j.esr.2023.101180
74. Golbaz, D., et al.: Layout and design optimization of ocean wave energy converters: a scoping review of state-of-the-art canonical, hybrid, cooperative, and combinatorial optimization methods. Energy Rep. **8**, 15446–15479 (2022). https://doi.org/10.1016/j.egyr.2022.10.403
75. Yang, B., et al.: Wave energy converter array layout optimization: A critical and comprehensive overview. Renew. Sustain. Energy Rev. **167**, 112668 (2022)
76. Lian, J., Wang, X., Wang, X., Wu, D.: Research on wave energy converters. Energies **17**(7), 1577 (2024). https://doi.org/10.3390/en17071577
77. Elatife, K., El Marjani, A.: Optimized blade design of a radial implulse turbine for wave energy conversion. In: 2015 3rd International Renewable and Sustainable Energy Conference (IRSEC), pp. 1–6 (2015). https://doi.org/10.1109/IRSEC.2015.7454955
78. Ning, D., Zhang, X., Wang, R., Zhao, M.: Hydrodynamic performance of an integrated system of breakwater and a multi-chamber OWC wave energy converter. China Ocean Eng. **38**(4), 543–556 (2024). https://doi.org/10.1007/s13344-024-0043-9

79. Arrosyid, W.A., et al.: Hydrodynamic performance and multi-objective optimization of multi-cylinder floating point absorber wave energy converter. Ocean Eng. **317**, 120040 (2025). https://doi.org/10.1016/j.oceaneng.2024.120040
80. Housner, S., Wynn, N.: Numerical Modeling and Optimization of the iProTech Pitching Inertial Pump (PIP) Wave Energy Converter (WEC) (Cooperative Research and Development Final Report, CRADA Number: CRD-22-22968). National Renewable Energy Laboratory (NREL), Golden, CO, USA; iProTech, Redwood City, CA, USA, NREL/TP-5000-92188; CRD-22-22968 (2024). https://doi.org/10.2172/2478103
81. Li, B., Zhang, X., Liu, T., Adan, H.S.: Bionic raft design and performance investigation of a two-raft wave energy converter. J. Mar. Sci. Eng. **12**(12), 2114 (2024). https://doi.org/10.3390/jmse12122114
82. Talaat, M., et al.: Monolithic design of self-adaptive CMOS converter and robust event-triggered consensus control for integration of multi-renewable energy sources with battery storage system. J. Energy Storage **88**, 111498 (2024). https://doi.org/10.1016/j.est.2024.111498
83. Li, L., Yuan, Z., Gao, Y.: Maximization of energy absorption for a wave energy converter using the deep machine learning. Energy **165**, 340–349 (2018). https://doi.org/10.1016/j.energy.2018.09.093
84. Liu, Z., Wang, Y., Hua, X.: Prediction and optimization of oscillating wave surge converter using machine learning techniques. Energy Convers. Manag. **210**, 112677 (2020). https://doi.org/10.1016/j.enconman.2020.112677
85. Giannini, G., et al.: Wave energy converter power take-off system scaling and physical modelling. J. Mar. Sci. Eng. **8**(9), 632 (2020). https://doi.org/10.3390/jmse8090632
86. Pinto Júnior, É.A., et al.: Geometric evaluation of the hydro-pneumatic chamber of an oscillating water column wave energy converter employing an axisymmetric computational model submitted to a realistic sea state data. J. Mar. Sci. Eng. **12**(9), 1620 (2024). https://doi.org/10.3390/jmse12091620
87. Lee, C.F., Fjermedal, S., Ong, M.C.: Design and analysis of taut mooring systems for a combined floating offshore wind and wave energy system at intermediate water depth. Ocean Eng. **312**, 119174 (2024). https://doi.org/10.1016/j.oceaneng.2024.119174
88. Ezhilsabareesh, K., Suchithra, R., Thandayutham, K., Samad, A.: Surrogate based optimization of a bi-directional impulse turbine for OWC-WEC: effect of guide vane lean and stagger angle for pseudo-sinusoidal wave conditions. Ocean Eng. **226**, 108843 (2021). https://doi.org/10.1016/j.oceaneng.2021.108843
89. Sharp, C., DuPont, B.: Wave energy converter array optimization: a genetic algorithm approach and minimum separation distance study. Ocean Eng. **163**, 148–156 (2018). https://doi.org/10.1016/j.oceaneng.2018.05.071
90. Shadman, M., Estefen, S.F., Rodriguez, C.A., Nogueira, I.C.M.: A geometrical optimization method applied to a heaving point absorber wave energy converter. Renew. Energy **115**, 533–546 (2018). https://doi.org/10.1016/j.renene.2017.08.055
91. Tournant, P., Perret, G., Smaoui, H., Sergent, P., Marin, F.: Shape parameters optimisation of a quayside heaving rectangular wave energy converter. Appl. Energy **343**, 121232 (2023). https://doi.org/10.1016/j.apenergy.2023.121232
92. Garcia-Teruel, A., Roberts, O., Noble, D.R., Henderson, J.C., Jeffrey, H.: Design limits for wave energy converters based on the relationship of power and volume obtained through multi-objective optimisation. Renew. Energy **200**, 492–504 (2022). https://doi.org/10.1016/j.renene.2022.09.053
93. Cotten, A., Forehand, D.I.M.: Multi-objective optimisation of a sloped-motion, multibody wave energy converter concept. Renew. Energy **194**, 307–320 (2022). https://doi.org/10.1016/j.renene.2022.05.030
94. Esmaeilzadeh, S., Alam, M.-R.: Shape optimization of wave energy converters for broadband directional incident waves. Ocean Eng. **174**, 186–200 (2019). https://doi.org/10.1016/j.oceaneng.2019.01.029

95. Rahimi, A., Rezaei, S., Mansourzadeh, S., Parvizian, J.: Dimensional optimization of a two-body wave energy converter under irregular waves for the strait of hormuz. Ocean Eng. **292**, 116539 (2024). https://doi.org/10.1016/j.oceaneng.2023.116539
96. Rodríguez, C.A., Rosa-Santos, P., Taveira-Pinto, F.: Hydrodynamic optimization of the geometry of a sloped-motion wave energy converter. Ocean Eng. **199**, 107046 (2020). https://doi.org/10.1016/j.oceaneng.2020.107046
97. Bouali, B., Larbi, S.: Contribution to the geometry optimization of an oscillating water column wave energy converter. Energy Procedia **36**, 565–573 (2013). https://doi.org/10.1016/J.EGYPRO.2013.07.065
98. Guo, W., Zhou, Y., Zhang, W., Zhao, Q.: Hydrodynamic analysis and power conversion for point absorber WEC with two degrees of freedom using CFD. China Ocean Eng. **32**(6), 718–729 (2018). https://doi.org/10.1007/s13344-018-0073-2
99. Manawadu, N.H.D.S., Nissanka, I.D., Karunasena, H.C.P.: SPH-based numerical modelling and performance analysis of a heaving point absorber type wave energy converter with a novel buoy geometry. Renew. Energy **228**, 120595 (2024). https://doi.org/10.1016/j.renene.2024.120595
100. Shadmani, A., Nikoo, M.R., Gandomi, A.H.: Adaptive systematic optimization of a multi-axis ocean wave energy converter. Renew. Sustain. Energy Rev. **189**, 113920 (2024)
101. Hall, C.M., Sheng, W., Yavuz, H., Aggidis, G.: PTO control design for a multi-axis WEC device. In: The 34th International Ocean and Polar Engineering Conference, OnePetro (2024)
102. Rusu, L., Onea, F.: The performance of some state-of-the-art wave energy converters in locations with the worldwide highest wave power. Renew. Sustain. Energy Rev. **75**, 1348–1362 (2017). https://doi.org/10.1016/j.rser.2016.11.123
103. Zhao, M., Ning, D.: A review of numerical methods for studying hydrodynamic performance of oscillating water column (OWC) devices. Renew. Energy **233**, 121177 (2024). https://doi.org/10.1016/j.renene.2024.121177
104. Song, L., Wu, Q., Xie, Y.: Numerical study of the hydrodynamic performance of the offshore oscillating water column device with varying tilt angle. In: The 34th International Ocean and Polar Engineering Conference, OnePetro (2024)
105. Qian, K., Chen, L., Zhou, Y., Ning, D.: Hydrodynamics of an offshore multi-chamber OWC wave energy converter. Energy **304**, 132239 (2024). https://doi.org/10.1016/j.energy.2024.132239
106. Zhang, H., Sheng, W., Zha, Z., Aggidis, G.: A preliminary study on identifying biomimetic entities for generating novel wave energy converters. Energies **15**(7), 2485 (2022). https://doi.org/10.3390/en15072485
107. Rosati, M., Ringwood, J.V.: Electric energy maximization for oscillating water column wave energy systems using a receding-horizon pseudospectral control approach. IEEE Trans. Sustain. Energy **15**(4), 2769–2776 (2024). https://doi.org/10.1109/TSTE.2024.3443228
108. Elhanafi, A., Kim, C.J.: Experimental and numerical investigation on wave height and power take–off damping effects on the hydrodynamic performance of an offshore–stationary OWC wave energy converter. Renew. Energy **125**, 518–528 (2018). https://doi.org/10.1016/j.renene.2018.02.131
109. Golbaz, D., et al.: Ocean Wave Energy Converters Optimization: A Comprehensive Review on Research Directions (2021). https://doi.org/10.48550/arxiv.2105.07180
110. Meng, W., Chen, M., Peng, H., Qiu, W.: Performance evaluation and optimization of a hinged-type wave energy converter. Int. J. Offshore Polar Eng. **30**(04), 403–413 (2020). https://doi.org/10.17736/ijope.2020.mm25
111. Vakili, A., Pourzangbar, A., Ettefagh, M.M., Abdollahi Haghghi, M.: Optimal control strategy for enhancing energy efficiency of Pelamis wave energy converter: a Simulink-based simulation approach. Renew. Energy Focus **53**, 100685 (2025). https://doi.org/10.1016/j.ref.2025.100685
112. Peymani, M., Nikseresht, A.H., Bingham, H.B.: A 3D numerical investigation of the influence of the geometrical parameters of an I-beam attenuator OWC on its performance at the resonance period. Energy **286**, 129542 (2024). https://doi.org/10.1016/j.energy.2023.129542

113. Optimization of overtopping type wave energy converters on existing breakwaters—ProQuest. https://www.proquest.com/openview/612e546643e81f2878b5e32ffa917bff/1?cbl=2026366&diss=y&pq-origsite=gscholar. Accessed 14 Mar. 2025
114. An, S.-H., Kim, G.-G., Lee, J.-H.: Optimal design of the overtopping wave energy converter based on fluid-structure interaction simulation. J. Coast. Res. **116**(SI), 578–582 (2024). https://doi.org/10.2112/JCR-SI116-117.1

Chapter 4
Layout Design Characteristics and Cost Evaluation

Abstract This chapter examines the critical relationship between wave farm layout design and economic feasibility of ocean wave energy projects. The spatial arrangement of wave energy converters (WECs) within a farm significantly influences both energy capture efficiency and project economics through its effects on infrastructure requirements, installation procedures, and maintenance operations. Understanding the complex interplay between technical design considerations and economic implications is essential for developing commercially viable wave energy projects that can compete with other renewable energy technologies in the global energy market. The chapter begins with an introduction to wave farm layout fundamentals, exploring basic concepts and historical approaches to spatial arrangement of WECs. Section 4.2 delves into crucial design considerations and constraints, including hydrodynamic interactions between devices, environmental impact limitations, navigational safety requirements, and mooring system configurations. Section 4.3 presents methodologies for layout optimization focusing on cost efficiency, covering analytical frameworks for levelized cost of energy calculations, multi-objective optimization techniques, and economic implications of different spatial arrangements. Finally, Sect. 4.4 provides illuminating case studies from existing wave energy projects worldwide, offering practical insights into the technical and economic trade-offs observed in real-world implementations across various scales, technologies, and oceanographic conditions.

Keywords Wave farm layout · Economic optimization · Array effects · Infrastructure design · Levelized cost of energy (LCOE)

4.1 Introduction to Wave Farm Layout Design

Wave farms, composed of arrays of wave energy converters (WECs), are pivotal in the large-scale utilization of ocean wave energy. Their layout is a key determinant of energy output, operational effectiveness, and overall project feasibility. The strategic arrangement of WECs impacts energy capture efficiency, maintenance demands,

A. Shadmani et al., *Ocean Wave Energy Technology*,
https://doi.org/10.1007/978-3-031-95040-7_4

environmental compatibility, and economic viability, making layout design a critical component of wave farm development [1].

The design of a wave farm layout is a critical factor that determines the efficiency, reliability, and environmental sustainability of energy extraction from ocean waves. WECs are generally arranged in arrays to maximize the collective capture of wave energy while minimizing destructive interactions between devices [2]. Unlike traditional power plants, where the resource is stationary and predictable, wave farms deal with a resource that is dynamic, nonlinear, and subject to a variety of environmental, spatial, and operational constraints. Hence, designing the layout of a wave farm is not just about arranging devices in an arbitrary pattern but requires careful consideration of wave propagation, hydrodynamic effects, device interactions, and site-specific factors [3]. Additionally, the optimization of wave farm layouts often involves a trade-off between maximizing energy yield and minimizing costs, environmental impacts, and maintenance complexity [4, 5].

The primary objective of layout design is to optimize energy capture by ensuring that each device in the array operates at its highest efficiency. This is achieved by strategically positioning WECs to harness the most energy from incident waves while accounting for the wake effects generated by upstream devices. Wake effects, a phenomenon in which energy is reduced downstream of a device due to wave absorption, can significantly reduce the overall performance of a wave farm if not properly managed. Hydrodynamic simulations and computational models are commonly used to predict and mitigate these interactions by optimizing the spacing between devices [6]. For example, staggered and clustered configurations have been studied extensively to identify optimal placements that can enhance constructive wave interference while avoiding destructive interactions. Furthermore, site-specific wave characteristics, including wave height, period, and direction, dictate the optimal layout since different configurations may be better suited to particular wave climates [7].

Another essential aspect of wave farm layout design involves considering the structural and mechanical integrity of the devices and their mooring systems. Ocean conditions are highly variable and can subject WECs to extreme forces, particularly during storms and high-energy wave events. Therefore, designers must ensure that devices are not only optimally placed for energy capture but also resilient against mechanical stresses [8]. Floating WECs require robust mooring systems that can accommodate dynamic wave loads while maintaining stability. Fixed-bottom devices, on the other hand, rely on seabed conditions to provide anchoring strength. Layout designs must also minimize the risk of mechanical failure and reduce maintenance demands by ensuring that devices are easily accessible for repair and inspection without interfering with neighboring units [3].

In addition to hydrodynamic and structural considerations, environmental and regulatory factors heavily influence the layout design of wave farms. Marine ecosystems are sensitive to changes in hydrodynamic flows, noise pollution, and seabed disturbance, all of which can be exacerbated by improperly designed arrays. Environmental Impact Assessments (EIAs) are therefore integral to layout planning, identifying sensitive ecological zones that should be avoided or mitigated [9]. Regulations concerning marine spatial planning and biodiversity protection impose constraints

on the location and density of wave farms, which in turn affect layout decisions. For instance, in regions where marine biodiversity is particularly high, arrays may be dispersed more widely to reduce ecological impacts while sacrificing some degree of energy efficiency [10]. Developers must strike a balance between optimizing layout efficiency and complying with environmental regulations to ensure long-term project sustainability [11].

Economic considerations also play a significant role in wave farm layout design. Optimal layouts not only maximize energy yield but also minimize construction, operation, and maintenance costs. The financial feasibility of a wave farm is influenced by factors such as proximity to the shore, grid connectivity, and ease of installation. Clustering devices closer to shore may reduce transmission losses and infrastructure costs but can limit access to higher-energy waves typically found further offshore [4]. The integration of cost-benefit analyses in layout design ensures that the financial return on investment is maximized without compromising on performance or environmental standards. Hybrid systems that combine wave energy with other offshore renewables, such as wind and solar, are increasingly being explored as a means of enhancing financial viability while optimizing space utilization [12].

Advancements in computational modeling, data analytics, and machine learning have revolutionized wave farm layout design in recent years. State-of-the-art simulation tools allow developers to model various design configurations and predict their performance under real-world conditions. Multi-objective optimization algorithms are commonly employed to assess trade-offs between conflicting objectives, such as energy maximization, cost minimization, and ecological protection [13]. These tools enable dynamic adjustments to the layout as new data becomes available during project development, ensuring that the design remains adaptable to changing environmental conditions or regulatory requirements. Furthermore, real-time monitoring systems can be integrated into the layout to provide continuous feedback on device performance, enabling proactive maintenance and operational adjustments [8].

In conclusion, the design of wave farm layouts is a complex, multi-disciplinary process that requires careful integration of hydrodynamic, structural, environmental, and economic factors. Successful layout design not only maximizes energy output but also ensures long-term sustainability and financial viability by addressing potential risks and challenges at the outset. With continued advancements in computational tools and hybrid energy systems, wave farms have the potential to play a significant role in the global transition to renewable energy. However, achieving this potential will require ongoing research and development to refine layout optimization techniques and address the unique challenges posed by ocean environments. In addition, a properly designed wave farm layout balances multiple objectives, for instance, maximizing energy yield, minimizing costs, and mitigating environmental impacts. This mixed problem requires integrating site-specific wave characteristics, technical constraints, and financial considerations. This chapter explores the intricacies of wave farm layout design, discussing its foundational principles, optimization strategies, and case studies that highlight practical implementations. Through a comprehensive evaluation of design considerations, this chapter provides insights into achieving cost-effective and sustainable wave energy extraction.

4.2 Design Considerations and Constraints

The design and layout of ocean wave farms rely on a multidisciplinary approach that balances the technical potential of the site, the interplay between wave energy devices, environmental regulatory limitations, and economic viability. An optimized layout is critical to ensure both maximum power generation and long-term sustainability of the wave farm. This section explores the core design aspects and constraints, focusing on the site characteristics, device interactions, environmental regulations, and economic considerations (Fig. 4.1).

4.2.1 Site Characteristics

Identifying an appropriate site is the first and most fundamental step in wave farm design. Site-specific parameters influence energy generation to installation logistics and long-term maintenance requirements, mainly classified as follows:

- Wave climate: Optimal layout design demands a thorough analysis of local wave conditions, including wave height, period, and directional distribution. Seasonal and inter-annual variability must be accounted for to ensure consistent energy production.
- Bathymetry: The underwater topography influences device positioning, mooring configurations, and hydrodynamic interactions between WECs. Shallow regions or irregular seabed often necessitate customized solutions.
- Seabed composition: The mechanical properties of the seabed dictate foundation and anchoring options. Sediment layers may require additional reinforcement, whereas rocky substrates pose anchoring challenges.
- Distance to shore: The proximity of the site to the shore affects the length and cost of subsea power transmission infrastructure. Nearshore installations may offer lower transmission costs but could face stricter environmental regulations.

Site selection begins with evaluating the wave resource potential, including wave height, frequency, and directional consistency. Coastal areas with high wave energy

Fig. 4.1 Design considerations and constraints factors

potential, such as western coastlines exposed to prevailing winds, are often ideal locations [4, 14]. Wave farms benefit most when deployed in regions with a consistent wave climate, as fluctuations can lead to intermittent energy production. However, wave energy is not the only consideration. Seabed composition, such as the presence of rocky, sandy, or muddy substrates, affects the stability and anchoring of WECs. Hard seabed generally provides a firm foundation, while soft seabed require more robust anchoring solutions [15, 16]. The wave resource is the primary driver of site selection, with developers seeking regions of high and consistent wave energy. Wave height, wave period, and directionality are crucial parameters that determine the energy yield of the wave farm. Seasonal variability in these characteristics can influence the efficiency and reliability of power output. Seasonal and directional variability are analyzed via wave roses and monthly averages to ensure the farm can harness prevailing swell directions and handle seasonal shifts. Extreme conditions must also be quantified: design standards call for withstanding the 50-year or 100-year return period storm at the site. For instance, North Sea wave farms are engineered for extreme waves exceeding 20 m height in a centennial storm [17]. As highlighted in [11], understanding the spatial distribution and temporal variations of wave resources helps in optimizing device placement and ensuring a stable energy output. Furthermore, advanced forecasting tools and models are often employed to predict wave behavior and improve overall performance planning. Water depth also plays a critical role in determining the suitability of a site. Shallow waters may create favorable conditions for nearshore installations, but excessive drag and wave breaking can reduce energy capture efficiency. Deep waters, on the other hand, require floating systems, increasing costs related to mooring and maintenance. Local ocean dynamics like currents and tides also affect WEC siting. Strong tidal currents can alter the incident wave field through Doppler shift and refraction, and they superimpose additional forces on devices and moorings. Currents on the order of ~ 10% of wave group velocity can measurably modify wave energy transport and cause spatial variations in power levels across a site. In device design, currents are treated as part of the metocean loading. Design condition definitions include not just extreme waves but concurrent wind and current profiles robust farm design considers the worst-case combination (e.g. peak storm waves plus peak currents) for structural stability. Currents can also influence device orientation (especially free-yaw floating WECs) and fatigue on moorings, necessitating careful analysis of wave–current interaction effects during site evaluation.

Additionally, proximity to the shore and the electrical grid is essential for reducing transmission losses and infrastructure costs. Sites with easy grid access can enhance the project's overall financial viability by minimizing logistical and transmission expenses [13]. Site accessibility for operations & maintenance (O&M) tends to diminish with distance and harsher offshore weather. Maintenance vessels face longer transit times and smaller weather windows. Extended gaps between suitable weather windows can significantly increase downtime and O&M costs. A recent accessibility analysis in the Irish wave sector showed that high-energy sites often suffer from reduced access (fewer calm periods), which can raise overall O&M costs and LCOE.

In addition to resource availability, bathymetry and seabed conditions at the deployment site are critical. A stable seabed with minimal slope ensures that devices are properly anchored while minimizing risks of structural failure or scouring [18]. Sites with soft substrates, such as sand or silt, may require more robust and costly anchoring systems compared to rocky seabed. Seabed composition influences the long-term maintenance requirements for mooring and anchoring systems, as soft sediment can lead to shifting anchors over time, necessitating regular inspection and reinforcement. Although rocky seabed offers superior stability, they may present installation challenges requiring specialized drilling or mounting techniques. Understanding these site-specific conditions allows designers to develop cost-effective and durable mooring solutions. Proximity to onshore electrical grids significantly affects the overall cost-effectiveness of the wave farm. Longer transmission distances increase capital investment for subsea cabling and power conversion systems. Remote locations may require additional infrastructure such as substations and voltage boosters. A study highlighted that excessive distances to the grid can render otherwise optimal locations economically unfeasible [19]. Emerging technologies, including floating substations, direct current (DC) transmission, and wireless power transfer, are being explored to address these challenges.

Beyond technical considerations, logistical factors play a significant role. Sites accessible to maintenance vessels and equipment reduce operational costs and improve the feasibility of long-term maintenance programs. Coastal regions with existing port facilities provide logistical advantages, allowing for faster deployment, servicing, and repairs. Conversely, remote locations may require the development of new infrastructure, which could significantly inflate project costs and timelines. Strategic planning for logistical support is, therefore, essential to project success. By incorporating integrated coastal management practices and participatory decision-making, developers can align their projects with environmental and community goals [17].

Finally, spatial variability across the farm area is assessed to ensure a coherent resource. Wave energy can vary within a few kilometers due to the bathymetry and wave–current effects. Prior studies recommend avoiding sites with highly localized wave peaks (small-scale “hot spots”), as these can complicate power estimation and device loading. Instead, developers seek a relatively homogeneous resource across the planned WEC array footprint so that each device experiences similar wave climates. Strategically spacing devices over an area can allow the farm to capture a broader wave front and marginally smooth out power output. In summary, selecting a wave farm site requires a holistic appraisal of the wave resource (mean and extreme), water depth and seabed conditions, and practical access considerations. These site characteristics set the fundamental constraints within which the WEC array must be designed and operated.

4.2.2 Device Interactions

The dynamic interactions between WECs within an array have significant implications for overall performance. Proper spacing and orientation are essential to minimize energy losses due to hydrodynamic interference.

- Wake effects: As waves propagate through an array, downstream devices may encounter reduced wave energy, leading to diminished power output. Accurate modeling of wake effects is necessary to mitigate these losses.
- Spacing between WECs: Overly dense layouts exacerbate interference, while overly sparse layouts underutilize available space. The optimal inter-device distance ensures maximum energy extraction without excessive infrastructure costs.

When multiple wave energy converters operate in proximity, their hydrodynamic fields overlap, leading to complex wave–device interactions that can significantly alter performance. Each WEC both absorbs and scatters waves; thus, in an array, devices influence the incoming waves for their neighbors via wave radiation and diffraction effects. These interactions can be either constructive or destructive depending on geometry and spacing [20]. As waves propagate through a wave farm, some energy may be extracted or redirected by upstream units, creating downstream "shadows" or altered wave patterns often termed wake effects. In contrast to wind farms (where wakes are velocity deficits), wave farm wake effects manifest as reduced wave height and energy in the lee of devices. For example, one study of multi-body WEC arrays found that a device placed directly down-wave of another can experience significantly diminished incident wave energy (a strong shielding effect) [21]. Such destructive interference was observed as an interaction factor, q, below 1 (meaning the pair produced less combined power than if widely separated), emphasizing that certain layouts (like devices in-line with wave direction) are suboptimal [21]. On the other hand, constructive interference can occur if devices are spaced such that radiated waves from one reinforce the excitation of another. Achieving these positive interactions often requires careful tuning of spacing to fractions of the dominant wavelength and phasing of device oscillations (Fig. 4.2).

Researchers commonly quantify array interaction effects using the q-factor (interaction factor). This metric is defined as the ratio of total power output of an array to the sum of the power outputs of each device operating in isolation. A q-factor > 1 indicates constructive interactions (array gains), while $q < 1$ signifies losses due to destructive interference [22]. Many early wave farm studies reported q-factors slightly below 1 for random or loosely optimized layouts, implying that unmanaged interactions often cause a small performance deficit. However, optimized configurations can attain $q \approx 1$ or even exceed it, meaning a well-designed array can equal or outperform the simple sum of its parts. This optimization hinges on both spacing and relative positioning (staggering). Optimal spacing is highly site- and device-specific; it often lies on the order of one wavelength or more between units to minimize near-field overlaps, but smaller spacings can be favorable for tightly coupled devices

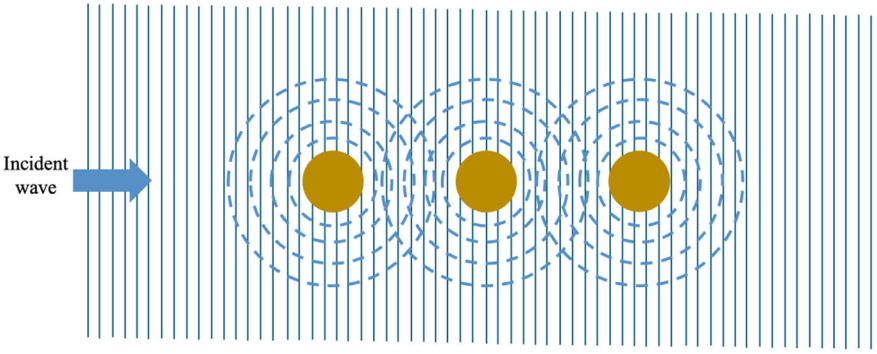

Fig. 4.2 Schematic of the modification of the wave resource in a WEC array

designed for constructive phasing. Empirical wave tank tests and numerical models have shown that even small arrays (3–5 WECs) can exhibit measurable interaction effects—positive or negative—depending on arrangement [23]. As array size grows, cumulative effects can lead to diminishing returns in power if layout is not adjusted accordingly.

Array configuration (the geometric layout of devices) thus plays a critical role. Common layouts studied include linear rows (devices aligned side-by-side or in tandem), staggered grids (e.g. a triangular lattice), and clustered groupings. Simulation studies for oscillating surge converters (flap-type WECs) found that staggering units (offsetting them in adjacent rows) yielded better overall efficiency than a single long line, by reducing direct shadowing [23]. Similarly, optimal layouts have been proposed for specific WEC types like OWCs and point absorbers, often involving multiple rows with spacing tuned to the dominant wavelength [23]. For instance, identified an improved arrangement for flap-type converters that maximized constructive interference while minimizing wake losses [24]. A general finding is that not a single layout fits all conditions. A configuration optimal for a narrow wave direction spread may underperform if wave directionality changes. Therefore, some array designs incorporate directional robustness, spacing devices to handle a range of wave approach angles without severe performance degradation.

Hydrodynamic modeling approaches underpin these interaction analyses. Linear potential flow models (using boundary element methods and analytical solutions) are widely used to predict array behavior in the frequency domain. These models capture radiation/diffraction effects efficiently for simplified geometries. For more complex WEC shapes or highly nonlinear behaviors, numerical methods like CFD or hybrid models are employed at the cost of higher computation [21]. Semi-analytical techniques (e.g. using Green's functions or eigenfunction expansions) can estimate interactions more quickly for preliminary optimization. These models allow designers to iterate on array spacing and configuration to seek maximum energy absorption. For example, by varying separation distances and evaluating q-factors, one can identify spacing that yields local maxima in power (constructive peaks) or avoid distances

that cause destructive interactions [25]. In practice, array design often also considers practical constraints like available sea space and cable lengths, leading to a compromise between pure hydrodynamic optimality and engineering feasibility. It is also crucial to consider scaling effects as the number of devices increases. A small array might achieve a q-factor > 1 by constructive tuning, but as array size grows, edge devices and interior devices experience different wave environments. Large farms may asymptotically trend toward a q-factor around 1 or slightly less if many devices mutually shadow each other. Indeed, theoretical studies of infinite or periodic arrays show that strong interactions can emerge, sometimes reducing incremental gains as more rows are added [26]. Therefore, designers typically simulate incrementally larger array sizes to observe when additional devices yield diminishing marginal returns. Spacing guidelines often emerge from such studies—for instance, keeping devices at least one to two device diameters apart for point absorbers, or one wavelength apart for terminator-style devices, to ensure the second row still receives sufficient wave energy [27].

In designing wave farms, wake effects and interference mean that downstream WECs generally have lower input wave energy if placed directly behind upstream ones. To mitigate this, array layouts are often staggered such that no device sits strictly in the wake of another for the dominant wave direction [28]. The goal is to distribute the extraction more evenly across the wave front. Some advanced concepts even dynamically reconfigure or tune WECs to adapt to changing wave directions, aiming to maintain an even load distribution. Additionally, combining different WEC types in one farm (hybrid arrays) is being explored to leverage complementary absorption characteristics and reduce coherent interference. Regardless of approach, performance metrics like total output and q-factor, normalized by isolated performance, remain key yardsticks. By employing high-fidelity models and optimization algorithms, recent research has demonstrated array designs that maximize energy capture while accounting for device interaction physics [29]. This ensures that wave farms are laid out not only to fit the site, but also to harness constructive interactions wherever possible and avoid mutual interference that would constrain overall efficiency.

4.2.3 Environmental and Regulatory Constraints

The development of wave energy farms must be carefully integrated within broader marine spatial planning frameworks to ensure their compatibility with other existing and planned uses of the ocean, such as fishing, shipping lanes, and recreational activities. Marine spatial planning is a crucial process for analyzing and planning the sustainable use of marine resources, aiming to minimize conflicts and promote coexistence between different sectors. Recent research has explored the application of marine spatial planning techniques in the context of emerging marine technologies, such as offshore aquaculture farms powered by WECs [30]. These studies highlight the potential for synergistic co-location of different marine activities, where wave energy farms could potentially provide a clean and reliable power source for

aquaculture operations, leading to more efficient use of ocean space and reduced reliance on traditional power sources [31]. The development of sophisticated spatial modeling tools is also playing an increasingly important role in marine spatial planning for offshore renewable energy projects. These tools can incorporate a wide range of data layers related to ocean environments and human activities, such as transportation routes, natural resource distribution, national security concerns, fisheries, and other ocean industries. By analyzing these data, decision-makers can gain a more holistic understanding of potential conflicts and synergies, enabling more informed and transparent decisions regarding the siting of wave energy farms. Ultimately, effective marine spatial planning is essential for the sustainable development of wave energy, ensuring that these projects can proceed in a manner that minimizes negative impacts on marine ecosystems and other ocean users while maximizing their contribution to renewable energy goals [32].

The development of wave energy farms necessitates a thorough consideration of potential environmental impacts on marine ecosystems. These considerations include factors such as the noise generated by the devices during operation, the creation of electromagnetic fields from subsea cables, and the potential for disruption to marine habitats and ecosystems. Recent studies have investigated these potential impacts. Research suggests that while a wave energy farm can have a noticeable influence on the local wave hydrodynamics in its immediate vicinity, these effects may gradually diminish as the distance from the farm increases towards the coastline [33]. This understanding is important for assessing potential impacts on coastal processes like erosion and sediment transport. Furthermore, the introduction of artificial structures, such as the foundations of WECs, into the marine environment can create new hard substrates that may be colonized by various marine organisms. While this can potentially benefit some species by providing new habitat, it can also alter existing ecological communities, and the long-term effects of large-scale deployments require further investigation [34]. Thorough EIAs are typically a mandatory requirement for wave energy projects. These assessments aim to identify potential negative environmental effects early in the planning process and to develop appropriate mitigation strategies to minimize or avoid these impacts. Mitigation measures might include careful selection of locations for subsea and onshore cables to avoid sensitive habitats, implementing noise reduction technologies, and designing structures in a way that minimizes disruption to marine life. Ongoing research continues to evaluate the potential environmental consequences of wave energy farms to ensure their sustainable and responsible development [35].

The development and deployment of wave energy farms are subject to various regulatory constraints, which often involve obtaining permits and licenses from relevant governmental and environmental authorities. Navigating these regulatory frameworks can be a complex and time-consuming process. Recent analyses have highlighted the challenges posed by the current regulatory landscape for ocean energy technologies, including wave energy [36]. One study pointed out that a significant barrier to the development of ocean energy in the EU is the lack of specific zones designated for these innovative technologies within maritime spatial plans [37]. This absence of clearly defined areas can lead to uncertainty for project developers and

potential conflicts with other established marine activities. Furthermore, the study noted that there is often a lack of regulations that are specifically tailored to the unique characteristics and requirements of ocean energy technologies. This, coupled with a limited understanding of their potential environmental impacts, can result in complex and lengthy approval procedures involving multiple regulatory bodies, which can ultimately discourage investment and hinder the progress of wave energy projects. The study recommends that ocean energy technologies should be recognized on an equal footing with more established marine-based renewables, such as offshore wind, and that dedicated regulatory frameworks should be introduced to address the specific needs of wave, tidal, and other ocean energy technologies [35]. Such tailored regulations could help to streamline the permitting process, reduce the risk of project failure, and ultimately support the permanent integration of ocean energy into the broader renewable energy mix. Therefore, the establishment of clear, supportive, and technology-specific regulatory frameworks is crucial for unlocking the full potential of wave energy and facilitating its transition towards commercial viability.

4.2.4 Economic Considerations

Economic factors are paramount in determining the feasibility and viability of wave energy projects, and infrastructure costs represent a significant portion of the overall investment. These costs are associated with various components, including subsea cables for power transmission, shared or individual mooring systems for the WECs, and the necessary transmission equipment to connect the wave farm to the electricity grid. Recent analyses of the WEC market indicate that high initial capital investment costs for establishing this infrastructure have been a major factor impeding the widespread development and scaling of the technology [38]. Setting up commercial-scale WEC farms requires substantial upfront expenditures for the procurement and installation of specialized devices designed to harness energy from ocean waves. These devices need to be securely moored to the seabed, and the power they generate must be transmitted back to onshore grids via undersea cables. Additionally, the costs associated with specialized vessels, deployment machinery, and ocean engineering services further contribute to the high initial capital requirements of these projects. However, there is a growing recognition that adopting modular and scalable designs for wave energy devices could potentially lead to a reduction in these infrastructure costs over time. This approach allows for incremental improvement and deployment, which can help drive down costs as the technology matures and economies of scale are achieved [39]. Furthermore, the market for submarine power cables is projected to experience significant growth in the coming years, reflecting the increasing global focus on offshore energy development, which could potentially lead to cost reductions through increased competition and technological advancements. In the context of offshore wind energy, cable costs have been shown to represent a substantial portion of the overall project expenses, a trend that is likely to be similar for wave

energy farms. The cost of subsea power cables can be significant, with estimates exceeding 2.5 million per kilometer [40]. Therefore, a thorough understanding and optimization of these infrastructure costs are essential for improving the economic competitiveness of wave energy technology.

Several cost components are particularly sensitive to array design: infrastructure costs (moorings, foundations, cables, and grid connection), installation and O&M logistics, and end-of-life decommissioning. Recent techno-economic analyses have broken down wave farm capital expenditures (CAPEX) into major categories. The WEC devices themselves (prime movers and PTOs) typically account for roughly one-third of CAPEX [41]. The balance of plant—which includes mooring systems, foundations, subsea cables, offshore substations, and onshore grid tie-in—can constitute a similar or larger share, often on the order of 40% of total CAPEX. For example, one study estimated foundation and mooring hardware around 19% of CAPEX and electrical grid connection around 8% [41]. Mooring costs alone have been cited as ~ 10% of a device's structural cost (and up to 30% in some cases) [42], reflecting the substantial steel or synthetic rope lengths and heavy anchors required offshore. Underwater cables and connectors are also expensive: as a rough figure, array interconnection cables might cost on the order of €40–€80 per meter, and export cables even more [43]. Furthermore, an offshore step-up substation (if needed for larger farms transmitting at high voltage) can add on the order of a million euros or more. These costs underscore why array layout optimization isn't only about hydrodynamics, but also electrical and structural economics—a compact layout shortens cable lengths (reducing cost and transmission losses), whereas very large spacing increases energy yield but incurs more cabling and support structure expense. Thus, designers conduct trade-off analysis to find an optimal spacing and layout that balances maximum energy capture with acceptable infrastructure cost [29] (Fig. 4.3).

The logistical challenges and associated costs involved in the installation of WECs play a crucial role in the overall economic feasibility of wave energy projects. These logistics encompass a range of factors, including the requirements for specialized vessels to transport and deploy the devices, the techniques and equipment needed for mooring and connecting the converters, and the potential for achieving economies of scale during the deployment process. Recent research has highlighted the potential advantages of built-in wave energy converters (BI-WECs) in terms of simplifying installation logistics [44, 45]. By integrating the energy conversion technology directly into existing marine structures, such as floating buoys or vessels, the need for complex and costly standalone installation procedures might be reduced. This approach could lead to more streamlined deployment processes and potentially lower overall project costs. In the more mature offshore wind energy sector, it has been observed that installation costs can represent a significant portion, sometimes as much as 20–30%, of the total capital expenditure for a wind farm. This suggests that the installation phase is also a major cost driver for offshore energy projects in general, and likely for wave energy as well. Therefore, optimizing the installation process through efficient planning, the use of appropriate vessels and equipment, and the potential for economies of scale when deploying larger arrays of devices are

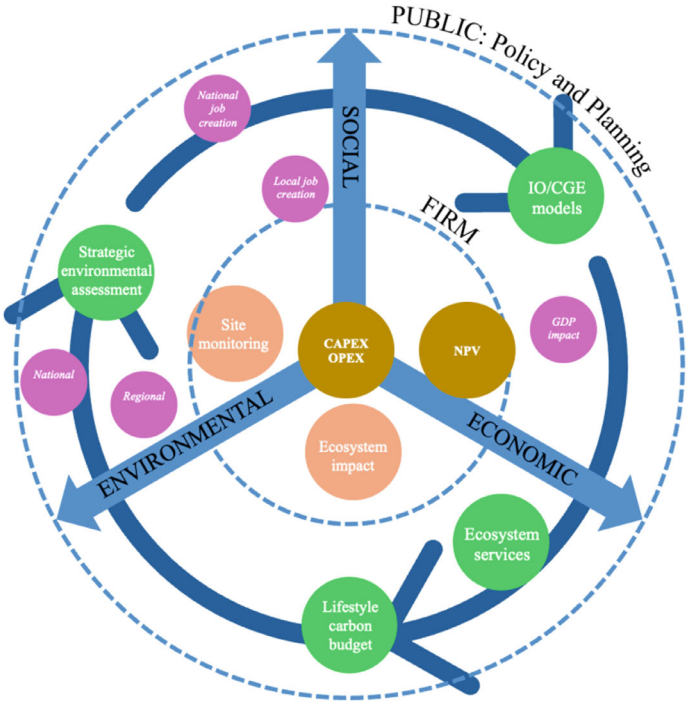

Fig. 4.3 Economics pillar and connectivity with socioeconomics and the environment

all critical considerations for reducing the overall cost of wave energy projects and making them more economically competitive with other renewable energy sources.

In a wave energy farm consisting of multiple devices, the efficient and cost-effective transmission of the generated electricity requires careful optimization of the array cable layout. This involves minimizing the total length of subsea cables needed to connect all the WECs and to transmit the power to a central point within the farm for onward transmission to shore. Recent research efforts have focused on developing strategies and tools for this optimization [46]. The National Renewable Energy Laboratory (NREL) is actively involved in developing modeling toolsets specifically designed for optimizing the array designs of large-scale floating offshore wind farms, which includes the crucial aspect of subsea power cabling. While this work is primarily focused on wind energy, the principles and methodologies developed are likely to be transferable and applicable to wave energy farms as well, given the similar challenges in connecting multiple offshore devices [47]. One of the objectives of such research is to create a holistic optimization framework that considers the coupled design of the array layout, the mooring systems, and the power cabling under realistic site-specific conditions. This integrated approach is essential because these different aspects of a wave farm are often interconnected, and optimizing one in isolation might not lead to the most efficient overall system. Furthermore, the

concept of shared mooring systems, which is being explored for floating wind farms, could also have implications for array cable optimization in wave energy farms. By reducing the number of required anchors and mooring lines, shared mooring systems might also simplify the inter-device electrical connections and potentially reduce the total length of array cables needed. Therefore, research and development in array cable optimization are crucial for minimizing the infrastructure costs and maximizing the efficiency of power transmission within wave energy farms, contributing to the overall economic viability of these projects [27, 43].

The power output from ocean waves is inherently variable and can fluctuate significantly depending on the sea state. To ensure the stable and reliable integration of wave energy into the electricity grid, effective power smoothing strategies are essential. These strategies aim to reduce the magnitude of power fluctuations and provide a more consistent and predictable supply of electricity. Recent research has explored various techniques for achieving power smoothing in wave energy farms [48]. One common approach involves the use of energy storage systems, such as batteries and supercapacitors, which can capture excess energy during periods of high wave activity and release it during calmer periods when the power generation is lower. Integrating energy storage at the level of individual WECs or at a central point within the wave farm can help to dampen the fluctuations in the overall power output. Furthermore, the potential for combining different types of ocean renewable energy sources, such as wave and tidal energy, has been highlighted as a promising strategy for power smoothing. The generation profiles of these different technologies can be complementary, with wave energy potentially being more abundant at different times or under different conditions than tidal energy, and vice versa. By combining these sources, a more stable and reliable overall power output might be achieved. Research has also explored the use of specific layout configurations and control algorithms within a wave farm to help reduce power fluctuations. For example, strategically arranging devices or coordinating their operation could potentially lead to a more consistent total power output [41, 49]. Therefore, the development and implementation of effective power smoothing techniques are critical for facilitating the seamless integration of wave energy into existing electricity grids and enhancing its value as a reliable renewable energy source.

Planning for the end-of-life phase of a wave energy farm, including the costs and considerations associated with decommissioning, is an important aspect of the overall economic analysis of these projects. While the wave energy industry is still relatively young compared to more established sectors like offshore wind, it is crucial to consider the eventual removal of devices and infrastructure based on the initial layout decisions. Recent literature provides some insights into the potential costs involved. For instance, the decommissioning cost for a Pelamis WEC in the Pacific region was estimated to be between US 0 and 1.0 million [50]. Drawing parallels from the offshore wind industry, which is further advanced in its lifecycle, studies suggest that decommissioning costs for offshore wind farms can be around 3–4% of the initial capital costs, with the removal of the turbines and their foundations being the most expensive stages. These figures can provide a useful benchmark for considering the potential decommissioning expenses for wave energy projects,

although the specific costs will likely depend on the type of WEC, the foundation design, the distance to shore, and the prevailing regulatory requirements at the time of decommissioning. There is also a growing interest in exploring the possibilities of reusing or repurposing offshore energy infrastructure at the end of its operational life. This could potentially reduce the overall decommissioning costs and environmental impact. Therefore, from the outset of a wave energy project, it is important to factor in the potential costs and logistical considerations associated with decommissioning to ensure a comprehensive economic analysis and to plan for the responsible end-of-life management of the wave farm.

Achieving an optimal and cost-effective layout design for a wave energy farm necessitates a comprehensive trade-off analysis. This involves carefully balancing the potential energy yield of the farm against the associated infrastructure costs and various other economic factors. Recent research has emphasized that the layout configuration that maximizes energy capture might not necessarily be the most economically viable option. For instance, a highly complex array designed to maximize constructive hydrodynamic interactions might also require significantly more expensive mooring systems or inter-device cabling, potentially leading to a higher overall LCoE. To address these complex trade-offs, researchers and developers utilize techno-economic models that allow for a comprehensive assessment of project feasibility [51]. These models typically consider various economic indicators, such as the net present value (NPV), the LCOE, and the discounted payback time (DPBT), under different scenarios that might involve variations in energy selling prices, investment costs, inflation rates, and the capacity factor of the energy produced [52]. Furthermore, studies have indicated that co-locating wave energy farms with other offshore renewable energy projects, such as wind farms, could potentially lead to a reduction in the cost of energy for both technologies through shared infrastructure and operational synergies. Ultimately, the goal of a thorough trade-off analysis is to identify the wave farm layout and design parameters that strike the right balance between maximizing energy production and minimizing the overall economic costs, thereby leading to a commercially viable and sustainable wave energy project.

4.3 Layout Optimization for Cost Efficiency

Layout optimization in the context of wave energy farms refers to the strategic arrangement of individual WECs within a designated area to maximize energy capture while minimizing costs associated with deployment, operation, and maintenance. This involves considering a multitude of factors, including the hydrodynamic interactions between devices, the prevailing wave climate, the reliability of individual WECs, and the potential environmental and social impacts of the farm. This section aims to provide a comprehensive analysis on layout optimization for cost-efficient wave energy farms. It will examine the mathematical and computational models employed, the inherent cost-energy trade-offs, the importance of reliability and redundancy, and the considerations for environmental and social impacts. The

subsequent subsections will explore each of these aspects in several case studies, synthesizing the current state of knowledge and highlighting emerging trends and gaps in the research.

4.3.1 Mathematical and Computational Models

The foundation of effective layout optimization for wave energy farms lies in accurately modeling the hydrodynamic interactions between individual WECs and the surrounding wave field. The performance of a WEC array is significantly affected by how each device scatters and radiates waves, which in turn influence the waves incident upon neighboring devices. Linear wave theory, based on the assumptions of a non-viscous, non-rotational, and incompressible fluid, provides a fundamental framework for understanding these interactions. This theory simplifies the complex fluid dynamics through basic equations, making it computationally efficient for modeling wave propagation and interaction with structures, as discussed in Sect. 2.2. Its prevalence in wave farm modeling stems from this balance between its ability to capture essential hydrodynamic phenomena and its relatively low computational cost, especially when dealing with many WECs.

Hydrodynamic interactions are a key determinant of the overall performance of wave energy farms. Accurate modeling of these interactions is therefore crucial for effective layout optimization. Linear potential flow theory serves as the dominant approach due to its balance between accuracy in capturing essential interactions and computational feasibility. However, the approximations inherent in analytical methods and the significant computational expense associated with numerical methods, especially for large arrays, represent limitations. Current models often face challenges in accurately representing highly complex and stochastic wave environments, as well as the nonlinear behavior of wave energy devices themselves. The prevalence of linear potential flow theory indicates a necessary compromise between computational manageability and the fundamental physics of wave-device interaction. Real-world ocean condition frequently exhibits nonlinear characteristics, and the operational dynamics of WECs can also introduce nonlinearities that linear theory might not fully capture. This trade-off motivates ongoing research into more advanced modeling techniques or refined approximations capable of bridging this gap. Furthermore, the availability of specialized software such as WAMIT and NEMOH signifies a notable level of maturity in the computational tools supporting hydrodynamic modeling [53].

Once a suitable hydrodynamic model is established, as details are explained in Sect. 2.4, computational optimization algorithms are employed to identify the most cost-effective layout of WECs within a wave energy farm. These algorithms systematically search through a vast number of possible arrangements to find the configuration that optimizes a predefined objective function, such as maximizing energy production or minimizing the LCoE. Optimization algorithms used in this context can be broadly

categorized into metaheuristic algorithms, mathematical programming techniques, and machine learning approaches [54].

Metaheuristic algorithms, inspired by natural processes, are widely used for their ability to tackle complex, nonlinear optimization problems with large search spaces, which are characteristics of wave farm layout optimization. Genetic algorithm (GA), for example, mimic the process of natural selection, iteratively evolving a population of potential layouts by applying genetic operators like crossover and mutation to find optimal or near-optimal solutions for WEC positions and other design parameters [55]. The presence of numerous local minima in the solution space makes the global search capabilities of GAs particularly advantageous. For instance, one study utilized a numerical optimization framework based on the WAMIT hydrodynamic model in conjunction with a GA to maximize the annual absorption of wave energy in the Aegean Sea [56]. Another research effort presented an optimization tool based on a GA to identify the optimal spatial configuration of wave energy parks, examining arrays with varying numbers of devices and demonstrating the algorithm's ability to find similar optimal layouts across different array sizes [57]. Furthermore, GAs have been integrated with surrogate models and gradient-based optimizers to enhance computational efficiency in solving layout optimization problems [58]. The robustness of GAs in navigating intricate solution landscapes makes them a valuable tool for identifying globally efficient wave farm layouts.

Particle swarm optimization (PSO) is another popular metaheuristic inspired by the social behavior of bird flocks or fish schools. It uses a swarm of particles that move through the solution space, guided by their own best-found position and the best position found by the entire swarm, making it effective for multi-objective optimization of layout designs. Other metaheuristic algorithms like different evolution, gray wolf algorithm, and glowworm optimization algorithm have also been applied to wave farm layout problems. PSO and its variants, such as Multi-Objective PSO (MOPSO) and Improved Quantum-behaved PSO (IQPSO), have also been frequently applied to the problem of wave farm layout optimization [59]. One study applied a semi-analytical method and numerical simulation using a MOPSO algorithm based on surrogate models to optimize the layout of a wave energy park, with the objectives of maximizing power output and power smoothing, while considering constraints related to WEC safety and the occupied sea area [60]. The use of surrogate models, such as radial basis functions, helps to improve the computational efficiency of the optimization process. Other research has also highlighted the application of PSO with surrogate models for layout optimization [61]. While primarily focused on wind farms, the application of PSO to optimize layouts with respect to the LCoE demonstrates its potential relevance for wave energy as well. The ability of PSO to efficiently explore the search space and the effectiveness of multi-objective versions in handling multiple performance metrics make it a popular choice for wave farm layout optimization.

Mathematical programming techniques, such as non-linear programming optimization, are also utilized, particularly for problems requiring optimization across a moderately large parameter space while adhering to non-linear constraints that often arise in layout design. The integration of machine learning (ML) and artificial

intelligence (AI) is an emerging trend in wave farm layout optimization [62]. Artificial neural networks (ANNs), for instance, can learn complex relationships between layout parameters, wave conditions, and farm performance, enabling efficient optimization and prediction of optimal layouts. There is increasing interest in leveraging AI and ML for not only optimizing the initial layout but also for improved control and monitoring of wave energy farms during operation [22]. While traditionally less prevalent than metaheuristic algorithms like GAs and PSO, gradient-based methods are increasingly being explored for wave farm layout optimization, often in combination with other techniques. These methods leverage the sensitivity of the objective function to changes in the design variables. For example, gradient-based optimizers have been used in conjunction with multi-start approaches, where an initial solution obtained from a GA is refined using a gradient-based method [27]. A novel numerical framework based on a gradient-flow formulation has also been introduced for the combined optimization of wave energy park layout and control parameters [63]. In the context of wind farm layout optimization, which shares similarities with wave farm optimization, gradient-based solvers like sequential least-squares programming (SLSQP) have been used to integrate complex domain boundaries by utilizing analytical gradients of the distances between turbine locations and boundaries [61]. Although gradient-based methods can be very efficient, they are often considered local search algorithms and may get trapped in local optima. However, their scalability to problems with a large number of variables and constraints is a significant advantage, making them a valuable tool when combined with global search strategies or when analytical gradients can be efficiently computed.

The computational cost associated with these optimization processes, particularly when coupled with high-fidelity hydrodynamic models and applied to large-scale farms, remains a significant challenge. Additionally, gradient-based optimization methods, while potentially faster for certain types of problems, can be sensitive to the initial starting configuration, potentially leading to suboptimal solutions [41]. The trend towards multi-objective optimization signifies a greater recognition of the need to find a balance between various crucial aspects of wave farm design, including energy production, economic performance, and environmental sustainability. Early optimization efforts often prioritized only energy capture, but the practical viability of a wave farm necessitates a holistic approach that considers all these interconnected factors. Therefore, a summary of recent mathematical models for wave farm layout optimization is presented in Table 4.1.

The objective functions used in these optimization processes vary depending on the specific goals of the study. Common objectives include maximizing the total power output of the wave farm, minimizing various costs such as CAPEX, operational expenditure (OPEX), and the LCOE, or performing multi-objective optimization that simultaneously considers several competing factors like energy production, cable length, and the marine area occupied by the farm [73]. To mitigate the significant computational cost associated with repeatedly running hydrodynamic simulations during the optimization process, especially for large arrays, surrogate models are often employed [74]. These models are computationally cheaper approximations of the more complex hydrodynamic models. Specialized design tools like DTOcean

Table 4.1 Summary of recent works on wave farm layout optimization

Authors	Model description	Hydrodynamic theory	Objective(s)	Optimization algorithms
Guo et al. [57]	Semi-analytical, numerical	Linear potential flow, Matched eigen-function expansions	Maximize power output Maximize power smoothing Minimize sea area occupancy	Multi-objective PSO
Ojeda et al. [62]	Numerical	SWAN	Maximize power production Minimize LCOE	Binary GA
Lyu et al. [56]	Integrated hydrodynamic and control	Boundary element method	Maximize q-factor	GA, Gradient-based
Moarefdoost et al. [59]	Analytical heuristic	Point absorber approximation	Maximize q-factor	Iterative heuristic
Li et al. [64]	Numerical stochastic	Linear potential theory	Maximize power smoothing	Stochastic optimization
Bergillos et al. [30]	Numerical ANN	SWAN	Maximize power	Bayesian
Peña Sanchez et al. [65]	Numerical	Boundary element method	Maximize energy absorption	GA
Ekweoba et al. [66]	Numerical	Linear potential flow WAMIT	Maximize AEP	GA
Neshat et al. [67]	Numerical	Semi-analytical	Maximize AEP	Random search
Neshat et al. [68]	Numerical	Semi-analytical	Maximize AEP Optimal spacing	Partial evolution
Neshat et al. [69]	Numerical	Analytical	Optimal placement	$1 + 1$ evolution algorithm
Neshat et al. [70]	Numerical	Hydrodynamic model	Optimal placement	Smart iterative local search + smart mutation
Neshat et al. [71]	Numerical	Hydrodynamic analytical	Optimal placement	Covariance matrix adaptation evolution strategy
Neshat et al. [72]	Numerical	Analytical	Maximize AEP Maximize power	Differential evolution Improved differential evolution

have also been developed to assist project developers in designing wave and tidal energy arrays. DTOcean includes computational modules for hydrodynamic array layout optimization, electrical system architecture, moorings and foundations, and installation and maintenance procedures, with optimization based on the LCOE [75].

The selection of an appropriate objective function is critical for guiding the layout optimization process. A primary objective in many studies is the maximization of power capture from the wave farm [59]. In one instance, the objective function used in a GA-based tool was the negative value of the total power production of the wave energy park, effectively aiming to minimize this negative value to achieve maximum power output. The total power output of the farm is typically calculated as the sum of the power produced by each individual WEC within the array [57].

Another commonly used objective function for maximizing power capture is the q-factor, which represents the ratio of the total output power of a WEC array to the sum of the potential power generated by each device if it were operating in isolation. Mathematically, the q-factor can be expressed as:

$$q = \frac{\sum_{n=1}^{N} P_n}{N.P_0} \tag{4.1}$$

where P_n is the power absorbed by the n-th device in the array, N is the total number of WECs, and P_0 is the power absorbed by a single, isolated device. The total mean power absorbed by an array of N identical WECs oscillating in one mode of motion can be given by a more complex equation involving hydrodynamic parameters. In some studies, the objective is formulated as maximizing the energy absorbed over a specific time horizon, which can be represented as:

$$\max \int_{t_0}^{t_f} P(t)dt \tag{4.2}$$

where $P(t)$ is the PTO rate of the WEC. The specific formulation of the objective function, whether it focuses on total power, the q-factor, or energy over time, can influence the optimization results and the characteristics of the resulting wave farm layout.

Beyond maximizing energy capture, minimizing costs has become an increasingly important objective in wave farm layout optimization. The ultimate goal of wave energy development is to achieve economically competitive energy production. The LCOE is a widely used metric for evaluating the economic viability of energy projects, including wave energy [43]. One study focused on optimizing a wave energy converter farm by considering a variable sea bottom and using genetic algorithms with the LCOE as the objective function to be minimized. Another research effort detailed a layout optimization process aimed at minimizing the LCOE of an offshore floating hybrid wind-wave farm. The general equation for LCOE is given by:

$$LCOE = \frac{\sum_{t=0}^{LT} \frac{TC_t}{(1+r)^t}}{\sum_{t=0}^{LT} \frac{q_t}{(1+r)^t}} \tag{4.3}$$

where TC represents the total costs in year t, r is the discount rate, and q_t is the yearly energy production in period t over the project's lifetime (LT) [61]. The net present value (NPV) has also been used as an objective function, particularly in wind farm layout optimization, as it incorporates both costs and energy production over the project's lifespan [19]. A NPV-based objective function can be formulated as:

$$NPV = \sum_{i=1}^{N} (AEP(x_i, y_i).p_{kwh} - OPEX(x_i, y_i)).a - CAPEX(x_i, y_i) \tag{4.4}$$

where NPV is the annual energy production, p_{kwh} is the price of electricity, $OPEX$ and $CAPEX$ are the operational and capital expenditures respectively, and a is the annuity factor [76]. In some cases, a cost indicator, such as the ratio of the total submerged volume of the WEC to the overall power capture, is used as an objective function to be minimized, aiming for a more resource-efficient energy extraction [77]. The inclusion of cost minimization in the objective function reflects the practical imperative for wave energy to be economically competitive with other energy sources.

Recognizing the multifaceted nature of wave farm design, there is an increasing trend towards multi-objective optimization, where several objectives are optimized simultaneously [57]. For instance, studies have aimed to maximize both power output and power smoothing of an array, while also minimizing sea area occupancy and power fluctuations. Multi-objective optimization acknowledges the often conflicting nature of design goals and allows for the identification of Pareto-optimal solutions that represent the best possible trade-offs between different performance metrics. This approach provides a more realistic and comprehensive framework for wave farm layout optimization. Therefore, a summary of most important objective functions utilized in layout optimization presented in Table 4.2.

4.3.2 Cost-Energy Trade-Offs

Achieving cost-effectiveness in wave energy farm design necessitates a careful analysis of the interplay between the layout of the farm and its overall economic performance. Research in this area focuses on optimizing both the number of WECs deployed and their spatial arrangement to maximize the energy produced for a given cost. Studies have shown that simply maximizing energy output may not lead to the most economically viable solutions. For instance, investigations into cost-effective configurations of WEC arrays have revealed that factors such as the placement of WECs in proximity to reflective structures like seawalls and the spacing between devices can significantly influence the cost-effectiveness of energy capture [77].

Table 4.2 Objective functions and corresponding mathematical equations in recent literature

Objective function	Mathematical Equation	References
Maximize total power	$P(t) = \sum_{i=1}^{N_b} P_i(t)$	[57]
Maximize q-factor	$q = \frac{\sum_{n=1}^{N} P_n}{N.P_0}$	[78]
Maximize energy absorbed	$\max \int_{t_0}^{t_f} P(t)dt$	[79]
Minimize LCOE	$LCOE = \frac{\sum_{t=0}^{LT} \frac{TC_t}{(1+r)^t}}{\sum_{t=0}^{LT} \frac{q_t}{(1+r)^t}}$	[61]
Maximize NPV	$NPV = \sum_{i=1}^{N} (AEP(x_i, y_i).p_{kwh} - OPEX(x_i, y_i)).a - CAPEX(x_i, y_i)$	[80]
Minimize cost indicator	Ratio of total submerged volume to overall power capture	[81]

These studies utilized a cost indicator defined by the ratio of the total submerged volume of the WEC to the overall power captured, demonstrating that a strategic arrangement can enhance power capture without a proportional increase in material or deployment costs. Furthermore, optimizing the array layout can lead to substantial increases in the q-factor, suggesting that well-designed layouts can improve the energy output per device and thus contribute to better cost-effectiveness. The consideration of cost alongside energy production is essential for the practical realization of wave energy technology.

The LCOE serves as a critical benchmark for evaluating the economic viability of wave energy projects and for comparing different design choices. This metric provides a comprehensive measure of the average cost of producing one unit of electricity over the entire lifespan of the project, taking into account all relevant expenditures, including capital investment, operational costs, and decommissioning, as well as the total energy generated. Optimizing a wave energy converter farm with the LCOE as the primary objective allows for a direct assessment of the economic performance of different layouts under various site conditions. Analyzing the cost breakdown of wave energy using LCOE for different WEC technologies and deployment locations further helps in identifying potential areas for cost reduction and in comparing the economic competitiveness of wave energy with other renewable energy sources. The widespread use of LCOE underscores its importance in guiding the development of economically sustainable wave energy farms.

NPV is another crucial economic metric that assesses the profitability of a wave energy project by discounting all future cash flows back to the present and comparing the present value of expected revenues with the present value of expected costs. A positive NPV indicates that the project is expected to be profitable. Other relevant economic metrics include the discounted payback time (DPBT), which estimates the

time required for the project's cumulative discounted cash flows to equal the initial investment, and the internal rate of return (IRR), which represents the discount rate at which the NPV of the project becomes zero. Additionally, some studies utilize cost indicators defined as the ratio of the total submerged volume of the WECs to the overall power capture, providing a measure of the cost-effectiveness of the WEC configuration [79]. In the context of layout optimization, it is essential to consider both the energy production potential of a given layout and its associated economic implications to determine the most cost-effective configuration.

In general, the economical model aims to evaluate the financial performance of a wave energy park by calculating CAPEX, OPEX, NPV, and LCOE. It integrates device level, electrical system costs, installation and decommissioning, and AEP into a consistent framework. The goal is to use this model within an optimization routine to minimize LCOE, a key metric in renewable energy viability. The total CAPEX sums the main components of CAPEX including cost of the WECs, electrical system (cabling and substations), installation process, and the decommissioning of the park. It provides a comprehensive upfront cost estimation essential for determining investment needs, and expressed in Eq. (4.5)

$$CAPEX = CAPEX_{WECs} + CAPEX_{ES} + CAPEX_{Inst} + CAPEX_{Dec} \tag{4.5}$$

The $CAPEX_{WECs}$, expressed in Eq. (4.6) details the breakdown of WEC cost components. It includes the physical parts of the system like the buoy, generator casing, and foundation, as well as labor and auxiliary materials. Each term reflects a specific portion of the cost structure needed to construct a single WEC.

$$\begin{aligned} CAPEX_{WECs} = {} & C_{buoy} + C_{casing} + C_{foundation} + C_{stator} \\ & + C_{translator} + C_{labour} + C_{extra-material} \end{aligned} \tag{4.6}$$

Additionally, $CAPEX_{ES}$ and $CAPEX_{cables}$ calculate the cost of electrical infrastructure. The total includes both the cabling (intra-array (l_{wc}), communication (l_{cc}), and transmission to shore (l_{sc})) and the marine substations, stated in Eqs. (4.7) and (4.8). Cable costs scale with length, and different cable types have distinct unit prices.

$$CAPEX_{WECs} = CAPEX_{cables} + CAPEX_{SS} \tag{4.7}$$

$$CAPEX_{buoy} = l_{wc}C_{wc} + l_{cc}C_{cc} + l_{sc}C_{sc} \tag{4.8}$$

where C_{wc}, C_{cc}, C_{sc} are corresponding costs per meter. Following these equations, the total cost of the electrical substations can be calculated by summing the rated power (RPW) connected to each substation, multiplied by a cost per kilowatt (C_{SS}), Eq. (4.9). It allows differentiation in cluster sizes and reflects the scalability of substation costs in wave energy park based on power demand.

$$CAPEX_{SS} = \sum_{j=1}^{n_{ss}} \left(C_{SS}.RPW_j \right) \tag{4.9}$$

Moreover, each component, e.g., WECs, substations, and cables, has its own cost per day and installation rate, means the $CAPEX_{Inst}$ is the summation of $CAPEX_{Inst-WECs}$ and $CAPEX_{Inst-ES}$.

The annual operational costs, which include repairs for buoy and generator failures and insurance is calculated as follows. These recurring costs are crucial for LCOE calculation and affect the long-term financial sustainability of the project.

$$OPEX_y = OPEX_{r-buoy,y} + OPEX_{r-gen,y} + C_{insurance,y} \tag{4.10}$$

The yearly repair cost of WEC components are as follows:

$$OPEX_{r-buoy,y} = n_b f_{rb} \left(C_{rep,buoy} + \frac{C_{inst,dive}}{I_{dive}} \right) \tag{4.11}$$

$$OPEX_{r-gen,y} = n_b f_{rg} \left(C_{rep,gen} + \frac{C_{inst,WEC}}{I_{WEC}} + \frac{C_{inst,dive}}{I_{dive}} \right) \tag{4.12}$$

where n_b is the number of WECs, f_{rb}, f_{rg} are failure rates, C_{rep} is repair cost, and I is the installation rate (units/day).

The profitability of the wave energy park over its lifetime by discounting annual revenues and $OPEX$ is expressed by NPV, in Eq. (4.13). A positive NPV indicates a viable project, while a negative value suggests it is not financially attractive under current assumptions.

$$NPV = \sum_{y=1}^{L} \frac{\left(AEP_y.FIT - OPEX_y \right)}{(1+r)^y} - CAPEX \tag{4.13}$$

where AEP_y is annual energy production in MWh/y, FIT is feed-in tariff in \$/MWh, r is discount rate, and L is the project lifetime. Subsequently, $LCOE$ represents the average cost of generating one unit of electricity over the park's lifetime. It balances all discounted costs against discounted energy output, serving as the key figure of merit for comparing different energy technologies or project configurations.

Layout choices significantly influence various cost components of a wave energy farm. The CAPEX is directly affected by the number of devices deployed. Mooring and foundation costs can vary depending on water depth and the complexity of the layout. The electrical infrastructure costs, including inter-array cables connecting the WECs to an offshore substation and the export cable transmitting power to shore, are highly dependent on the distances between devices and the location of the substation. OPEX can also be influenced by the layout. For instance, the spacing between devices can affect the accessibility for maintenance and repairs, potentially impacting the associated costs. Inspection and repair costs, as well as decommissioning costs at the

end of the project's life, can also be indirectly influenced by the initial layout design. To effectively optimize the layout for cost efficiency, some studies employ multi-parametric objective functions that combine the annual energy production with the costs that are directly dependent on the layout, such as cable lengths and foundation requirements.

The number of WECs in a farm and their spatial arrangement, particularly the spacing between them, have a significant impact on both the total energy yield and the overall costs of the project. Accordingly, there is likely an optimal number of devices and an ideal spacing that balances energy production with cost efficiency. While increasing the number of WECs generally leads to higher energy output, it also results in greater capital investment and operational expenses. Hydrodynamic interactions between closely positioned WECs can either enhance or diminish the energy captured by individual devices, making the determination of optimal spacing a complex task. Studies have found that similar optimal layouts can emerge for arrays with different numbers of devices, indicating a potential for scalability in design. Furthermore, specific configurations, such as placing WECs near a seawall, have been shown to intensify the wave fields around the devices, leading to more cost-effective energy extraction due to enhanced power absorption. These marks emphasize the need to carefully consider the trade-offs between the number of WECs, their spacing, and the resulting energy production and costs to achieve an economically optimized wave farm layout.

The configuration of a wave energy farm, including the spacing and arrangement of WECs, has a direct impact on both the total energy captured and the overall costs of the project. Hydrodynamic interactions between closely spaced WECs can either enhance or reduce the energy absorbed by individual devices and the farm. Dense layouts might lead to higher power output per unit area due to constructive wave interference but could also result in increased interaction losses and potentially higher cabling costs for connecting the devices. Conversely, sparse layouts reduce interaction losses but require a larger marine area and may increase the costs associated with moorings, foundations, and inter-array cables (Table 4.3).

Several methodologies explicitly aim to minimize the LCOE or maximize the NPV of wave energy projects through strategic layout optimization [26]. These approaches often involve integrating detailed cost models with energy production models within an optimization framework. For example, optimization algorithms can be used to find layouts that minimize the total length of inter-array cables required to connect the WECs, thereby reducing both CAPEX and energy losses [43].

Layout optimization is indeed a critical factor in achieving cost-effective wave energy farms, as it allows for a careful balancing of energy production and various cost elements throughout the project lifecycle. The LCOE serves as a key metric for evaluating this intricate trade-off. However, accurately modeling the costs associated with wave energy technology remains a significant challenge due to the technology's relatively early stage of development and the considerable variability in site-specific conditions that can influence both capital and operational expenditures. Consequently, many research efforts still tend to prioritize the maximization of power

Table 4.3 Recent studies on cost-energy trade-offs in wave farm layout optimization

Authors	WEC type	Number of WECs	Layout parameters	Objective function(s)	Key finding(s)	Cost metric
Shadmani et al. [26]	Multi-axis point absorber	15, 30, 45	Aligned Staggered Arrow	Maximize AEP Maximize power	Showed how particular design choices can lead to cost-effective manufacturing and deployment of WECs	LCoE ($/MWh) NPV ($)
Ojeda et al. [82]	Cylindrical	10	Spatial arrangement	Minimize LCoE Maximize power production	Linear orientation of WECs found to be optimal for both LCOE and power maximization; LCoE optimization resulted in a farm closer to the onshore substation, reducing cable costs	LCOE (€/MWh)
Guo et al. [57]	Point absorber	Variable	Global geometry Separating distance	Minimize sea area occupancy Minimize power fluctuations	Multi-objective optimization showed trade-offs between minimizing sea area and power fluctuations; specific layouts achieved better performance under different wave conditions	Sea area (m^2) Power fluctuation (%)
Lyu et al. [56]	Cylindrical buoys	3, 5, 7	Dimensions (radius, draft) Array layout	Maximize q-factor	Optimizing both WEC dimensions and array layout simultaneously leads to a higher q-factor, improving energy absorption and potentially reducing the number of devices needed for a given power output	q-factor
Meyer et al. [83]	Heaving point absorber	24	Array layout	Assess accuracy of mid-fidelity hydrodynamic models for wave farm design	Accurate and efficient modeling tools for cost-effective design and optimization of wave farms	Power output

(continued)

Table 4.3 (continued)

Authors	WEC type	Number of WECs	Layout parameters	Objective function(s)	Key finding(s)	Cost metric
Behzad and Sanaei [84]	Oscillating wave surge converter	5	Arrowhead up and down Linear	Maximize AEP	Variation in the lateral spacing (perpendicular to the wave direction) of the converters changes the energy absorption slightly and the shape of energy diagram and its peak period remain the same	AEP
Giassi et al. [43]	Point absorber	10, 20, 50	Optimized	Minimize LCOE	the hydrodynamical interaction has a large impact on the optimal design of wave energy parks, and that the length of the intra-array cable does not play a significant role in the economical layout optimization routine for the studied wave energy park system	LCOE (€/MWh)

output as the primary objective, sometimes overlooking a more comprehensive optimization that fully integrates all relevant cost factors. The substantial impact of OPEX on the overall cost of wave energy projects underscores the importance of considering long-term operational aspects right from the initial layout design phase. Decisions regarding the arrangement and spacing of WECs can significantly affect the accessibility for maintenance, the potential for device failures due to hydrodynamic loading, and the efficiency of routine operations, all of which have a direct bearing on the long-term economic viability of the wave farm. Furthermore, the parallels drawn between wave energy farm layout optimization and the more established field of offshore wind farm layout optimization suggest a valuable opportunity for knowledge transfer and methodological adaptation. Offshore wind energy has already addressed many of the challenges related to optimizing layouts for energy capture and cost efficiency, particularly concerning wake effects, electrical grid design, and cost modeling.

4.3.3 Environmental and Social Impact Consideration

The development and deployment of wave energy farms, while offering a promising avenue for clean energy generation, necessitate careful consideration of their potential environmental and social impacts [34]. A thorough understanding of these impacts is essential for ensuring the sustainable and responsible growth of the wave energy sector.

The interaction of wave energy farms with marine ecosystems is a key area of concern. The presence of WEC devices can potentially disrupt marine habitats and the behaviors of marine life. Concerns include the risk of collisions or entanglements for marine mammals, particularly those that may not be able to detect the devices through sound signals. The physical presence of the structures might also lead to alterations in the migration patterns and behaviors of various marine species as they seek to avoid interactions [31]. Furthermore, the electromagnetic fields generated by wave energy installations could have implications for the feeding and orientation of some marine species. The extraction of energy from waves can also lead to changes in wave characteristics, which in turn might influence sediment movement, ocean currents, and the overall structure of the water column. Research has also examined the potential ecological impacts on rocky shore intertidal communities due to changes in wave exposure caused by wave energy extraction, with findings suggesting that the impacts of broader climate change on wave exposure might be more significant than those of industrial-scale wave energy extraction [85]. While generally considered environmentally benign, careful assessment and mitigation strategies are necessary to minimize any adverse effects on marine ecosystems.

Noise pollution from wave energy farms is another potential environmental concern that has been investigated. Underwater noise generated during the construction and operation of wave energy converters could potentially affect marine life, which relies on sound for communication, navigation, and hunting [86]. However,

studies on certain wave energy converter prototypes have indicated that the underwater noise levels produced during operation are very low and unlikely to significantly impact marine mammals. The noise generated during the construction phase, which may involve activities like pile driving for certain types of installations, could be more significant. The overall impact of noise pollution appears to vary depending on the specific technology and the stage of development, but ongoing research aims to better understand and mitigate any potential noise-related effects on marine fauna.

The visual impact of wave energy farms on coastal landscapes and seascapes is a social consideration that needs to be addressed. Compared to other renewable energy technologies like large-scale wind farms, wave energy devices often have a lower visual profile, particularly when they are submerged or have low-lying structures. Some wave energy technologies, such as those that attach converters to existing shoreline infrastructure like breakwaters, can further minimize their visual footprint [87]. The height of the devices above sea level and their distance from the coast are key factors influencing their visibility and potential impact on the aesthetic value of coastal areas. While generally considered to have a low visual impact, this aspect can still be a concern for some coastal communities, highlighting the importance of careful planning and consideration of local perspectives.

The deployment of wave energy farms can also lead to interactions with other marine users, such as fishing vessels, shipping traffic, and recreational activities [88]. The spatial requirements of wave farms might potentially overlap with traditional fishing grounds or shipping lanes, leading to conflicts. Ensuring the safety of navigation around wave energy installations is also a critical consideration, requiring appropriate marking and navigational aids. Engaging with local communities and stakeholders, including fishermen and other marine users, is essential to address their concerns, minimize disruptions to their livelihoods and activities, and find mutually acceptable solutions for the coexistence of wave energy farms and other ocean uses. Careful site selection, taking into account existing marine activities and environmental sensitivities, is crucial for minimizing potential conflicts and ensuring the successful integration of wave energy farms into the marine environment (Tables 4.4 and 4.5).

Accordingly, layout optimization strategies play a vital role in mitigating the potential negative environmental and social consequences of wave energy farms while maximizing their benefits. Strategic site selection is paramount to avoid sensitive marine habitats, minimize visual impacts from the shore, and reduce potential conflicts with existing marine users. Optimizing the spacing and arrangement of WECs within the farm can help minimize alterations to wave patterns and sediment transport processes in the surrounding environment. Layout design can also consider the potential for artificial reef effects, perhaps by strategically placing devices to enhance biodiversity in certain areas while avoiding disruption in others [31]. Implementing appropriate safety features, such as marker buoys, navigational lighting, and radar reflectors, is essential to ensure the safety of navigation and minimize risks to marine life.

Engaging with local communities and stakeholders from the early stages of project planning is crucial for addressing their concerns, incorporating their feedback, and

Table 4.4 Summary of potential environmental impacts of wave energy farms

Type of impact	Specific effects observed or predicted	Mitigation strategies proposed	References
Marine life disturbance	• Potential collisions or entanglements of marine mammals • Alterations in migration patterns and behaviors; disruption of feeding and orientation due to electromagnetic fields	• Careful device design to minimize entanglement risks • Acoustic deterrents to reduce collision risk • Thorough environmental impact assessments before deployment	[86]
Changes in wave patterns and hydrodynamics	• Potential effects on sediment transport, ocean currents, and shoreline erosion	• Site selection to minimize impacts on coastal processes • Hydrodynamic modeling to predict and mitigate changes	[40]
Noise pollution	• Underwater noise during construction (e.g., pile driving) and operation potentially affecting marine animal communication, navigation, and behavior	• Use of noise reduction technologies during construction • Careful selection of operational technologies that minimize noise	[33]
Habitat modification	• Small-scale seafloor disturbances from mooring anchors • Potential for devices to act as artificial reefs	• Selection of mooring systems with minimal seafloor impact • Monitoring of ecological changes around deployed devices	[85]

Table 4.5 Social impacts and mitigation measures for wave energy farms

Type of social impact	Specific effects	Stakeholder concerns	Mitigation strategies	References
Visual impact	• Potential alteration of coastal aesthetics due to the presence of above-water structures	• Concerns from coastal communities and tourism industry about impacts on scenic views	• Use of low-profile or submerged devices • Locating farms further offshore • Careful color selection	[37]
Conflicts with fishing	• Potential overlap with fishing grounds, restricting access or affecting fish populations	• Concerns from fishing communities about loss of fishing areas and potential impacts on fish stocks	• Thorough mapping of fishing areas • Consultation with fishing communities during site selection • Potential for compensation or co-use strategies	[89]
Impact on navigation	• Potential hazard to shipping traffic	• Concerns from maritime industry about safety of navigation	• Implementation of appropriate navigational aids (e.g., marker buoys, lights, radar reflectors) • Communication with maritime authorities • Inclusion of wave farm locations on nautical charts	[36]
Economic opportunities	• Creation of jobs in manufacturing, installation, operation, and maintenance • Potential for local economic development	• Interest from local communities in new employment opportunities and economic benefits	• Prioritizing local hiring and supply chains • Engaging with local businesses	[9]

fostering a sense of ownership and support for the project [88]. In some cases, the strategic layout of wave farms can even contribute to coastal protection by reducing wave energy reaching the shore, offering a dual benefit of energy generation and coastal defense.

Subsequently, a comprehensive understanding of the long-term and large-scale environmental and social impacts of wave energy farms is still an area of ongoing research. Quantifying these impacts accurately and effectively integrating them into the layout optimization frameworks can be a complex undertaking. The potential for wave farms to offer coastal protection presents an interesting opportunity where

layout optimization could be designed to achieve dual objectives, i.e., efficient energy generation and effective coastal defense. By strategically positioning WECs, it might be possible to attenuate wave energy before it reaches the coastline, thereby reducing erosion and providing protection to coastal communities. Optimizing the layout for this dual purpose would necessitate considering both the energy extraction efficiency of the array and its wave attenuation characteristics. Furthermore, the critical importance of community buy-in for the success of renewable energy projects underscores the essential role of social impact considerations in the planning of wave farm layouts. As demonstrated by the failure of an offshore wind project due to community opposition, neglecting the concerns and perspectives of residents and stakeholders can lead to significant challenges and even project failure. Therefore, proactive engagement with communities, thorough assessment of potential social impacts (both positive and negative), and the integration of community feedback into the layout design process are paramount for ensuring the successful and sustainable development of wave energy farms.

4.4 Case Studies: Wave Farm Layout and Cost Analysis

4.4.1 Optimizing Layout for Energy Maximization

Recent work has explored several procedures and methodologies for optimizing wave farm layouts to enhance energy production. The employed methods often utilize the q-factor, a metric representing the ratio of the total power absorbed by an array of WECs to the power that would be absorbed if the same number of WECs operated in isolation, as the primary measure of farm performance. Such heuristic approaches offer a practical means of addressing the computational challenges associated with the combinatorial nature of WEC placement optimization, allowing researchers to explore complex solution spaces and identify layouts that significantly improve energy extraction without requiring exhaustive computational resources. Several objective functions have been used to guide the optimization process for energy maximization. Maximizing the q-factor is a common approach, as it directly quantifies the benefit of deploying WECs in an array by comparing the array's power output to that of individually operating devices. Another key objective is maximizing the AEP of the wave farm. This metric is crucial for assessing the long-term economic viability of a project, as it represents the total energy generated over a year, considering the site's specific wave climate. Some studies also aim to balance power production with the separation distance between WECs, recognizing the practical limitations and costs associated with deploying devices too close together.

GA have also been widely adopted for optimizing both the individual characteristics of WECs and their spatial arrangement within a wave farm to achieve maximum energy output [80]. This algorithm is particularly effective in navigating the complex and non-linear performance landscapes inherent in wave farm design, where multiple

local optima might exist. By maintaining a population of potential solutions and iteratively applying processes of selection, crossover, and mutation, GAs can explore a broad range of design possibilities and converge towards configurations that yield high energy capture rates. Studies have demonstrated that optimizing WEC dimensions concurrently with the array layout can lead to substantial increases in the overall energy production of a wave farm [55, 90].

In some studies, particularly for initial assessments and theoretical analyses, the point absorber approximation is employed. This approximation assumes that the WECs are small relative to the wavelength of the incident waves, simplifying the analysis of wave interactions and often allowing for analytical or semi-analytical solutions that can provide rapid insights into the impact of array configuration on energy maximization [91, 92]. Accordingly, the optimization of wave farm layouts for energy maximization relies heavily on accurate mathematical models that can simulate wave propagation and the interaction of waves with WEC devices. Linear potential flow theory is a widely used approach for modeling the hydrodynamic behavior of WECs and their interactions within an array [93]. This theory, while based on simplifying assumptions, provides a computationally efficient means of capturing the fundamental hydrodynamic effects that govern the performance of a wave farm, particularly in the initial stages of design and optimization. The BEM is another commonly employed technique for analyzing the hydrodynamic performance of both individual WECs and entire wave farms [26]. BEM is particularly well-suited for wave-structure interaction problems as it reduces the dimensionality of the problem by only requiring the discretization of the surfaces of the WECs and the boundary of the fluid domain. This can lead to significant computational savings compared to methods that require the discretization of the entire fluid volume.

Regular geometric layouts, such as those employing cylindrical, triangular, quadrilateral, and octagonal arrangements of WECs, have been investigated [55, 70, 71, 75]. These regular patterns offer simplicity in design and analysis, providing a foundation for further optimization. For smaller arrays of heaving WECs, a rhombus-like layout has been identified as a potentially optimal configuration for maximizing energy extraction. The performance of linear and staggered arrays has also been analyzed under different wave conditions, with the optimal choice often depending on the prevailing wave direction and the need to mitigate wake effects between devices.

A novel hybrid algorithm for optimized solutions in WECs was presented to enhance the PTO parameters and site selection, tailored for oscillating wave surge converter (OWSC) [94]. This work does not directly address multi-device array layout configurations, but rather focuses on optimizing site selection and PTO system parameters to enhance the energy output of a single WEC unit. The optimization is grounded in the environmental conditions of the southern Caspian Sea and used a hybrid metaheuristic algorithm, namely Hill Climbing—Explorative Gray Wolf Optimizer (HC-EGWO), for maximizing absorbed wave energy. Unlike typical layout optimization involving spatial positioning of multiple WECs, this study's optimization focused on parameter-space exploration to identify the most effective configuration of a single OWSC unit under real wave conditions. The proposed HC-EGWO

algorithm outperforms five GWO variants in both benchmark and OWSC-specific optimization tasks. A power output improvement of up to 3.31% over other algorithms was observed, affirming the robustness and generalization capacity of the hybrid approach. Notably, the optimized configuration corresponds to wave conditions found near Kiashahr Port (37.6°N, 50.1°E), confirming this site's suitability for OSWEC deployment.

In another study, a comprehensive and novel approach for optimizing the layout of WEC arrays using the honey badger algorithm (HBA) has been presented [95]. The main objective of the study was to maximize the overall power output of WEC arrays by strategically positioning fully submerged three-tether buoys to exploit constructive hydrodynamic interactions and minimize destructive interference effects. The research systematically evaluates different configurations involving 2, 4, 10, and 20 WECs and compares the performance of HBA with five well-known metaheurtistic algorithms, such as GA, ACO, PSO, GSO, and GWO, as well as conventional linear and shared mooring layouts. The layout optimization problem involves determining the spatial positions of WEC buoys within a defined sea area, ensuring safe spacing and maximizing total power output. The design variables are the two-dimensional coordinates (x_i, y_i) of each WEC (F).

Their optimization approach iteratively searches the solution space and identify buoy arrangements that improve the performance index, particularly the q-factor, which is the ratio of array power output to the sum of outputs from isolated WECs. Their utilized approach is benchmarked against other layouts under different scenarios, where outperformed other metaheuristic algorithms in maximizing total power output and improving q-factors. In addition, the optimized arrays achieved q-factors of 1.039 (2-buoys), 1.027 (4-buoys), 1.056 (10-buoys), and 0.969 (20-buoys). It also showed a high power improvement efficiency, up to 7.19% in the 10-buoy case.

Following this type of WEC, a triple-layered chaotic differential evolution algorithm has been employed to optimizing the spatial arrangement of WECs [96]. The core objective was to maximize the total power output of an array by intelligently accounting for complex hydrodynamic interactions under multiple wave scenarios. The optimization approach enhances local search efficiency while maintaining global exploration, addressing the challenges of nonlinearity and high-dimensional optimization in WEC farms. The optimization problem is defined as selecting the optimal spatial coordinates for each WEC buoy in an array to maximize the total annual absorbed power, taking into account the constructive or destructive hydrodynamic interactions among buoys. The algorithm operates within a constrained domain, where each buoy must maintain a minimum safe Euclidean distance from others to ensure feasibility and avoid collision. The layout search space is large and complex, especially for large arrays, e.g., 16 WECs, where the number of hydrodynamic interaction evaluations increases exponentially. To address this, the triple-layered chaotic differential evolution algorithm is used to explore the layout space efficiently through a hierarchical, chaos-enhanced evolution strategy. Therefore, their proposed algorithm outperformed seven benchmark evolutionary algorithms, e.g., DE, IDE, CJADE, CMA-ES, and LS-NM, in all four wave conditions for 4- and 16-buoy

arrays. For instance, in the 4-buoy case, constructive hydrodynamic interactions were achieved in three out of four wave models, with $q > 1$, indicating effective layout optimization. In larger arrays, the algorithm maintained its robustness, identifying layouts with enhanced energy output despite increasing computational costs.

4.4.2 Optimizing Layout for LCOE Minimization

For wave energy to achieve widespread adoption as a viable renewable energy source, minimizing the LCOE is of paramount importance. The LCOE represents the average cost of generating one unit of electricity over the entire lifespan of a power generation project. The layout of a wave farm plays a critical role in determining the LCOE by influencing both the total energy production and the various capital and operational costs associated with the project.

Recent works highlights several procedures and methodologies for optimizing wave farm layouts with the specific goal of minimizing the LCOE. A prominent approach involves the development and application of integrated models that combine the simulation of wave energy conversion with detailed cost models. These integrated frameworks allow researchers to directly assess the economic implications of different layout choices alongside their impact on energy production. By considering both the revenue generated from electricity and the total costs incurred over the project's lifetime, these models enable the identification of layouts that offer the most economically efficient means of harnessing wave energy.

A study highlighted that the LCOE for wave energy projects varies widely, from 0.07 to 0.92 $/kWh, depending on the WEC technology, wave climate, and scale of deployment [97]. These values are significantly higher than the LCOE for mature renewable systematic optimization of both device design and project configuration to bring wave energy closer to commercial competitiveness.

Several research efforts have focused on the optimization WEC arrays and subsystems with the goal of minimizing LCOE. The optimization techniques used vary in complexity and computational demand but typically combine hydrodynamic modeling, economic analysis, and evolutionary algorithms. For instance, studies utilizing GA and DE methods have demonstrated the benefits of optimizing multiple design parameters simultaneously, such as the number of WEC units, spacing, orientation, and PTO control strategies, to achieve lower LCOEs. In one notable case involving the WaveSub device, a shift from a single-float to a six-float configuration led to a 21% reduction in LCOE, primarily due to cost efficiencies in mooring, installation, and electrical infrastructure [98]. In addition to system architecture and array layout, subsystem reliability and lifecycle performance also play a significant role in LCOE. The DTOcean framework incorporates detailed modeling of logistics, failure rates, and component-level reliability to simulate LCOE variability across different scenarios [99]. This approach acknowledges that LCOE is not a single deterministic value, but a probabilistic outcome influenced by the stochastic nature of wave climates and unplanned maintenance events. Their findings show that smaller arrays

are particularly sensitive to component failures, and investments in higher-quality electrical cables or connectors can reduce both the expected LCOE by up to 2.5% and its variability by over 50%. This underscores the importance of integrating reliability engineering and maintenance planning into early-stage project design, rather than treating them as operational afterthoughts.

A detailed framework for optimizing the spatial arrangement and electrical configuration of WEC arrays, with a strong emphasis on minimizing the LCOE has been presented in [43]. This work introduced an integrated modeling approach combining hydrodynamic modeling, economic modeling, and GA-based optimization, aimed at enhancing both energy output and economic viability of large-scale wave parks. The core focus of the layout optimization in this study is on identifying the optimal positions of multiple point-absorber WECs within a constrained marine area. The devices are arranged in clusters connected to one or more offshore electrical substations. Each substation serves a group of WECs, and their placement is determined such that intra-array cable lengths are minimized. A GA is employed to iteratively refine the layout toward configurations that minimize the LCOE, which serves as the primary objective function, as shown in Figs. 4.4 and 4.5. The GA encodes each potential layout as a chromosome, where genes represent the (x_i, y_i)

coordinates of each WEC. The algorithm initializes a population of random layouts and applies evolutionary operators—selection, crossover, and mutation—to evolve the population over multiple generations. A custom k-means clustering method is integrated into the GA to determine the optimal grouping of WECs to substations. This method minimizes the total cable length while allowing flexible placement of substations and ensuring an efficient electrical configuration (Fig. 4.6).

Another critical factor in reducing LCOE is the increased AEP through improved energy capture efficiency and control strategies. While the design of optimal layouts can mitigate destructive hydrodynamic interactions, which reduce AEP, control strategies such as adaptive damping and phase optimization further enhance energy

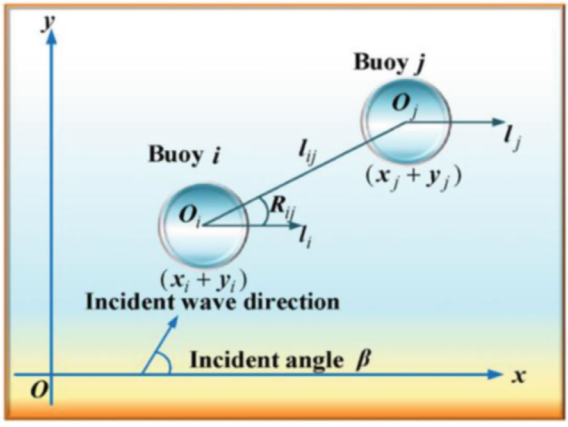

Fig. 4.4 Design variable for layout optimization [95]

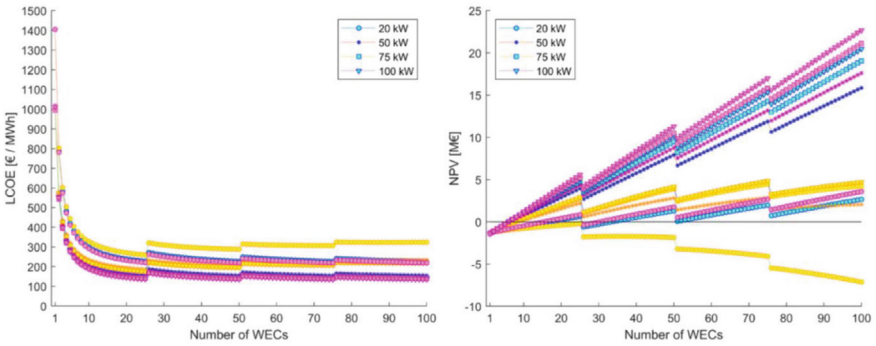

Fig. 4.5 Minimization of LCOE as well as maximization of NPV for different number of WECs [43]

extraction. AEP improvements of 12 to 55% were reported in studies that implemented advanced control techniques, which, when combined with CAPEX and OPEX reductions of 45–75%, could bring LCOEs below the often-cited commercialization threshold of 0.3 $/kWh [97]. The use of BEM, hybrid analytical-numerical models, and high-resolution wave resource assessments facilitates more accurate predictions of AEP, which are vital inputs in LCOE optimization workflows. Ultimately, the cost structure of wave energy projects is heavily front-loaded, with CAPEX constituting the largest share, often exceeding 60% of total costs. Device structure, PTO system, foundations, and installation dominate this phase. However, OPEX becomes increasingly relevant as arrays scale up or operate in harsher marine environments. Strategies such as modular device design, shared mooring systems, and optimized maintenance schedules contribute to reducing both CAPEX and OPEX. Projects that emphasize modularity and scalability, as seen in multi-float or array-on-device configurations, benefit from economies of scale that significantly improve LCOE. For example, a study showed that such configurations not only reduce grid connection costs but also maintain similar capacity factors, reinforcing their economic attractiveness [98].

In general, reducing the LCOE of wave energy projects is a multi-dimensional challenge that requires integrated optimization of WEC design, array layout, control strategies, and subsystem reliability. The combination of accurate techno-economic modeling, site-specific environmental assessment, and advanced computational optimization techniques provides a credible pathway toward achieving commercially viable wave energy systems. While current LCOE values remain above market-competitive levels, the cumulative impact of improvements across the project lifecycle, especially in PTO design, array configuration, and O&M strategies, suggest that wave energy is approaching a tipping point in its journey toward grid parity and widespread deployment.

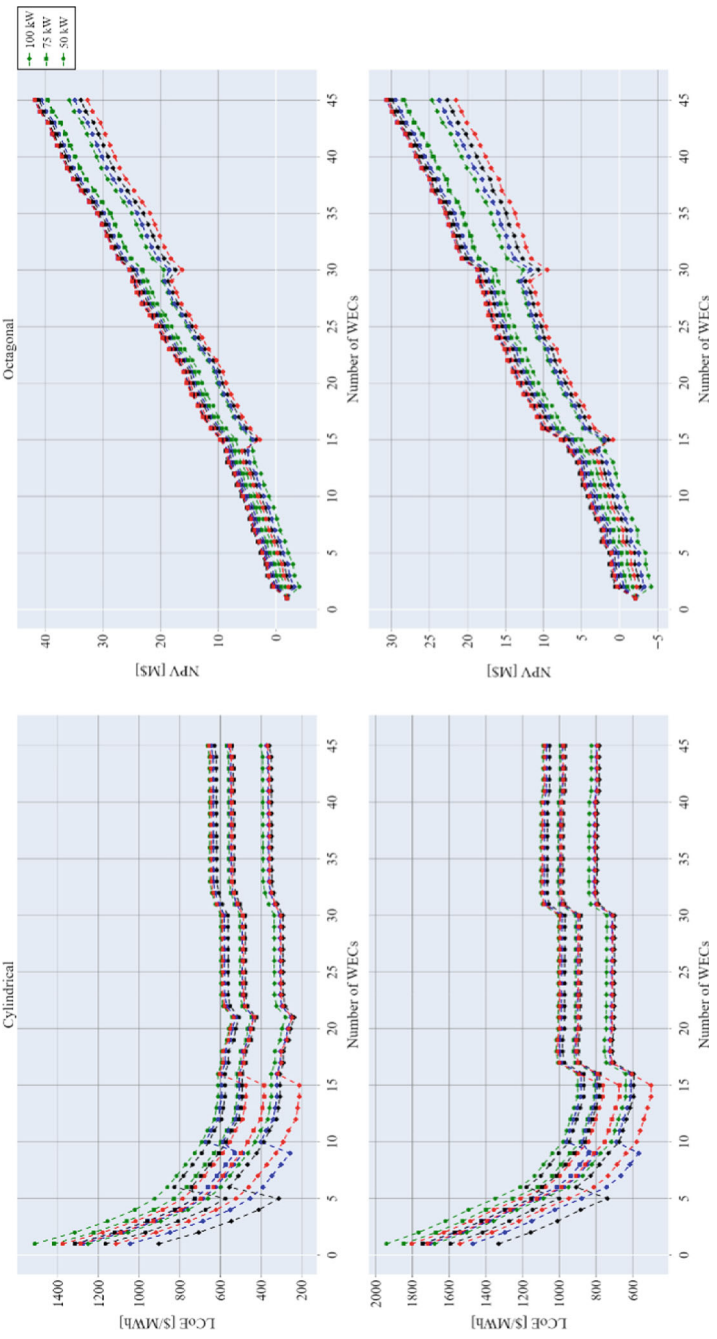

Fig. 4.6 LCOE and NPV results for various number of WECs [26]

4.4.3 *Multi-objective Optimization*

The development of commercially viable wave energy farms necessitates the consideration of multiple objectives that extend beyond simply maximizing energy production or minimizing the LCOE. Real-world wave farm design involves balancing economic performance with factors such as environmental impact, power grid integration requirements, and the reliability and survivability of the infrastructure. Consequently, multi-objective optimization techniques have gained prominence in recent research as a means of simultaneously addressing these various objectives and identifying a set of Pareto-optimal solutions that represent the best possible compromises [57].

Recent studies demonstrated how multi-objective optimization can be effectively used to optimize WEC placement, configuration, and operational parameters by simultaneously considering objectives such as energy production, hydrodynamic interaction efficiency, spatial compactness, and cost-effectiveness.

One study utilized NSGA-III algorithm to optimize WEC arrays along the coast of Oman, focusing on two main objectives, including maximizing the AEP and maximizing the q-factor, which quantifies the constructive or destructive hydrodynamic interactions between devices [93]. AEP is computed using wave data from SWAN simulations and stochastic modeling of sea states via Latin hypercube sampling. The q-factor is derived from comparing the array's power output to that of isolated devices. The optimization is applied to layouts with 4, 8, and 16 WECs depicted in Fig. 4.7, with findings indicating that different configurations, such as diagonal or multi-row arrangements, are optimal depending on the array size and wave conditions, demonstrated in Fig. 4.8. The study showed that strategic spacing and layout orientation can significantly influence both energy performance and interference effects.

Another study broadens the optimization framework significantly by including six objectives, including maximizing energy absorption and fluid velocity, while minimizing inter-device spacing, LCOE, NPV, and q-factor [26]. This work applied three different evolutionary algorithms, namely NSGA-III, R-NSGA-III, and MOEA/D,

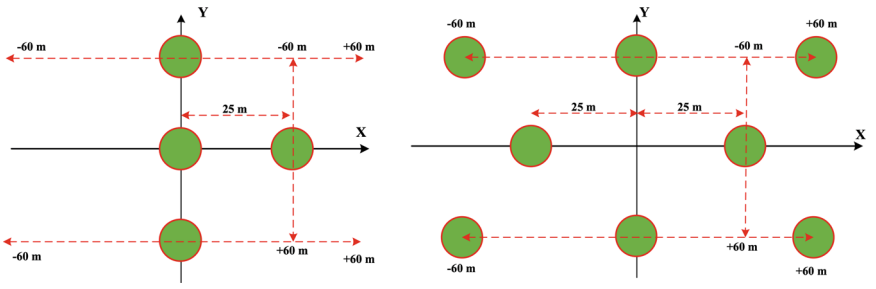

Fig. 4.7 Initial state of the WECs in the four and eight layout design [93]

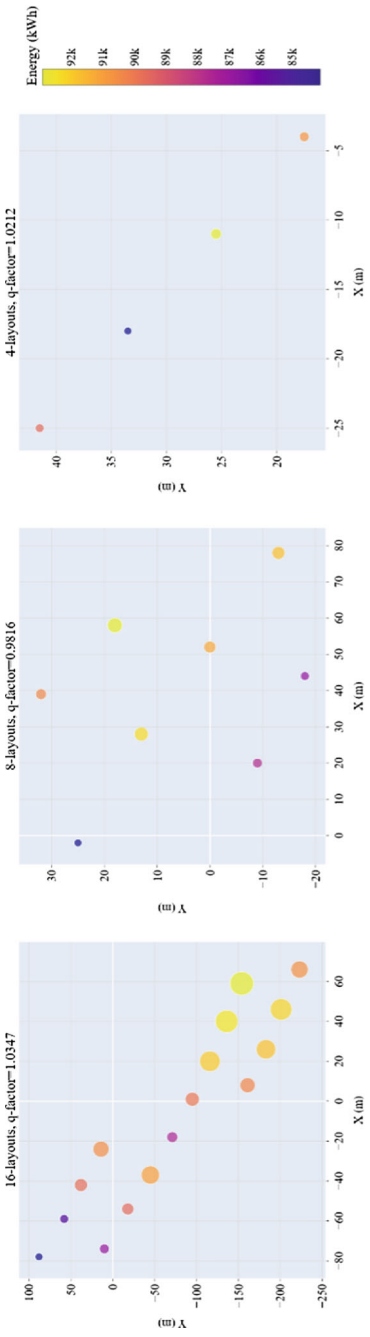

Fig. 4.8 Optimal layouts obtained from multi-objective optimization for different arrangements [93]

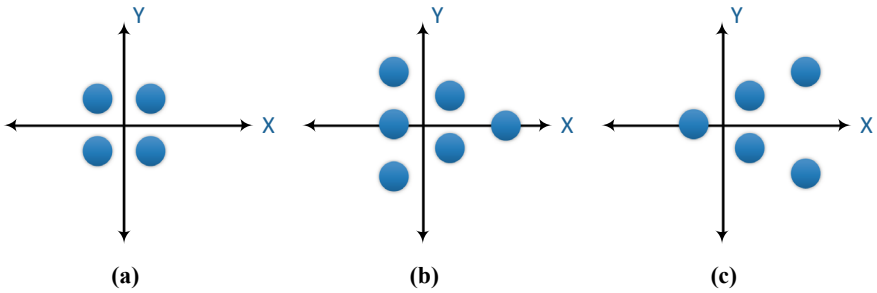

Fig. 4.9 Layout configuration designed for array optimization [26]

to explore a large solution space involving multiple WEC shapes, sizes, and configurations, showed in Fig. 4.9. One key insight was the influence of hull geometry on layout effectiveness. For example, arrow-shaped layouts of 30 cylindrical devices, as depicted in Fig. 4.10, showed high energy performance and low LCOE, demonstrating that geometric and spatial factors must be co-optimized for economic viability. This study also highlights that layouts must be tailored to site-specific wave climates and deployment constraints.

Both works, device spacing and number of WECs are treated as critical design variables. Tight spacing can lead to destructive wave interference and reduced power output, while excessive spacing increases cable costs and infrastructure complexity. Both studies enforce minimum spacing constraints to ensure practical feasibility and safe operations. Additionally, both studies recognized that the optimal number of devices does not necessarily scale linearly with energy production, adding more WECs without accounting for layout effects may lead to diminishing returns or even losses due to interference. Thus, finding the balance between array size and layout efficiency is essential. The modeling in both studies relied on frequency-domain hydrodynamic solvers and used simplifying assumptions such as constant depth, regular wave conditions, and linear PTO models. Despite these simplifications, the optimization results are validated using realistic wave data and robust performance metrics. Importantly, both research provide Pareto-optimal fronts, offering decision-makers a spectrum of solutions that trade-off between energy production, cost, and space. This enables flexible adaptation of designs based on project-specific priorities and regulatory or logistical constraints.

Several studies illustrated the significant advancements in multi-objective optimization techniques for WEC array design and operation. These studies reflected a shared understanding that optimizing only for energy output is insufficient for achieving viable wave energy systems. Instead, a multi-dimensional approach is necessary, integrating hydrodynamic performance, spatial planning, structural loading, infrastructure cost, and even operational adaptability. By combining numerical modeling tools, evolutionary algorithm, and, in one case, machine learning, these works demonstrated both complexity and the practicality of holistic wave energy farm optimization.

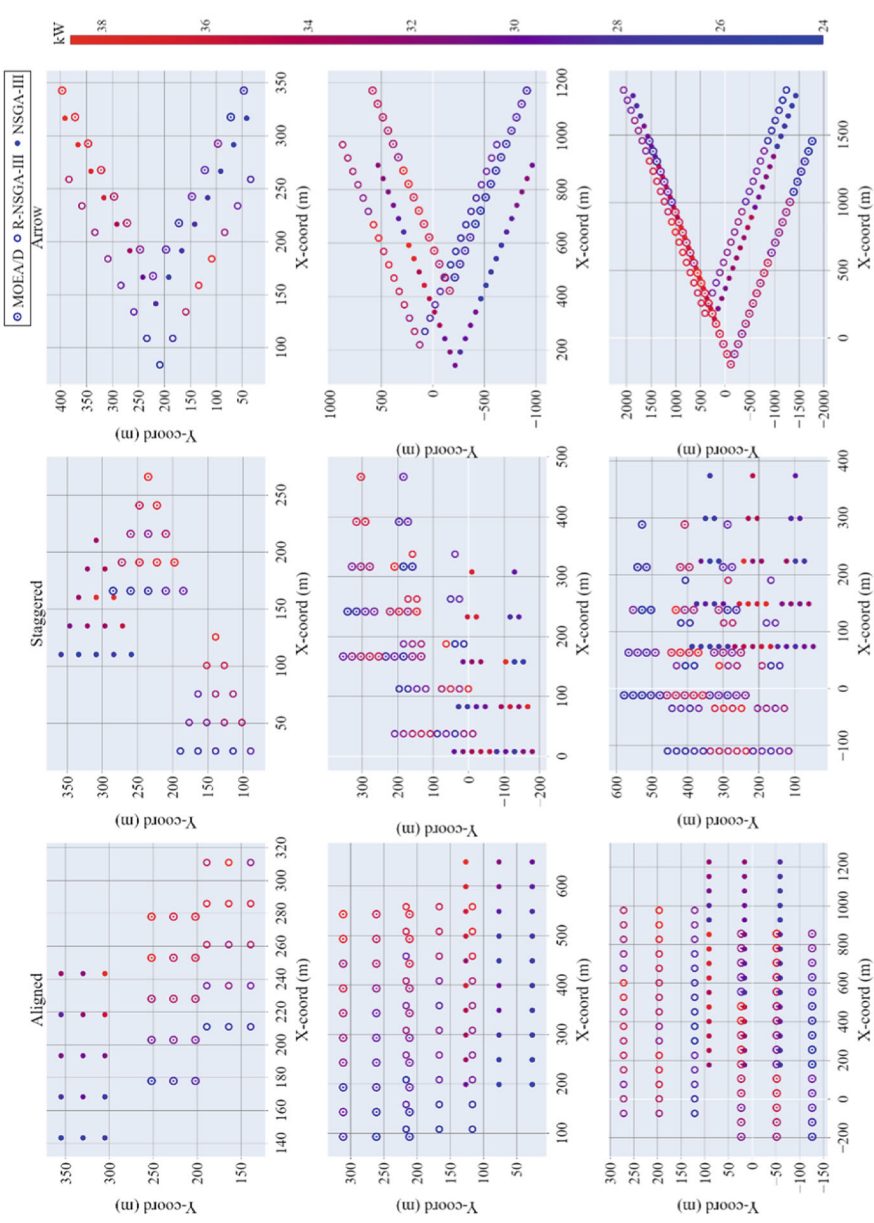

Fig. 4.10 Layout design of cylindrical WEC with 15, 30, and 45 device [26]

For instance, the optimization framework, i.e., evolutionary multi-objective optimization, balances four competing objectives, i.e., maximizing power, minimizing cable length, number of foundations, and structura loads, investigated in [73]. The study implemented three array layout schemes, including linear array model, random array model, and grid array model, each with its own variable structure and constraints on inter-device spacing and shared foundations. Their findings underscored that minimzing infrastructure costs through compact layouts can inadvertently increase destructive wave interferene, reducing overall energy performance. This illustrated the need for carefully tuned trade-offs between economics and hydrodynamics, which multi-objective optimization framewors such as theirs can robustly navigate. Their evolutionary algorithm produced a wide range of Pareto-optimal configurations, giving developers flexible design pathways depending on project priorities. Additionally, another study takes a more computationally efficient route by combining ANN with an adaptive GA to optimize array layouts solely for maximum energy output [100]. By training a surrogate model on simulation results, this work drastically reduce computational costs, making the method scalable for larger arrays or more frequent assessments. While the objective is narrower, focused only on energy production, the study still maintained important physical constraints, such as minimum and maximum inter-device spacing. This approach is highly relevant in early-stage planning or in scenarios where simulations costs are prohibitive, and it offers a compelling case for the integration of machine learning into renewable energy system design.

In contrast, the multi-body WEC optimization framework, investigated in [101], integrated not only layout design but also control optimization, allowing for adaptive configuration under differnet wave conditions. The use of a two-phase evolutionary framework, employed by U-NSGA-III and AGE-MOEA-II, supported by boundary element modeling, enables the system to respond dynamically to wave scenarios by altering the leg angles of the devices. This provided a significant advantage in ensuring both high energy output and low mechanical stress. While the optimization focuses on a relative small array, as shown in Fig. 4.11, the principles demonstrated, particularly the coupling of layout and operational control, represented a scalable strategy for real-time adaptive WEC farms.

In conclusion, the reviewed studies demonstrate that multi-objective optimization has become an indispensable tool in the advancement of WEC array design. By simultaneously accounting for hydrodynamic efficiency, spatial configuration, cost, and operational adaptability, multi-objective optimization frameworks enable the development of more robust and economically viable wave energy projects. The integration of numerical hydrodynamic modeling, evolutionary algorithms, and, increasingly, machine learning techniques offers flexible yet powerful pathways for optimizing both layout and control strategies. These approaches have revealed that trade-offs—particularly between compactness, energy output, and infrastructure cost—must be carefully balanced, and that site-specific conditions often necessitate customized array configurations.

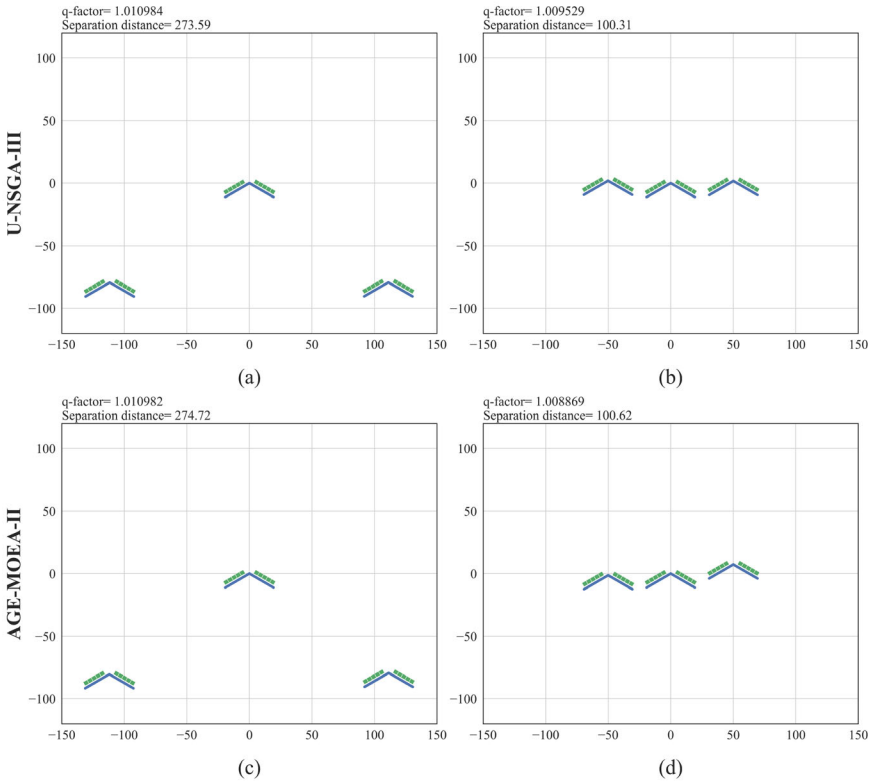

Fig. 4.11 Layout design using evolutionary multi-objective optimization [101]

Looking forward, future trends in this field will likely involve deeper integration of real-time adaptive control systems, uncertainty quantification, and machine learning-assisted surrogate models for faster and more scalable optimization. Hybrid frameworks that couple operational control with economic forecasting and reliability analysis will become increasingly relevant as WEC technologies mature toward commercialization. Furthermore, the expansion of optimization objectives to include environmental impact, marine spatial planning, and grid integration constraints will allow for more holistic and sustainable wave farm development. The convergence of high-fidelity modeling, intelligent algorithms, and interdisciplinary design considerations marks a promising trajectory for the future of wave energy systems.

References

1. Shi, Y.: Array design and levelized cost of energy of wave energy farm. Laurea, Politecnico di Torino. https://webthesis.biblio.polito.it/30624/ (2024). Accessed 23 Mar 2025
2. Bozzi, S., et al.: Wave energy farm design in real wave climates: the Italian offshore. Energy **122**, 378–389 (2017). https://doi.org/10.1016/j.energy.2017.01.094
3. Clemente, D., Rosa-Santos, P., Taveira-Pinto, F., Martins, P.: Influence of platform design and power take-off characteristics on the performance of the E-motions wave energy converter. Energy Convers. Manag. **244**, 114481 (2021). https://doi.org/10.1016/j.enconman.2021.114481
4. Aderinto, T., Li, H.: Ocean wave energy converters: status and challenges. Energies **11**(5), 1250 (2018). https://doi.org/10.3390/en11051250
5. Aderinto, T., Li, H.: Review on power performance and efficiency of wave energy converters. Energies **12**(22), 4329 (2019)
6. Pérez-Collazo, C., Greaves, D., Iglesias, G.: A review of combined wave and offshore wind energy. Renew. Sustain. Energy Rev. **42**, 141–153 (2015). https://doi.org/10.1016/j.rser.2014.09.032
7. Lehmann, M., Karimpour, F., Goudey, C.A., Jacobson, P.T., Alam, M.-R.: Ocean wave energy in the United States: current status and future perspectives. Renew. Sustain. Energy Rev. **74**, 1300–1313 (2017). https://doi.org/10.1016/j.rser.2016.11.101
8. Trueworthy, A., DuPont, B.: The wave energy converter design process: methods applied in industry and shortcomings of current practices. J. Mar. Sci. Eng. **8**(11), 932 (2020). https://doi.org/10.3390/jmse8110932
9. Leeney, R.H., Greaves, D., Conley, D., O'Hagan, A.M.: Environmental impact assessments for wave energy developments—learning from existing activities and informing future research priorities. Ocean Coast. Manag. **99**, 14–22 (2014). https://doi.org/10.1016/j.ocecoaman.2014.05.025
10. Frid, C., et al.: The environmental interactions of tidal and wave energy generation devices. Environ. Impact Assess. Rev. **32**(1), 133–139 (2012). https://doi.org/10.1016/j.eiar.2011.06.002
11. Azam, A., et al.: Wave energy evolution: knowledge structure, advancements, challenges and future opportunities. Renew. Sustain. Energy Rev. **205**, 114880 (2024). https://doi.org/10.1016/j.rser.2024.114880
12. Dalton, G.: Ocean energy—wave and tide. In: Building Industries at Sea—'Blue Growth' and the New Maritime Economy. River Publishers (2018)
13. Emmanouil, G., Galanis, G., Kalogeri, C., Zodiatis, G., Kallos, G.: 10-year high resolution study of wind, sea waves and wave energy assessment in the Greek offshore areas. Renew. Energy **90**, 399–419 (2016). https://doi.org/10.1016/j.renene.2016.01.031
14. Bouhrim, H., El Marjani, A., Nechad, R., Hajjout, I.: Ocean wave energy conversion: a review. J. Mar. Sci. Eng. **12**(11), 2024 (1922). https://doi.org/10.3390/jmse12111922
15. Flocard, F., Ierodiaconou, D., Coghlan, I.R.: Multi-criteria evaluation of wave energy projects on the south-east Australian coast. Renew. Energy **99**, 80–94 (2016). https://doi.org/10.1016/j.renene.2016.06.036
16. Qiao, D., Haider, R., Yan, J., Ning, D., Li, B.: Review of wave energy converter and design of mooring system. Sustainability **12**(19), 8251 (2020). https://doi.org/10.3390/su12198251
17. Moore, D., Eftekhari, A., Nash, S.: Weather window analysis for the deployment, operation, and maintenance of marine renewable energy devices in Irish coastal waters. J. Ocean Eng. Mar. Energy **10**(4), 711–729 (2024). https://doi.org/10.1007/s40722-024-00340-2
18. OES | Design of the next generation of the Oyster wave energy converter. https://www.ocean-energy-systems.org/publications/icoe/icoe-2010/document/design-of-the-next-generation-of-the-oyster-wave-energy-converter/. Accessed 24 Mar 2025
19. Göteman, M., Giassi, M., Engström, J., Isberg, J.: Advances and challenges in wave energy park optimization—a review. Front. Energy Res. **8**, 26 (2020)

20. Kang, Y. (康元顺), Zeng, X. (曾晓辉), Cui, Z. (崔哲华), Chen, J. (陈嘉昊): Hydrodynamic responses and layout optimization of wave energy converter arrays consisting of five-degree-of-freedom truncated cylinders in front of a vertical wall. Phys. Fluids **36**(1), 017102 (2024). https://doi.org/10.1063/5.0184849
21. Zeng, X., Wang, Q., Kang, Y., Yu, F.: A novel type of wave energy converter with five degrees of freedom and preliminary investigations on power-generating capacity. Energies **15**(9), 3069 (2022). https://doi.org/10.3390/en15093069
22. Yang, B., et al.: Wave energy converter array layout optimization: a critical and comprehensive overview. Renew. Sustain. Energy Rev. **167**, 112668 (2022)
23. Flanagan, T., Wengrove, M., Robertson, B.: Coupled wave energy converter and nearshore wave propagation models for coastal impact assessments. J. Mar. Sci. Eng. **10**(3), 370 (2022). https://doi.org/10.3390/jmse10030370
24. Noad, I.F., Porter, R.: Optimisation of arrays of flap-type oscillating wave surge converters. Appl. Ocean Res. **50**, 237–253 (2015). https://doi.org/10.1016/j.apor.2015.01.020
25. Astariz, S., Iglesias, G.: Enhancing wave energy competitiveness through co-located wind and wave energy farms. A review on the shadow effect. Energies **8**(7), 7344–7366 (2015). https://doi.org/10.3390/en8077344
26. Shadmani, A., Nikoo, M.R., Gandomi, A.H.: Adaptive systematic optimization of a multi-axis ocean wave energy converter. Renew. Sustain. Energy Rev. **189**, 113920 (2024)
27. Abdulkadir, H., Abdelkhalik, O.: Optimization of heterogeneous arrays of wave energy converters. Ocean Eng. **272**, 113818 (2023)
28. Peña-Sanchez, Y., García-Violini, D., Penalba, M., Zarketa, A., Nava, V., Ringwood, J.: Spectral control co-design of wave energy converter array layout. In: Proceedings of the European Wave and Tidal Energy Conference (2023)
29. Garcia-Rosa, P.B., Bacelli, G., Ringwood, J.V.: Control-informed optimal array layout for wave farms. IEEE Trans. Sustain. Energy **6**(2), 575–582 (2015). https://doi.org/10.1109/TSTE.2015.2394750
30. Bergillos, R.J., Rodriguez-Delgado, C., Iglesias, G.: Optimization of wave farm location and layout for coastal protection. In: Bergillos, R.J., Rodriguez-Delgado, C., Iglesias, G. (eds.) Ocean Energy and Coastal Protection: A Novel Strategy for Coastal Management Under Climate Change, pp. 9–27. Springer International Publishing, Cham (2020). https://doi.org/10.1007/978-3-030-31318-0_2
31. Want, A., Waldman, S., Burrows, M.T., Side, J.C., Venugopal, V., Bell, M.C.: Predicted ecological consequences of wave energy extraction and climate-related changes in wave exposure on rocky shore communities. ICES J. Mar. Sci. **81**(7), 1263–1281 (2024). https://doi.org/10.1093/icesjms/fsae086
32. Bedard, R.: Economic and social benefits from wave energy conversion marine technology. Mar. Technol. Soc. J. **41**(3), 44–50 (2007). https://doi.org/10.4031/002533207787442123
33. Tougaard, J.: Underwater noise from a wave energy converter is unlikely to affect marine mammals. PLoS ONE **10**(7), e0132391 (2015). https://doi.org/10.1371/journal.pone.0132391
34. Foteinis, S.: Wave energy converters in low energy seas: current state and opportunities. Renew. Sustain. Energy Rev. **162**, 112448 (2022). https://doi.org/10.1016/j.rser.2022.112448
35. Rahman, A., Farrok, O., Haque, M.M.: Environmental impact of renewable energy source based electrical power plants: solar, wind, hydroelectric, biomass, geothermal, tidal, ocean, and osmotic. Renew. Sustain. Energy Rev. **161**, 112279 (2022). https://doi.org/10.1016/j.rser.2022.112279
36. Al-Shetwi, A.Q.: Sustainable development of renewable energy integrated power sector: trends, environmental impacts, and recent challenges. Sci. Total. Environ. **822**, 153645 (2022). https://doi.org/10.1016/j.scitotenv.2022.153645
37. Hu, H., Xue, W., Jiang, P., Li, Y.: Bibliometric analysis for ocean renewable energy: an comprehensive review for hotspots, frontiers, and emerging trends. Renew. Sustain. Energy Rev. **167**, 112739 (2022). https://doi.org/10.1016/j.rser.2022.112739
38. Arena, F., Laface, V., Malara, G., Romolo, A.: Estimation of downtime and of missed energy associated with a wave energy converter by the equivalent power storm model. Energies **8**(10), 11575–11591 (2015). https://doi.org/10.3390/en81011575

39. Astariz, S., Iglesias, G.: Wave energy vs. other energy sources: a reassessment of the economics. Int. J. Green Energy **13**(7), 747–755 (2016). https://doi.org/10.1080/15435075.2014.963587
40. Al Mubarak, F., Rezaee, R., Wood, D.A.: Economic, societal, and environmental impacts of available energy sources: a review. Eng **5**(3), 1232 (2024). https://doi.org/10.3390/eng5030067
41. Guo, C., Sheng, W., De Silva, D.G., Aggidis, G.: A review of the levelized cost of wave energy based on a techno-economic model. Energies **16**(5), 2144 (2023). https://doi.org/10.3390/en16052144
42. Xu, S., Wang, S., Guedes Soares, C.: Review of mooring design for floating wave energy converters. Renew. Sustain. Energy Rev. **111**, 595–621 (2019). https://doi.org/10.1016/j.rser.2019.05.027
43. Giassi, M., Castellucci, V., Göteman, M.: Economical layout optimization of wave energy parks clustered in electrical subsystems. Appl. Ocean Res. **101**, 102274 (2020). https://doi.org/10.1016/J.APOR.2020.102274
44. Giglio, E., Petracca, E., Paduano, B., Moscoloni, C., Giorgi, G., Sirigu, S.A.: Estimating the cost of wave energy converters at an early design stage: a bottom-up approach. Sustainability **15**(8), 6756 (2023). https://doi.org/10.3390/su15086756
45. Correia da Fonseca, F.X., Amaral, L., Chainho, P.: A decision support tool for long-term planning of marine operations in ocean energy projects. J. Mar. Sci. Eng. **9**(8), 810 (2021). https://doi.org/10.3390/jmse9080810
46. Said, H.A., Ringwood, J.V.: Grid integration aspects of wave energy—overview and perspectives. IET Renew. Power Gener. **15**(14), 3045–3064 (2021). https://doi.org/10.1049/rpg2.12179
47. Thomas, J.J., et al.: A comparison of eight optimization methods applied to a wind farm layout optimization problem. Wind Energy Sci. **8**(5), 865–891 (2023). https://doi.org/10.5194/wes-8-865-2023
48. Castro-Santos, L., Bento, A.R., Guedes Soares, C.: The economic feasibility of floating offshore wave energy farms in the North of Spain. Energies **13**(4), 806 (2020). https://doi.org/10.3390/en13040806
49. Roberts, O., et al.: Bringing structure to the wave energy innovation process with the development of a techno-economic tool. Energies **14**(24), 8201 (2021). https://doi.org/10.3390/en14248201
50. Abhinav, K.A., et al.: Offshore multi-purpose platforms for a blue growth: a technological, environmental and socio-economic review. Sci. Total. Environ. **734**, 138256 (2020). https://doi.org/10.1016/j.scitotenv.2020.138256
51. Dalton, G., et al.: Economic and socio-economic assessment methods for ocean renewable energy: public and private perspectives. Renew. Sustain. Energy Rev. **45**, 850–878 (2015). https://doi.org/10.1016/j.rser.2015.01.068
52. Sirigu, S.A., et al.: Techno-economic optimisation for a wave energy converter via genetic algorithm. J. Mar. Sci. Eng. **8**(7), 482 (2020). https://doi.org/10.3390/jmse8070482
53. Han, M., Cao, F., Shi, H., Zhu, K., Dong, X., Li, D.: Layout optimisation of the two-body heaving wave energy converter array. Renew. Energy **205**, 410–431 (2023). https://doi.org/10.1016/j.renene.2023.01.100
54. Shadmani, A., Nikoo, M.R., Gandomi, A.H., Wang, R.-Q., Golparvar, B.: A review of machine learning and deep learning applications in wave energy forecasting and WEC optimization. Energy Strategy Rev. **49**, 101180 (2023). https://doi.org/10.1016/j.esr.2023.101180
55. Sharp, C., DuPont, B.: Wave energy converter array optimization: a genetic algorithm approach and minimum separation distance study. Ocean Eng. **163**, 148–156 (2018). https://doi.org/10.1016/j.oceaneng.2018.05.071
56. Lyu, J., Abdelkhalik, O., Gauchia, L.: Optimization of dimensions and layout of an array of wave energy converters. Ocean Eng. **192**, 106543 (2019). https://doi.org/10.1016/j.oceaneng.2019.106543

57. Guo, X., Liu, Y., Zhang, X.: Layout optimization of wave energy park based on multi-objective optimization algorithm. In: ASME 2024 43rd International Conference on Ocean, Offshore and Arctic Engineering, American Society of Mechanical Engineers Digital Collection (2024). https://doi.org/10.1115/OMAE2024-120859
58. Azad, S., Khanal, S., Herber, D.R., Jia, G.: Integrated Design for Wave Energy Converter Farms: Assessing Plant, Control, Layout, and Site Selection Coupling in the Presence of Irregular Waves (2024). https://doi.org/10.48550/arXiv.2405.15717. *arXiv*: arXiv:2405.15717
59. Moarefdoost, M.M., Snyder, L.V., Alnajjab, B.: Layouts for ocean wave energy farms: models, properties, and optimization. Omega **66**, 185–194 (2017). https://doi.org/10.1016/j.omega.2016.06.004
60. Snyder, L.V.: Lawrence V. Snyder (2022). https://doi.org/10.1287/483ca90f-76d7-48ca-8808-7e85d4b7b688
61. Khanal, K., DeGoede, N., Vitale, O., Haji, M.N.: Multi-objective multidisciplinary optimization of wave energy converter array layout and controls. In: Social Science Research Network, Rochester, NY: 4891821 (2024). https://doi.org/10.2139/ssrn.4891821
62. Optimization of a wave energy park using a spectral wave model and a binary genetic algorithm | Tethys Engineering. https://tethys-engineering.pnnl.gov/publications/optimization-wave-energy-park-using-spectral-wave-model-binary-genetic-algorithm. Accessed 26 Mar 2025
63. Gambarini, M., Ciaramella, G., Miglio, E.: A gradient flow approach for combined layout-control design of wave energy parks (2024). https://doi.org/10.48550/arXiv.2409.10200. *arXiv*: arXiv:2409.10200
64. Li, C., Liu, Y., Hong, Y., Pan, J.: Optimal layout configuration of a wave energy farm considering the power smoothing effect. In: The 11th IET International Conference on Advances in Power System Control, Operation and Management (APSCOM 2018), p. 91. https://doi.org/10.1049/cp.2018.1824
65. Peña-Sanchez, Y., et al.: Control co-design for wave energy farms: Optimisation of array layout and mooring configuration in a realistic wave climate. Renew. Energy **227**, 120506 (2024). https://doi.org/10.1016/j.renene.2024.120506
66. Ekweoba, C., et al.: Geometry optimization of a floating platform with an integrated system of wave energy converters using a genetic algorithm. Renew. Energy **231**, 120869 (2024). https://doi.org/10.1016/j.renene.2024.120869
67. Neshat, M., Alexander, B., Sergiienko, N.Y., Wagner, M.: A hybrid evolutionary algorithm framework for optimising power take off and placements of wave energy converters. In: Proceedings of the Genetic and Evolutionary Computation Conference, in GECCO '19, pp. 1293–1301. Association for Computing Machinery, New York, NY, USA (2019). https://doi.org/10.1145/3321707.3321806
68. Neshat, M., Alexander, B., Sergiienko, N.Y., Wagner, M.: Optimisation of large wave farms using a multi-strategy evolutionary framework. In: Proceedings of the 2020 Genetic and Evolutionary Computation Conference, in GECCO '20, pp. 1150–1158. Association for Computing Machinery, New York, NY, USA (2020). https://doi.org/10.1145/3377930.3390235
69. Neshat, M., Alexander, B., Wagner, M., Xia, Y.: A detailed comparison of meta-heuristic methods for optimising wave energy converter placements. In: Proceedings of the Genetic and Evolutionary Computation Conference, in GECCO '18, pp. 1318–1325. Association for Computing Machinery, New York, NY, USA (2018). https://doi.org/10.1145/3205455.3205492
70. Neshat, M., Alexander, B., Sergiienko, N.Y., Wagner, M.: New insights into position optimisation of wave energy converters using hybrid local search. Swarm Evol. Comput. **59**, 100744 (2020)
71. Neshat, M., Alexander, B., Wagner, M.: A hybrid cooperative co-evolution algorithm framework for optimising power take off and placements of wave energy converters. Inf. Sci. **534**, 218–244 (2020). https://doi.org/10.1016/j.ins.2020.03.112
72. Neshat, M., et al.: A new bi-level optimisation framework for optimising a multi-mode wave energy converter design: a case study for the Marettimo Island, Mediterranean Sea. Energies **13**(20), 5498 (2020). https://doi.org/10.3390/en13205498

73. David, D.R., Kurniawan, A., Wolgamot, H., Hansen, J.E., Rijnsdorp, D., Lowe, R.: Nearshore submerged wave farm optimisation: a multi-objective approach. Appl. Ocean Res. **124**, 103225 (2022). https://doi.org/10.1016/j.apor.2022.103225
74. Golbaz, D., et al.: Ocean Wave Energy Converters Optimization: A Comprehensive Review on Research Directions (2021). https://doi.org/10.48550/arxiv.2105.07180
75. Neshat, M., Alexander, B., Sergiienko, N.Y., Wagner, M.: Optimisation of large wave farms using a multi-strategy evolutionary framework. In: Proceedings of the 2020 Genetic and Evolutionary Computation Conference, pp. 1150–1158 (2020). https://doi.org/10.1145/3377930.3390235
76. Hietanen, A.I., Snedker, T.H., Dykes, K., Bayati, I.: A novel techno-economical layout optimization tool for floating wind farm design. Wind Energy Sci. **9**(2), 417–438 (2024). https://doi.org/10.5194/wes-9-417-2024
77. Natarajan, S.K., Cho, I.H.: Cost-effective optimization of an array of wave energy converters in front of a vertical seawall. Energies **17**(1), 128 (2023)
78. Castro-Santos, L., Cordal-Iglesias, D., Filgueira-Vizoso, A.: Floating wave energy farms: how energy calculations shape economic feasibility? Heliyon **10**(22), e39672 (2024). https://doi.org/10.1016/j.heliyon.2024.e39672
79. Izquierdo-Pérez, J., Brentan, B.M., Izquierdo, J., Clausen, N.-E., Pegalajar-Jurado, A., Ebsen, N.: Layout optimization process to minimize the cost of energy of an offshore floating hybrid wind-wave farm. Processes **8**(2), 139 (2020). https://doi.org/10.3390/pr8020139
80. Teixeira-Duarte, F., Rosa-Santos, P., Taveira-Pinto, F.: Multi-objective optimization of co-located wave-wind farm layouts supported by genetic algorithms and numerical models. Renew. Energy **241**, 122362 (2025). https://doi.org/10.1016/j.renene.2025.122362
81. Carballo, R., Iglesias, G.: Wave farm impact based on realistic wave-WEC interaction. Energy **51**, 216–229 (2013). https://doi.org/10.1016/j.energy.2012.12.040
82. Santiago-Ojeda, E., García-Nava, H., Gutiérrez-López, E.: Optimization of a wave energy park using a spectral wave model and a binary genetic algorithm.
83. Meyer, J., Windt, C., Hildebrandt, A., Schlurmann, T.: Mechanically coupled wave farms: on the accuracy of a mid-fidelity hydrodynamic model under consideration of varying calibration approaches. Ocean Eng. **305**, 117874 (2024). https://doi.org/10.1016/j.oceaneng.2024.117874
84. Behzad, H., Sanaei, P.: On optimizing the wave energy converters configuration in a farm (2019)
85. Galparsoro, I., et al.: A new framework and tool for ecological risk assessment of wave energy converters projects. Renew. Sustain. Energy Rev. **151**, 111539 (2021). https://doi.org/10.1016/j.rser.2021.111539
86. Martínez, M.L., et al.: A systemic view of potential environmental impacts of ocean energy production. Renew. Sustain. Energy Rev. **149**, 111332 (2021). https://doi.org/10.1016/j.rser.2021.111332
87. Ringwood, J.V., Zhan, S., Faedo, N.: Empowering wave energy with control technology: possibilities and pitfalls. Annu. Rev. Control. **55**, 18–44 (2023). https://doi.org/10.1016/j.arcontrol.2023.04.004
88. Zhou, Y.: Ocean energy applications for coastal communities with artificial intelligencea state-of-the-art review. Energy AI **10**, 100189 (2022). https://doi.org/10.1016/j.egyai.2022.100189
89. Buenau, K.E., Garavelli, L., Hemery, L.G., García Medina, G.: A review of modeling approaches for understanding and monitoring the environmental effects of marine renewable energy. J. Mar. Sci. Eng. **10**(1), 94 (2022). https://doi.org/10.3390/jmse10010094
90. Abbaspour, M., Farshforoush, A.: Optimal arrangements for semi-submersible cylindrical wave energy converters: a study in layout optimization and power extraction efficiency. Ocean Eng. **296**, 116833 (2024). https://doi.org/10.1016/j.oceaneng.2024.116833
91. Göteman, M., Engström, J., Eriksson, M., Isberg, J.: Optimizing wave energy parks with over 1000 interacting point-absorbers using an approximate analytical method. Int. J. Mar. Energy **10**, 113–126 (2015). https://doi.org/10.1016/j.ijome.2015.02.001

92. Wang, X., Wang, T., Lv, H., Wang, H., Zeng, F.: Analytical modeling and experimental verification of a multi-DOF spherical pendulum electromagnetic energy harvester. Energy **286**, 129428 (2024). https://doi.org/10.1016/j.energy.2023.129428
93. Shadmani, A., Reza Nikoo, M., Etri, T., Gandomi, A.H.: A multi-objective approach for location and layout optimization of wave energy converters. Appl. Energy **347**, 121397 (2023). https://doi.org/10.1016/j.apenergy.2023.121397
94. Mehdipour, H., Amini, E., Naeeni, S.T., Neshat, M.: A Novel Hybrid Algorithm for Optimized Solutions in Ocean Renewable Energy Industry: Enhancing Power Take-Off Parameters and Site Selection Procedure of Wave Energy Converters (2023). https://doi.org/10.48550/arXiv.2309.10606. *arXiv*: arXiv:2309.10606
95. Yang, B., et al.: Optimal array layout design of wave energy converter via honey badger algorithm. Renew. Energy **234**, 121182 (2024). https://doi.org/10.1016/j.renene.2024.121182
96. Zhang, Z., Yu, Q., Yang, H., Li, J., Cheng, J., Gao, S.: Triple-layered chaotic differential evolution algorithm for layout optimization of offshore wave energy converters. Expert Syst. Appl. **239**, 122439 (2024). https://doi.org/10.1016/j.eswa.2023.122439
97. Chang, G., Jones, C.A., Roberts, J.D., Neary, V.S.: A comprehensive evaluation of factors affecting the levelized cost of wave energy conversion projects. Renew. Energy **127**, 344–354 (2018). https://doi.org/10.1016/j.renene.2018.04.071
98. Faraggiana, E., Chapman, J.C., Williams, A.J., Masters, I.: Genetic based optimisation of the design parameters for an array-on-device orbital motion wave energy converter. Ocean Eng. **218**, 108251 (2020). https://doi.org/10.1016/j.oceaneng.2020.108251
99. Topper, M.B.R., et al.: Reducing variability in the cost of energy of ocean energy arrays. Renew. Sustain. Energy Rev. **112**, 263–279 (2019). https://doi.org/10.1016/j.rser.2019.05.032
100. Zhu, K., Shi, H., Han, M., Cao, F.: Layout study of wave energy converter arrays by an artificial neural network and adaptive genetic algorithm. Ocean Eng. **260**, 112072 (2022). https://doi.org/10.1016/j.oceaneng.2022.112072
101. Hoseini Karani, M.M., Nikoo, M.R., Dolatshahi Pirooz, H., Shadmani, A., Al-Saadi, S., Gandomi, A.H.: Multi-objective evolutionary framework for layout and operational optimization of a multi-body wave energy converter. Energy **313**, 134045 (2024). https://doi.org/10.1016/j.energy.2024.134045

Chapter 5
Power Take-Off Control of WECs

Abstract This chapter addresses the critical role of Power Take-Off (PTO) control systems in maximizing energy extraction from ocean waves. The effectiveness of wave energy converters (WECs) depends significantly on how well their PTO systems can respond to the irregular and variable nature of ocean waves. PTO control represents one of the most promising pathways for improving WEC performance without substantial increases in capital costs, potentially reducing the levelized cost of energy (LCOE) for wave energy projects. Advanced control strategies enable WECs to adapt to changing sea states, optimize power capture across a broad frequency spectrum, and protect devices during extreme conditions, ultimately determining the commercial viability of wave energy technologies. The chapter begins with Sect. 5.1 which introduces fundamental concepts of PTO systems, including mechanical, hydraulic, pneumatic, and direct drive configurations, and their inherent control challenges. Section 5.2 explores methodologies for evaluating PTO control strategies, presenting analytical and numerical approaches for quantifying performance improvements under various wave conditions. Section 5.3 examines optimization techniques for PTO systems, covering both passive and active control methods, reactive control, and machine learning applications in real-time control systems. Section 5.4 provides detailed case studies of PTO control implementation in operational wave energy projects, offering practical insights into successes and challenges in real-world applications. Finally, Sect. 5.5 investigates emerging trends in PTO control technology, including predictive control algorithms, distributed control architectures, and integration with energy storage systems to enhance grid compatibility.

Keywords Power take-off (PTO) · Control strategies · Energy efficiency · Reactive control · Real-time optimization

The power take-off (PTO) system is a critical component of WECs, responsible for converting mechanical energy from ocean waves into electrical power. Over the past decade, there has been significant research aimed at optimizing PTO control strategies to maximize energy extraction, improve reliability, and reduce maintenance costs. Various control methods have been proposed, including passive, reactive,

A. Shadmani et al., *Ocean Wave Energy Technology*,
https://doi.org/10.1007/978-3-031-95040-7_5

and advanced predictive control strategies, each tailored to different WEC designs and environmental conditions. This literature review explores the fundamentals of PTO systems, the performance evaluation of different control strategies, optimization techniques, real-world case studies, and emerging trends shaping the future of wave energy technology.

Currently, several WECs exist with different absorption mechanisms and subsystems. Hence, a general formulation to describe the dynamics of all possible devices is a non-trivial task. This section provides practical, condensed information, and derivations for the dynamics of oscillating bodies, as this category comprises most WECs, and relevant literature is recommended for more technical information.

Section 5.1, PTO System Fundamentals, provides an in-depth overview of the different PTO types and the underlying principles guiding their functionality. It sets the stage by exploring the mechanical, electrical, and hydraulic subsystems that collectively enable wave energy capture and conversion. In Sect. 5.2, the text progresses to a detailed analysis of various performance evaluation approaches for PTO control strategies, covering simulation studies, laboratory tests, and field experiments. Readers will gain insight into how these evaluation methods can be used to compare and optimize different PTO systems under realistic ocean conditions.

Building on this, Sect. 5.3 addresses PTO optimization by discussing advanced control algorithms designed to enhance energy absorption across varying wave climates. This section examines both model-based and model-free approaches, illustrating how properly tuned algorithms can adapt in real time to shifting wave environments, ultimately improving power output. Section 5.4, Case Studies: PTO Control in Wave Energy Projects, presents real-world applications of these control strategies, showcasing how theoretical insights are put into practice and what lessons have been learned from operational wave energy farms. These case studies underscore the influence of site-specific conditions and project objectives on final technology selection.

Lastly, Sect. 5.5 sheds light on Emerging Trends in PTO Control Technology, touching on cutting-edge topics such as data-driven control, artificial intelligence, and hybrid energy systems integration. The chapter wraps up by discussing how ongoing innovations may shape future WEC designs, with an eye toward improving cost-effectiveness, durability, and scalability. By the end of this chapter, readers will have a clear understanding of the principal PTO control concepts, the methodologies used to assess performance, and the direction of emerging technologies in wave energy conversion.

5.1 PTO System Fundamentals

The PTO system serves as the intermediary between the wave motion and the electrical grid, playing a crucial role in energy conversion efficiency. PTO mechanisms can be broadly classified into hydraulic, mechanical, pneumatic, and direct-drive systems, as shown in Fig. 5.1 [1]. Functioning as the interface between the initial

wave energy absorption stage and the subsequent delivery to the electrical grid or energy storage solutions, the PTO system faces the significant challenge of efficiently converting the inherent irregular, bidirectional, and low-frequency motion characteristic of WECs into a stable and grid-compatible electrical output. The fundamental difficulty in this process lies in accommodating the highly variable nature of wave energy, marked by continuous fluctuations in both amplitude and frequency. Consequently, the PTO system must process the capability to manage these dynamic variations and ensure a consistent power supply that meets the stringent demands of electrical grids, where the usage percentage of each PTO system is demonstrated in Fig. 5.2.

Hydraulic PTO systems are a prevalent choice, utilizing an incompressible fluid, typically oil, to transfer the mechanical power generated by the WEC's motion to a hydraulic motor. This motor, in turn, drives an electrical generator. Hydraulic systems are particularly well-suited for the low-frequency, high-power density characteristics of ocean waves. These systems often incorporate hydraulic gas accumulators to store absorbed peak loads and smooth the energy conversion process from the hydraulic motor. The ability of hydraulic PTOs to operate efficiently at low speeds and generate high torque makes them advantageous for floating WECs [2].

Direct-drive mechanical PTO systems offer an alternative approach by directly converting the oscillating mechanical energy from the WEC into electricity using a rotary electrical generator. This conversion is facilitated by a mechanical interface, which can include components such as gearboxes and pulley systems. By minimizing intermediate energy conversion stages, direct-mechanical drives hold the potential

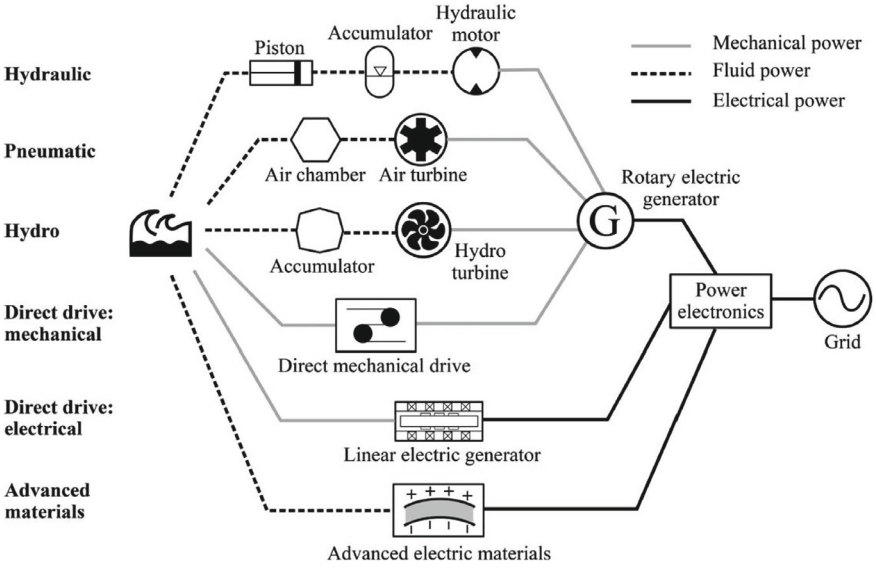

Fig. 5.1 Various types of PTO systems [1]

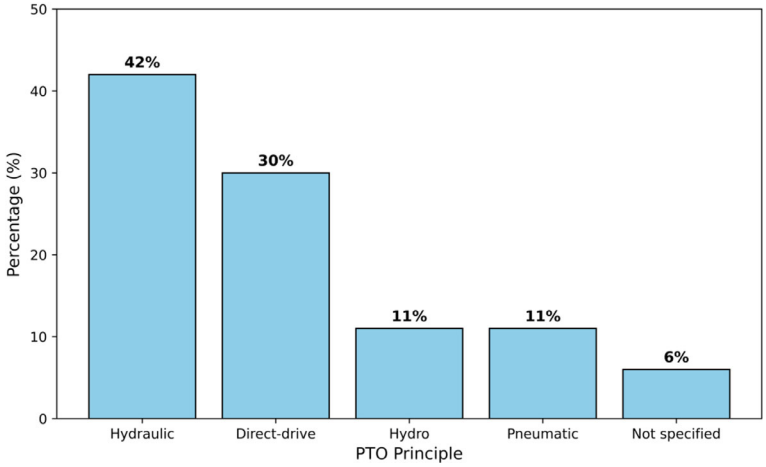

Fig. 5.2 Breakdown of WECs depending on the utilized PTO principles

for high efficiency and enhanced reliability. The simplicity of this approach, with a more direct transfer of energy, can lead to reduced losses within the system [2].

Another category is direct-drive electrical PTO systems, where the mechanical energy captured by the primary converter is directly coupled to the moving part of a linear electrical generator. Recent advancements in permanent magnet technology and the field of power electronics have significantly increased the attractiveness of this solution. Since the wave motion is directly converted to electricity, a rectification stage is typically necessary before the power can be transformed into a sinusoidal waveform with fixed voltage and frequency suitable for grid connection. The elimination of mechanical interfaces like gearboxes in direct-electrical drives can potentially lead to increased reliability and reduced maintenance requirements. Pneumatic PTO systems, utilizing air turbines, are commonly employed in Oscillating Water Column (OWC) type WECs. In these systems, the motion of the waves within a chamber compresses and decompresses air, creating a bidirectional airflow that drives the turbine. A key innovation in this area is the development of self-rectifying turbines, such as the Wells turbine, which can rotate in a single direction regardless of the airflow direction, overcoming a significant limitation of conventional turbines in this application [3].

Finally, hydro turbine PTO systems find application in overtopping wave energy converters or in systems that utilize hydraulic pumps with seawater as the working fluid. In overtopping devices, water that flows over a ramp is collected in a basin, and its potential energy is then converted into electricity using low-head hydro turbines coupled with generators. Hydro turbines represent a mature technology with high efficiency values and relatively low maintenance requirements, making them a reliable option for WEC designs that can provide a consistent flow of water [4].

Each of these PTO system types comprises a unique set of key components that are essential for its specific energy conversion mechanism. In a hydraulic PTO, the

primary components include the oscillating body of the WEC, a hydraulic cylinder or ram that is activated by this motion, check valves that act as a rectifier to ensure unidirectional flow of the hydraulic fluid, a high-pressure accumulator for energy storage and smoothing of pressure fluctuations, a hydraulic motor that converts the hydraulic energy into mechanical energy, an electrical generator coupled to the motor, a flow control valve to regulate the flow of hydraulic fluid, and often a low-pressure accumulator to prevent cavitation [5]. A direct-drive mechanical PTO typically consists of a mechanical linkage, such as a gearbox or pulleys, connected to a rotary electrical generator. In a direct-drive electrical PTO, the main components are a translator, which houses permanent magnets, and a stator, containing the electrical coils, along with necessary power electronics for rectification. A pneumatic PTO in an OWC system includes the air chamber where the waves interact, a self-rectifying turbine (like a Wells or impulse turbine), and an electrical generator. For a hydro turbine PTO, the key elements are the water basin in overtopping devices and the hydro turbine itself, which is coupled to a generator [6].

5.1.1 Dynamics of PTO Systems

The dynamics of WECs are generally characterized by a set of nonlinear equations from the hydrodynamic loads, mooring, structural behavior, and PTO systems with their respective control strategy. Nonlinearities are relevant in WEC dynamics because their natural frequency is usually set within the sea spectrum range, which increases the energy transferred from waves to WECs, and leads to large displacements. Based on that, the use of time-domain models is a common practice in the wave energy field due to its capability to deal with nonlinearities. In such models, the system dynamics are deterministically solved in time via numerical integration using a specific time series of wave elevation/forces. Strictly speaking, several of the aforementioned methods can be classified as time-domain models, such as linear/nonlinear potential flow models and computational flow dynamics (CFD) models. Hereafter, this section will focus mainly on time-domain models based on the Cummins equation [7, 8], which relies on existing experiences from the offshore and ship industry. This type of model has been proved to be effective after extensive application to WECs. In addition, the foundation of the Cummins equation can be related straightforwardly to the frequency-domain model, presented in the following subsection, which is based on linear wave potential theory.

Let us consider general WECs dynamics, in which the main sources of loads are:

$$M\ddot{x}(t) = F_e + F_r + F_s + F_v + F_{add} \tag{5.1}$$

where the first four right-hand terms refer to the loads caused by wave-structure interactions; F_e, F_r, F_s and F_v refer to the wave excitation, wave radiation, hydrostatic, and viscous drag forces and moment terms respectively; the last term, F_{add}, denotes

additional forces, such the ones from the power take-off, mooring system, control strategy, and motion constraint forces.

For the majority of WECs, first-order wave excitation analysis provides sufficiently accurate predictions of body displacements, as the natural frequency of the power absorption mode typically falls within the dominant range of the sea state spectrum. However, as the design progresses, incorporating higher-order excitations becomes necessary for more detailed analysis. In the case of an irregular sea state, the wave excitation is commonly modeled as a linear combination of N sinusoidal load components, expressed as [1]:

$$F_e(t) = \Re\left[\sum_{i=1}^{N} \eta_i \omega_i H_{Fe,i}(\omega_i) e^{(-i\omega_i t + \beta_{\eta,i})}\right] \tag{5.2}$$

where the subscript i denotes the i-th frequency component, η denotes the amplitude of wave elevation, which can be obtained from the sea spectrum as $\eta_i(\omega_i) = \sqrt{2S_\eta(\omega_i)\Delta\omega}$; $H_{Fe,i}(\omega_i)$ denotes the transfer function that relates the wave excitation loads and the wave elevation at frequency ω_i; $\beta_{\eta,i}$ is the wave surface phase angle, which is assumed to be uniformly distributed within $[0, 2\pi]$ radians. Note that for a regular sea state, the wave is composed of a single frequency.

The wave radiation loads may be represented by Cummins equation [1]:

$$F_r(t) = -A_\infty \ddot{x}(t) - \int_{-\infty}^{t} K_{rad}(t-\tau)\dot{x}(t)d\tau \tag{5.3}$$

The term $A_\infty = lim_{\omega\to\infty} A_m(\omega)$ represents the added mass matrix at infinite frequency, while K_{rad} refers to the radiation impulse response function matrix—also known as the memory function matrix. This term accounts for the influence of the free surface, where the motion of the body generates radiated waves. The resulting radiation forces are dependent on the history of the body's motion, which is reflected in the integration limits of the convolution term. In practice, the effect of this convolution integral tends to diminish after a relatively short period—typically between 20 to 80 s for many devices. Therefore, in offshore engineering applications, it is common to compute the convolution integral over a finite time window when using direct numerical integration. To reduce computational effort, several approximation methods have been developed to avoid evaluating the full convolution integral in Eq. 5.3. These include system identification techniques applied in the frequency domain, time domain, and using approaches such as Prony's method.

Hydrostatic forces (F_s) rise from the static pressure of still water acting on the submerged surface of a WEC. These forces play a crucial role in determining the device's dynamic behavior and stability. Since hydrostatic force varies with displacement, it is typically modeled using a hydrostatic stiffness matrix along with a constant restoring force component. Viscous drag loads, on the other hand, are

commonly represented using a modified version of Morison's equation, which characterizes the drag as a quadratic function of relative velocity. Originally developed to estimate wave-induced forces on vertical piles, Morison's equation has undergone various adaptations to better suit offshore and wave energy applications. In the context of WECs, viscous drag is typically computed using the relative velocity between the device and the wave particle motion for translational degrees of freedom ($\dot{x}_{rel,i} = \dot{x}_i - u_i$), and the absolute structure velocity for rotational modes. For translational motion, the viscous drag force component is often expressed as:

$$F_{v,j}(t) = -1/2\rho C_{D,i} S_{\perp,j} \dot{x}_{rel,j}(t) \left| \dot{x}_{rel,j}(t) \right|, for\, j = [1, 2, 3] \tag{5.4}$$

where $C_{D,j}$ denotes the viscous drag coefficient in the *j-th* mode, and $S_{\perp,j}$ is the cross-sectional area of the structure perpendicular to the *j-th* direction. The drag coefficient is usually obtained via experimental results or CFD simulations; its magnitude is dependent on the geometry, Reynolds number, roughness number, and Keulegan-Carpenter number [9].

Additional forces act on the WEC dynamics, which are dependent on the characteristics of the devices. For example, some WECs might be connected to mooring systems composed of tethers connected to their PTO system, while others use catenary lines to restrain their motion [10]. The PTO system can be composed of hydraulic, pneumatic, mechanical, and electrical systems. Hence, different numerical models can be employed to describe additional loads, based on the characteristics of each device and assumptions.

The primary goal of a WEC and its PTO system is to harness and convert the energy carried by ocean waves into usable mechanical or electrical power. In this context, the mean mechanical power absorbed by the PTO system over a time period T can be expressed as:

$$\overline{P}_{pto} = -\frac{1}{T} \int_0^T F_{pto}(t) \dot{x}(t) dt \tag{5.5}$$

where F_{pto} is the PTO force, which was included as an additional force in Eq. 5.1. Assuming a mechanical PTO system, composed of a linear damper, the mean power absorbed is given by:

$$\overline{P}_{pto} = -\frac{1}{T} \int_0^T B_{pto} \dot{x}^2 dt \tag{5.6}$$

where B_{pto} is the magnitude of the linear damping coefficient from the PTO system.

Time-domain simulations are typically more computationally intensive than frequency-domain analyses. As a result, time-domain simulations are generally employed after extensive frequency-domain studies have been conducted, once the

key characteristics of the WEC have been established. These simulations help validate the device's performance and control strategy under real operating conditions. In the early stages of analysis, WEC dynamics are typically studied in the frequency domain, as it allows for an efficient evaluation of the system's response to wave excitation. In frequency-domain analysis, the wave-structure interaction is often modeled using linear potential theory, which assumes the waves are small and the system's response is linear. Other forces, such as those generated by the PTO system, mooring systems, and control mechanisms, are approximated around an operating point by linearizing them through a Taylor series expansion, retaining only the first-order terms. This linearization simplifies the system's behavior, making it possible to apply superposition and linear combination principles to analyze the system. These methods provide a manageable way to analyze WECs under a variety of wave conditions and control strategies, with the assumption that the interactions remain linear during normal operation.

Considering harmonic excitation loads, the vector of response has also an harmonic motion that oscillates at same frequency and can be represented as:

$$x(t) = \Re\left\{X(\omega)e^{-i\omega t}\right\} \tag{5.7}$$

where X is the vector of complex amplitude of the body displacement. Based on Eq. (5.7), the velocity and acceleration can be obtained as:

$$\dot{x}(t) = \Re\left\{-i\omega X(\omega)e^{-i\omega t}\right\} \tag{5.8}$$

$$\ddot{x}(t) = \Re\left\{-\omega^2 X(\omega)e^{-i\omega t}\right\} \tag{5.9}$$

Based on the above equations, the WEC linear dynamics can be expressed in the frequency domain as:

$$-\omega^2(M + A_m(\omega)) - i\omega(B + B_{rad}(\omega)) + K]X = F_e(\omega) \tag{5.10}$$

In this formulation, the matrices M, B, and K represent the system's inertia, damping, and stiffness, respectively. The hydrodynamic coefficients—including the added mass $A_m(\omega)$, radiation damping, $B_{rad}(\omega)$, and excitation force, $F_e(\omega)$—are typically obtained using BEM solvers or analytical methods. Additional forces arising from the PTO system, mooring lines, and control mechanisms are generally modeled as functions of displacement and velocity and are thus incorporated into the overall damping and stiffness matrices B and K through linear approximations. However, it's important to note that some PTO configurations—such as those employing translators or flywheels—introduce significant inertial contributions, which are then included in the inertia matrix M. It is also worth mentioning that certain nonlinear effects, such as viscous drag under conditions of zero current velocity, may be eliminated during the linearization process. As a result, while

linear models offer analytical simplicity and computational efficiency, they may omit important nonlinear behaviors present in real-world WEC operation.

Based on Eq. (5.10), the transfer function of the linear system dynamics can be established to relate the WEC response and excitation forces:

$$H_x(\omega) = \left[-\omega^2(M + A_m(\omega)) - i\omega(B + B_{rad}(\omega)) + K\right]^{-1} \tag{5.11}$$

In the offshore engineering field, the response is also usually expressed based on the response amplitude operator (RAO), which establishes a transfer function between the body response amplitude and the wave amplitude. Once the transfer function is derived, the dynamics can be obtained straightforwardly by solving the system of algebraic linear equations [11]. For irregular sea states, the stochastic response can be expressed in terms of the power spectrum density (PSD) through the response spectrum matrix as:

$$S_x(\omega) = H_x S_f H_x^{T^*} \tag{5.12}$$

where superscript T^* denotes the transpose conjugate of the matrix, and S_f is the force spectrum matrix given by:

$$S_f(\omega) = H_{F_e} S_\eta H_{F_e}^{T^*} \tag{5.13}$$

where S_η denotes the wave spectrum.

In Eq. (5.10), the damping matrix (B) contains contributions from several sources of loads that can exist in the WEC's dynamics, such as those from the PTO system (B_{pto}) [12]. In this regard, the mean power absorbed by a linear PTO system in an irregular sea state can be calculated in the frequency domain as:

$$\overline{P}_{pto} = B_{pto} \int \omega^2 S_x d\omega \tag{5.14}$$

The PTO system itself exerts a reaction force back onto the WEC, and this interaction can be conveniently modeled using the concept of control impedance, denoted as $Z_{pto}(\omega) = j\omega M_{pto} + D_{pto} + \frac{K_{pto}}{j\omega}$. Here, M_{pto}, D_{pto}, and K_{pto} represent the PTO's inertia, damping, and stiffness, respectively, and ω is the angular frequency of the wave. The force exerted by the PTO can then be expressed as $F_{pto} = -Z_{pto}(\omega)\dot{x}$. This impedance modifies the dynamic response of the WEC and plays a crucial role in determining the wave reflection, transmission, and ultimately, the power absorption characteristics of the device. Representing the PTO as an impedance allows for analyzing its effect on the WEC's response and optimizing its parameters to achieve maximum power absorption through a process akin to impedance matching [13].

Specific PTO mechanisms also have their own mathematical models. For hydraulic PTOs, these models often involve continuity equations that describe the

pressure dynamics of the compressible hydraulic fluid within the cylinders, considering the effective bulk modulus of the fluid, the volume of the piston chamber, and the area of the piston. For instance, the rate of change of pressure in a hydraulic cylinder chamber ($\dot{p}_A$) can be described by an equation like $\dot{p}_A = V_0 - A_p z \beta_e \left(A_p \dot{z} - \dot{V}_1 + \dot{V}_4\right)$, where β_e is the effective bulk modulus, V_0 is the initial volume, A_p is the piston area, z and $\dot{z}$ are the piston displacement and velocity, and V_1 and $\dot{V}_4$ are volumetric flow rates through valves. Flow through the control valves is often modeled using the orifice equation, which relates the flow rate to the pressure difference across the valve and the area of the orifice. The efficiency of hydraulic PTOs can be further modeled by considering factors such as the viscosity of the hydraulic fluid and the efficiency of the hydraulic motor [14].

For direct-drive electrical PTOs that utilize linear generators, the mathematical models are based on Faraday's law of induction, which describes the relationship between the induced voltage in a conductor and the rate of change of magnetic flux through it. A simplified representation of the induced voltage (E) in a linear generator is given by $E = Blv$, where B is the magnetic flux density, l is the length of the conductor moving through the magnetic field, and v is the relative velocity between the conductor and the magnetic field [15]. More complex models account for factors such as the magnetic circuit design, the number of turns in the coils, and the electrical parameters of the generator, including resistance and inductance. Similarly, mathematical models for direct-drive mechanical PTOs involve the dynamic characteristics of the mechanical interface, such as the gear ratio and inertia, coupled with the model of the electrical generator. For pneumatic PTOs using Wells turbines, models relate the airflow rate and direction to the pressure differential across the turbine blades and the resulting rotational speed and torque of the turbine. These mathematical models are indispensable tools for the simulation, analysis, and optimization of the performance of these various PTO mechanisms [16].

5.2 Performance Evaluation of PTO Control Strategies

5.2.1 Control Strategies

PTO control mechanisms govern the conversion of wave-induced motion into usable electrical energy, directly influencing energy capture efficiency, device durability, and power quality. Various strategies have been proposed, each with distinct advantages and trade-offs. Recent research has focused on optimizing these strategies using advanced control algorithms, machine learning approaches, and adaptive real-time tuning techniques. This section evaluates passive, reactive, and hybrid PTO control methods, comparing their performance across different WEC types and wave conditions [17].

The PTO system forms the centerpiece of a WEC and serves multiple roles:

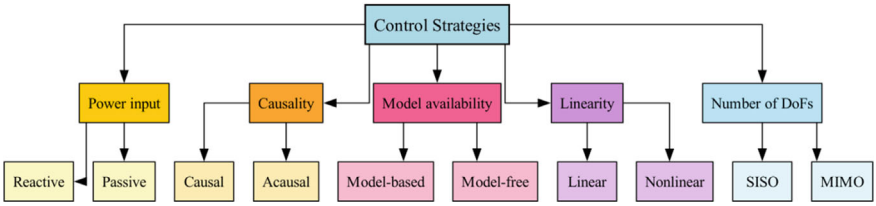

Fig. 5.3 Classification of WEC control strategies

- it converts the mechanical energy generated by the WEC's moving parts into electrical power
- it enhances the device's hydrodynamic efficiency to maximize power absorption under different sea conditions
- it ensures that the WEC operates safely in the demanding offshore environment.

In practical implementations, the wave energy device's motion must be controlled to maximize power capture within the limits of its equipment—such as peak amplitude, velocity, and load force. This control is executed by the PTO system , which applies a load force on the oscillating body to tune its dynamic behavior. Factors influencing the development of control strategies for wave energy systems include (i) PTO capabilities, (ii) the availability and complexity of the system model, (iii) the availability of information about the incident wave field, and (iv) the number of controlled variables. These considerations enable grouping control algorithms in the manner depicted in Fig. 5.3 [18].

One of the primary classifications of PTO systems is based on whether they permit unidirectional or bidirectional power flow. In reactive control, the PTO force is expressed as $\left(F_{pto}(t) = B_{pto}\dot{x}(t) + K_{pto}x(t)\right)$, allowing the system not only to extract energy from wave-induced motion but also to inject energy back into the WEC during parts of the oscillation cycle. This bidirectional power exchange is typically facilitated by integrating energy storage components, such as hydraulic accumulators or mechanical springs. One of the earliest applications of this method was in the Edinburgh Duck (also known as Salter's Duck), where the load force was proportional to both velocity and displacement—an approach commonly referred to as complex-conjugate control. In contrast, passive control operates under the principle $\left(F_{pto}(t) = B_{pto}\dot{x}(t)\right)$, where energy is only extracted from the system without being returned. This approach is generally compatible with simpler machinery, such as conventional electrical generators [18]. Within passive control strategies, two variations exist: phase control, achieved through techniques like latching or declutching, and resistive control, which employs a tunable damper to adapt to wave conditions. In terms of performance, reactive control has been shown to be more effective than passive methods, as it fully utilizes the potential of the oscillating body. Both reactive and latching strategies are capable of achieving phase optimality, or resonance with the wave excitation force—a key condition for maximizing energy absorption. In

contrast, passive control lacks this capability, which typically results in lower overall efficiency [18, 19].

Passive control, which involves applying a constant damping force, is the simplest approach but often results in suboptimal energy capture. Reactive control, on the other hand, actively adjusts PTO forces in response to wave dynamics, significantly increasing energy output. Liao et al. [20] demonstrated that reactive control can improve energy capture efficiency by up to 50% compared to passive damping but requires high-fidelity wave prediction models and increased computational power.

Latching control has also been widely studied, particularly for OWC-WECs. This method involves temporarily locking the WEC at optimal positions to enhance power conversion efficiency. A hybrid torque coefficient control strategy is proposed that reduces peak loads while stabilizing energy output [21]. However, latching control requires precise wave phase prediction, which is difficult in highly variable sea states. The recent trend towards deep reinforcement learning (DRL)-based PTO control, aims to address these challenges by training AI models to learn optimal PTO responses in real-time, eliminating the need for explicit wave forecasting [22].

The simplest PTO control method is passive damping, where a fixed damping coefficient is applied to the system. This approach offers robust and maintenance-free operation but is generally suboptimal in energy extraction because it does not adapt to varying wave conditions. Passive PTO control systems tend to operate efficiently only within a narrow frequency range and struggle with highly irregular sea states. It is also proved that passive PTOs typically achieve 40–60% energy conversion efficiency, with significant losses occurring in off-resonance conditions [23]. In contrast, reactive control dynamically adjusts PTO damping forces based on wave conditions, significantly increasing energy capture efficiency. This method requires real-time wave prediction models and sophisticated feedback control algorithms. Model Predictive Control (MPC) has been extensively studied for reactive PTO control, allowing WECs to anticipate and optimize energy absorption for incoming waves. It has been found that reactive PTO control increased energy capture efficiency by up to 80% compared to passive damping, particularly in moderate and high-energy sea states [24].

Another form of reactive control is latching control, where the WEC's motion is temporarily halted at optimal positions to maximize energy extraction. This approach has been shown to improve power output in point absorber WECs, particularly in low-energy wave climates. However, latching control requires precise timing mechanisms and predictive algorithms, making it computationally expensive and difficult to implement in real-time applications. A growing trend in WEC control is the integration of hybrid PTO strategies, which combine elements of passive, reactive, and predictive control to balance energy capture efficiency and operational reliability. Another innovative approach involves power-limiting control, which reduces PTO forces in extreme wave conditions to prevent mechanical overloading and structural fatigue. This method has been particularly useful for large-scale WEC deployments in storm-prone regions. It is found that PTO power-limiting strategies reduced peak loads by 30%, extending WEC lifespan while maintaining high energy production during moderate sea states [24].

Furthermore, the integration of machine learning and artificial intelligence (AI) into PTO control has opened new avenues for real-time performance optimization. Reinforcement learning (RL)-based controllers can adapt to changing wave climates without requiring explicit hydrodynamic models, significantly reducing computational complexity. A study explored the application of self-learning AI algorithms in PTO tuning, showing that intelligent control systems improved energy capture efficiency by 20% compared to manually tuned systems [25].

Determining the optimal phase and amplitude for a WEC is relatively straightforward in environments with regular, sinusoidal waves. However, real ocean conditions are inherently irregular and stochastic. To maximize energy absorption using an optimally controlled PTO force, it becomes necessary to predict incoming wave excitation forces ahead of time. This makes the control problem fundamentally acausal, as it relies on future wave information. Achieving such predictive control often involves the use of up-wave sensors and wave forecasting models, such as auto-regressive algorithms or augmented Kalman filters. However, the accuracy of these forecasts declines as the prediction horizon increases, affecting the reliability of acausal control strategies [26].

In contrast, causal controllers do not depend on future wave data but operate using only current and past measurements. One method to achieve causality involves integrating knowledge of the sea state's energy spectrum into the system model, forming the basis for linear-quadratic-Gaussian (LQG) control [27]. Another approach replaces the non-causal transfer function between optimal velocity and wave excitation force with a frequency-dependent gain. Additionally, controllers that adjust parameters such as spring-damper coefficients in response to the peak frequency of the incoming wave spectrum also fall under the causal category [28].

When comparing acausal and causal control strategies, acausal methods, such as MPC, typically offer superior power extraction—provided that wave force predictions are highly accurate. However, this performance gain comes with added complexity [18]. Acausal control demands high peak-to-average power ratios, large energy storage capacities, and strong control forces. As with other aspects of wave energy system design, the implementation of advanced control techniques must be carefully weighed against their economic and technical feasibility.

Most low-cost WEC control models rely on linear potential theory, which simplifies the system's hydrodynamics for easier analysis. Optimization-based control methods, such as MPC, DP, and LQC, aim to maximize power output while respecting physical and operational constraints [12]. The success of these techniques depends heavily on the fidelity of the WEC model used in the optimization process. Other strategies, like complex-conjugate control and latching, do not directly compute control forces from the model, but still use it to determine optimal parameters.

On the other hand, non-model-based control strategies seek to optimize power capture without relying on a physical model of the WEC. A notable example is Maximum Power Point Tracking (MPPT), widely used in wind energy systems. However, due to the irregular nature of ocean waves, MPPT has not proven as effective for WEC applications when compared to model-based controls [29]. Most existing control approaches are based on linear system assumptions and therefore cannot

fully account for nonlinear effects, such as viscous drag and other complex hydrodynamic phenomena. To address this, control methods like the Phi-method derive the optimal PTO force from a nonlinear analytical model, although their accuracy depends heavily on the quality of the model. DP and Shape-Based (SB) Control are capable of handling nonlinearities but often involve high computational costs, making them less suitable for real-time control [30].

To date, the majority of WEC control systems have been developed for devices operating in a single degree of freedom (DoF)—typically heave or surge. These systems are treated as single–input-single-output (SISO), simplifying control design by avoiding the complexity of coupled state variables. However, as WEC technologies evolve to harness multiple motion modes, there is growing interest in designing control systems for multiple-input-multiple-output (MIMO) configurations [31].

Lastly, assessing WEC performance requires looking beyond just the mechanical power captured. Losses occur throughout the power conversion chain, including within the PTO machinery, transmission components (e.g., hydraulic or mechanical drivetrains), electrical generators (rotary or linear), and power converters. Therefore, evaluating the total system efficiency, or the efficiency of each individual subsystem, is essential for understanding the overall commercial viability of a WEC system.

5.2.2 *Performance Metrics*

The power conversion efficiency (mechanical-to-electrical) gauges how effectively the PTO machinery transforms its mechanical power input into an electrical power output [32]:

$$\eta_{eff,M\to E} = \frac{E_{power}}{M_{power}} \tag{5.15}$$

Because this efficiency depends on PTO input parameters (e.g., force and velocity, torque and angular speed, pressure difference and flow rate), it is often expressed in the form of a matrix. For holistic WEC performance—particularly how much available wave energy is captured, delivered to the generator, and converted into electricity—an alternative measure is the wave-to-electrical efficiency:

$$\eta_{eff,M\to E} = \frac{E_{power}}{H_{power}} \tag{5.16}$$

In the case of a regular wave acting on a heaving, axisymmetric WEC, the available hydrodynamic power can be computed accordingly.

Maximum or peak values of power, force, speed, and displacement establish design requirements for PTO components (drivetrain, hydraulic system, generator, etc.). However, identifying these peak loads can be highly dependent on both the

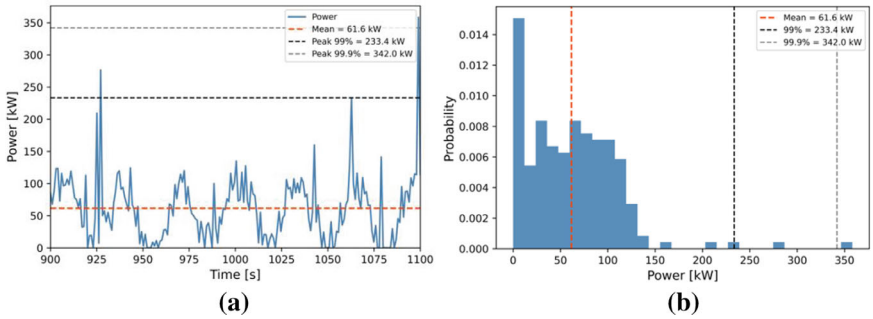

Fig. 5.4 Statistical estimation of peak power based on power time-series data: **a** instantaneous power in the time domain and **b** associated histogram of the power distribution

length of numerical or physical tests and the phasing of incoming waves. Consequently, it is practical to report "statistical peak" values at particular confidence levels (e.g., 95%, 99%, or 99.9%) [33] (Fig. 5.4).

Peak-to-average ratios of power, control force, or speed are also essential for the electrical elements of a WEC. For instance, an electric generator operates most efficiently at its nominal speed, torque, and current, but can tolerate brief overloads. Thus, the peak-to-average ratio informs whether the electrical system should be sized according to the average power or the peak power demands, which can vary significantly depending on the hydrodynamic control strategy [34]. If a signal has a zero mean, its peak-to-average ratio may be computed using the root-mean-square value instead of the mean. Slew rate (of force or speed) captures how quickly that quantity changes over time, expressed typically in $[N/s]$ for force or $\left[m/s^2\right]$ for speed. It reflects the required response rate of the PTO's mechanical or electrical subsystems [35].

Damage equivalent loading (DEL) is widely used in offshore engineering to determine a structure's ability to endure its entire loading spectrum and has recently been applied to wave energy device design optimization. In particular, this includes analyzing the DEL of PTO assemblies with welded joints [36]. The calculation involves:

- Generating time-series of the PTO force,
- Converting force to stress,
- Counting stress cycles,
- Relating these cycles to S-N curves for the specific material/joint, and
- Estimating the accumulated damage.

Additionally, flicker describes rapid voltage fluctuations in the power grid caused by WECs once they are connected, thereby influencing power quality. The short-term flicker severity captures flicker over a 10-min interval, while the long-term flicker severity is derived by taking the cubic average of short-term flicker over two hours [37].

Another important performance metric is energy capture efficiency, which indicates the proportion of incident wave energy that a WEC successfully converts into usable power. It is defined as the ratio of the average power extracted by the WEC to the average power available in the incoming wave resource. This relationship can be expressed as [38, 39]:

$$\eta = \frac{P_{extracted}}{P_{wave}} \tag{5.17}$$

where η is the efficiency, $P_{extracted}$ is the average power harnessed by the WEC, and P_{wave} represents the average available power in the incident wave.

A closely related performance indicator is the capture width ratio (CWR), which relates the absorbed power to the power available in a wave front of a certain width. Most PTO control strategies aim to maximize energy capture efficiency as a primary design goal [39].

Another key consideration is power smoothing, which plays a vital role in maintaining the quality of electricity delivered to the grid. Because ocean waves are naturally irregular, WEC output tends to fluctuate over time. PTO control strategies that mitigate these fluctuations help deliver a more stable and reliable power supply. Power smoothing can be assessed using the peak-to-average power ratio or through specific metrics like the power fluctuation ratio (PFR), defined as [40]:

$$PFR = \frac{P_{\max} - P_{\min}}{P_{avg}} \tag{5.18}$$

where $P_{\max}$ and $P_{\min}$ are the maximum and minimum power outputs over a given time period, and P_{avg} is the average power output. Minimizing power fluctuations not only enhances grid compliance but also reduces mechanical and electrical stress on the PTO system and associated components.

Finally, system reliability is a crucial performance metric that reflects the ability of the PTO system and the implemented control strategy to operate consistently and without failure over the intended operational lifetime of the WEC. Factors that contribute to reliability include the robustness of the system to extreme wave conditions, the maintenance requirements of the PTO mechanism, and the complexity of the control system itself. Evaluating reliability often involves conducting failure analysis, assessing the fatigue life of critical components under the dynamic loads imposed by the waves and the control strategy, and considering the impact of the control strategy on the structural integrity of the WEC. A control strategy that enhances energy capture but significantly compromises the reliability of the system may not be practically viable in the long term.

A comparative study assessed different PTO strategies using these metrics across multiple WEC types, presented in Table 5.1 [41].

The study found that passive PTO control scored highest in stability but lowest in energy efficiency, while reactive and hybrid control methods exhibited superior energy capture at the cost of increased computational complexity. This analysis

Table 5.1 Comparative analysis of various performance metrics in PTO control

PTO strategy	Energy efficiency	Mechanical durability	Computational complexity	Operational adaptability
Passive PTO	Low (40–60%)	High (low wear and tear)	Low	Poor
Reactive PTO	High (70–80%)	Moderate	High	Good
Latching control	Moderate (60–75%)	Moderate	High	Excellent
Hybrid PTO	Very high (85–90%)	Moderate	Very high	Excellent

underscores the trade-offs between efficiency, durability, and control complexity, highlighting the need for customized PTO solutions tailored to specific WEC applications, where optimization techniques can be used for this task.

5.3 PTO Optimization of WECs

The optimization of PTO systems in WECs is critical to improving their efficiency, reliability, and economic feasibility. PTO systems must be tuned to operate efficiently under varying wave conditions while minimizing mechanical stress and maintenance costs. It also involves tuning damping coefficients, force control algorithms, and power conversion mechanisms to maximize energy yield. This process typically includes:

- Hydrodynamic analysis: Understanding the interaction between the WEC and the wave environment to model the system's dynamic behavior.
- Control strategy development: Designing control algorithms that can adapt to changing wave conditions and optimize energy extraction.
- Parameter tuning: Adjusting system parameters, such as damping and stiffness, to achieve optimal performance.
- Simulation and validation: Using numerical simulations to predict system behavior and validate control strategies before deployment.

The objective functions employed in PTO optimization for WECs are varied and reflect the different goals that researchers and developers aim to achieve. Maximizing the power output of the WEC is a primary objective, with the goal of extracting the greatest possible amount of energy from the incident ocean waves. Objective functions designed to achieve this can be formulated to maximize either the average power produced over a period of time or the peak power output under specific, representative wave conditions. Minimizing the energy cost, often expressed as the Levelized Cost of Energy (LCOE), is another critical objective. Optimization efforts focused on reducing LCOE take into account a range of economic factors, including

the initial capital costs of the WEC and PTO system, the ongoing operational and maintenance expenses, and the total amount of energy generated by the system over its expected operational lifetime. Improving the overall reliability and survivability of the WEC system, particularly in harsh marine environments, is also a significant goal [42]. Objective functions aimed at this may focus on minimizing the mechanical stress and fatigue experienced by the PTO system and the main structure of the WEC, thereby ensuring reliable long-term operation and the ability to withstand extreme sea states. For effective integration of wave energy into electrical grids, smoothing the power output from the WEC is often an important objective. Optimization techniques can be used to minimize fluctuations and intermittency in the generated power, leading to a more stable and predictable energy supply [43]. Finally, maximizing the energy conversion efficiency of the PTO system itself is a common objective, focusing on minimizing the energy losses that occur during the process of converting the mechanical energy of the waves into usable electricity [44].

The optimization of PTO systems often involves a multi-objective approach, recognizing that a balance must be achieved between these sometimes competing goals. For example, striving for the absolute maximum power output might necessitate a more complex and expensive PTO system, potentially increasing the overall LCOE. Similarly, focusing solely on minimizing the initial costs might lead to a compromise in the energy capture efficiency or the long-term reliability of the WEC. Multi-objective optimization techniques are valuable in such scenarios as they can help identify a set of Pareto-optimal solutions, representing the best possible trade-offs between the various objectives, allowing designers and developers to make informed decisions based on their specific priorities [45].

Among the various optimization techniques, genetic algorithm (GA) and particle swarm optimization (PSO) have been widely applied. It has been shown that PSO-optimized PTO settings could achieve up to 30% higher energy extraction compared to conventionally tuned systems [46]. These evolutionary algorithms are particularly effective for WEC arrays, where inter-device hydrodynamic interactions complicate the optimization process.

Another major development in PTO optimization is adaptive damping control, where PTO resistance is dynamically adjusted based on wave conditions. For instance, a Sea-State-Dependent Control Strategy (SSCS) is introduced, which limits power surges in extreme waves while maximizing energy absorption in moderate conditions [20]. This dual-mode approach has proven effective in balancing WEC survivability with energy production.

A comprehensive classification of PTO systems, including hydraulic, pneumatic, hydro turbine, direct mechanical, direct linear electrical, and hybrid designs, with an emphasis on MPC and AI-driven techniques that enhance power output, resilience, and operational efficiency. Accordingly, a two-body WEC with a mechanical motion rectifier (MMR) PTO, employing a ball screw mechanism to convert bidirectional wave motion into unidirectional generator rotation is introduced, achieving mechanical efficiencies exceeding 67% through rigorous dynamic modeling and validation via wave tank experiments. In addition, an analysis of multi-degree-of-freedom (multi-DOF) WECs, underscoring the significance of optimized damping coefficients

and stiffness matrices in enhancing power absorption, especially when integrated with AI-enhanced MPC frameworks is examined in another study [12].

The impact of MPC structures on a hydraulic PTO-based WEC is investigated and highlighting that integrating PTO dynamics within the MPC model improves power output by 23% compared to hydrodynamics-only models [19]. Moreover, a co-design optimization approach for oscillating-surge WECs (OSWECs), incorporating PTO and control systems into the geometric design phase is also proposed [47]. An active mechanical motion rectifier (AMMR)-based PTO that utilizes electromagnetic clutches for active engagement, offering enhanced controllability, reduced power losses, and better adaptation to varying wave conditions [48]. The economic impact of PTO constraints on LCOE through a control co-design methodology, highlighted that optimal PTO force and stroke constraints significantly influence both capital expenditure and energy output [49].

Hydraulic PTOs, while offering high load capacities, are hindered by mechanical complexity and maintenance challenges. Direct mechanical and linear electrical PTOs offer simplified structures but face efficiency losses under low-speed wave conditions. Emerging technologies like triboelectric nanogenerators (TENGs) provide promising solutions for low-power applications, while hybrid PTOs combining multiple renewable sources present a robust approach for continuous energy harvesting. MPC stands out for its real-time adaptive control, allowing WECs to respond dynamically to varying marine conditions, with AI algorithms further enhancing this adaptability through real-time data processing and optimal control predictions.

As previously discussed, MPC inherently involves an optimization step at each control interval to determine the sequence of optimal control actions for the PTO based on predictions of the system's future behavior. The selection of the most appropriate optimization technique is contingent upon several factors, including the complexity of the PTO system being considered, the number of design and control parameters that need to be optimized, and the computational resources that are available for performing the optimization process. Certain optimization problems may be efficiently solved using gradient-based methods, while others, characterized by non-linear or multi-modal objective functions, may necessitate the use of more robust global optimization techniques such as GA or PSO. Bayesian optimization proves particularly advantageous in scenarios, where evaluating the performance of a given set of parameters requires significant computational time or resources, as is often the case with detailed hydrodynamic modeling.

Therefore, this section is primarily divided into two parts to address the key aspects of PTO optimization: (i) hydrodynamic and structural optimization, and (ii) refinement of control algorithms. Several studies comparing different optimization techniques in this context are discussed accordingly.

5.3.1 Hydrodynamic and Structural Optimization of PTO Systems

One of the key areas of PTO optimization involves hydrodynamic modeling and numerical simulation, which allow researchers to fine-tune WEC-PTO interactions for maximum energy absorption. The efficient capture of wave energy is fundamentally linked to the hydrodynamic performance of the WEC and the structural integrity of its components, including the PTO system. Hydrodynamic optimization aims to maximize the energy transfer from the waves to the WEC's moving parts, while structural optimization focuses on ensuring the WEC and PTO system can withstand the forces exerted by the ocean environment over their operational lifespan, often with a focus on cost reduction. Hydrodynamic optimization of WECs, including those integrated with PTO systems, has seen significant advancements through the application of sophisticated numerical modeling and simulation techniques. Researchers frequently employ computational software such as NEMOH, REEF 3D, MATLAB, WEC-Sim, and DualSPHysics to analyze and refine WEC designs and their interaction with various wave characteristics, thereby enhancing hydrodynamic efficiency [50–52].

CFD simulations and multi-physics coupling methods have been widely used to model wave-structure interactions and optimize PTO damping settings. For instance, high-fidelity hydrodynamic models can improve PTO efficiency by 25% by optimizing force transmission pathways between WEC structures and PTO units [50]. Furthermore, the scaling effects of PTO systems have been investigated to enhance energy extraction for both single WECs and wave farm arrays.

Optimized designs of conical-bottom floating buoys have been proposed and studied using CFD simulations with different PTO systems. The novel design incorporating a tuned inertial mass has also been explored to significantly increase energy absorption and broaden the operational bandwidth, with numerical investigations using WAMIT demonstrating increased power generation in irregular sea conditions [53]. Furthermore, the study of two-body floating point absorber WECs has led to the establishment of heave motion models, with software like ANSYS-AQWA being further developed to account for PTO effects in motion simulations [54]. Innovative bulbous-bottomed buoy designs have shown potential for higher absorption efficiencies compared to non-bulbous shapes through frequency-domain analyses and spectral modeling in ANSYS-AQWA [55]. The development of a point absorber WEC utilizing a Magnus effect driven turbine generator, simulated using MATLAB Simulink, represents another novel approach. Comparisons between two-buoy and single-buoy floating bodies have been conducted using modified nonlinear versions of WEC-Sim to understand the impact of system configuration on energy capture.

Geometric modifications to WECs have also proven effective in enhancing energy capture. A hydrodynamic optimization study of a sloped-motion point absorber WEC, for example, demonstrated substantial increases in energy production [56]. This design likely alters the WEC's natural oscillation period, allowing it to resonate more effectively with a wider range of wave frequencies. Similarly, the hydrodynamic

optimization of a floating flapping-panel WEC using CFD highlighted that different WEC types necessitate specific hydrodynamic optimization strategies tailored to their unique operating principles [57]. For OWCs, geometric factors such as the internal length or width, the inclination angle of the front wall, and the depth of immersion significantly influence hydrodynamic efficiency [58].

Continuous research efforts are dedicated to improving WEC design to increase energy capture efficiency, reflecting the dynamic nature of this field with ongoing advancements. The development of novel performance indices, such as the hydrodynamic capacity for wave energy conversion used in the optimization of a sloped-motion WEC, indicates a move towards more comprehensive metrics for evaluating WEC performance beyond traditional measures like capture width ratio.

Structural optimization of PTO systems is essential for addressing the high structural costs that currently hinder the widespread commercialization of wave energy converters. A primary driver of these costs is the need to design WEC components to withstand peak loads from extreme wave events, often leading to overdesign of the PTO capacity. This overdesign, while ensuring survivability, comes at a higher cost, especially when the increased capacity is only utilized for a small fraction of the operational lifetime. Balancing the need for robustness with cost-effectiveness is a key challenge in structural optimization. In general, structural optimization approach involves modular PTO designs, which allow different configurations to be deployed based on site-specific conditions. For instance, the bionic raft WEC utilizes a two-raft PTO system, improving wave energy capture efficiency by 30% by mimicking natural oscillation patterns found in marine organisms [59].

Optimization algorithms are increasingly being used to guide structural design choices. For example, GAs have been employed to optimize the maximum output power of the PTO system, providing a theoretical foundation for structural optimization design and material selection. Accurate modeling of PTO components, such as hydraulic systems, which are common in WECs, is crucial for both structural and performance optimization. Mathematical models that consider factors like fluid Reynolds numbers and leakage are being developed to better understand the structural behavior of these systems under wave loads. Therefore, structural optimization is recognized as an integral part of the overall WEC design process, encompassing the internal mechanical components of the PTO system that need to be both structurally sound and optimized for energy conversion. For built-in WECs, the inertial force acting on the PTO mechanism is a key structural consideration, highlighting that different WEC types have unique structural requirements for their PTOs. Ultimately, the structural integrity of the WEC and its PTO system is paramount to ensure the device can withstand the harsh marine environment and achieve its intended operational lifespan while maximizing energy absorption.

Efforts to integrate hydrodynamic performance with structural robustness are evident in the development of advanced WEC designs. The TALOS-WEC, for instance, features a fully enclosed PTO system that aims for both high energy conversion efficiency and enhanced durability by protecting the PTO from the corrosive marine environment. Numerical analysis and optimization of hinged-type WECs, focusing on PTO damping and geometrical parameters, demonstrate the benefits of

simultaneously considering hydrodynamic and structural aspects to achieve better overall performance. A holistic design approach that considers hydrodynamic performance, structural reliability, and economic data from the early predesign stage is crucial for successful WEC development, ensuring that all relevant factors are addressed to avoid major setbacks and result in a viable final design.

5.3.2 Control Algorithm Refinements for PTO Optimization

Optimizing PTO control involves adaptive algorithms that adjust damping, force application, and energy conversion rates in real time. Various control strategies have been developed and refined in recent years, each with its own advantages and limitations. These strategies often aim to either maximize the power absorbed by the WEC or the power delivered to the grid, while also considering practical constraints such as the PTO power and force limits.

One of the most effective control strategies is MPC, which predicts incoming wave conditions and adjusts PTO parameters accordingly. Instantaneous power variations in heaving-buoy WECs, revealing that MPC-based PTO optimization increased energy output by 22% compared to conventional passive control strategies [37]. MPC has emerged as a powerful advanced control strategy for WECs. MPC utilizes a model of the WEC and predictions of future wave conditions to optimize power extraction while adhering to system constraints. This approach is promising for maximizing energy capture by proactively adjusting the PTO's operation based on anticipated wave behavior and the WEC's dynamic response. Research indicates that MPC strategies that incorporate detailed models of both the WEC's hydrodynamics and the PTO system's dynamics can achieve significantly higher power output compared to approaches that only consider the hydrodynamics. Furthermore, Nonlinear MPC (NMPC) can outperform simpler control methods by taking into account real-world system characteristics such as the efficiency of the PTO system in the control law [60]. Hybrid MPC methods, such as those using a variable damper to regulate efficiency, are also being explored to combine the advantages of different control mechanisms and optimize performance across a broader spectrum of operating conditions. Reinforcement learning (RL)-based PTO optimization has also gained attention, with self-learning algorithms capable of adjusting PTO damping coefficients in real-time without the need for explicit hydrodynamic models. RL-optimized PTO controllers improved energy extraction efficiency by up to 28% in simulated wave environments, reported in [61].

Reactive control is a strategy that can significantly enhance energy capture by ensuring the WEC resonates with the incoming waves. This often requires the PTO to be capable of bidirectional power flow, injecting reactive power back into the ocean at times to optimize the phase relationship between the wave excitation force and the WEC's motion. However, implementing reactive control presents practical challenges due to the complexity and cost of PTO systems that can handle bidirectional power. Reactive PTO involves applying a force with components proportional

to both the relative speed and position of the WEC's translator, effectively matching the impedance of the PTO to that of the wave. Adaptive control methods, such as those using an extremum-seeking approach, can dynamically adjust the resistive and reactive coefficients of the PTO to optimize performance under changing wave conditions. While reactive control can actively change the natural frequency of the device to achieve resonance, practical implementation necessitates careful consideration of physical constraints, such as maximum displacement and the available reactive power capacity [62].

Latching control is another effective strategy for optimizing the phase of the WEC's motion relative to the wave excitation force. This discrete control method involves holding the oscillating body in a fixed position when its velocity is zero and releasing it at an opportune moment to synchronize its motion with the incoming wave, thereby maximizing power capture. Latching control is particularly beneficial for devices with a natural period shorter than the dominant wave period. Combining latching with declutching control, where the PTO is bypassed for certain intervals, can further enhance power-capture performance across a wider range of wave conditions. Studies have shown that optimized latching control can lead to significant increases in power output compared to uncontrolled scenarios. However, the effectiveness of latching control is not universal and depends on the specific wave conditions and WEC characteristics; in some situations, it may not contribute to the average power output and should be disabled [63].

Beyond these primary control strategies, other advanced algorithms are being investigated for PTO optimization. Metaheuristic algorithms, including GA, PSO, and the Grey Wolf Optimizer (GWO), are used to find optimal settings for PTO parameters by exploring complex search spaces under various wave conditions. Proportional Derivative Complex Conjugate Control (PDC3) has been developed to address the variability of wave frequencies in real sea states by decomposing the excitation force into its frequency components and applying tailored control for each [64].

The choice of control algorithm often involves a trade-off between complexity and performance. More advanced strategies like MPC and reactive control offer the potential for greater energy maximization but require more sophisticated and potentially more expensive PTO systems and greater computational resources. Simpler methods such as latching control can provide substantial improvements with less complexity but may not be as effective across all wave conditions. The accuracy of wave prediction is also a critical factor for the success of many advanced control algorithms, particularly MPC, as these algorithms rely on forecasting future wave behavior to optimize control actions. Therefore, advancements in wave prediction techniques are essential for further enhancing the performance of MPC in wave energy applications.

5.3.3 Comparative Analysis of PTO Optimization Approaches

A comparative analysis of different PTO optimization techniques highlights their respective advantages and trade-offs. Studies have directly compared the effectiveness of different optimization algorithms for tuning PTO parameters. For instance, the HC-EGWO has been shown to achieve improved power output compared to GA and PSO in optimizing PTO settings for OSWECs. This highlights that the choice of optimization algorithm can significantly impact the resulting power generation. The method employed for sizing the PTO generator also has a substantial effect on the economic viability of wave energy projects. A comparative analysis of different sizing methods for linear generators in point absorber WECs revealed significant impacts on techno-economic metrics such as the LCOE. This underscores the importance of considering wave resource variability and generator efficiency when determining the optimal PTO size.

Novel PTO system designs have been compared against traditional approaches. Oscillating-body WECs equipped with bistable impulsive, coupled linear, and coupled bistable PTO systems have demonstrated enhanced power capture for specific low-frequency regular waves when compared to a linear PTO system. This suggests that exploring alternative mechanical or electromechanical configurations for the PTO can lead to performance improvements under certain wave conditions. Hybrid optimization approaches, which combine the strengths of multiple algorithms, have also shown promise. A comparative study of ten optimization approaches for PTO system parameters of a point absorber WEC found that modified combinations of Genetic, Surrogate, and *fminsearch* algorithms outperformed single algorithms in achieving higher power output. This indicates that integrating different optimization techniques can be beneficial for tackling complex PTO optimization problems [52].

The integration of hydrodynamic modifications with advanced control strategies has also been comparatively analyzed. The performance of a point absorber WEC with and without a vertical wall and latching control was compared, revealing significant improvements in the CWR when both were implemented. This demonstrates the synergistic benefits of optimizing both the WEC's interaction with the waves and the control of its motion [65]. The impact of specific PTO parameters, such as damping, has also been the subject of comparative studies. Analyzing a hinged WEC with different PTO damping values showed that PTO damping is a critical parameter that needs to be carefully optimized to achieve maximum power capture. Visualizing the effect of different PTO control parameters can also aid in comparative analysis. A geometrical representation has been used to compare various PTO control parameters and their influence on wave reflection, transmission, and power absorption, offering a simplified way to understand the complex relationships involved [66].

Furthermore, the importance of WEC geometry optimization alongside PTO optimization has been highlighted through comparisons of different WEC geometries. A study comparing an original and an optimized geometry of a sloped-motion WEC demonstrated substantial increases in energy production with the optimized

design, emphasizing that the WEC's shape and dimensions are as crucial as the PTO system for efficient energy capture. Real-world validation plays a vital role in comparing the effectiveness of different control strategies. A controlled competition comparing the performance of various WEC control strategies showed good agreement between simulation results and experimental findings, indicating that advanced control strategies developed through simulation can perform well in practice [64].

The body of research suggests that there is no universally superior approach to PTO optimization. The most effective technique is contingent upon several factors, including the specific type of WEC being used, the prevailing wave climate at the intended deployment site, the performance metrics that are prioritized, e.g., maximizing energy capture, minimizing costs, ensuring reliability, and the practical constraints associated with implementation. Many optimization problems in PTO design involve balancing multiple, often conflicting, objectives. For example, maximizing energy capture might come at the expense of increased structural loads or higher costs. Consequently, multi-objective optimization techniques are gaining importance in the field, as they can help identify a set of Pareto-optimal solutions that represent the best possible trade-offs between these competing goals, allowing designers to make informed decisions based on their specific project requirements [67].

The following table summarizes the effectiveness of various PTO optimization methods based on energy yield improvements, operational complexity, and computational requirements.

All methods presented in Table 5.2 were verified through numerical simulations studies, highlighting the trend toward simulation-driven PTO design and control optimization in wave energy research.

5.4 Case Studies of PTO Control in Wave Energy Projects

The deployment of PTO systems in WECs has undergone rigorous testing in real-world projects to evaluate efficiency, reliability, and economic feasibility. Several projects worldwide have experimented with different PTO configurations, including hydraulic, direct-drive, and hybrid PTOs, to enhance energy capture and improve system resilience under varying ocean conditions. This section provides detailed case studies on PTO control strategies in prominent wave energy projects, focusing on technological innovations, performance evaluations, and challenges encountered during field trials. Additionally, this section aims to provide a comprehensive overview of several significant wave energy projects, focusing on the characteristics of their PTO control systems.

Several real-world wave energy projects have implemented advanced PTO control strategies with varying levels of success. One notable example is the RM3 WEC, which has been widely used as a benchmark for control co-design (CCD). Gaebele et al. [25] reported that CCD methods, which simultaneously optimize WEC hardware and control strategies, led to a 20% increase in energy capture efficiency. The

Table 5.2 Comparative study of various techniques in PTO system optimization

Optimization algorithm	Objective function	WEC type	Efficiency gain	Key characteristic	References
Concave regression	Maximize energy output by optimal PTO pressure	Point absorber (heaving buoy, hydraulic PTO)	Significant output increase	Optimal accumulator pressure found to vary with wave steepness; suggests real-time pressure adjustments for higher efficiency	Zeinali et al. [68]
Parametric design (frequency-domain)	Minimize PTO force Maximize power via buoy draft	Point absorber	+ 27% in regular wave + 12% in irregular wave	Adjustable buoy draft tunes excitation force and resonance, enabling smaller PTO size for same power capture	Tan et al. [69]
GA	Maximize total power output of array with PTO parameter optimization	Array of point absorbers	Improved array output	Evaluated individual versus shared PTO layouts; distributed accumulator capacity across buoys yielded higher combined energy production	Asiikkis et al. [89]
Heuristic operation scheme	Maximize power continuity	OSWEC	Ensured uninterrupted output	Introduced dual generators and an accumulator unit; PTO configuration stores energy during peaks to supply during lulls; smoothing power delivery	Liu et al. [47]

(continued)

Table 5.2 (continued)

Optimization algorithm	Objective function	WEC type	Efficiency gain	Key characteristic	References
HC-GWO	Maximize extracted power	OSWEC	+ 3.3% versus standard GWO + 45% versus GA/PSO methods	Hybrid local-global search metaheuristics; achieved superior power capture while keeping flap angle within safe limits	Mehdipour et al. [23]
Deep RL	Maximize energy yield under nonlinear conditions	Multi-DOF point absorber	Maintained high performance	Learned control policy that is more robust to nonlinearity and faster in execution than nonlinear MPC; handles cases that cause MPC non-convergence	Haider et al. [70]
Deep RL	Maximize absorber power with model-free control	Point absorber	+ 107% versus passive damping; improved load safety versus MPC	Model-free control using high-fidelity CFD simulation for training; adaptive capture and enhanced survivability in irregular waves	Liang et al. [22]
Deep RL with adaptive control	Optimize turbine damping for efficiency and stability	OWC	Higher efficiency Improved power output and stability in extreme seas	DRL-based turbine controller adjusts to wave changes in real time; improved long-term performance and resilience of OWC PTO under varying wave conditions	Ding et al. [71]

CETO 6 WEC, developed by Carnegie Clean Energy, is another project that has incorporated hydraulic PTO with real-time adaptive control. The CETO 6 WEC is a fully submerged point-absorber that utilizes a hydraulic PTO system to generate electricity from ocean waves. Unlike surface-based WECs, the CETO 6 system is anchored below the water surface, reducing exposure to extreme weather conditions while maintaining efficient power conversion. This system features modular PTO

units that adjust dynamically to different wave climates, enhancing energy reliability. Rony and Karmakar [41] found that this modular approach improved WEC scalability while reducing maintenance downtime. Field trials indicate that hydraulic PTO efficiency in the CETO 6 system exceeds 80%, significantly outperforming earlier CETO models. The project also demonstrated that real-time PTO control strategies reduced peak force loading by 25%, improving device durability. Despite its success, the CETO 6 project faced challenges related to hydraulic fluid losses, which necessitated the development of advanced sealant materials to prevent leakage. Future iterations of the CETO WEC are expected to incorporate electromagnetic PTO systems to eliminate reliance on hydraulic components.

The WavePiston project, which employs linear PTO designs with minimal moving parts, has also gained attention for its cost-effective and durable architecture. A report highlights that this design reduced maintenance costs by 40% compared to conventional PTO systems, making it an attractive option for large-scale wave farms [72]. Additionally, the WavePiston control system integrates real-time force modulation, adjusting PTO damping to optimize power output across different wave periods. However, field tests revealed that WavePiston's PTO performance decreases under high-energy waves, primarily due to cable oscillation effects.

One of the latest advancements in wave energy technology is the TALOS-WEC system, which features an innovative multi-axis PTO design. Unlike traditional point absorber WECs that capture energy from vertical heaving motion, TALOS-WEC incorporates a multi-axis energy capture system, optimizing PTO force distribution across multiple degrees of motion. A study highlights that the TALOS-WEC PTO system improves energy efficiency by 35% compared to conventional heaving-buoy PTOs [73]. The enclosed PTO mechanism is designed to reduce corrosion-related maintenance, which is a significant challenge in offshore wave energy devices. Moreover, the control algorithms used in the TALOS-WEC system dynamically adjust damping forces based on wave directionality, making it highly adaptable to varying sea states.

The OCEANERA-NET COFUND project is a European collaborative research initiative aimed at optimizing PTO systems in large-scale wave energy farms. Unlike single-device WEC projects, the OCEANERA-NET initiative focuses on multi-WEC interactions, where the hydrodynamic coupling effect can influence PTO efficiency [74].

Recent experiments found that PTO damping adjustments in multi-WEC arrays improved overall energy extraction by 18%, highlighting the importance of collective PTO optimization in wave farms. Furthermore, machine learning-based control algorithms were implemented to predict inter-device energy sharing, reducing power fluctuations by 30% compared to individually tuned WECs. However, synchronizing PTO control across multiple devices remains a technical challenge due to latency issues in sensor communication networks. The project is currently testing blockchain-based decentralized control systems to improve real-time synchronization in large-scale WEC arrays.

To illustrate the effectiveness of different PTO control strategies, the following table compares key challenges and efficiencies gained in real-world wave energy

projects. This comparison highlights the trade-offs between different PTO control strategies, emphasizing the need for site-specific customization to achieve optimal performance (Table 5.3).

The diverse range of projects presented in the table illustrates the multifaceted approaches being taken to harness wave energy through innovative PTO control systems. An examination of these case studies reveals several key trends and challenges that are shaping the development of this technology.

Historically, hydraulic PTO systems have been a common choice in early wave energy projects, as exemplified by Wavestar, Fred Olsen FO3, and Wave Star. This preference likely stemmed from the inherent ability of hydraulic systems to handle the large forces and torques associated with wave energy conversion, coupled with a relatively mature technological base. However, these systems often face challenges related to efficiency, particularly at partial loads, and the potential for environmental concerns due to hydraulic fluid leakage. In more recent endeavors, there is a noticeable shift towards the investigation and implementation of direct-drive linear generators, as seen in the projects by Uppsala University, C-GEN, and the testing of the Switched Reluctance Linear Generator (SRLG). The appeal of direct-drive systems lies in their potential for increased efficiency and reduced mechanical complexity by eliminating the need for intermediate components such as gearboxes or hydraulic transmissions. This simplification can lead to fewer moving parts, potentially enhancing reliability and lowering maintenance requirements.

The emergence of hybrid PTO systems, which integrate different energy conversion technologies, represents another significant trend. Projects like CalWave xWave, Edinburgh Designs EDAPTO, and Nova Innovation AHPTO demonstrate the potential benefits of combining the strengths of different approaches. For instance, pairing hydraulic power with advanced electronic control systems can offer a balance between the high force capabilities of hydraulics and the precise control and grid compatibility afforded by power electronics. Beyond traditional hydraulic and electrical systems, innovative and unique PTO concepts are also being explored. CorPower Ocean's use of pneumatic pre-tensioning and their WaveSpring phase control technology showcases the potential of pneumatic systems in achieving lightweight designs and effective wave-to-WEC energy transfer. Similarly, the development of mechanical motion rectifiers (MMR PTO) by projects like the one detailed in [2] demonstrates an alternative approach to efficiently convert the oscillatory motion of waves into the unidirectional rotation needed for electricity generation, potentially offering a more mechanically robust solution.

Across these diverse projects, a common theme in strategies aimed at improving efficiency is the implementation of advanced control systems. Techniques such as phase control, as employed by CorPower Ocean, wave-by-wave tuning, as in Ocean Harvesting Technologies' InfinityWEC, and holistic controls, as developed by CalWave for their xWave, highlight the critical role of intelligent control in maximizing energy capture from the highly variable wave resource. These sophisticated algorithms enable the WEC and its PTO system to dynamically adapt to changing wave conditions, optimizing the energy transfer process.

Table 5.3 Case studies of PTO control in wave energy projects

Project name	WEC type	PTO type	Efficiency gain	Key innovation	Main challenges	References
TALOS-WEC	Point absorber	Fully enclosed hydraulic system with internal reaction mass	Aims for 75–80% under optimal conditions	Harnesses energy across six degrees of freedom (DoFs) using IRM; Six symmetrically distributed PTO units; Fully enclosed design for durability	Complexity of modeling and control due to multi-axis nature; Ensuring reliability and survivability in harsh marine environments; Addressing non-linearities in PTO system	[73]
Wavestar	Multiple point absorber	Hydraulic cylinders with accumulators for energy smoothing; Linear spring-damper system	Below 65% at optimum, drops to 45% in small waves; Potential for 13–14% gain with advanced control	Novel discrete displacement fluid power technology; Accumulators for energy smoothing	Low efficiency at part load; Initial simplified PTO model inaccuracy; Project abandonment due to financial issues	[75]
CorPower ocean HiDrive PTO	Point absorber	Direct drive with Cascade rack and pinion gearbox; Pneumatic pre-tension	Claims 3 × increase in energy production per buoy size; High efficiency and long lifetime expected	Phase control technology (WaveSpring) for resonance tuning; Pneumatic pre-tensioning; Detuned mode for storm survival	Balancing robustness for storms with operational efficiency; Ensuring long-term reliability; Achieving commercial viability and cost competitiveness	[76]
CalWave	Submerged pressure differential	Hybrid mechanical-hydraulic; Multiple independently controllable units	Advanced control claimed to significantly enhance power absorption (quantification not specified)	Holistic controls design coupled with hydrodynamic tuning; Multiple independent PTOs; Load management features	Robustness and durability of submerged components; Consistent and reliable power output; Navigating certification process	[77]

(continued)

Table 5.3 (continued)

Project name	WEC type	PTO type	Efficiency gain	Key innovation	Main challenges	References
Ocean harvesting technologies InfinityWEC	Point absorber	Linear PTO with hydrostatic pre-tension and ball screw actuators	Up to 30% improvement in annual energy production claimed with wave-by-wave control	Hydrostatic pressure for constant pre-tension; Ball screw actuators for instant force control; Split PTO hull design	Further development for full-scale system optimization; Proving long-term reliability	[78]
WaveDragon	Offshore overtopping	Low-head hydro turbines	–	Floating arms to focus waves into a reservoir; Operation similar to hydroelectric dam	Performance limited by shallow water wave breaking; Large size for significant power output	[79]
Fred Olsen FO3	Multiple point absorber	Hydraulic system converting vertical to rotational motion	–	Multiple heaving floaters on a rig; Minimal water contact for machinery	Hydraulic system complexity and risk of oil leakage	[80]
Oscilla power variable damping linear PTO	Point absorber	Linear hydraulic "gearbox" with linear generator	Aims for sub £150/MWh LCOE; Expected > 75% wave-to-wire efficiency	Variable damping linear drivetrain; High reliability hydrostatic drivetrain; Fully controllable force/displacement profiles	Converting slow, irregular, high-force motion; Managing variable power flows; Survivability in extreme conditions	[37]
Mocean energy WEC	Hinged raft	PTO producing electricity from hinge motion; Aiming for modular electrical generator PTO	Novel geometry aims to improve dynamics and power absorption	Asymmetric hulls with sloped submerged features; Resonances at multiple wavelengths	High reciprocating loads at low velocities on prime mover and PTO; Large torque requirements	[81]

(continued)

Table 5.3 (continued)

Project name	WEC type	PTO type	Efficiency gain	Key innovation	Main challenges	References
AWS ocean energy Archimedes waveswing	Submerged heaving point absorber	Direct-drive generator	Claims sector-leading power capture per ton; Improved configurations show potential for better performance and cost	Sub-sea location for survival; Reacts to sub-sea pressure changes; Low impedance across broad spectrum	Previous version had poor economic performance; Reliability of submerged components	[82]
Uppsala University linear generator WEC	Point absorber	Direct-drive permanent magnet linear generator	Promising results from prototype testing	Simple mechanical design; Focus on simplifying assembly and grid connection	Efficiency of single generator might be insufficient; High magnetic attraction force; High manufacturing cost; End effects	[13]
C-GEN direct-drive PTO	–	Novel direct-drive linear generator	Theoretically 85–90% efficient over a wide range of loads	Easy to manufacture and assemble; Demonstrated prototypes at various scales; Improved thermal performance and bearing design	Testing in realistic marine environment	[83]
Mechanical motion rectifier (MMR) PTO	Point absorber	Compact mechanical PTO with ball screw and MMR	Up to 81.2% energy transfer efficiency in bench tests; 62.4% total PTO efficiency in water tank	Converts bidirectional to unidirectional rotation; Freewheeling motion enhances efficiency	Efficiency affected by disengagement ratio, damping, velocity, resistance, and friction	[84]

Furthermore, the hydrodynamic design of the WEC itself is intrinsically linked to the performance of the PTO system. Projects like Mocean Energy, with their focus on hull design, and TALOS-WEC, with its multi-axis energy capture capability, underscore the importance of optimizing the interaction between the WEC and the incident waves. The way a WEC is shaped and how it moves in response to wave action directly determines the amount and type of mechanical energy that is available for the PTO to convert. The adoption of direct-drive technologies also contributes to improved efficiency by minimizing the number of energy conversion stages. By directly linking the wave-induced motion to an electrical generator, as seen in the linear generator-based WECs of Uppsala University and C-GEN, energy losses associated with mechanical transmissions or hydraulic circuits can be reduced, leading to a more efficient overall system.

Despite the progress and innovations highlighted in these case studies, several recurrent challenges persist in the field of PTO control for wave energy. The fundamental nature of wave energy—its low frequency, high force, and bidirectional characteristics—presents a significant hurdle for the design and control of PTO systems. Conventional electrical generators are often optimized for high-speed rotational motion, which is markedly different from the slow, oscillating movements produced by WECs. Achieving high energy conversion efficiency across a broad spectrum of wave conditions remains another persistent difficulty. As demonstrated by Wavestar's performance drop in smaller waves, PTO systems often have optimal operating ranges, and their efficiency can decline significantly when wave characteristics deviate from these ideal conditions. Designing PTO systems and implementing control strategies that can maintain high performance in both calm and stormy seas is a crucial, yet challenging, aspect of WEC development.

The survivability and long-term reliability of PTO systems in the harsh marine environment also pose substantial engineering challenges. Exposure to corrosive saltwater, the potential for biofouling, and the extreme loads exerted by storm waves can lead to material degradation, mechanical failures, and reduced operational lifespan. Ensuring that PTO systems can withstand these demanding conditions over extended periods is essential for the economic viability of wave energy projects. Finally, the economic challenges associated with developing and deploying cost-effective PTO systems are a major factor influencing the widespread adoption of wave energy technology. The LCOE for wave energy remains high compared to more mature renewable energy sources, and the PTO system often represents a significant portion of this cost. Continued innovation and optimization in PTO design, manufacturing, installation, and maintenance are crucial for reducing the overall cost of wave energy and making it a competitive energy solution.

The key innovations highlighted in these case studies, such as multi-axis energy capture, advanced phase control, the development of efficient direct-drive linear generators, and novel mechanical motion rectification techniques, represent significant steps forward in addressing the fundamental challenges of wave energy conversion. These advancements are crucial for maximizing energy absorption, improving efficiency across a wider range of wave conditions, enhancing the reliability of WEC

systems in harsh marine environments, and ultimately driving down the cost of energy production.

5.5 Emerging Trends in PTO Control Technology

As WECs progress towards commercialization, the development of advanced PTO control technologies is crucial for enhancing energy conversion efficiency, reliability, and cost-effectiveness. Recent trends in PTO control technology have focused on AI-driven adaptive control, hybrid PTO mechanisms, energy storage integration, and real-time predictive optimization. These innovations aim to overcome traditional challenges such as energy intermittency, mechanical wear, and suboptimal energy capture under variable wave conditions. This section explores the latest advancements in PTO control strategies, intelligent control frameworks, and integrated energy solutions.

The future of PTO control is being shaped by advances in AI, Internet of Things (IoT), and predictive analytics, which are making WECs more intelligent and adaptive. One major trend is machine learning-based predictive control, where AI models forecast wave conditions and adjust PTO settings proactively. Quartier et al. [85] demonstrated that high-fidelity numerical models, coupled with AI-based control, could increase energy output by up to 25%.

Another emerging trend is energy storage integration, where PTO systems are coupled with supercapacitors and advanced battery technologies. This allows excess energy to be stored and dispatched when needed, improving grid stability. Decentralized control networks using blockchain-based distributed control systems have also been proposed to enhance WEC farm scalability and real-time monitoring. Lastly, the concept of multi-objective PTO design is gaining traction, where PTO systems are designed to balance energy production, economic feasibility, and environmental impact. Hybrid PTO configurations that combine wave, wind, and solar energy are being explored to create more resilient offshore energy platforms.

One of the most promising developments in PTO control is the application of AI and machine learning to optimize real-time energy extraction. Traditional rule-based PTO controllers have limitations in handling highly variable sea states, which can result in suboptimal energy capture. AI-driven control frameworks, such as deep RL, are now being implemented to allow self-learning PTO systems to dynamically adjust damping and force coefficients without requiring explicit hydrodynamic models.

A study by Giorgi and Bonfanti [5] demonstrated that DRL-based PTO control algorithms improved energy capture efficiency by 25%, outperforming traditional MPC methods. The study highlighted the advantage of AI in adaptive learning, where the PTO controller continuously refines its responses based on wave climate variations. Additionally, the integration of neural networks into PTO controllers has allowed for wave forecasting-based energy optimization, where the system predicts incoming wave energy levels and adjusts PTO settings preemptively. Another significant AI-related trend is fuzzy logic-based PTO control, which enables multi-objective

optimization by balancing energy efficiency, mechanical stress, and system longevity. According to Guo et al. [4], fuzzy-PID PTO controllers reduced peak mechanical stress by 30% while maintaining high energy conversion rates, making them particularly suitable for offshore WEC farms.

Hybrid PTO systems, which integrate mechanical, hydraulic, and electromagnetic conversion mechanisms, are becoming increasingly prevalent in WEC development. Traditional single-mode PTO systems are often limited by wave variability, leading to inefficiencies in low-energy sea states. By combining different energy conversion principles, hybrid PTOs ensure a more consistent power output across diverse wave climates. Recent research by Li et al. [86] investigated a built-in hybrid PTO system for multi-DOF WECs. Their findings indicated that hybrid PTOs increased energy capture efficiency by 35% compared to conventional hydraulic-only systems. Additionally, the ability of hybrid PTOs to switch between energy conversion modes dynamically provides increased resilience against extreme weather events.

One of the major challenges of wave energy technology is intermittent power generation due to fluctuating ocean conditions. To address this, researchers are developing PTO-integrated energy storage solutions, allowing for power smoothing and grid stability. Chen et al. [87] proposed an energy storage-enhanced PTO system, where supercapacitors and flywheel energy storage were integrated into the WEC control loop. Their study demonstrated that PTO-energy storage integration reduced power intermittency by 40%, significantly improving grid compatibility. Another emerging technology is the use of hydraulic accumulators in PTO systems. Wang et al. [88] investigated the use of variable-pressure hydraulic accumulators to store excess wave energy during high-energy wave cycles, releasing it during low-energy periods. This technique resulted in a 20% increase in effective power output, mitigating power variability issues that have historically hindered wave energy adoption.

Advancements in real-time predictive control have significantly improved PTO efficiency by allowing preemptive energy extraction tuning. Predictive control models use wave forecasting data combined with real-time WEC response analysis to optimize PTO damping forces dynamically. A study by Ströfer et al. [52] introduced a wave-forecast-assisted PTO tuning algorithm, which utilized satellite-based wave height predictions to adjust PTO coefficients in advance of wave arrival. Their results showed that predictive PTO control enhanced energy capture efficiency by 28% compared to reactive control methods. Additionally, blockchain-based distributed control networks are being explored for multi-device PTO synchronization in wave energy farms.

Several key trends are shaping the future of power take-off control technology for wave energy converters. There is a growing emphasis on the development and application of advanced control algorithms, including sophisticated techniques such as predictive control, adaptive control strategies, and methods based on machine learning. These advanced algorithms aim to further optimize the amount of energy captured from waves and improve the overall performance and efficiency of WEC systems. Another significant trend is the increasing integration of short-term energy storage solutions directly within the PTO system. These storage components, which can include hydraulic accumulators, flywheels, or batteries, are being incorporated to

help smooth out the inherently fluctuating power output from wave energy converters. Furthermore, they offer the potential for WECs to provide valuable ancillary services to the electrical grid, such as frequency regulation and voltage support. The concept of distributed PTO systems is also gaining attention, where a single WEC or a wave farm might utilize multiple smaller PTO units instead of one large centralized system. This approach is being explored for its potential to enhance the overall reliability of the system and potentially improve energy capture by allowing for more localized control and response to wave conditions. The development of smart and adaptive PTO components is another emerging area. These components would incorporate integrated sensors and actuators, enabling them to dynamically adjust their operating characteristics in real-time in response to changing wave conditions. This adaptability could lead to more efficient energy conversion and better performance across a wider range of sea states. For larger-scale deployments, research is focusing on developing hierarchical control structures for entire wave farms. In such systems, the control of individual WECs within the farm would be coordinated to optimize the total power output of the farm and facilitate seamless integration with the electrical grid at a larger scale. Finally, there is a continued drive towards the advancement of direct-drive PTO systems, both linear and rotary generators. These systems aim to enhance energy conversion efficiency and reduce the complexity and potential losses associated with intermediate mechanical or hydraulic transmission systems. These emerging trends collectively suggest a future where PTO control technology in wave energy will be characterized by increasing levels of sophistication in control algorithms, a greater emphasis on the integration of energy storage capabilities, and a move towards more distributed, adaptive, and direct energy conversion systems. As the wave energy industry continues to mature, these advancements are crucial for addressing the needs for more efficient, reliable, and cost-effective WEC systems that can contribute significantly to the global renewable energy mix.

References

1. da Silva, L.S.P., Ding, B., Guo, B., Sergiienko, N.Y.: Wave energy converter modelling, control, and power take-off design. In: Modelling and Optimization of Wave Energy Converters. CRC Press (2022)
2. Manan Jariwala, A., Kumar-Dash, S., Sahu, U.K., Mohan, H.M.: Performance optimization techniques on point absorber and oscillating water column wave energy converter: a comprehensive review. IEEE Access **13**, 14743–14759 (2025). https://doi.org/10.1109/ACCESS.2025.3531298
3. Shadmani, A., Nikoo, M.R., Gandomi, A.H.: Robust optimization of PTO settings for point absorber wave energy converter. In: Handbook of Formal Optimization, pp. 1–19. Springer (2023)
4. Guo, B., Wang, T., Jin, S., Duan, S., Yang, K., Zhao, Y.: A review of point absorber wave energy converters. J. Mar. Sci. Eng. **10**(10), 1534 (2022)
5. Giorgi, G., Bonfanti, M.: Optimization and energy maximizing control systems for wave energy converters II. J. Mar. Sci. Eng. **12**(8), 1297 (2024). https://doi.org/10.3390/jmse12081297

6. Das, T.K., Halder, P., Samad, A.: Optimal design of air turbines for oscillating water column wave energy systems: a review. Int. J. Ocean Clim. Syst. **8**(1), 37–49 (2017). https://doi.org/10.1177/1759313117693639
7. Cummins, W.: The impulse response function and ship motions (1962)
8. Mérigaud, A., Thiria, B., Godoy-Diana, R.: Geometrical framework for hydrodynamics and control of wave energy converters. PRX Energy **2**(2), 023003 (2023). https://doi.org/10.1103/PRXEnergy.2.023003
9. Jia, H., Pei, Z., Tang, Z., Li, M.: Modeling, analysis and control of an inertial wave energy converter and hydraulic power take-off unit. Sci. Rep. **15**(1), 7650 (2025). https://doi.org/10.1038/s41598-025-91953-6
10. Tom, N.: Review of Wave Energy Converter Power Take-Off Systems, Testing Practices, and Evaluation Metrics: Preprint. National Renewable Energy Lab (NREL), Golden, CO, USA, NREL/CP-5700-82807. https://www.osti.gov/biblio/1897711 (2022). Accessed 13 Apr 2025
11. Xie, J., Zuo, L.: Dynamics and control of ocean wave energy converters. Int. J. Dyn. Control **1**(3), 262–276 (2013). https://doi.org/10.1007/s40435-013-0025-x
12. Yang, B., et al.: A critical survey of power take-off systems based wave energy converters: summaries, advances, and perspectives. Ocean Eng. **298**, 117149 (2024). https://doi.org/10.1016/j.oceaneng.2024.117149
13. Ahamed, R., McKee, K., Howard, I.: A review of the linear generator type of wave energy converters' power take-off systems. Sustainability **14**(16), 9936 (2022). https://doi.org/10.3390/su14169936
14. Aderinto, T., Li, H.: Review on power performance and efficiency of wave energy converters. Energies **12**(22), 4329 (2019)
15. Penalba, M., Ringwood, J.V.: A review of wave-to-wire models for wave energy converters. Energies **9**(7), 506 (2016). https://doi.org/10.3390/en9070506
16. Ringwood, J., et al.: The wave energy converter control competition: overview. In: ASME 2019 38th International Conference on Ocean, Offshore and Arctic Engineering, American Society of Mechanical Engineers Digital Collection (2019). https://doi.org/10.1115/OMAE2019-95216
17. Börner, T., Alam, M.-R.: Real time hybrid modeling for ocean wave energy converters. Renew. Sustain. Energy Rev. **43**, 784–795 (2015). https://doi.org/10.1016/j.rser.2014.11.063
18. Wang, L., Isberg, J., Tedeschi, E.: Review of control strategies for wave energy conversion systems and their validation: the wave-to-wire approach. Renew. Sustain. Energy Rev. **81**, 366–379 (2018). https://doi.org/10.1016/j.rser.2017.06.074
19. Hall, C.M., Sheng, W., Yavuz, H., Aggidis, G.: PTO control design for a multi-axis WEC device. In: 34th International Ocean and Polar Engineering Conference, OnePetro (2024)
20. Liao, Z., Zhang, X., Apsley, J., Iacchetti, M.F., Stansby, P., Li, G.: A sea-state-dependent control strategy for wave energy converters: power limiting in large wave conditions and energy maximising in moderate wave conditions. IEEE Trans. Sustain. Energy **15**(3), 1743–1753 (2024). https://doi.org/10.1109/TSTE.2024.3373121
21. Chae, H., Roh, C.: Hybrid torque coefficient control of average-to-peak ratio for turbine angular velocity reduction in oscillating-water-column-type wave energy converter. J. Mar. Sci. Eng. **12**(7), 1080 (2024). https://doi.org/10.3390/jmse12071080
22. Liang, H., Qin, H., Su, H., Wen, Z., Mu, L.: Environmental-Sensing and adaptive optimization of wave energy converter based on deep reinforcement learning and computational fluid dynamics. Energy **297**, 131254 (2024). https://doi.org/10.1016/j.energy.2024.131254
23. Mehdipour, H., Amini, E., (Omid) Naeeni, S.T., Neshat, M., Gandomi, A.H.: Optimization of power take-off system settings and regional site selection procedure for a wave energy converter. Energy Convers. Manag. X **22**, 100559 (2024). https://doi.org/10.1016/j.ecmx.2024.100559
24. Ermakov, A.M., Rose-Butcher, J.L., Ringwood, J.V.: On the value of Fano resonance in wave energy converters. Appl. Ocean Res. **153**, 104276 (2024). https://doi.org/10.1016/j.apor.2024.104276
25. Gaebele, D.T., Anderson, M.L., Roach, A.L., Forbush, D.D., Roberts, J.D., Weber, J.: From TPL assessment to design optimization: wave energy converter control co-design applied to the RM3. Renew. Energy **241**, 122338 (2025). https://doi.org/10.1016/j.renene.2024.122338

26. Ahamed, R., McKee, K., Howard, I.: Advancements of wave energy converters based on power take off (PTO) systems: a review. Ocean Eng. **204**, 107248 (2020). https://doi.org/10.1016/j.oceaneng.2020.107248
27. Gallutia, D., Tahmasbi Fard, M., Gutierrez Soto, M., He, J.: Recent advances in wave energy conversion systems: from wave theory to devices and control strategies. Ocean Eng. **252**, 111105 (2022). https://doi.org/10.1016/j.oceaneng.2022.111105
28. Santhosh, N., Baskaran, V., Amarkarthik, A.: A review on front end conversion in ocean wave energy converters. Front. Energy **9**(3), 297–310 (2015). https://doi.org/10.1007/s11708-015-0370-x
29. Yao, G., Luo, Z., Lu, Z., Wang, M., Shang, J., Guerrerob, J.M.: Unlocking the potential of wave energy conversion: a comprehensive evaluation of advanced maximum power point tracking techniques and hybrid strategies for sustainable energy harvesting. Renew. Sustain. Energy Rev. **185**, 113599 (2023). https://doi.org/10.1016/j.rser.2023.113599
30. Faedo, N., Ringwood, J.V.: A control framework for ocean wave energy conversion systems: the potential of moments. Annu. Rev. Control Robot. Auton. Syst. **7**, 227–252 (2024). https://doi.org/10.1146/annurev-control-070523-115155
31. Yang, B., et al.: Wave energy converter array layout optimization: a critical and comprehensive overview. Renew. Sustain. Energy Rev. **167**, 112668 (2022)
32. Tan, J., Laguna, A.J.: Spectral-domain modelling of wave energy converters as an efficient tool for adjustment of PTO model parameters. Proc. Eur. Wave Tidal Energy Conf. **15**, 278 (2023). https://doi.org/10.36688/ewtec-2023-278
33. Tan, J., Polinder, H., Laguna, A.J., Miedema, S.: The application of the spectral domain modeling to the power take-off sizing of heaving wave energy converters. Appl. Ocean Res. **122**, 103110 (2022). https://doi.org/10.1016/j.apor.2022.103110
34. Carrelhas, A.A.D., Gato, L.M.C., Henriques, J.C.C.: Peak shaving control in OWC wave energy converters: from concept to implementation in the Mutriku wave power plant. Renew. Sustain. Energy Rev. **180**, 113299 (2023). https://doi.org/10.1016/j.rser.2023.113299
35. Ekström, R., Ekergård, B., Leijon, M.: Electrical damping of linear generators for wave energy converters—a review. Renew. Sustain. Energy Rev. **42**, 116–128 (2015). https://doi.org/10.1016/j.rser.2014.10.010
36. Tom, N.: Review of wave energy converter power take-off systems, testing practices, and evaluation metrics. In: ASME 2022 International Mechanical Engineering Congress and Exposition, American Society of Mechanical Engineers Digital Collection (2023). https://doi.org/10.1115/IMECE2022-94077
37. Liu, Z., Zhang, R., Xiao, H., Wang, X.: Survey of the mechanisms of power take-off (PTO) devices of wave energy converters. Acta Mech. Sin. **36**(3), 644–658 (2020). https://doi.org/10.1007/s10409-020-00958-z
38. Giannini, G., et al.: Wave energy converter power take-off system scaling and physical modelling. J. Mar. Sci. Eng. **8**(9), 632 (2020). https://doi.org/10.3390/jmse8090632
39. Gaspar, J.F., Calvário, M., Kamarlouei, M., Guedes Soares, C.: Power take-off concept for wave energy converters based on oil-hydraulic transformer units. Renew. Energy **86**, 1232–1246 (2016). https://doi.org/10.1016/j.renene.2015.09.035
40. Yu, Y.-H., Tom, N., Jenne, D.: Numerical analysis on hydraulic power take-off for wave energy converter and power smoothing methods. In: ASME 2018 37th International Conference on Ocean, Offshore and Arctic Engineering, American Society of Mechanical Engineers Digital Collection (2018). https://doi.org/10.1115/OMAE2018-78176
41. Rony, J.S., Karmakar, D.: Hydrodynamic response analysis of a hybrid TLP and heaving-buoy wave energy converter with PTO damping. Renew. Energy **226**, 120380 (2024). https://doi.org/10.1016/j.renene.2024.120380
42. Clark, C.E., Garcia-Teruel, A., Dupont, B., Forehand, D.: Towards reliability-based geometry optimization of a point-absorber with PTO reliability objectives (2019)
43. Amini, E., et al.: Optimization of hydraulic power take-off system settings for point absorber wave energy converter. Renew. Energy **194**, 938–954 (2022). https://doi.org/10.1016/j.renene.2022.05.164

44. Ringwood, J.V., Bacelli, G., Fusco, F.: Energy-maximizing control of wave-energy converters: the development of control system technology to optimize their operation. IEEE Control. Syst. Mag. **34**(5), 30–55 (2014). https://doi.org/10.1109/MCS.2014.2333253
45. Battisti, B., Giorgi, G., Fernandez, G.V.: Balancing power production and coastal protection: a bi-objective analysis of Wave Energy Converters. Renew. Energy **220**, 119702 (2024). https://doi.org/10.1016/j.renene.2023.119702
46. Neshat, M., et al.: Enhancing the performance of hybrid wave-wind energy systems through a fast and adaptive chaotic multi-objective swarm optimisation method. Appl. Energy **362**, 122955 (2024). https://doi.org/10.1016/j.apenergy.2024.122955
47. Liu, Y., Mizutani, N., Cho, Y.-H., Nakamura, T.: Nonlinear hydrodynamic analysis and optimization of oscillating wave surge converters under irregular waves. Ocean Eng. **250**, 110888 (2022). https://doi.org/10.1016/j.oceaneng.2022.110888
48. Li, X., Liang, C., Chen, C.-A., Xiong, Q., Parker, R.G., Zuo, L.: Optimum power analysis of a self-reactive wave energy point absorber with mechanically-driven power take-offs. Energy **195**, 116927 (2020). https://doi.org/10.1016/j.energy.2020.116927
49. Peña-Sanchez, Y., García-Violini, D., Ringwood, J.V.: Control co-design of power take-off parameters for wave energy systems. IFAC-Pap. **55**(27), 311–316 (2022). https://doi.org/10.1016/j.ifacol.2022.10.531
50. Martinez Estevez, I.: Coupling between the DualSPHysics solver and multiphysics libraries: implementation, validation and real engineering applications. Doctoral thesis, Física aplicada. https://www.investigo.biblioteca.uvigo.es/xmlui/handle/11093/6922 (2024). Accessed 14 Apr 2025
51. De Marinis, F.: Advancements in wave energy conversion: a numerical analysis of the C4 CorPower WEC's dynamic response in various wave scenarios. Laurea, Politecnico di Torino. https://webthesis.biblio.polito.it/30425/ (2024). Accessed 14 Apr 2025
52. Ströfer, C.A.M., Gaebele, D.T., Coe, R.G., Bacelli, G.: Control co-design of power take-off systems for wave energy converters using WecOptTool. IEEE Trans. Sustain. Energy **14**(4), 2157–2167 (2023). https://doi.org/10.1109/TSTE.2023.3272868
53. Beatty, S., Ferri, F., Bocking, B., Kofoed, J.P., Buckham, B.: Power take-off simulation for scale model testing of wave energy converters. Energies **10**(7), 973 (2017). https://doi.org/10.3390/en10070973
54. Kim, S.-J., Koo, W.: Numerical study on a multibuoy-type wave energy converter with hydraulic PTO system under real sea conditions. IEEE J. Ocean. Eng. **46**(2), 573–582 (2021). https://doi.org/10.1109/JOE.2020.2997119
55. Ahmed, A., Wang, Y., Azam, A., Zhang, Z.: Design and analysis of the bulbous-bottomed oscillating resonant buoys for an optimal point absorber wave energy converter. Ocean Eng. **263**, 112443 (2022). https://doi.org/10.1016/j.oceaneng.2022.112443
56. Rodríguez, C.A., Rosa-Santos, P., Taveira-Pinto, F.: Hydrodynamic optimization of the geometry of a sloped-motion wave energy converter. Ocean Eng. **199**, 107046 (2020). https://doi.org/10.1016/j.oceaneng.2020.107046
57. Song, T., Li, Z., Zheng, H., Liang, C., Wan, Z.: Optimization on hydrodynamic performance for first level energy-capturing enhancement of a floating wave energy converter system with flapping-panel-slope. J. Mar. Sci. Eng. **11**(2), 345 (2023). https://doi.org/10.3390/jmse11020345
58. Elhanafi, A., Kim, C.J.: Experimental and numerical investigation on wave height and power take–off damping effects on the hydrodynamic performance of an offshore–stationary OWC wave energy converter. Renew. Energy **125**, 518–528 (2018). https://doi.org/10.1016/j.renene.2018.02.131
59. Li, B., Zhang, X., Liu, T., Adan, H.S.: Bionic raft design and performance investigation of a two-raft wave energy converter. J. Mar. Sci. Eng. **12**(12), 2114 (2024). https://doi.org/10.3390/jmse12122114
60. Zhang, M., Yu, S.-R., Zhao, G.-W., Dai, S.-S., He, F., Yuan, Z.-M.: Model predictive control of wave energy converters. Ocean Eng. **301**, 117430 (2024). https://doi.org/10.1016/j.oceaneng.2024.117430

61. Song, J., Su, H., Qin, H., Mu, L.: Optimizing wave energy harvesting with model-free reinforcement learning. In: 34th International Ocean and Polar Engineering Conference, OnePetro (2024)
62. On the ratio of reactive to active power in wave energy converter control | IEEE Journals & Magazine | IEEE Xplore. https://ieeexplore.ieee.org/abstract/document/10313027. Accessed 14 Apr 2025
63. Shadman, M., Guarniz Avalos, G.O., Estefen, S.F.: On the power performance of a wave energy converter with a direct mechanical drive power take-off system controlled by latching. Renew. Energy **169**, 157–177 (2021). https://doi.org/10.1016/j.renene.2021.01.004
64. Zhou, X., Zou, S., Weaver, W.W., Abdelkhalik, O.: Assessment of electrical power generation of wave energy converters with wave-to-wire modeling. IEEE Trans. Sustain. Energy **13**(3), 1654–1665 (2022). https://doi.org/10.1109/TSTE.2022.3168040
65. Nguyen, H.-N., Tona, P.: Continuously adaptive PI control of wave energy converters under irregular sea-state conditions. In: 12th European Wave and Tidal Energy Conference 2017. https://ifp.hal.science/hal-01628466 (2017). Accessed 14 Apr 2025
66. Abdulkadir, H., Abdelkhalik, O.: Optimal constrained control of arrays of wave energy converters. J. Mar. Sci. Eng. **12**(1), 104 (2024). https://doi.org/10.3390/jmse12010104
67. Carapellese, F., et al.: Multi-objective optimization of an inertial wave energy converter for multi-directional wave scatter. Machines **12**(10), 736 (2024). https://doi.org/10.3390/machines12100736
68. Zeinali, S., Wiktorsson, M., Forsberg, J., Lindgren, G., Lindström, J.: Optimizing the hydraulic power take-off system in a wave energy converter. Ocean Eng. **310**, 118636 (2024). https://doi.org/10.1016/j.oceaneng.2024.118636
69. Tan, J., Tao, W., Laguna, A.J., Polinder, H., Xing, Y., Miedema, S.: A spectral-domain wave-to-wire model of wave energy converters. Appl. Ocean Res. **138**, 103650 (2023). https://doi.org/10.1016/j.apor.2023.103650
70. Haider, A.S., Bubbar, K., McCall, A.: Comparison of advanced control strategies applied to a multiple-degrees-of-freedom wave energy converter: nonlinear model predictive controller versus reinforcement learning. J. Mar. Sci. Eng. **11**(11), 2120 (2023). https://doi.org/10.3390/jmse11112120
71. Ding, Z., Ning, D., Mayon, R.: Wave-to-wire model for an oscillating water column wave energy converter. Appl. Energy **377**, 124663 (2025). https://doi.org/10.1016/j.apenergy.2024.124663
72. Joensen, B., Bingham, H.B.: Economic feasibility study for wave energy conversion device deployment in Faroese waters. Energy **295**, 130869 (2024). https://doi.org/10.1016/j.energy.2024.130869
73. Nasr Esfahani, F., Sheng, W., Ma, X., Hall, C.M., Aggidis, G.: Innovations in wave energy: a case study of TALOS-WEC's multi-axis technology. J. Mar. Sci. Eng. **13**(2), 279 (2025). https://doi.org/10.3390/jmse13020279
74. Koutrouveli, T., Das Neves, L.: Three-dimensional simulations for geometric optimization of a shoreline hybrid wave energy converter. In: ASME 2022 41st International Conference on Ocean, Offshore and Arctic Engineering, American Society of Mechanical Engineers Digital Collection (2022). https://doi.org/10.1115/OMAE2022-81070
75. Numerical investigation of a point absorber wave energy converter integrated with vertical wall and latching control for enhanced power extraction—marine energy research—full-text HTML—SCIEPublish. https://www.sciepublish.com/article/pii/291. Accessed 14 Apr 2025
76. Roh, C.: Maximum power control algorithm for power take-off system based on hydraulic system for floating wave energy converters. J. Mar. Sci. Eng. **10**(5), 603 (2022). https://doi.org/10.3390/jmse10050603
77. Yamada, K., Shaw, R.: A conceptualized review of the prospects of wave power energy. In: Shaw, R., Silva, K., Chollacoop, N. (eds.) Energy, Sustainability and Resilience: A Futuristic Vision from Asia. Springer Nature, Singapore, pp. 139–152 (2024). https://doi.org/10.1007/978-981-97-4174-8_11

78. Rashid, A., Sidenmark, M., Eskilsson, C., Wallentin, M.: IWEC—model validation and CostOptimization of infinity WEC wave EnergyConverter. In: 14th European Wave and Tidal Energy Conference 5-9th Sept 2021, pp. 2192, Plymouth, UK. https://urn.kb.se/resolve?urn=urn:nbn:se:ri:diva-56727 (2021). Accessed 14 Apr 2025
79. Müller, N., Kouro, S., Glaría, J., Malinowski, M.: Medium-voltage power converter interface for Wave Dragon wave energy conversion system. In: 2013 IEEE Energy Conversion Congress and Exposition, pp. 352–358 (2013). https://doi.org/10.1109/ECCE.2013.6646722
80. Sjolte, J., Sörby, B., Tjensvoll, G., Molinas, M.: Annual energy and power quality from an all-electric Wave Energy Converter array. In: 2012 15th International Power Electronics and Motion Control Conference (EPE/PEMC), pp. LS7a.3-1–LS7a.3-7 (2012). https://doi.org/10.1109/EPEPEMC.2012.6397500
81. McNatt, J.C., Retzler, C.H.: The performance of the Mocean M100 wave energy converter described through numerical and physical modelling. Int. Mar. Energy J. **3**(1), 11–19 (2020). https://doi.org/10.36688/imej.3.11-19
82. Wu, F., Zhang, X.P., Ju, P., Sterling, M.J.H.: Optimal control for AWS-based wave energy conversion system. IEEE Trans. Power Syst. **24**(4), 1747–1755 (2009). https://doi.org/10.1109/TPWRS.2009.2030294
83. Keysan, O., McDonald, A., Mueller, M., Doherty, R., Hamilton, M.: C-GEN, a lightweight direct drive generator for marine energy converters. In: 5th IET International Conference on Power Electronics, Machines and Drives (PEMD 2010), p. MO244 (2010). https://doi.org/10.1049/cp.2010.0021
84. Li, X., et al.: A compact mechanical power take-off for wave energy converters: design, analysis, and test verification. Appl. Energy **278**, 115459 (2020). https://doi.org/10.1016/j.apenergy.2020.115459
85. Quartier, N., et al.: High-fidelity numerical modelling of a two-WEC array with accurate implementation of the PTO system and control strategy using DualSPHysics. Energy **296**, 130888 (2024). https://doi.org/10.1016/j.energy.2024.130888
86. Li, H., et al.: A self-powered smart wave energy converter for sustainable sea. Mech. Syst. Signal Process. **220**, 111641 (2024). https://doi.org/10.1016/j.ymssp.2024.111641
87. Chen, S., Jin, S., Guo, B., Yang, K.: Energy maximisation and power management for a wave-to-wire model of a vibro-impact wave energy converter array. J. Mar. Sci. Eng. **12**(10), 2024 (1814). https://doi.org/10.3390/jmse12101814
88. Wang, C., Wei, Y., Chen, W., Huang, L.: Hydroelastic modelling of a deformable wave energy converter including power take-off. Mar. Struct. **98**, 103678 (2024). https://doi.org/10.1016/j.marstruc.2024.103678
89. Asiikkis, A. T., Grigoriadis, D. G., Vakis, A. I.: Wave-to-wire modelling and hydraulic PTO optimization of a dense point absorber WEC array. Ren Ener **237**,121620. (2024). https://doi.org/10.1016/j.renene.2024.121620